FSRU RAVENNA

Model tests - Jetty Mooring and Side By Side Jetty mooring

Text Report

Report No.	:	35255-3-OB
Date	:	May 2024
Version	:	1.0

FSRU RAVENNA

Model tests - Jetty Mooring and Side By Side Jetty mooring

Text Report

MARIN order No.	:	35255
Ship model No.	:	M10446-M10447
Model scale ratio	:	30
Water density	:	1.025 [tonnes/m^3]
Number of pages	:	240

:

Reported by : R. Mulders, R. Engelenburg
Reviewed by : J. de Wilde

Version	Date	Version description
0.1	April 9th, 2024	draft
1.0	April 11th, 2024	draft report for client review
1.1	May 17th. 2024	Final version

CONTENTS PAGE

Appendices:

REVIEW OF TABLES, FIGURES AND PHOTOS

Tables in the report:

Tables in the Table section:

Figures in the report:

Figures in the Figure section:

Photos in the Photo section:

REVIEW OF DELIVERABLES

Report type		Content
Text report	MARIN report No. 35255-3-OB – Volume I	Present report
FTP transfer	MARIN report No. 35255-3-OB – Volume II	Processed data deliverables Photos and videos of the model tests Digital version of the reports

EXECUTIVE SUMMARY

T.EN Italy Solutions S.p.A. and SNAM Rete Gas S.p.A. are working on a floating storage and regasification unit (FSRU) in the Adriatic Sea that is scheduled to be installed by the end of 2024. The existing BW Singapore is foreseen as the FSRU in this project. Technip Energies awarded the Maritime Research Institute Netherlands (MARIN) the order for wave basin model tests to study the vessel motion behavior and the mooring loads in different sea states in shallow water.

This report concerns the performed wave basin model tests with the FSRU in jetty mooring with and without the LNGC moored alongside. The station keeping model tests were carried out in order to check the numerical model of the FSRU vessel in regular and irregular wave conditions by assessing:

- the natural periods and hydrodynamic damping of the moored FSRU and the alongside moored LNGC at the appropriate water depth;
- the statistical motions during operating conditions;
- the motion behaviour of the vessel in operational and critical irregular wave conditions;
- the extreme and statistical accelerations at given locations;
- the relative wave elevation in extreme conditions;
- the motion RAO for the jetty moored FSRU;
- the motion, velocities and accelerations at the jetty loading arm location and the relative motions between FSRU and LNGC at the SBS-loading arms;
- the mooring line tensions and fender loads.

Tests were performed with two MARIN stock models representing respectively the FSRU and the LNGC. The ship models were moored in two basic setups:

- Station keeping tests of the FSRU in jetty mooring;
- Side-by-Side (SBS) mooring of a LNGC alongside the FSRU in the jetty mooring.

Earlier seakeeping model tests of the FSRU in soft-mooring were performed in November/December 2023 and were reported in report 35225-1-OB.

The results of the station keeping model tests can be used to verify the validity of numerical calculated results by applying a “model the model” approach.

It is noted that the loads and motions obtained from the present test campaign are for waves only and only wave frequent response is assessed in the scope of this report.

1 INTRODUCTION

1.1 Background

Technip Energies and SNAM are working on a floating storage and regasification unit (FSRU) in the Adriatic Sea that is scheduled to be installed by the end of 2024. The existing BW Singapore is foreseen as the FSRU in this project. The FSRU is to be moored to a jetty at a water depth of approximately 15.4 m. A breakwater will be installed to provide shelter against waves from the predominant incident heading.

As part of the engineering design, hydrodynamic simulations are performed of the moored FSRU. Technip Energies awarded the Maritime Research Institute Netherlands (MARIN) the order for wave basin model tests to study the vessel motion behavior and the mooring loads in different sea states in shallow water. The basin test results will be used for tuning and validating numerical calculations.

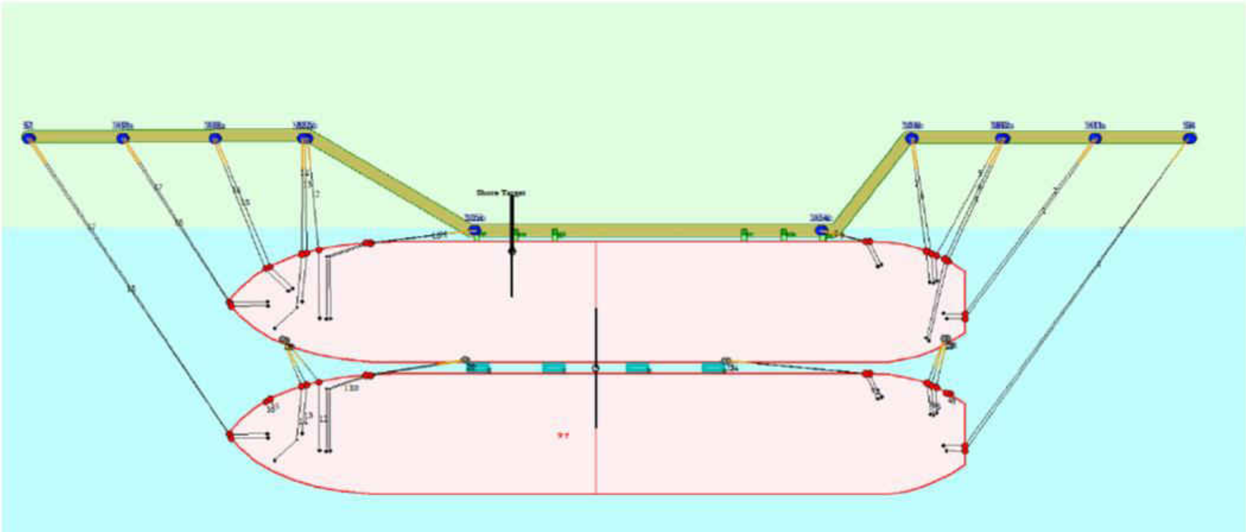

Figure 1-1: top view of the schematic layout of the FSRU Terminal

1.2 Objectives

The performed tests were split in three phases of which phase 2 and 3 are considered in this report:

Phase 1: Seakeeping tests performed in soft mooring;
Phase 2: Station keeping tests of the FSRU in jetty mooring;
Phase 3: Side-by-Side (SBS) mooring of a LNGC alongside the FSRU in the jetty mooring.

Note: the main difference between Phase 1 and Phase 2 is that Phase 2 includes the effect of the jetty mooring on the motion response and accelerations of the vessel. It is expected that these effects are non-negligible.

This report concerns the performed wave basin model tests with the FSRU in the jetty mooring with and without the LNGC moored alongside it. The station keeping model tests were carried out in order to check the numerical model of the FSRU vessel in regular and irregular wave conditions by assessing:

- the natural periods and hydrodynamic damping of the moored FSRU and the alongside moored LNGC at the appropriate water depth;
- the statistical motions during operating conditions;
- the motion behaviour of the vessel in operational and critical irregular wave conditions;

- the extreme and statistical accelerations at given locations;
- the relative wave elevation in extreme conditions;
- the motion RAO for the jetty moored FSRU;
- the motion, velocities and accelerations at the jetty loading arm location and the relative motions between FSRU and LNGC at the SBS-loading arms;
- the mooring line tensions and fender loads.

Only wave-frequent response is considered.

The test results enable the client to verify the validity of the numerical calculated results by applying a “model the model” approach.

1.3 Content of the report

In this report the following topics are addressed:

- Description of the sign conventions
- Description of the model used for the test campaign
- Description of the facility and environmental conditions
- Description of the applied software
- Description of the measurements and data acquisition
- Description of the experimental procedures
- Description of the data and analysis performed on the results
- Discussion of the results
- Conclusions and recommendations

1.4 Content of delivered dataset

The present report is accompanied by a dataset with time trace data, supplementary figures, and other deliverables. Throughout the report, this dataset will be referred to as “Volume II”. The dataset was delivered to the client through an FTP.

An overview of deliverables for each type of test is presented in Section 4.6. The organisation of the data structure and test labelling is described in Section 5.1. The delivered dataset contains an “Overviews” directory that stores review tables of the delivered tests, including hyperlinks that can be used to navigate through the dataset.

1.5 General conventions

The following general conventions are used in this report:

- All results are presented as full scale values unless explicitly stated otherwise.
- The metric system of units (SI) is used.

A right-handed coordinate system is used with upward z-axis. The applied coordinate system is described in Appendix I05.

1.6 Relation to other reports

A diffraction analysis has been performed for the original hull geometry. These numerical calculations were performed by DNV and presented in the report with reference number: 2023-0726, Rev. 01, dated 31-08-2023. Due to the short timescale of the tests, the scale model tests were pragmatically performed with a MARIN stock model very similar to the intended BW Singapore.
To be able to relate the basin model tests to the numerical scope performed by DNV, diffraction calculations were also performed by MARIN for the stock model geometry as used in the basin tests. A

technical note of these diffraction calculations is delivered in MARIN report 35225-2-CPO v1. Results of the diffraction analysis are incorporated in the results of the phase 1 test report , with MARIN report number: 35225-1-OB.

Phase 2 and phase 3 testing have been performed together in the MARIN Offshore basin from February 19th through March 1st 2024. Phase 1 testing has been performed in November/December 2023.

2 MODEL, APPLIED SOFTWARE / FACILITIES AND EXPERIMENTAL SETUP

2.1 Model

A stock model LNGC with model number 10446 of MARIN was used to represent the FSRU. The model scale was selected at 1/30 in order to match the dimensions of the BW Singapore as closely as possible. The bilge keels of the model were replaced in order to represent the bilge keels of the BW Singapore with a height of 40 cm and a length of 90 meter. For the phase 2+3 model testing, the model was unaltered from the model as used in ballast condition for phase 1 testing. (instrumentation on the model was altered, this is later addressed)

The FSRU model is shown in the drawings in FIGURE 1 and in PHOTO 1 through PHOTO 9. The main particulars of the used stock model M10446 are presented in TABLE 1 for ballast condition such as used for all tests for phase 2 and phase 3.

The LNGC model is shown in the drawings in FIGURE 2 and in PHOTO 10 through PHOTO 14. The main particulars of the used stock model M10447 are presented in TABLE 2 for full load condition such as used for all tests for phase 2 and phase 3.

2.2 Wave basin test facility

The scale model was tested in the Offshore Basin (OB). Water depth during regular testing was 0.513 meter (15.4m full scale). See appendix F01 for more information about the Offshore Basin.

2.3 Sign convention

An overview of the used sign conventions is delivered in Appendix I05. Note that during the tests, the ship heading and the incident wave headings are both used. In the overviews in TABLE 41 and TABLE 42 both angles are indicated for clarification purposes.

2.4 Scale factors

All results of the model tests are presented as prototype values in the tables and figures in this report unless denoted otherwise. The model tests results are converted from the model scale values applying Froude’s law of similitude. For scale λ of 1:**30**, this means that the conversion factors of Table 2-1 can be applied.

Table 2-1: Scaling factors

Quantity	Model	Prototype	Ratio
Linear dimension	1 [m]	30 [m]	λ
Area	1 [m^2]	900 [m^2]	λ^2
Volume	1 [m^3]	27,000 [m^3]	λ^3
Time	1 [s]	5.477 [s]	$\sqrt{\lambda}$
Velocity	1 [m/s]	5.477 [m/s]	$\sqrt{\lambda}$
Acceleration	1 [m/s^2]	1 [m/s^2]	1
Angle	1 [deg]	1 [deg]	1
Angular velocity	1 [deg/s]	0.183 [deg/s]	$1/\sqrt{\lambda}$
Mass	1 [kg]	27.7 [tonne]	$\rho\lambda^3/1{,}000$
Force	1 [N]	27.7 [kN]	$\rho\lambda^3/1{,}000$
Moment	1 [Nm]	830.3 [kNm]	$\rho\lambda^4/1{,}000$

The ratio ρ = **1.025** between the specific weight of salt water and the fresh water in the basin indicates that all test results apply to seawater.

2.5 Test setup

Decay tests and inclination tests of the FSRU and LNGC were performed free floating.

Tests in waves were performed with the FSRU moored to the jetty. This was done either with only the FSRU moored to the jetty (phase 2 testing) or with the FSRU moored to the jetty in side by side with a LNGC (phase 3 testing).

2.5.1 Jetty

The jetty was modelled to make an overly stiff construction with attachment points for all fender positions and mooring line boulders. It was constructed of a Prolyte truss system. The jetty as constructed on the basin floor is depicted in Figure 2-1.

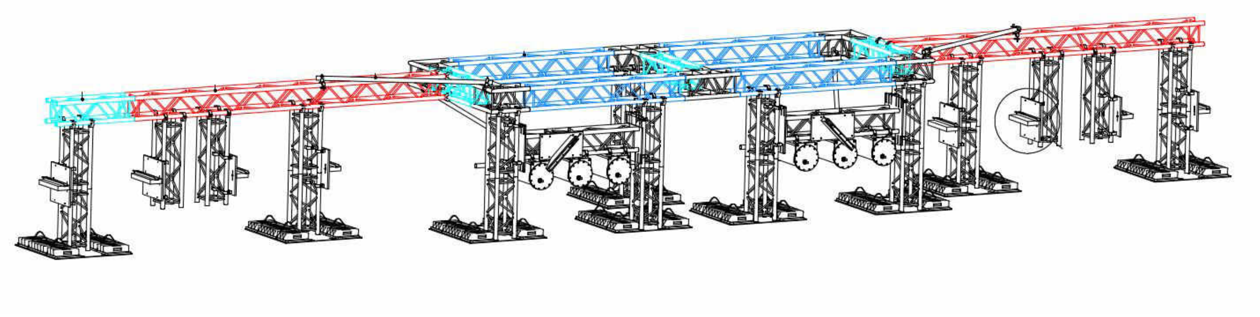

Figure 2-1: jetty as constructed on the basin floor

For shallow water, long crested waves in the offshore basin can only be generated accurately from 180° or 270° in the basin. Therefore, to measure wave responses from waves coming in from different angles, the jetty had to be rotated in the basin. Table 2-2 gives an overview of the used jetty headings and the corresponding wave incidence headings.
In situ, the jetty will be placed behind a breakwater. However, this breakwater will still be under construction during the first two years of operations. The wave incidence angles to be tested were specified by the client, based on uninterrupted waves without the breakwater and the diffracted waves behind the breakwater for the permanent phase.

Table 2-2: Jetty headings and corresponding wave incidence angles

Jetty heading	Wave heading	Wave incidence heading (ship fixed)
80°	180°	100°
80°	270°	190°
225°	180°	315°
225°	270°	45°
260°	180°	280°
260°	270°	10°

All fender and fairlead positions on the jetty were specified by the client. The specified coordinate system is defined by client in file Tec_Coordinates.pdf, by Tecnoconsult. All positions are translated into coordinates on a different ship fixed coordinate system or a earth fixed coordinate system for either locations on the jetty or on the FSRU/LNGC.
Because the stock models used by MARIN are not exactly the same geometry as the specified vessels by the client, the positions of the fairleads and SBS fenders in x-direction, were scaled with the ratio of LPP's of the stock model M10446 and the BW Singapore. This has also been done for the specified LNGC geometry and the stock model M10447.

Fenders and mooring lines were pretensioned before the tests. The procedure for this pretensioning is described in section 5.3.5. The specified pretensions of all mooring lines and fenders, does not exactly lead to the specified exact location of the vessel due to small round off errors. To increase the accuracy of the model tests, the exact equilibrium state was determined. In a numerical model made by MARIN, the specified equilibrium state was used as input. Then, after "releasing" the location of the vessel from its fixed position, the vessel will move to its new equilibrium position. The new resulting pretensions and locations from this numerical model are presented in TABLE 34 and TABLE 36. By using these equilibrium positions as reference for the scale model values, the accuracy of the model tests is increased.

2.5.2 Jetty fenders

The 6 fenders on the jetty consist of 2 rubber Trelleborg fenders placed in parallel above each other on a boulder, mounted on a breasting dolphin. An isometric view of one of the fenders is presented in Figure 2-2. The specified locations for all fenders are transformed into earth fixed coordinates as presented in TABLE 15. The jetty has 6 of these equally composed fenders. The fender stiffness to be taken into account for the model tests is the dolphin stiffness combined in series with the two Trelleborg fenders in parallel. The specified stiffnesses for the dolphins, fenders and combined stiffnesses are presented in TABLE 16. These combined stiffnesses are modelled as the stiffness as presented in TABLE 17 and FIGURE 12.

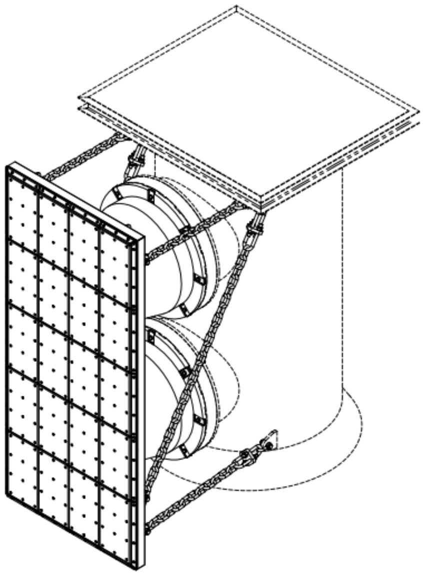

Figure 2-2: isometric view of jetty fenders

The fenders are modelled by electronical actuators manufactured inhouse by MARIN. These actuators deliver a force depending on the position of the actuator. The actuator, which is displayed in PHOTO 23, is placed in a watertight casing attached to the jetty in an overly stiff construction.

PHOTO 23 shows the calibration procedure of the fenders. A 500kg weight was placed in a pendulum with known length. The reaction force and location was then measured for each fender while swinging the weight against the actuator. Calibration results of the fender stiffness are presented in FIGURE 13 through FIGURE 18.

2.5.3 SBS fenders

The fenders used for the SBS mooring are specified to be Yokohama fenders of 4500x9000mm with an inner pressure of 50 kPA. The specified locations of the SBS fenders are presented in TABLE 18. The locations are converted with the procedure as referred to in section 2.5.1. This leads to the as-built fender locations as presented in TABLE 19. Note that the height of the fenders is taken to be 1.75m above the waterline.
The fenders have a stiffness which is specified in TABLE 20. The stiffness is modelled by springs with a linear stiffness. Unlike the jetty fenders, the spring stiffness is modelled with a mechanical spring instead of an electronic actuator spring. The moving part of the mechanical spring fenders is built inside the hull of the LNGC model. The springs are connected to the actuating fender rods as is shown in PHOTO 22 The as-built fender stiffness is presented in TABLE 21. The specified and as-built fender deflection curves are presented in FIGURE 19.

2.5.4 Fender bearings

The jetty fenders and SBS fenders are equipped with air bearings on the ends of the fender actuator rods. These air bearings are made of a porous graphite material. By pumping air into the air bearings, a uniform layer of air is formed between the bearing and the vessel. Due to the low friction no or negligible damping for surge is introduced at the fenders. The air bearings with attached blue air hoses are shown in PHOTO 19.
Since the jetty fenders are mounted on the jetty and the SBS fenders are mounted in the LNGC, the air bearings for all fenders act on the hull of the FSRU. This can be seen in the photos section in several photographs such as PHOTO 24 and PHOTO 25.

2.5.5 Modelling mooring lines

The FSRU is moored to the jetty with 18 mooring lines. Likewise, the LNGC is moored to the FSRU and the jetty with 16 mooring lines. For the model tests, the number of mooring lines is reduced. Lines originating from the same location on the jetty are represented in the model tests by a single (bundled) line. This division is graphically represented in Figure 2-3.

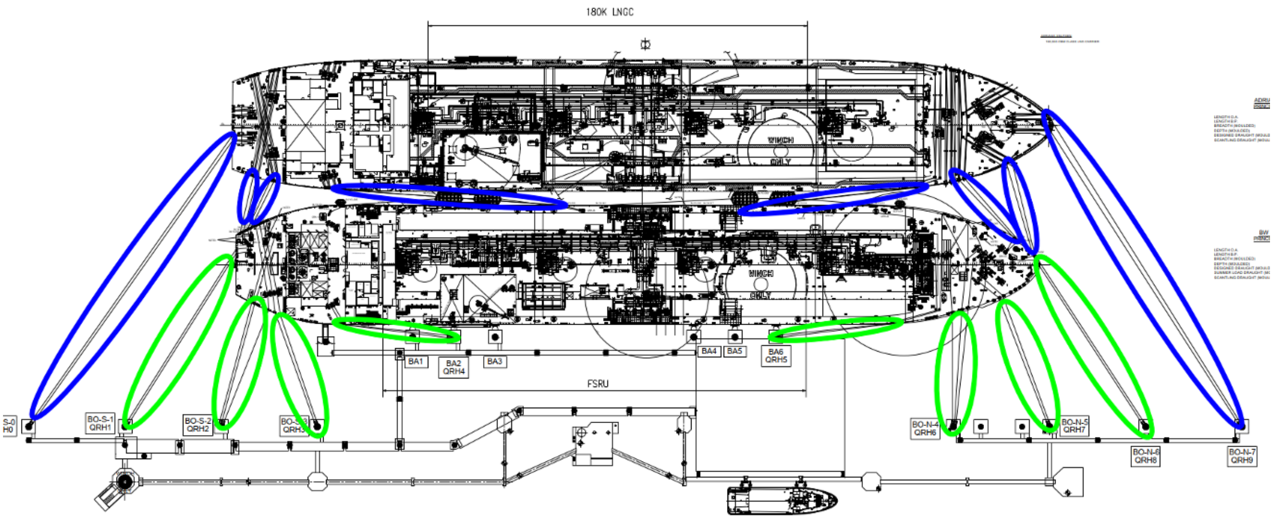

Figure 2-3: Grouped jetty lines to be bundled in modelling (Green=FSRU lines, Blue = LNGC lines)

The positions of the fairleads and jetty anchoring points for the bundled lines are determined by taking the weighted average of all represented lines. The average is weighted based on the specified pretension in the lines. This method prevents the introduction of moments in the model. These bundled positions are presented in TABLE 22 for the FSRU jetty mooring lines and in TABLE 28 for the SBS mooring lines

Since the fairlead positions from TABLE 22 are specified and derived from the geometry of the BW Singapore, they do not necessarily coincide with the outside of geometry of MARIN stock model M10446 as used for the model testing. The coordinates are therefore shifted along the bundled lines to coincide with the geometry of the stock model. For this, the models are aligned on station 10, centreline and keel. This again prevents the introduction of moments in the model. The resulting coordinates of all anchoring points are presented in TABLE 23.
Likewise, the fairlead positions from TABLE 28 are shifted to compensate for this. However, due to practical reasons, the fairlead points on the LNGC (which contain the dual spring system) cannot be placed below deck. This leads to different heights for the fairlead points of the SBS mooring lines on the LNGC. The fairlead positions are placed on the deck of the M10447 model directly above the projected fairlead point on the hull. All as-built coordinates are supplied in sections below. The resulting as-built fairlead positions for the SBS mooring lines are presented in TABLE 29.

The stiffness of all bundled lines is determined in two steps. First, the stiffness of the specified 22m nylon tail (Timm Flex 8 used rope stiffness) is combined in series with the specified stiffness of the steel wire for the remaining line length. Then, the stiffnesses of the lines to be bundled are combined as parallel line stiffnesses. The load elongation curves of these combined stiffnesses are represented in TABLE 24 and TABLE 25 for the FSRU jetty mooring lines and in TABLE 26 and TABLE 27 for the SBS mooring lines. These load-elongation curves can also be represented graphically as in FIGURE 20 and FIGURE 21. Note that for the SBS mooring, the lengths of the lines on deck were not specified and therefore not used for the mooring line stiffnesses of the model.

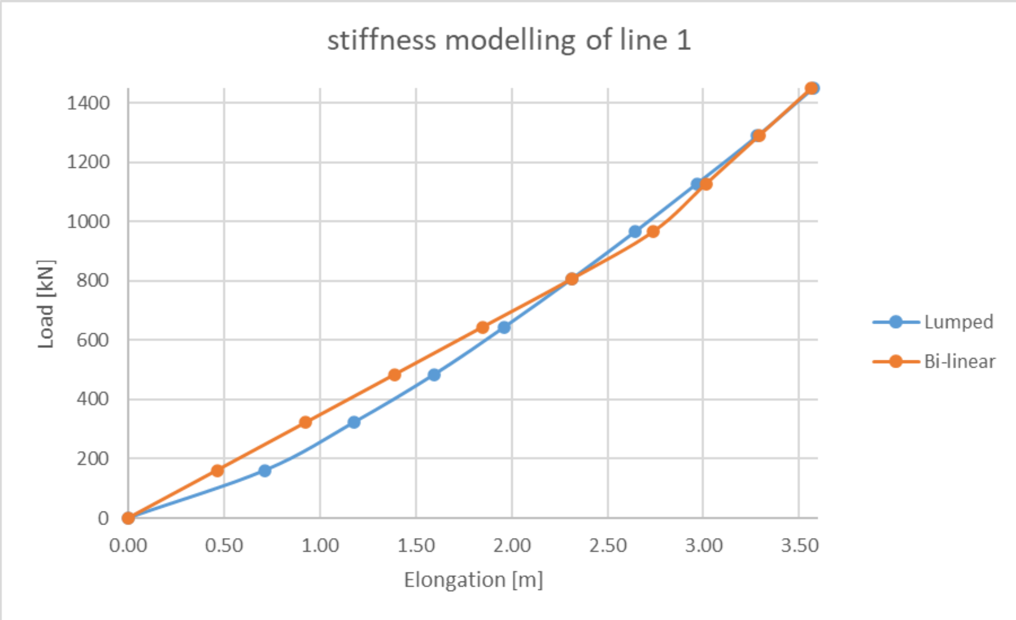

Figure 2-4: Example of bilinear stiffness modelling of bundled jetty line1

When using a linear spring to model the line stiffness, the stiffness cannot be accurately modelled for the entire elongation curve of the lines. To increase the accuracy, the elongation curves of the mooring lines as presented in Figure 2-4 are fitted with a bi-linear spring system. This spring system consists of two springs in series where the deflection of one of these springs is maximized. This results in a bi-linear stiffness curve (2 linear segments). The remaining line in the model tests is an overly stiff metal line. The stiffness of the springs is chosen such that the stiffness during model tests at the pretension load is equal to the theoretical bundled mooring line stiffness. The bi-linearized stiffnesses are given in TABLE 30 and TABLE 31 for the FSRU jetty mooring lines and TABLE 32 and TABLE 33 for the SBS mooring lines. A graphical representation of such a bi-linear fit is given in Figure 2-4. A graphical overview of all bi-linearizations of all mooring lines is given in FIGURE 22 through FIGURE 25.

3 SIMULATION OF ENVIRONMENTAL CONDITIONS

3.1 General

The environmental conditions generated in the Offshore Basin are presented in this chapter. Furthermore, the procedures to calibrate the environmental conditions are described. A general description of the wave, current and wind generation capabilities of the Offshore Basin can be found in Appendix F01 and E01.

Prior to the model tests, the waves were calibrated by measurements at the design position of the FSRU (without FSRU present in the basin). During the calibration and model tests, the waves were monitored at the reference positions.

3.1.1 Waves

The irregular seas were adjusted such that the spectral density distribution corresponds with the required theoretical energy distribution at the design position of the model in the basin. The wave spectra used throughout the tests were JONSWAP and white noise wave spectra. Also a set of regular waves was calibrated. A detailed description of different types of wave spectra formulations is given in Appendix E03. The JONSWAP spectra are formulated as follows:

$$S_\zeta(\omega) = \frac{C \cdot H_s^2 \cdot \omega_p^4}{\omega^5} \cdot \exp\left(-1.25 \cdot \frac{\omega_p^4}{\omega^4}\right) \cdot \gamma^{\exp\left(-\left(\frac{\omega-\omega_p}{\omega_p \cdot \sigma \cdot \sqrt{2}}\right)^2\right)}$$

with

$$C \cong \frac{0.597 + 0.3125 \cdot \gamma}{1.27 + 1.47 \cdot \gamma + 0.168 \cdot \gamma^2}$$

in which

$S_\zeta(\omega)$	=	spectral density at wave frequency ω, [m^2 s]
ω	=	circular wave frequency, [rad/s]
ω_p	=	peak frequency = $2\pi/T_P$, [rad/s]
T_P	=	peak period, [s]
H_s	=	significant wave height, [m]
γ	=	peak enhancement factor, 3.3

and $\sigma = \begin{bmatrix} \sigma_a \text{ for } \omega \le \omega_p \\ \sigma_b \text{ for } \omega > \omega_p \end{bmatrix}$ or $\sigma = \begin{bmatrix} \sigma_a \text{ for } T \ge T_P \\ \sigma_b \text{ for } T < T_P \end{bmatrix}$

The dimensionless shape parameters σ_a and σ_b were taken as:

σ_a	=	0.07
σ_b	=	0.09

The significant wave height is defined as: $H_S = 4 \cdot \sqrt{\int_0^\infty S_\varsigma(\omega)d\omega} = 4 \cdot \sqrt{m_{\varsigma 0}}$

where $\sqrt{m_{\zeta 0}}$ is the area beneath the wave spectrum.

3.1.2 Wave calibration procedure

The wave calibration procedure is described in Appendix E04. Note that only the first order wave spectrum can be calibrated. The second order group wave spectrum and the maximum crest amplitudes cannot be calibrated and are a result of the applied wave seed.

3.1.3 Irregular waves

An overview of target and realized irregular waves is listed in TABLE 3 and TABLE 4.

4 MEASUREMENTS, DATA ACQUISITION AND POST PROCESSING

4.1 General

An overview of the measured signals as well as their definitions and sign conventions is given in this chapter. Furthermore, the applied instrumentation is listed and some key information of the measurement system is given. Finally, an overview of the signals that were derived from the measured signals is given. The location of the model instrumentation is presented in TABLE 5 and TABLE 6.

4.2 Data acquisition

The model tests were carried out in the MARIN Offshore Basin, see also Section 3. Part of the signals is measured using an analogue system and part of the applied measurement systems has a direct digital output.

For the data acquisition of the analogue signals the MARIN Measurement System (MMS2) was used. Before sampling an on-line anti-aliasing filter was applied. All the signals were sampled and stored at a sampling rate of 200 Hz. The sampling rate of 200 Hz results in a time interval of respectively 0.02739 seconds (prototype values) between each two subsequent samples.

The digital signals were measured with the MSES system. For the digital signals no on-line filtering and sampling is required. The digital signals included the measured displacements from the optical measurement systems and the logging of system feedback signals. The applied sampling rate for the digital signals was 100 Hz.

The irregular wave tests each had a duration of ½ + 3 + ½ hours (prototype values). This means that at a sample rate of 100 Hz 262,907 data points are available for the statistical analysis of each measured channel. The first half hour of the measurement is considered as start up time to let possible transient phenomena vanish. In total 197,180 data points are used for the data analysis. This is assumed to be sufficient to allow a reliable statistical analysis on low frequency as well as wave frequency phenomena.

4.3 Instrumentation and measured quantities

This section summarizes the instrumentation that was installed in the basin and on the model during the test campaign. The following signals were measured and recorded at a sampling frequency of 100 Hz or 200 Hz:

- *Reference wave heights*
  Resistance type wave probes.
- *Translations (X, Y, Z) and rotations (ϕ, θ, ψ) of the model*
  NDI contact-less optical position measurement system (above water). The system determines the model motions based on the recorded positions of three infrared LEDs on a position target placed on the model. Based on the measured motions of the three LEDs the NDI system calculates the 6 degrees of freedom (3 translations and 3 rotations). All motions are defined in the basin-fixed (BF) system of axes, except roll and pitch which are defined in the ship-fixed (SFT0) system of axes.
- *Accelerations on the model*
  3 dof Piezo-type accelerometers at 4 locations. This configuration allows to calculate the accelerations in 6 dof at any required position on board of the model.
- *Relative wave heights along the model*
  Resistance type wave probes.
- *Fender loads*
  Rod shaped actuators.

- *Side-by-side line tensions*
  Ring-shaped strain gauge force transducers placed in the each line at fairlead position.

TABLE 7 to TABLE 10 represent lists of measured quantities including their designation, sign conventions and measuring devices. The locations of the instruments are shown in TABLE 5 and TABLE 6 and FIGURE 3 and FIGURE 4.

4.4 Derived quantities

In TABLE 13 and TABLE 14, reviews of the signals derived from the measured signals are presented. The signals that were derived from the measured signals are as follows:

- Accelerations of the model at CoG (6DOF).
- Motions of the model at CoG (6DOF) and at other points (3DOF).
- Relative motions at the manifold position at the jetty side and at the LNGC side.

The formulas used to calculate the derived signals are described in Appendix D12. The derived signals include for example the motions and accelerations at any point of the model.

4.5 Examples of signals in irregular wave tests

The records of the signals during the tests were of one of the following types:

- The type I record consists of a fast oscillating value, of which the frequency corresponds to the frequency of the wave (WF).

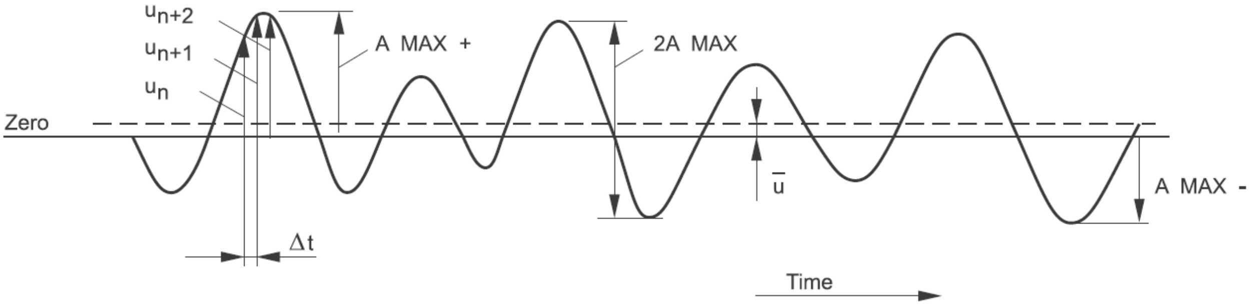

Figure 4-1: Type I signal with WF oscillations

- The type II record consists of a fast oscillating value, which is superimposed on a slowly varying value (LF).

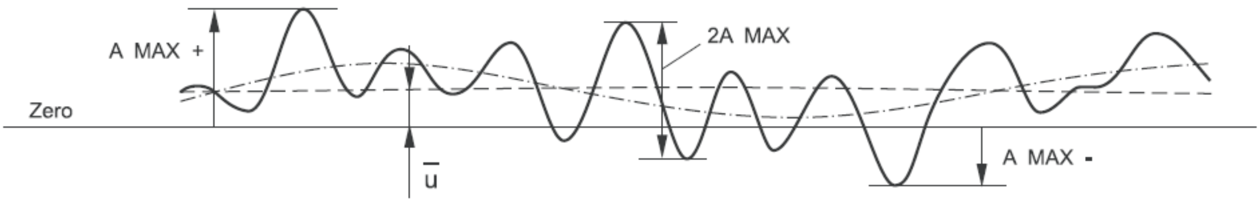

Figure 4-2: Type II signal with combined WF and LF oscillations

- The type III record consists also of an oscillating signal of which the frequency corresponds to the wave frequency, superimposed on a slowly varying signal. But in this case the fast oscillating part is small compared to the slowly varying signal.

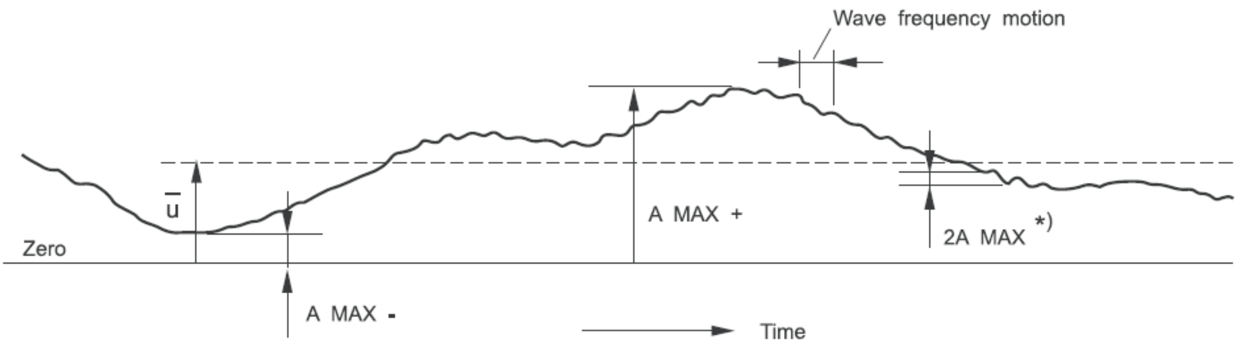

Figure 4-3: Type III signal with LF oscillations

- The type IV record is typical for slamming loads as well as green water on deck.

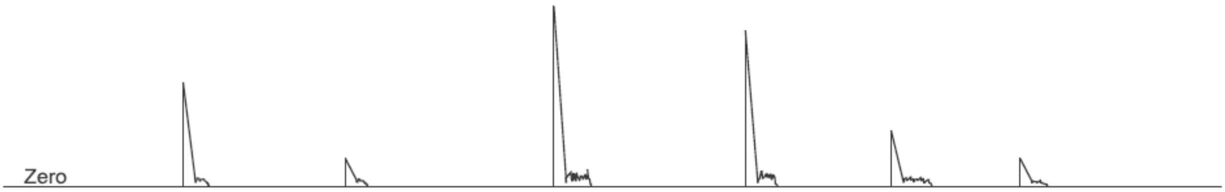

Figure 4-4: Type IV signal for impact loads

4.6 Types of data reduction

Each paragraph of this chapter discusses types of analyses that have been applied to present the model test results.

4.6.1 Statistical analysis

The two types of statistical analysis that can be done on the measured data are described in the Appendix D03 at the end of this report. They are referred to as Statistical and Extrema Statistical analysis later on in this report.

4.6.2 Signal filtering

For a selection of signals a Low Frequency (LF) and Wave Frequency (WF) filtering, including a statistical analysis was carried out. The boundary of all filter settings are documented in Table 4-1. The Nyquist frequency ω_{NY} is about 114.7 rad/s.

Table 4-1: Filter settings in [rad/s]

Tests	UF	LF	WF
Tests in Waves	0.0 – ω_{NY}	0.0 – 0.40	0.40 – 3.0

The scope of this report is to determine the RAO's of the FSRU and LNGC (response) for the wave frequent domain. A typical frequency domain response signal for the FSRU would look like the response in Figure 4-5 in which the wave frequent response is dominated by 1st order forces.

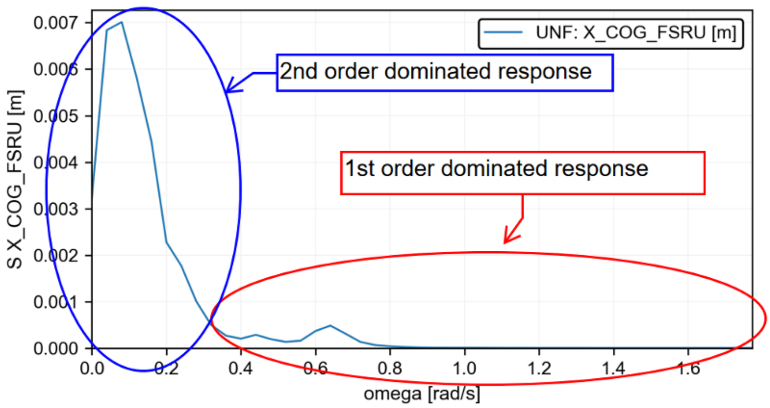

Figure 4-5: Total frequency domain response for measurement 35225_02OB_04_015_001_01

4.6.3 Decay Analysis

The decay tests are analysed in order to determine the natural periods and damping coefficients. The method used to analyse the damping coefficients based on a decay test are described in Appendix D01.

4.6.4 Weibull fits

For the extreme values of a number of signals (e.g. roll motion) a 3-parameter Weibull fit was made through 10, 25 and 50% of the highest peak or through values. The percentage of peaks to be used for the Weibull fit was selected by MARIN. This fitted line was used to determine the most probable maximum (MPM) values of the signals. A description of this methodology is given in Appendix D05.

4.6.5 Response Spectra

The motion response spectrum was determined for all irregular wave tests. A mathematical description of irregular phenomena is given in Appendix D02.

4.6.6 Response Amplitude Operator (RAO)

The motion RAO was determined for all wave tests. The lead signal is the calibrated wave. The theoretical background of the RAO is described in Appendix D06.

4.6.7 Fast Fourier transform (FFT)

Several analysis needs an FFT, like the response spectra or the filtered extrema statistical analysis. The FFT is always applied on resampled data to avoid issues due to non equidistant data.

4.6.8 Harmonic analysis

For the regular wave tests the signal is decomposed into a primary component and its higher harmonics (amplitude and phase). The theory behind this harmonic analysis is documented in Appendix D09.

4.7 Data analysis and deliverables for each type of test

4.7.1 Regular wave calibration

Channels:

- Wave probe at the centreline of the basin (position of the FSRU)

Deliverables

- Harmonic Analysis of the measured regular wave
- Time traces – plotted and in H5M format

Channels:

- Other wave probes

Deliverables

- Time traces – in H5M format

4.7.2 Irregular wave calibration

Channels:

- Wave probe at the centreline of the basin (position of the FSRU)

Deliverables

- (Extrema) statistics of measured wave elevation
- Comparison measured vs. specified wave spectrum
- Comparison of measured vs. specified significant wave height H_s
- Comparison of measured vs. specified peak period T_p
- Comparison of wave crest probability distribution to the Rayleigh and Forristall distributions (plot)
- Comparison of measured vs. theoretical wave group spectrum
- Time traces – H5M format

Channels:

- Other wave probes

Deliverables

- Time traces – H5M format

4.7.3 Decay Tests

Channels:

- 6DOF motions at CoG

Deliverables:

- PQ analysis
- Time trace plot of measured quantity (for example, roll for a roll decay) combined with a fit based on the derived PQ values
- Time traces – plotted and in H5M format

Channels:

- Fender forces
- Side by side lines

- Time traces – H5M format

4.7.4 Model Tests in Regular Waves

Channels:

- Reference basin wave elevations
- 6DOF motions at COG and at the manifold location
- 3DOF angular accelerations at the CoG
- 3DOF accelerations at CoG
- Relative wave elevations around the hull
- Fender forces
- Side by side lines
- Relative motions at the manifold location

Deliverables:

- Time trace plots of the same time frame as the harmonical analysis
- Time traces of the measured and derived quantities – H5M format
- Harmonic analysis of all relevant signals for the same time frame as selected for the wave calibration

4.7.5 Model Tests in Irregular Waves

Channels:

- Reference basin wave elevations
- 6DOF motions at COG and at the manifold location
- 3DOF angular accelerations at the CoG
- 3DOF accelerations at CoG
- Relative wave elevations around the hull
- Fender forces
- Side by side lines
- Relative motions at the manifold location

Deliverables:

- Time trace plots of the unfiltered measured and derived quantities
- Time traces of the unfiltered measured and derived quantities – H5M format
- Time traces of a selection of filtered measured and derived quantities (LPF+WPF) – H5M format
- Table of extremes of the unfiltered measured and derived quantities – H5M format
- (Extrema) Statistical mean crossing statistical analysis of unfiltered signals (UF)
- (Extrema) Statistical mean crossing statistical analysis of filtered signals (LF+WF)
- Spectrum response plots and tables for relevant signals
- RAO plots and tables for relevant signals
- Weibull Analysis for relevant signals

4.8 Visualization

During the model tests and the preparations still photographs were taken. Furthermore, video recordings were made.

Still photographs

Still photographs were taken of the models in the workshop, the test set-up in the basin and during a selected number of model tests. A selection of the photographs is shown on the photo pages at the end of this report.

Video recordings

Video recordings were made to obtain a good overall impression of the behaviour of the vessels.

5 TEST REVIEW AND EXPERIMENTAL PROCEDURES

5.1 Test review

In this section, a brief overview of the model tests performed is given. A more complete overview is shown in at the end of this report.

- Decay tests [see TABLE 37 and TABLE 38]
- Jetty mooring tests in regular waves [see TABLE 39]
- SBS mooring tests in regular waves [see TABLE 40]
- Jetty mooring tests in irregular waves [see TABLE 41]
- SBS mooring tests in regular waves [see TABLE 42]

5.2 Test labelling and organisation

All tests have a unique number, see explanation below.

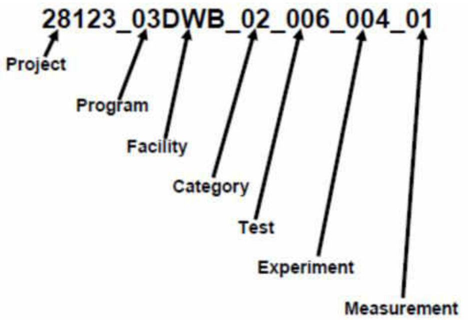

All deliverables (digital files) start with this unique number.

- Project — MARIN Project number
- Program — Test programme number in a facility
- Facility — Facility in which the tests are performed
- Category — Each combination of configurations, loading condition and/or basin fixed model heading. For this project used for the basin set-up
  - 02 Wave calibration tests
  - 03 Jetty mooring tests at model heading 80 deg
  - 04 Jetty mooring tests at model heading 225 deg
  - 05 Side by side mooring tests at model heading 225 deg
  - 06 Side by side mooring tests at model heading 260 deg
  - 07 Jetty mooring tests at model heading 260 deg
- Test — Test number, for this project mainly used to indicate the sea state. For system verification tests and decay tests usually test number 001 is used.
- Experiment — Experiment number, indicating test variations with same set-up and sea state. Note also current and wind only tests associated with wave conditions are measured within the Test number; these will be numbered by the experiment number.
- Measurement — Measurement number, for repeats of the same test. Usually 1, but consecutive in case of system errors or repeated (decay) tests.

In Volume II there are two levels of folder: first layer for the Category and second for the Test. Within the Category\Test folder all files associated with each measurement are located.

5.3 Experimental procedures

The test procedures applied in the different types of model tests performed in this project phase are described in this section.

5.3.1 Weight distribution procedure

Prior to any test in the basin, the weight distribution of the model is calibrated. The experimental procedure followed to prepare the weight distribution of the model is described in Appendix M05. The calibrated weight distributions are shown in TABLE 1 and TABLE 2.

5.3.2 Zero adjustment

All results presented in this report are given with respect to the 'zero values' taken after each setup change and at the beginning of every new day. In its zero-position, the floater is at the specified draft and at even keel. The zero values in each test represent the actual values of the respective quantities for the model in this starting position.

5.3.3 Wave calibration

Both regular and irregular waves were calibrated in the basin prior to the start of the model tests. The experimental procedure followed to calibrate waves is described in Appendix E04.

5.3.4 Inclination tests

Prior to any test in the basin and after calibration of the weight distribution on the Resonic table, inclination tests are conducted to verify the correctness of the roll stiffness. For the inclination tests, one weight located at midship is shifted in the transverse direction, and the resulting inclination roll angle is measured. Based on the shifting distance, shifted mass and displacement of the floater, the GM value is calculated.

5.3.5 Jetty mooring and side by side pretensioning

Prior to performing the mooring tests, the mooring lines and fenders are pretensioned. Furthermore, the measured equilibrium position is measured. This is done for every setup per jetty heading.

The following procedure was followed to set up the pretensions of the jetty mooring arrangement:

- The FSRU is connected to the jetty using wooden blocks and cables to lock the FSRU in the correct position relative to the jetty. This is the equilibrium position obtained from numerical calculations.
- The pretension in the mooring lines and the fenders is adjusted to the specified values.
- The stiff separators installed between the jetty and the FSRU are removed.
- Due to small movements of the vessel, the loads between the mooring lines and fenders are redistributed. A measurement is performed to check the resulting line and fender loads.

This procedure was repeated for all headings for the jetty mooring. For SBS mooring, the following procedure was applied to bring all SBS lines and SBS fenders to the correct pretension:

- The entire procedure for pretensioning the jetty mooring lines and jetty fenders was first followed, leading to the correct pretensions for those lines and fenders. Depending on the test schedule, then either phase 2 tests were performed to the FSRU, or the procedure for SBS pretensioning was started.
- The LNGC was placed alongside the FSRU. With wooden blocks and stiff steel cables, the LNGC was connected to the FSRU in the correct equilibrium position.
- The pretension in the SBS lines and SBS fenders is applied.

- The pretension of the mooring lines from the LNGC to the jetty is applied.
- The stiff separators installed between the LNGC and the FSRU are removed.
- Due to small movements of the vessel, the loads between the mooring lines and fenders are redistributed. A measurement is performed to check the resulting line and fender loads.

The effect of the pretensioning of the SBS mooring lines and SBS fenders on the jetty mooring lines of the FSRU is not prevented. It is measured, but no pretensions of any jetty mooring lines of the phase 2 testing setup were altered after starting the SBS pretension procedure.
All measured pretensions for all mooring lines and fenders for all headings are presented in TABLE 43 and TABLE 44.

5.3.6 Decay tests

Motion decay tests are carried out by pulling or pushing the model from its equilibrium position, after which it is released. In this project, decay tests were carried out for all degrees of freedom. The resulting decaying motions are recorded for later analysis. The experimental test procedure followed to carry out the decay tests is described in Appendix P03.

5.3.7 Tests in waves

The procedure followed to execute the tests in waves is described in Appendix P04 at the end of this report. The basin setup and mooring arrangement are depicted in FIGURE 3 through FIGURE 9.

5.4 Summary of QA/QC procedures

This section presents a selection of the main Quality Assurance/ Quality Control (QA/QC) steps that were performed during the project.

5.4.1 Model and basin preparations

- The model geometry is inspected.
- Positions of relative wave probes is checked.
- The channel numbering of the relative wave probes is verified.
- Draught lines and coordinates of line connection points were checked.
- The anchor positions and numbering on the basin floor are checked.

5.4.2 In basin (after each change in Loading Condition)

- The GM is measured.
- Roll natural frequencies are compared against theory.

5.4.3 In basin (mooring system)

- Mooring pretensions are checked regularly to check whether no major shifts of the model or spring deformations have occurred.

6 RESULTS AND DISCUSSION

6.1 General observations

This Chapter summarises the main outcomes of the model tests, with specific interest in the objectives listed in Section 1.2. The following aspects are addressed:

- Quality of environmental conditions
- Assessment of the realised weight distributions of the vessels
- Static loads of the mooring system
- Pretension and equilibrium positions of the vessels
- Natural periods and damping coefficients
- Motion RAOs
- Motions in irregular waves
- Relative wave heights
- Line and fender loads

6.2 Wave calibration results

TABLE 3 and TABLE 4 present comparisons between the measured and realised (significant) wave heights and (peak) periods. The measured values are within 5% of the specified values for all irregular waves. Note that wave irregular T7 was not calibrated, but only measured afterwards because of ad-hoc additions to the test programme.

The measured spectra of all calibrated irregular waves are presented in FIGURE 26 through FIGURE 32. Note that beside the wave frequent energy, a (smaller) amount of low frequent energy ($\omega < 0.2$ rad/s) is present in the basin. This energy will not be equal to the low frequent energy present in situ.

To save time, the regular waves were only measured, but not calibrated. Therefore, the values are further off from the specified values. Due to the academic nature of the wave tests to be performed with these waves, this has no effect on the accuracy of the wave tests performed with these regular waves.

6.3 Weight distribution

The weight distribution was assessed through Resonic measurements of the model (without mooring) and through inclination tests to assess the GM_T. The main particulars and weight distribution of the models are provided in TABLE 1 (FSRU) and TABLE 2 (LNGC).

For the FSRU, a stock model was used and the draught and model radii of gyration were calibrated to fit the specified values. Therefore the calibrated displacement varies more (~6,5%) than the weight distribution parameters, which are within 2% from what was specified.

For the LNGC, also a MARIN stock model of a LNG carrier was used. The displacement was chosen to match specified displacement. The distribution values of the LNGC model are also within 2% of the specified values. The model has slightly differing length, breadth, and depth from the specified LNGC values. Consequently the draught, metacentre and CoG height differ up to 8% of the specified values

6.4 Pretensions and equilibrium positions

For every setup per heading, pretensions are applied and measured. All measured pretensions are presented in TABLE 43 and TABLE 44.

Phase 2, with only the FSRU moored to the jetty

For the mooring lines, the maximum deviation in line tension is 5.0% from the specified equilibrium value. This is an outlier: the average deviation in the mooring lines is 0.7%. The maximum deviation in fender compression is 4.8% from the specified equilibrium values. The average deviation of fender compression is 1.86%.

Phase 3, with the FSRU and LNGC moored alongside to the jetty
For the mooring lines, the maximum deviation in line tension is 7.63% from the specified equilibrium value. The average deviation in the mooring lines is 2.8%. The maximum deviation in fender compression is 9.8% from the specified equilibrium values. The average deviation of fender compression is 5.6%.

The larger deviations for pretensions in the SBS mooring, is in confirmation of the larger effort it was to apply the pretensions for the SBS mooring, compared with the jetty mooring pretensions. The two most probable reasons for this are:

- The SBS mooring system is a double spring-mass system, whereas the jetty mooring system is a single spring-mass system.
- The mechanical SBS fenders are less accurate than the more sophisticated electronical fenders used as jetty mooring fenders.

After pretensioning all lines and fenders with the vessels locked in place, the models were released and pretensions were measured again. These are also presented in TABLE 43 and TABLE 44.

6.5 Natural periods and damping values

Decay tests for free floating and moored set-ups were performed to quantify the natural periods and damping values of the moored vessels. The procedures for these decay tests are described in section 5.3.6; the analysis of the decay test results is described in Section 4.7.3 and Appendix D01. An overview of natural periods and damping values (P, Q) is provided for each set-up in TABLE 37 and TABLE 38. Comparison figures between the measurement motion decay and the decay fit are presented in Volume II

6.6 Motion RAOs

The full range of all measured motion RAOs is delivered for all tests in waves in Volume II. A selection of RAOs for the white noise and irregular wave conditions are presented in FIGURE 33 through FIGURE 36 for wave tests with a wave incidence angle of 10 degrees. The white noise, regular and irregular wave tests generally lead to similar RAOs.

Motion statistics and extreme value analyses (Weibull distributions) are also presented for all irregular wave tests in Volume II. Further, a summary of key values per test is supplied in TABLE 45 and TABLE 46.

6.7 Mooring and side-by-side line loads and fender loads

TABLE 49 and TABLE 50 present an overview of maximum line loads for irregular wave tests in jetty mooring (phase II) and SBS mooring (phase III) respectively. The labelling of the lines is shown in FIGURE 3 and FIGURE 4. Note that all below mentioned loads are for bundled lines, which have the equivalent maximum break load (MBL) of either 2 or 3 mooring lines. Maximum relative loads can therefore occur in other tests and lines than the absolute maximum line loads.

6.7.1 Jetty mooring tests (phase II)

Line loads:
The absolute maximum occurring bundled line load during jetty mooring tests was 2040 kN. The maximum relative load was 42% of the MBL of the bundled line.

Fender loads:
Jetty fenders were compressed up to 91% of their maximum load during the jetty mooring tests. This is an absolute load of 3577 kN. As can be expected, fender loads especially reach high values during the beam-on wave conditions.

Note that for these jetty mooring tests, the values of test 35225_02OB_07_023_001_01 were disregarded, since line loads after the snapped mooring line were included in the maximum line load analysis.

6.7.2 SBS mooring tests (phase II)

Line loads:
The maximum occurring bundled line load in the jetty mooring lines of the FSRU during SBS mooring tests was 1580 kN. The maximum relative load was 33% of the MBL of the bundled line. For the SBS mooring lines, the absolute maximum load was 1013 kN. The relative maximum load was 79% of the MBL of the bundled line.

Fender loads:
Jetty fenders were compressed up to 63% of their maximum load during the SBS mooring tests. This is a load of 2502 kN. SBS fenders were compressed up to 1236 kN. This load leads to a maximum compression of 22% of the fenders.

6.8 Relative wave heights

TABLE 47 and TABLE 48 summarize the maximum relative wave heights measured with the wave gauges deployed alongside the hulls of the FSRU and LNGC. The measurements were obtained using conductivity-based wire wave gauges. The highest maximum wave heights measured reach up to 6.22 m for the irregular wave tests.

6.9 Other observations

The latest test: 35225_02OB_07_023_001_01 was with a Hs=7.8s and Tp=3m wave. During this test, one mooring line aft of the FSRU snapped. Investigation showed that the line did not snap due to excessive line loads. However, it is probable that due to the more excessive pitching motion of the FSRU the line got stuck in the line guiding block and sheared off. The test was not redone, because replacing the line would be too time consuming on the last day of testing.

7 CONCLUSIONS AND RECOMMENDATIONS

Technip Energies and SNAM are working on a floating storage and regasification unit (FSRU) in the Adriatic Sea that is scheduled to be installed by the end of 2024. The existing BW Singapore is foreseen as the FSRU in this project. The FSRU is to be moored to a jetty at a water depth of approximately 15.4 m. A breakwater will be installed to provide shelter against waves from the predominant incident heading.

As part of the engineering design, hydrodynamic simulations are performed of the moored FSRU. Technip Energies awarded the Maritime Research Institute Netherlands (MARIN) the order for wave basin model tests to study the vessel motion behaviour in different sea states. The basin test results can be used for tuning and validation of numerical calculations.

The performed tests were split in three phases of which phases 2 and 3 are considered in this report:

Phase 1: Seakeeping tests performed in soft mooring
Phase 2: Station keeping tests of the FSRU in jetty mooring.
Phase 3: Side-by-Side (SBS) mooring of a LNGC alongside the FSRU in the jetty mooring.

This report concerns the performed wave basin tests with the FSRU in the jetty mooring with and without the LNGC moored alongside. These station keeping model tests were carried out in order to check the numerical model of the FSRU vessel in regular and irregular wave conditions by assessing:

- the natural periods and hydrodynamic damping of the moored FSRU and the alongside moored LNGC at the appropriate water depth;
- the statistical motions during operating conditions;
- the motion behaviour of the vessel in operational and critical irregular wave conditions;
- the extreme and statistical accelerations at given locations;
- the relative wave elevation in extreme conditions;
- the motion RAO for the jetty moored FSRU;
- the motion, velocities and accelerations at the jetty loading arm location and the relative motions between FSRU and LNGC at the SBS-loading arms;
- the mooring line tensions and fender loads.

Only wave-frequent response is considered in the scope of this report.

The delivered test results enable the client to verify the validity of the numerical calculated results by applying a “model the model” approach for wave frequent motions. Low frequent energy on site will be different than the LF energy in the model basin. Therefore, it is advisable to investigate low frequent energy in situ and model the systems response to that low frequent energy when designing the mooring system.

Based on the results presented in this report, the following conclusions and recommendations seem justified:

- Results of the decay tests for both vessels, are presented in TABLE 37 and TABLE 38. Decay tests for roll were performed both in jetty mooring and free floating condition. The natural period for roll decreases slightly when comparing the free-floating model to the jetty moored model. It shifts from 14.8s to 14.1s.

- Damping values at the eigen periods are derived from the decay tests and are presented in TABLE 37 and TABLE 38 as P and Q values for linear and quadratic damping. To convert these values to a percentage of critical damping, the method as described in Appendix D01 can be used.

- The motion RAOs for the soft-moored configuration are determined and presented in Volume II of this report. The results for irregular waves show a high repeatability. A selection of RAOs for the white noise and irregular wave conditions are presented in FIGURE 33 through FIGURE 36 for wave tests with a wave incidence angle of 10 degrees.

- The maximum occurring bundled line load during jetty mooring tests was 2040 kN. The maximum relative load was 42% of the MBL of the bundled line.

- For the SBS mooring lines, the absolute maximum load for the performed irregular wave tests was 1013 kN. The relative maximum load was 79% of the MBL of the bundled line.

- Jetty fenders were compressed up to 91% of their maximum load for all performed wave tests. This is an absolute load of 3577 kN. As can be expected, fender loads especially reach high values during the beam-on wave conditions.

- SBS fenders were compressed up to 1236 kN. This load leads to a maximum compression of 22% of the fenders.

- The highest maximum relative wave heights measured reach up to 6.22 m for the irregular wave tests.

- The results of the performed tests can be used to verify the validity of numerical calculated results by applying a “model the model” approach.

Wageningen, May 2024
MARITIME RESEARCH INSTITUTE NETHERLANDS

Ir. O.J. Waals
Manager Offshore

REFERENCES

[1] Oil Companies International Marine Forum (OCIMF); *"Prediction of Wind and Current Loads on VLCCs"*, 2nd edition, 1994.

[2] Frédérick Jaouën, Olaf Waals, Martijn de Jong, Arne van der Hout, Marios Christou. "Methodology for the design of LNG terminals in a nearshore environment". OMAE2016-54724

[3] O.Waals. "On the application of advanced wave analysis in shallow water model testing (wave splitting)". OMAE2005-79413.

TABLES

TABLE 1 MAIN PARTICULARS FSRU (M10446) – BALLAST LOADING CONDITION

Designation	Symbol	Unit	Client	MARIN	
				Theoretical	Realized
Length between perpendiculars	LPP	m	277.00		
Beam	B	m	43.40		
Deck height	H	m	28.00		
Draft fwd (st. 20)	Tf	m	9.69		
Draft mean	T	m	9.90		
Draft aft (st. 0)	Ta	m	10.11		
Mass	M	ton	94,719	88,575	88,698
Displacement mass	D	ton	94,719	88,575	88,698
Longitudinal position CoG (st10)	LCG	m	2.07	-1.35	-1.30
Transverse position CoG	TCG	m	0	0.00	0.00
Vertical position CoG	KG	m		14.98	14.86
Transverse metacentric height	GM_t [1]	m	8.49		6.37
Transverse metacentric height (Free surface corrected)	$GM_{t\ (FSC)}$	m	6.35	6.35	-
Position transverse metacentre	KM_t [2]	m		21.33	21.23
Roll radius of gyration	k_{xx}	m	15.19		15.16
Pitch radius of gyration	k_{yy}	m	71.35		72.35
Yaw radius of gyration	k_{zz}	m	72.95		72.73

(1) GM_t as realized is determined by means of heeling tests in the basin.

(2) KMt as realized is derived from the measured GMt and measured (Resonic) KG.

TABLE 2 MAIN PARTICULARS LNGC (M10447) – FULL LOADING CONDITION

Designation	Symbol	Unit	Client	MARIN		
				Theoretical	To be built	Realized
Length between perpendiculars	LPP	m	293.60	295.00		
Beam	B	m	48.00	46.00		
Deck height	H	m	26.40	30.00		
Draft fwd (st. 20)	Tf	m	11.50	12.23		
Draft mean	T	m	11.50	12.23		
Draft aft (st. 0)	Ta	m	11.50	12.23		
Mass	M	ton	125,959	125,849	125,849	125,755
Displacement mass	D	ton	125,959	125,849	125,849	125,755
Longitudinal position CoG (st10)	LCG	m	-2.48	-1.65	-1.65	-1.63
Transverse position CoG	TCG	m	0	0.00	0.00	-0.01
Vertical position CoG	KG	m	18.73	18.73	17.49	17.28
Transverse metacentric height	GM_t [1]	m	3.84	2.60	3.84	3.79
Transverse metacentric height (Free surface corrected)	$GM_{t\,(FSC)}$	m	-	-	-	-
Position transverse metacentre	KM_t [2]	m	22.57	21.33	21.33	21.07
Roll radius of gyration	k_{xx}	m	15.36		15.36	15.16
Pitch radius of gyration	k_{yy}	m	73.40		73.40	73.38
Yaw radius of gyration	k_{zz}	m	73.40		73.40	73.56

(1) GM_t as realized is determined by means of heeling tests in the basin.
(2) KMt as realized is derived from the measured GMt and measured (Resonic) KG.

TABLE 3 REVIEW OF IRREGULAR WAVES WITHOUT MODEL

MARIN Test No. 35225_02OB_02_	Environment	Time	Irregular Sea Characteristics JONSWAP Type Spectrum				Error	
			Hs Specified / Measured	Tp Specified / Measured	Dir.	γ	Hs	Tp
		[hrs]	[m]	[s]	[deg]	[-]	%	%
010_003_01	WN - 180 deg	0.5 + 3.0	1.0 / 0.99	3.0-16.0	180	-	-1.00%	-
011_003_01	WN - 270 deg		1.0 / 1.01	3.0-16.0	270		1.00%	-
012_003_01	Irregular P1		1.21 / 1.21	3.80 / 3.98	180	3.3	0.00%	4.74%
013_002_01	Irregular P2		1.16 / 1.17	5.00 / 4.99	270		0.86%	-0.20%
014_003_01	Irregular P3		0.77 / 0.79	8.00 / 7.85	270		2.60%	-1.88%
015_003_01	Irregular P4		0.96 / 0.96	9.60 / 9.52	270		0.00%	-0.83%
016_003_01	Irregular P5		1.29 / 1.26	4.40 / 4.3	180		-2.33%	-2.20%
017_002_01	Irregular T1		2.00 / 1.98	6.63 / 6.55	180		-1.00%	-1.21%
018_002_01	Irregular T2		2.00 / 2.01	6.63 / 6.55	270		0.50%	-1.21%
019_002_01	Irregular T3		1.50 / 1.51	5.91 / 5.82	180		0.67%	-1.52%
020_002_01	Irregular T4		1.50 / 1.51	5.91 / 5.82	270		0.67%	-1.52%
021_003_01	Irregular T5		1.00 / 0.99	5.02 / 5.07	180		-1.00%	1.00%
022_002_01	Irregular T6		1.00 / 0.99	5.02 / 4.99	270		-1.00%	-0.60%
023_001_01*)	Irregular T7		3.00 / 3.05	7.80 / 7.66	270		1.67%	-1.79%

*) Measured after the tests

TABLE 4 REVIEW OF REGULAR WAVES WITHOUT MODEL

MARIN Test No. 35225_02OB_02_	Environment	Start time	End time	Regular Waves 2ζa Specified / measured	T Specified / Measured	Dir	Error 2ζa	T
		[s]	[s]	[m]	[s]	[deg]	%	%
060_001_01	Regular 1	350	480	1.50 / 1.42	5.0 / 5	180	-5.33%	0.00%
061_001_01	Regular 2	260	380	1.50 / 1.44	7.5 / 7.5		-4.00%	0.00%
062_001_01	Regular 3	220	380	1.50 / 1.54	10.0 / 10.01		2.67%	0.10%
063_001_01	Regular 4	250	400	1.50 / 1.04	12.5 / 12.49		-30.67%	-0.08%
064_001_01	Regular 5	220	460	1.50 / 1.4	15.0 / 15.03		-6.50%	0.20%
065_001_01	Regular 7	320	420	1.50 / 1.56	5.0 / 5	270	4.00%	0.00%
066_001_01	Regular 8	320	440	1.50 / 1.5	7.5 / 7.5		-0.01%	0.00%
067_001_01	Regular 9	380	540	1.50 / 1.68	10.0 / 10.01		12.00%	0.10%
068_001_02	Regular 10	180	300	1.50 / 0.92	12.5 / 12.57		-38.67%	0.56%
069_001_01	Regular 11	500	750	1.50 / 1.26	15.0 / 15		-16.00%	0.00%

TABLE 5 LOCATION OF INSTRUMENTATION FSRU

Location	X [m] w.r.t. St10	Y [m] w.r.t. CL	Z [m] w.r.t. Keel
TARGET	6.00	0.00	37.02
ACC PSF	101.01	14.55	25.92
ACC PSA	-108.99	14.55	25.92
ACC SBF	101.01	-14.55	25.92
ACC SBA	-108.99	-14.55	25.92

TABLE 6 LOCATION OF INSTRUMENTATION LNGC

Location	X [m] w.r.t. St10	Y [m] w.r.t. CL	Z [m] w.r.t. Keel
TARGET	0.00	-24.06	39.06
ACC PSF	105.60	16.50	27.18
ACC PSA	-104.10	16.50	27.18
ACC SBF	105.60	-16.50	27.18
ACC SBA	-104.10	-16.50	27.18

TABLE 7 DESIGNATION, NOTATION, SIGN CONVENTION AND MEASURING DEVICE OF MEASURED QUANTITIES - FSRU

[measuring frequency 100 Hz]

Designation	Notation	Positive for	Measured by
MOTIONS OF FSRU MODEL AT TARGET POSITION			
Translations:		**Model moving:**	NDI optical measuring system
Longitudinal motion	X_TARGET_FSRU	Forward	
Transverse motion	Y_TARGET_FSRU	To portside	
Vertical motion	Z_TARGET_FSRU	Upward	
Rotations:			
Around longitudinal axis	ROLL_FSRU	Starboard down	
Around transverse axis	PITCH_FSRU	Bow down	
Around vertical axis	YAW_FSRU	Bow to portside	

TABLE 8 DESIGNATION, NOTATION, SIGN CONVENTION AND MEASURING DEVICE OF MEASURED QUANTITIES - FSRU

[measuring frequency 200 Hz]

Designation	Notation	Positive for	Measured by
WAVE ELEVATIONS AT REFERENCE POINTS			
Long crested wave probes For locations see FIGURE 10 and FIGURE 11	WAVE_CL WAVE_X1 WAVE_X2 WAVE_X3 WAVE_X4 WAVE_X5 WAVE_X6 WAVE_Y1 WAVE_Y2 WAVE_Y3	Wave crest	Resistance type waveprobes
ACCELERATIONS OF FSRU AT ACCELEROMETER POSITIONS			
Port side fore: Longitudinal acceleration Transverse acceleration Vertical acceleration **Port side aft:** Longitudinal acceleration Transverse acceleration Vertical acceleration **Starboard fore:** Longitudinal acceleration Transverse acceleration Vertical acceleration **Starboard aft:** Longitudinal acceleration Transverse acceleration Vertical acceleration	 AX_PSF_FSRU AY_PSF_FSRU AZ_PSF_FSRU AX_PSA_FSRU AY_PSA_FSRU AZ_PSA_FSRU AX_SBF_FSRU AY_SBF_FSRU AZ_SBF_FSRU AX_SBA_FSRU AY_SBA_FSRU AZ_SBA_FSRU	**Model accelerating:** Forward To portside Upward Forward To portside Upward Forward To portside Upward Forward To portside Upward	Accelerometers
RELATIVE WAVE HEIGHTS FSRU			
Relative wave probes	REL_01_FSRU to REL_06_FSRU	Wave crest	Resistance type waveprobes
JETTY MOORING LINE FORCES			
Jetty mooring lines	F_01_JET to F_08_JET	Tension	Ring shaped force transducers
JETTY FENDER FORCES			
Fenders	F_FEN_01_JET to F_FEN_06_JET	Compression	Rod shaped actuators

TABLE 9 DESIGNATION, NOTATION, SIGN CONVENTION AND MEASURING DEVICE OF MEASURED QUANTITIES – LNGC

[measuring frequency 100 Hz]

Designation	Notation	Positive for	Measured by
MOTIONS OF LNGC MODEL AT TARGET POSITION			
Translations:		**Model moving:**	NDI optical measuring system
Longitudinal motion	X_TARGET_LNGC	Forward	
Transverse motion	Y_TARGET_LNGC	To portside	
Vertical motion	Z_TARGET_LNGC	Upward	
Rotations:			
Around longitudinal axis	ROLL_LNGC	Starboard down	
Around transverse axis	PITCH_LNGC	Bow down	
Around vertical axis	YAW_LNGC	Bow to portside	

TABLE 10 DESIGNATION, NOTATION, SIGN CONVENTION AND MEASURING DEVICE OF MEASURED QUANTITIES – LNGC

[measuring frequency 200 Hz]

Designation	Notation	Positive for	Measured by
WAVE ELEVATIONS AT REFERENCE POINTS			
Long crested wave probes For locations see figure	WAVE_CL WAVE_X1 WAVE_X2 WAVE_X3 WAVE_X4 WAVE_X5 WAVE_X6 WAVE_Y1 WAVE_Y2 WAVE_Y3	Wave crest	Resistance type waveprobes
ACCELERATIONS OF LNGC AT ACCELEROMETER POSITIONS			
Port side fore: Longitudinal acceleration Transverse acceleration Vertical acceleration	 AX_PSF_LNGC AY_PSF_LNGC AZ_PSF_LNGC	**Model accelerating:** Forward To portside Upward	Accelerometers
Port side aft: Longitudinal acceleration Transverse acceleration Vertical acceleration	 AX_PSA_LNGC AY_PSA_LNGC AZ_PSA_LNGC	 Forward To portside Upward	
Starboard fore: Longitudinal acceleration Transverse acceleration Vertical acceleration	 AX_SBF_LNGC AY_SBF_LNGC AZ_SBF_LNGC	 Forward To portside Upward	
Starboard aft: Longitudinal acceleration Transverse acceleration Vertical acceleration	 AX_SBA_LNGC AY_SBA_LNGC AZ_SBA_LNGC	 Forward To portside Upward	
RELATIVE WAVE HEIGHTS LNGC			
Relative wave probes	REL_01_LNGC to REL_02_LNGC	Wave crest	Resistance type waveprobes
SBS MOORING LINE FORCES			
SBS mooring lines	F_01_SBS to F_08_SBS	Tension	Ring shaped force transducers
SBS FENDER FORCES			
Fenders	F_FEN_01_SBS to F_FEN_04_SBS	Compression	Force transducers

TABLE 11 POINTS OF INTEREST FSRU

Location	X [m] w.r.t. St10	Y [m] w.r.t. Cl	Z [m] w.r.t. Keel
COG	-1.35	0.00	14.98
MAN_JETTY	31.74	-18.20	31.50
MAN_FSRU	2.17	18.60	31.50

TABLE 12 POINTS OF INTEREST LNGC

Location	X [m] w.r.t. St10	Y [m] w.r.t. Cl	Z [m] w.r.t. Keel
COG	-1.35	0.00	14.98
MAN_LNGC	-0.88	-19.65	31.50

TABLE 13 DESIGNATION, NOTATION AND SIGN CONVENTION OF DERIVED SIGNALS - FSRU

Designation	Notation	Positive for
TRANSLATIONS OF FSRU		
At centre of gravity:		**Model moving:**
Longitudinal motion	X_COG_FSRU	Forward
Transverse motion	Y_COG_FSRU	To portside
Vertical motion	Z_COG_FSRU	Upward
For other POI's see table 11		
LINEAR ACCELERATIONS OF FSRU		
At centre of gravity:		**Model accelerating:**
Longitudinal acceleration	AX_COG_FSRU	Forward
Transverse acceleration	AY_COG_FSRU	To portside
Vertical acceleration	AZ_COG_FSRU	Upward
ROTATIONAL ACCELERATIONS OF FSRU		
Around longitudinal axis	A_ROLL_FSRU	Starboard down
Around transverse axis	A_PITCH_FSRU	Bow down
Around vertical axis	A_YAW_FSRU	Bow to portside
RELATIVE MOTIONS AT THE JETTY MANIFOLD POSITION		
Longitudinal relative motion	REL_MAN_X_FSRU_JETTY	FSRU forward wrt jetty
Transverse relative motion	REL_MAN_Y_FSRU_JETTY	FSRU to port side wrt jetty
Vertical relative motion	REL_MAN_Z_FSRU_JETTY	FSRU upward wrt jetty

TABLE 14 DESIGNATION, NOTATION AND SIGN CONVENTION OF DERIVED SIGNALS - LNGC

Designation	Notation	Positive for
TRANSLATIONS OF LNGC		
At centre of gravity:		**Model moving:**
Longitudinal motion	X_COG_LNGC	Forward
Transverse motion	Y_COG_LNGC	To portside
Vertical motion	Z_COG_LNGC	Upward
For other POI's see table 12		
LINEAR ACCELERATIONS OF LNGC		
At centre of gravity:		**Model accelerating:**
Longitudinal acceleration	AX_COG_LNGC	Forward
Transverse acceleration	AY_COG_LNGC	To portside
Vertical acceleration	AZ_COG_LNGC	Upward
ROTATIONAL ACCELERATIONS OF LNGC		
Around longitudinal axis	A_ROLL_LNGC	Starboard down
Around transverse axis	A_PITCH_LNGC	Bow down
Around vertical axis	A_YAW_LNGC	Bow to portside
RELATIVE MOTIONS AT THE LNGC MANIFOLD POSITION		
Longitudinal relative motion	REL_MAN_X_FSRU_LNGC	LNGC forward wrt FSRU
Transverse relative motion	REL_MAN_Y_FSRU_LNGC	LNGC to port side wrt FSRU
Vertical relative motion	REL_MAN_Z_FSRU_LNGC	LNGC upward wrt FSRU

TABLE 15 SPECIFIED JETTY FENDER POSITIONS

Line [#]	x-coordinate [m]	y-coordinate [m]	z-coordinate [m]
Earth-Fixed-Coordinate System[1]			
1	-80.19	-24.07	4.70
2	-65.19	-24.07	4.70
3	-50.19	-24.07	4.70
4	22.15	-24.07	4.70
5	37.17	-24.07	4.70
6	52.17	-24.07	4.70

[1] The earth-fixed coordinate system is with respect to the waterline for the z-coordinate. Station 10 of the FSRU is used as the origin of the x-axis for the earth-fixed coordinate system and the centre line of the FSRU is used as the origin of the y-axis for the earth-fixed coordinate system.

TABLE 16 SPECIFIED LOAD-DEFLECTION CURVES FENDERS AND DOLPHINS

Combined fenders (2x)		Dolphin	
Applied Load [kN]	Deflection [m]	Applied Load [kN]	Deflection [m]
0	0.00	0	0.00
1338	0.08	318	0.05
2194	0.16	635	0.10
2890	0.24	941	0.15
3431	0.32	1248	0.20
3802	0.40	1543	0.25
3945	0.48	1849	0.30
3883	0.56	2110	0.35
3720	0.64	2371	0.40
3509	0.72	2586	0.45
3254	0.80	2802	0.50
3036	0.88	3006	0.55
2970	0.96	3187	0.60
3118	1.04	3357	0.65
3500	1.12	3516	0.70
3842	1.152	3709	0.75
		3913	0.80
		4242	0.85
		5000	0.90

Combined fender and dolphin	
Applied Load [kN]	Deflection [m]
0	0.000
1338	0.292
2194	0.529
2890	0.758
3431	0.993
3802	1.181
3945	1.287
3883	1.356
3720	1.403
3509	1.420
3036	1.434
2970	1.497
3118	1.616
3500	1.817
3842	1.941

TABLE 17 AS-BUILT LOAD-DEFLECTION CURVES JETTY FENDERS

All Jetty fenders	
Applied Load [kN]	Deflection [m]
0	0.00
1338	0.30
2194	0.53
2890	0.76
3431	0.99
3802	1.17
3945	1.28
3883	1.35
3720	1.39
3509	1.42
2970	1.50
3118	1.62
3500	1.81
3842	1.93

TABLE 18 SPECIFIED SBS FENDER POSITIONS

Line [#]	x-coordinate [m] (ST10)	y-coordinate [m] (CL)	z-coordinate [m] (BL)
FSRU-Fixed-Coordinate System			
1	52.58	24.2	13.93
2	38.78	24.2	13.93
3	-53.63	24.2	13.93
4	-67.44	24.2	13.93

TABLE 19 AS-BUILT SBS FENDER POSITIONS

Fender [#]	x-coordinate [m] (ST10)	y-coordinate [m] (CL)	z-coordinate [m] (BL)
LNGC-Fixed-Coordinate System			
1	45.94	-26.5	13.984
2	31.94	-26.5	13.984
3	-61.8	-26.5	13.984
4	-75.81	-26.5	13.984

Note: because of a shift of the LNGC forward, center of SBS fenders can be discplaced 1,95m forward.

TABLE 20 SPECIFIED LOAD-DEFLECTION CURVES SBS FENDERS

Fender 1		Fender 2	
Applied Load [kN]	Deflection [m]	Applied Load [kN]	Deflection [m]
0	0	0	0
182.2	0.338	182.2	0.338
462.6	0.715	462.6	0.715
1000.0	1.166	1000.0	1.166
1572.4	1.502	1572.4	1.502
2588.8	1.917	2588.8	1.917
3628.5	2.241	3628.5	2.241
4457.9	2.449	4457.9	2.449
5544.4	2.669	5544.4	2.669
Fender 3		**Fender 4**	
Applied Load [kN]	Deflection [m]	Applied Load [kN]	Deflection [m]
0	0	0	0
182.2	0.338	182.2	0.338
462.6	0.715	462.6	0.715
1000.0	1.166	1000.0	1.166
1572.4	1.502	1572.4	1.502
2588.8	1.917	2588.8	1.917
3628.5	2.241	3628.5	2.241
4457.9	2.449	4457.9	2.449
5544.4	2.669	5544.4	2.669

TABLE 21 AS-BUILT LOAD-DEFLECTION CURVES SBS FENDERS

Fender 1		Fender 2	
Applied Load [kN]	Deflection [m]	Applied Load [kN]	Deflection [m]
0	0	0	0
543	0.35	543	0.33
1086	0.69	1086	0.69
1629	1.03	1629	1.03
2172	1.38	2172	1.37
2715	1.72	2715	1.72
3258	2.08	3258	2.08
3801	2.44	3801	2.44
4344	2.78	4344	2.80
4887	3.13	4887	3.15
Fender 3		**Fender 4**	
Applied Load [kN]	Deflection [m]	Applied Load [kN]	Deflection [m]
0	0	0	0
543	0.34	543	0.33
1086	0.68	1086	0.69
1629	1.02	1629	1.03
2172	1.36	2172	1.37
2715	1.72	2715	1.72
3258	2.08	3258	2.08
3801	2.46	3801	2.44
4344	2.82	4344	2.80
4887	3.17	4887	3.15

TABLE 22 BUNDLED JETTY LINE POSITIONS FSRU

Line [#]	x-coordinate [m] (ST10)	y-coordinate [m] (CL)	z-coordinate [m] (BL)
FSRU, in the ship-fixed coordinate system			
1	-143.527	5.271	20.575
2	-135.033	-14.950	20.575
3	-129.085	-17.426	20.575
4	-105.584	-21.351	26.600
5	92.886	-21.053	26.600
6	116.406	-16.393	26.600
7	130.594	-11.061	26.600
8	143.977	-1.260	26.600
JETTY, in the Earth-Fixed-Coordinate system			
1	-189.733	-57.466	7.50
2	-156.404	-58.448	7.50
3	-124.617	-58.177	7.50
4	-67.193	-25.462	8.65
5	50.302	-25.447	8.65
6	114.576	-58.251	8.65
7	149.545	-57.973	8.65
8	184.509	-57.973	8.65

TABLE 23 AS-BUILT BUNDLED JETTY LINE POSITIONS

Line [#]	x-coordinate [m] (ST10)	y-coordinate [m] (CL)	z-coordinate [m] (BL)
FSRU, in the ship-fixed coordinate system			
1	-143.500	5.310	20.560
2	-135.310	-15.510	20.520
3	-129.050	-17.790	20.530
4	-102.520	-21.680	25.950
5	92.880	-21.050	26.590
6	116.400	-16.370	26.590
7	130.630	-11.170	26.570
8	144.540	-2.050	26.480
JETTY, in the Earth-Fixed-Coordinate system			
1	-189.698	-57.490	7.50
2	-156.404	-58.448	7.50
3	-124.606	-58.175	7.50
4	-67.193	-25.458	8.65
5	50.305	-25.457	8.65
6	114.549	-58.251	8.65
7	149.549	-57.973	8.65
8	184.548	-57.973	8.65

TABLE 24 THEORETICAL LINE-ELONGATION CURVES OF BUNDLED JETTY LINES (I/II)

Line 1		Line 2	
Applied Load [kN]	Elongation [m]	Applied Load [kN]	Elongation [m]
0.00	0.000	0.00	0.000
160.98	0.714	241.47	0.679
321.96	1.176	482.95	1.105
482.95	1.593	724.42	1.487
643.93	1.962	965.89	1.821
804.91	2.312	1207.37	2.135
965.89	2.645	1448.84	2.433
1126.87	2.966	1690.31	2.719
1287.86	3.282	1931.79	3.000
1448.84	3.574	2173.26	3.256
1609.82	3.873	2414.73	3.520
1770.80	4.158	2656.20	3.770
1931.79	4.439	2897.68	4.015
2092.77	4.716	3139.15	4.257
2253.75	4.982	3380.62	4.487
2414.73	5.254	3622.10	4.724
2575.71	5.508	3863.57	4.943
2736.70	5.763	4105.04	5.163
2897.68	6.015	4346.52	5.380
3058.66	6.266	4587.99	5.595
3219.64	6.516	4829.46	5.810
Line 3		**Line 4**	
Applied Load [kN]	Elongation [m]	Applied Load [kN]	Elongation [m]
0.00	0.000	0.00	0.000
160.98	0.678	160.98	0.673
321.96	1.102	321.96	1.092
482.95	1.483	482.95	1.468
643.93	1.815	643.93	1.796
804.91	2.128	804.91	2.103
965.89	2.425	965.89	2.395
1126.87	2.709	1126.87	2.674
1287.86	2.988	1287.86	2.949
1448.84	3.243	1448.84	3.199
1609.82	3.505	1609.82	3.456
1770.80	3.754	1770.80	3.700
1931.79	3.998	1931.79	3.939
2092.77	4.238	2092.77	4.174
2253.75	4.467	2253.75	4.398
2414.73	4.703	2414.73	4.628
2575.71	4.920	2575.71	4.841
2736.70	5.138	2736.70	5.054
2897.68	5.354	2897.68	5.265
3058.66	5.567	3058.66	5.473
3219.64	5.781	3219.64	5.682

TABLE 25 THEORETICAL LINE-ELONGATION CURVES OF BUNDLED JETTY LINES (II/II)

Line 5		Line 6	
Applied Load [kN]	Elongation [m]	Applied Load [kN]	Elongation [m]
0.00	0.000	0.00	0.000
160.98	0.674	241.47	0.675
321.96	1.094	482.95	1.097
482.95	1.471	724.42	1.474
643.93	1.799	965.89	1.804
804.91	2.107	1207.37	2.113
965.89	2.400	1448.84	2.407
1126.87	2.680	1690.31	2.688
1287.86	2.955	1931.79	2.965
1448.84	3.206	2173.26	3.217
1609.82	3.464	2414.73	3.476
1770.80	3.708	2656.20	3.722
1931.79	3.949	2897.68	3.963
2092.77	4.184	3139.15	4.200
2253.75	4.409	3380.62	4.426
2414.73	4.640	3622.10	4.659
2575.71	4.854	3863.57	4.874
2736.70	5.068	4105.04	5.089
2897.68	5.279	4346.52	5.301
3058.66	5.489	4587.99	5.512
3219.64	5.698	4829.46	5.723
Line 7		**Line 8**	
Applied Load [kN]	Elongation [m]	Applied Load [kN]	Elongation [m]
0.00	0.000	0.00	0.000
160.98	0.686	160.98	0.703
321.96	1.118	321.96	1.152
482.95	1.507	482.95	1.558
643.93	1.848	643.93	1.915
804.91	2.168	804.91	2.252
965.89	2.473	965.89	2.574
1126.87	2.765	1126.87	2.883
1287.86	3.053	1287.86	3.187
1448.84	3.316	1448.84	3.467
1609.82	3.586	1609.82	3.754
1770.80	3.843	1770.80	4.027
1931.79	4.095	1931.79	4.296
2092.77	4.343	2092.77	4.561
2253.75	4.580	2253.75	4.815
2414.73	4.823	2414.73	5.075
2575.71	5.049	2575.71	5.318
2736.70	5.275	2736.70	5.561
2897.68	5.499	2897.68	5.801
3058.66	5.720	3058.66	6.040
3219.64	5.942	3219.64	6.278

TABLE 26 AS-BUILT LINE-ELONGATION CURVES OF THE BUNDLED JETTY LINES (I/II)

Line 1		Line 2	
Applied Load [kN]	Elongation [m]	Applied Load [kN]	Elongation [m]
0.00	0.000	0.00	0.000
160.98	0.462	241.47	0.435
321.96	0.925	482.95	0.870
482.95	1.387	724.42	1.304
643.93	1.850	965.89	1.739
804.91	2.312	1207.37	2.174
965.89	2.740	1448.84	2.528
1126.87	3.015	1690.31	2.768
1287.86	3.290	1931.79	3.007
1448.84	3.565	2173.26	3.247
1609.82	3.839	2414.73	3.486
1770.80	4.114	2656.20	3.726
1931.79	4.389	2897.68	3.965
2092.77	4.664	3139.15	4.205
2253.75	4.939	3380.62	4.444
2414.73	5.213	3622.10	4.684
2575.71	5.488	3863.57	4.923
2736.70	5.763	4105.04	5.163
2897.68	6.038	4346.52	5.402
3058.66	6.313	4587.99	5.642
3219.64	6.588	4829.46	5.881
Line 3		**Line 4**	
Applied Load [kN]	Elongation [m]	Applied Load [kN]	Elongation [m]
0.00	0.000	0.00	0.000
160.98	0.452	160.98	0.427
321.96	0.904	321.96	0.854
482.95	1.357	482.95	1.282
643.93	1.809	643.93	1.709
804.91	2.246	804.91	2.136
965.89	2.488	965.89	2.490
1126.87	2.729	1126.87	2.723
1287.86	2.971	1287.86	2.956
1448.84	3.212	1448.84	3.189
1609.82	3.454	1609.82	3.422
1770.80	3.695	1770.80	3.656
1931.79	3.937	1931.79	3.889
2092.77	4.178	2092.77	4.122
2253.75	4.420	2253.75	4.355
2414.73	4.661	2414.73	4.588
2575.71	4.903	2575.71	4.821
2736.70	5.144	2736.70	5.054
2897.68	5.386	2897.68	5.287
3058.66	5.627	3058.66	5.521
3219.64	5.869	3219.64	5.754

TABLE 27 AS-BUILT LINE-ELONGATION CURVES OF THE BUNDLED JETTY LINES (II/II)

Line 5		Line 6	
Applied Load [kN]	Elongation [m]	Applied Load [kN]	Elongation [m]
0.00	0.000	0.00	0.000
160.98	0.529	241.47	0.437
321.96	1.057	482.95	0.875
482.95	1.586	724.42	1.312
643.93	1.947	965.89	1.750
804.91	2.189	1207.37	2.187
965.89	2.430	1448.84	2.502
1126.87	2.671	1690.31	2.737
1287.86	2.912	1931.79	2.972
1448.84	3.153	2173.26	3.208
1609.82	3.394	2414.73	3.443
1770.80	3.635	2656.20	3.678
1931.79	3.876	2897.68	3.913
2092.77	4.117	3139.15	4.148
2253.75	4.358	3380.62	4.383
2414.73	4.599	3622.10	4.619
2575.71	4.840	3863.57	4.854
2736.70	5.081	4105.04	5.089
2897.68	5.322	4346.52	5.324
3058.66	5.563	4587.99	5.559
3219.64	5.804	4829.46	5.794
Line 7		**Line 8**	
Applied Load [kN]	Elongation [m]	Applied Load [kN]	Elongation [m]
0.00	0.000	0.00	0.000
160.98	0.469	160.98	0.510
321.96	0.938	321.96	1.020
482.95	1.406	482.95	1.530
643.93	1.875	643.93	2.041
804.91	2.287	804.91	2.371
965.89	2.536	965.89	2.637
1126.87	2.786	1126.87	2.903
1287.86	3.035	1287.86	3.170
1448.84	3.285	1448.84	3.436
1609.82	3.534	1609.82	3.702
1770.80	3.784	1770.80	3.969
1931.79	4.033	1931.79	4.235
2092.77	4.283	2092.77	4.501
2253.75	4.532	2253.75	4.768
2414.73	4.782	2414.73	5.034
2575.71	5.031	2575.71	5.300
2736.70	5.281	2736.70	5.567
2897.68	5.530	2897.68	5.833
3058.66	5.780	3058.66	6.099
3219.64	6.030	3219.64	6.365

TABLE 28 SPECIFIED BUNDLED SBS LINE POSITIONS

Line [#]	x-coordinate [m] (ST10)	y-coordinate [m] (CL)	z-coordinate [m] (BL)
FSRU, in the FSRU coordinate system			
1	219.600	-58.600	25.700
2	142.349	3.844	26.600
3	136.239	9.046	26.600
4	43.911	21.700	26.600
5	-26.764	21.700	26.600
6	-139.339	13.200	20.600
7	-141.899	11.751	20.600
8	-221.900	-58.600	24.500
LNGC, in the LNGC coordinate system			
1	148.063	0.233	26.400
2	133.093	-12.601	26.400
3	115.654	-18.835	26.400
4	96.784	-21.664	26.400
5	-114.490	-21.951	26.400
6	-136.353	-19.267	21.500
7	-142.583	-17.829	21.500
8	-150.978	-4.267	21.500

TABLE 29 AS BUILT BUNDLED SBS LINE POSITIONS

Line [#]	x-coordinate [m] (ST10)	y-coordinate [m] (CL)	z-coordinate [m] (BL)
FSRU, in the FSRU coordinate system			
1	219.60	-58.186	18.6
2	142.31	3.98	26.600
3	137.60	7.45	26.600
4	47.11	21.700	26.600
5	-26.77	21.700	26.600
6	-139.20	13.83	20.560
7	-141.89	12.55	20.560
8	-221.90	-58.186	17.45
LNGC, in the LNGC coordinate system			
1	142.02	-5.93	31.95
2	133.74	-15.35	31.95
3	116.29	-19.59	30.45
4	96.83	-22.26	30.45
5	-101.59	-23.00	30.45
6	-136.33	-19.18	25.44
7	-142.56	-17.00	25.44
8	-152.84	-6.95	25.44

TABLE 30 THEORETICAL LINE-ELONGATION CURVES OF THE BUNDLED SBS LINES (I/II)

Line 1		Line 2	
Applied Load [kN]	Elongation [m]	Applied Load [kN]	Elongation [m]
0.00	0.000	0.00	0.000
160.98	0.477	160.98	0.361
321.96	0.841	321.96	0.598
482.95	1.199	482.95	0.817
643.93	1.520	643.93	1.009
804.91	1.832	804.91	1.191
965.89	2.142	965.89	1.366
1126.87	2.404	1126.87	1.527
1287.86	2.652	1287.86	1.683
Line 3		**Line 4**	
Applied Load [kN]	Elongation [m]	Applied Load [kN]	Elongation [m]
0.00	0.000	0.00	0.000
160.98	0.355	160.98	0.386
321.96	0.586	321.96	0.650
482.95	0.797	482.95	0.898
643.93	0.982	643.93	1.117
804.91	1.158	804.91	1.327
965.89	1.326	965.89	1.530
1126.87	1.482	1126.87	1.713
1287.86	1.633	1287.86	1.888

TABLE 31 THEORETICAL LINE-ELONGATION CURVES OF THE BUNDLED SBS LINES (II/II)

Line 5		Line 6	
Applied Load [kN]	Elongation [m]	Applied Load [kN]	Elongation [m]
0.00	0.000	0.00	0.000
160.98	0.425	160.98	0.341
321.96	0.732	321.96	0.556
482.95	1.029	482.95	0.750
643.93	1.292	643.93	0.919
804.91	1.546	804.91	1.079
965.89	1.795	965.89	1.231
1126.87	2.012	1126.87	1.374
1287.86	2.219	1287.86	1.514
Line 7		**Line 8**	
Applied Load [kN]	Elongation [m]	Applied Load [kN]	Elongation [m]
0.00	0.000	0.00	0.000
160.98	0.344	160.98	0.474
321.96	0.562	321.96	0.834
482.95	0.760	482.95	1.188
643.93	0.932	643.93	1.506
804.91	1.095	804.91	1.814
965.89	1.250	965.89	2.119
1126.87	1.396	1126.87	2.379
1287.86	1.539	1287.86	2.624

TABLE 32 AS-BUILT LINE-ELONGATION CURVES OF THE BUNDLED SBS LINES (I/II)

Line 1		Line 2	
Applied Load [kN]	Elongation [m]	Applied Load [kN]	Elongation [m]
0.00	0.000	0.00	0.000
160.98	0.477	160.98	0.361
321.96	0.892	321.96	0.631
482.95	1.194	482.95	0.811
643.93	1.496	643.93	0.990
804.91	1.799	804.91	1.170
965.89	2.101	965.89	1.350
1126.87	2.403	1126.87	1.529
1287.86	2.705	1287.86	1.709
Line 3		**Line 4**	
Applied Load [kN]	Elongation [m]	Applied Load [kN]	Elongation [m]
0.00	0.000	0.00	0.000
160.98	0.355	160.98	0.386
321.96	0.618	321.96	0.686
482.95	0.791	482.95	0.892
643.93	0.964	643.93	1.098
804.91	1.138	804.91	1.303
965.89	1.311	965.89	1.509
1126.87	1.484	1126.87	1.714
1287.86	1.658	1287.86	1.920

TABLE 33 AS-BUILT LINE-ELONGATION CURVES OF THE BUNDLED SBS LINES (II/II)

Line 5		Line 6	
Applied Load [kN]	Elongation [m]	Applied Load [kN]	Elongation [m]
0.00	0.000	0.00	0.000
160.98	0.425	160.98	0.341
321.96	0.775	321.96	0.586
482.95	1.023	482.95	0.744
643.93	1.270	643.93	0.902
804.91	1.518	804.91	1.060
965.89	1.765	965.89	1.219
1126.87	2.013	1126.87	1.377
1287.86	2.261	1287.86	1.535
Line 7		**Line 8**	
Applied Load [kN]	Elongation [m]	Applied Load [kN]	Elongation [m]
0.00	0.000	0.00	0.000
160.98	0.344	160.98	0.474
321.96	0.592	321.96	0.884
482.95	0.754	482.95	1.183
643.93	0.915	643.93	1.482
804.91	1.076	804.91	1.780
965.89	1.238	965.89	2.079
1126.87	1.399	1126.87	2.378
1287.86	1.560	1287.86	2.677

TABLE 34 NUMERICAL CALCULATED EQUILIBRIUM STATE JETTY MOORING

Position of the FSRU in the Earth Fixed Coordinate System			
x-coordinate [m]	y-coordinate [m]	yaw-angle [deg]	z-coordinate [m]
-0.00777076	0.132836	0.00201906	-9.85386
Jetty Fender Compression			
Fender 1 [kN]	Fender 2 [kN]	Fender 3 [kN]	Fender 4 [kN]
737.403	730.890	724.377	692.856
Fender 5 [kN]	Fender 6 [kN]		
686.338	679.367		
Jetty Lines Pretensions			
Line 1 [kN]	Line 2 [kN]	Line 3 [kN]	Line 4 [kN]
773.55	1085.78	612.12	748.31
Line 5 [kN]	Line 6 [kN]	Line 7 [kN]	Line 8 [kN]
338.12	1010.30	590.65	505.34

TABLE 35 ACHIEVED PRETENSIONS JETTY MOORING 80 DEGREES HEADING

TABLE 36 NUMERICAL CALCULATED EQUILIBRIUM STATE SBS MOORING

Position of the FSRU in the Earth Fixed Coordinate System			
x-coordinate [m]	y-coordinate [m]	yaw-angle [deg]	Draft [m]
-0.0143618	0.116106	9.6793e-04	-9.99398
Position of the LNGC in the Earth Fixed Coordinate System			
x-coordinate [m]	y-coordinate [m]	yaw-angle [deg]	Draft [m]
1.10392	49.5041	0.0071735	-12.423
Jetty Fender Compression			
Fender 1 [kN]	Fender 2 [kN]	Fender 3 [kN]	Fender 4 [kN]
758.254	753.162	748.069	723.401
Fender 5 [kN]	Fender 6 [kN]		
718.307	712.757		
Jetty Lines Pretensions			
Line 1 [kN]	Line 2 [kN]	Line 3 [kN]	Line 4 [kN]
779.213	1083.59	627.206	745.248
Line 5 [kN]	Line 6 [kN]	Line 7 [kN]	Line 8 [kN]
336.219	1012.74	588.443	502.140
SBS Fender Compression			
Fender 1 [kN]	Fender 2 [kN]	Fender 3 [kN]	Fender 4 [kN]
143.427	144.454	151.330	152.357
SBS Lines Pretensions			
Line 1 [kN]	Line 2 [kN]	Line 3 [kN]	Line 4 [kN]
93.9331	123.892	87.6079	171.863
Line 5 [kN]	Line 6 [kN]	Line 7 [kN]	Line 8 [kN]
110.240	119.843	118.499	82.7392

TABLE 37 OVERVIEW OF FSRU DECAY TESTS

MARIN Test No. 35225_02OB_03_	Test condition	Quantity	Natural Period [s]	P [-]	Q [1/motion]
Free Floating					
001_003_01	Roll	ROLL_FSRU	14.84	0.107	0.032
001_004_01			14.85	0.100	0.034
Jetty Moored					
002_001_01	Surge	X_COG_FSRU	56.90	1.560	-
002_005_01	Sway	Y_COG_FSRU	-	-	-
002_002_01	Roll	ROLL_FSRU	14.06	0.259	0.001
002_003_01			14.10	0.231	0.002
002_006_01	Yaw	YAW_FSRU	22.60	1.108	0.705

TABLE 38 OVERVIEW OF LNGC DECAY TESTS

MARIN Test No. 35225_02OB_05_	Test condition	Quantity	Natural Period [s]	P [-]	Q [1/motion]
Free Floating					
002_001_01	Roll	ROLL_LNGC	20.28	0.096	0.051
002_002_01			20.28	0.097	0.049
SBS Moored					
002_003_01	Surge	X_COG_LNGC	100.40	-	-
002_004_01	Sway	Y_COG_LNGC	68.12	1.145	0.271
002_005_01	Roll	ROLL_LNGC	19.48	0.262	0.003
002_006_01			19.47	0.260	0.004
002_007_01	Yaw	YAW_LNGC	41.22	-	-

TABLE 39 OVERVIEW OF JETTY-MOORING TESTS IN REGULAR WAVES

MARIN Test No. 35225_02OB_	Test	Start Time [s]	End Time [s]	Heading [deg]	Wave Characteristics				Comment
					2ζa [m]	Period [s]	Dir. [deg]	Incidence dir. [deg]	
07_060_001_02	Regular 1	350	480	260	1.50 / 1.42	5.0 / 5	180	280	
07_061_001_02	Regular 2	260	380		1.50 / 1.44	7.5 / 7.5			
07_062_001_01	Regular 3	220	380		1.50 / 1.54	10.0 / 10.01			
07_063_001_01	Regular 4	250	400		1.50 / 1.04	12.5 / 12.49			
07_064_001_01	Regular 5	220	460		1.50 / 1.4	15.0 / 15.03			
03_060_001_01	Regular 1	350	480	80	1.50 / 1.42	5.0 / 5	180	100	
03_061_001_01	Regular 2	260	380		1.50 / 1.44	7.5 / 7.5			
03_062_001_01	Regular 3	220	380		1.50 / 1.54	10.0 / 10.01			
03_063_001_01	Regular 4	250	400		1.50 / 1.04	12.5 / 12.49			
03_064_001_01	Regular 5	220	460		1.50 / 1.4	15.0 / 15.03			

TABLE 40 OVERVIEW OF SBS-MOORING TESTS IN REGULAR WAVES

MARIN Test No. 35225_02OB_	Test	Start Time [s]	End Time [s]	Heading [deg]	Wave Characteristics				Comment
					2ζa [m]	Period [s]	Dir. [deg]	Incidence dir. [deg]	
06_061_001_01	Regular 2	260	380	260	1.50 / 1.44	7.5 / 7.5	180	280	
06_066_001_01	Regular 8	320	440		1.50 / 1.5	7.5 / 7.5	270	10	
05_061_001_01	Regular 2	260	380	225	1.50 / 1.44	7.5 / 7.5	180	315	

TABLE 41 OVERVIEW OF JETTY-MOORING TESTS IN IRREGULAR WAVES

MARIN Test No. 35225_02OB_	Test	Time [hrs]	Heading [deg]	Wave Characteristics					Comment
				Hs [m]	Tp [s]	Dir. [deg]	γ [-]	Incidence dir. [deg]	
07_010_001_01	WN - 180 deg	0.5 + 3.0	260	1.00	3.0-16.0	180	-	280	
07_011_001_01	WN - 270 deg					270		10	
07_012_001_01	Irregular P1			1.21	3.80	180	3.3	280	
07_013_001_01	Irregular P2			1.16	5.00	270		10	
07_019_001_01	Irregular T3			1.50	5.91	180		280	
07_020_001_01	Irregular T4					270		10	
07_017_001_01	Irregular T1			2.00	6.63	180		280	
07_023_001_01	Irregular T7			3.00	7.80	270		10	
04_010_001_01	WN - 180 deg		225	1.00	3.0-16.0	180	-	315	
04_011_001_01	WN - 270 deg					270		45	
04_016_001_01	Irregular P5			1.29	4.40	180	3.3	315	
04_015_001_01	Irregular P4			0.96	9.60	270		45	
04_019_001_01	Irregular T3			1.50	5.91	180		315	
04_020_001_01	Irregular T4					270		45	
03_010_001_01	WN - 180 deg		80	1.00	3.0-16.0	180	-	100	
03_011_001_01	WN - 270 deg					270		190	
03_014_001_01	Irregular P3			0.77	8.00	270	3.3	190	
03_015_001_01	Irregular P4			0.96	9.60	270		190	
03_019_001_01	Irregular T3			1.50	5.91	180		100	
03_020_001_01	Irregular T4					270		190	

TABLE 42 OVERVIEW OF SBS-MOORING TESTS IN IRREGULAR WAVES

MARIN Test No. 35225_02OB_	Test	Time [hrs]	Heading [deg]	Wave Characteristics					Comment
				Hs [m]	Tp [s]	Dir. [deg]	γ [-]	Incidence dir. [deg]	
06_010_001_01	WN - 180 deg	0.5 + 3.0	260	1.00	3.0-16.0	180	-	280	
06_011_001_01	WN - 270 deg					270		10	
06_019_001_01	Irregular T3			1.50	5.91	180	3.3	280	
06_020_001_01	Irregular T4					270		10	
05_010_001_01	WN - 180 deg		225	1.00	3.0-16.0	180	-	315	
05_019_001_02	Irregular T3			1.50	5.91	180	3.3	315	

TABLE 43 MEASURED PRETENSIONS JETTY MOORING

Line/Fender	theoretical equilibrium state		With fixed position		difference	Released	
80 degrees jetty mooring							
F_01.JET	505.3	kN	505.2	kN	-0.04%	504.2	kN
F_02.JET	590.7	kN	588.8	kN	-0.31%	576.0	kN
F_03.JET	1010.3	kN	998.6	kN	-1.16%	941.5	kN
F_04.JET	338.1	kN	321.1	kN	-5.03%	286.3	kN
F_05.JET	748.3	kN	765.5	kN	2.30%	793.2	kN
F_06.JET	612.1	kN	609.7	kN	-0.39%	589.9	kN
F_07.JET	1085.8	kN	1073.4	kN	-1.14%	1024.9	kN
F_08.JET	773.6	kN	762.9	kN	-1.38%	730.7	kN
F_FEN_01.JET	679.4	kN	669.5	kN	-1.45%	579.5	kN
F_FEN_02.JET	686.3	kN	691.8	kN	0.79%	688.8	kN
F_FEN_03.JET	692.9	kN	665.2	kN	-4.00%	709.5	kN
F_FEN_05.JET	724.4	kN	713.2	kN	-1.54%	636.2	kN
F_FEN_06.JET	730.9	kN	721.7	kN	-1.26%	732.8	kN
F_FEN_07.JET	737.4	kN	745.6	kN	1.11%	764.8	kN
225 degrees jetty mooring							
F_01.JET	505.3	kN	503.8	kN	-0.30%	513.9	kN
F_02.JET	590.7	kN	589.7	kN	-0.16%	589.0	kN
F_03.JET	1010.3	kN	1007.7	kN	-0.26%	957.4	kN
F_04.JET	338.1	kN	341.8	kN	1.08%	288.3	kN
F_05.JET	748.3	kN	752.6	kN	0.57%	808.1	kN
F_06.JET	612.1	kN	614.2	kN	0.33%	604.8	kN
F_07.JET	1085.8	kN	1088.1	kN	0.21%	1028.3	kN
F_08.JET	773.6	kN	772.7	kN	-0.11%	734.0	kN
F_FEN_01.JET	679.4	kN	672.2	kN	-1.05%	640.8	kN
F_FEN_02.JET	686.3	kN	685.9	kN	-0.06%	690.8	kN
F_FEN_03.JET	692.9	kN	704.0	kN	1.61%	731.6	kN
F_FEN_05.JET	724.4	kN	720.8	kN	-0.49%	646.7	kN
F_FEN_06.JET	730.9	kN	727.0	kN	-0.53%	658.6	kN
F_FEN_07.JET	737.4	kN	760.6	kN	3.15%	771.4	kN
260 degrees jetty mooring							
F_01.JET	505.3	kN	505.9	kN	0.11%	490.5	kN
F_02.JET	590.7	kN	589.7	kN	-0.16%	561.8	kN
F_03.JET	1010.3	kN	1010.0	kN	-0.03%	945.5	kN
F_04.JET	338.1	kN	340.4	kN	0.68%	312.8	kN
F_05.JET	748.3	kN	746.6	kN	-0.23%	750.9	kN
F_06.JET	612.1	kN	612.2	kN	0.01%	597.6	kN
F_07.JET	1085.8	kN	1088.9	kN	0.29%	1055.3	kN
F_08.JET	773.6	kN	776.6	kN	0.40%	759.0	kN
F_FEN_01.JET	679.4	kN	670.5	kN	-1.31%	601.4	kN
F_FEN_02.JET	686.3	kN	709.6	kN	3.38%	633.8	kN
F_FEN_03.JET	692.9	kN	690.2	kN	-0.39%	695.1	kN
F_FEN_05.JET	724.4	kN	759.0	kN	4.78%	737.0	kN
F_FEN_06.JET	730.9	kN	753.1	kN	3.04%	731.6	kN
F_FEN_07.JET	737.4	kN	763.9	kN	3.59%	811.3	kN

TABLE 44 MEASURED PRETENSIONS SBS MOORING

Line/Fender	theoretical equilibrium state		With fixed position		difference	Released	
225 degrees SBS mooring							
LNGC_SBS_F1	93.9	kN	94.2	kN	0.24%	86.6	kN
F_02_SB	123.9	kN	123.7	kN	-0.14%	124.1	kN
F_03_SB	87.6	kN	86.5	kN	-1.23%	105.9	kN
F_04_SB	171.9	kN	173.7	kN	1.09%	154.1	kN
F_05_SB	110.2	kN	113.2	kN	2.72%	130.4	kN
F_06_SB	119.8	kN	125.3	kN	4.56%	116.6	kN
F_07_SB	118.5	kN	124.2	kN	4.85%	118.1	kN
LNGC_SBS_F8	82.7	kN	86.1	kN	4.07%	78.5	kN
F_FEN_01.sbs	143.4	kN	154.5	kN	7.71%	150.5	kN
F_FEN_02.sbs	144.5	kN	133.8	kN	-7.37%	148.7	kN
F_FEN_03.sbs	151.3	kN	163.3	kN	7.92%	121.1	kN
F_FEN_04.sbs	152.4	kN	155.4	kN	2.00%	122.5	kN
260 degrees SBS mooring							
LNGC_SBS_F1	93.9	kN	101.1	kN	7.63%	97.6	kN
F_02_SB	123.9	kN	126.5	kN	2.10%	119.2	kN
F_03_SB	87.6	kN	88.8	kN	1.35%	92.5	kN
F_04_SB	171.9	kN	162.2	kN	-5.62%	149.3	kN
F_05_SB	110.2	kN	110.0	kN	-0.20%	118.6	kN
F_06_SB	119.8	kN	113.6	kN	-5.23%	113.0	kN
F_07_SB	118.5	kN	121.7	kN	2.69%	125.2	kN
LNGC_SBS_F8	82.7	kN	83.1	kN	0.38%	71.1	kN
F_FEN_01.sbs	143.4	kN	143.0	kN	-0.32%	155.8	kN
F_FEN_02.sbs	144.5	kN	139.2	kN	-3.66%	138.2	kN
F_FEN_03.sbs	151.3	kN	166.1	kN	9.77%	143.1	kN
F_FEN_04.sbs	152.4	kN	161.4	kN	5.91%	107.7	kN

TABLE 45 MOTIONS FSRU IN JETTY MOORING

MARIN Test No.	Hs	Tp	WaveIncHeading	X_COG_FSRU [m]				Y_COG_FSRU [m]				Z_COG_FSRU [m]				ROLL_FSRU [deg]				PITCH_FSRU [deg]				YAW_FSRU [deg]			
35225_02OB_	[m]	[s]	[deg]	Mean	StdDev	Min	Max	Mean	StdDev	Min	Max	Mean	StdDev	Min	Max	Mean	StdDev	Min	Max	Mean	StdDev	Min	Max	Mean	StdDev	Min	Max
03_010_001_01	1	3.0-16.0	100	-0.11	0.05	-0.39	0.05	0.04	0.19	-0.53	0.91	0.04	0.10	-0.32	0.39	0.48	0.37	-1.16	2.18	0.01	0.06	-0.25	0.24	0.01	0.07	-0.32	0.29
03_011_001_01	1	3.0-16.0	190	-0.09	0.03	-0.19	0.03	0.00	0.01	-0.06	0.05	0.08	0.02	0.02	0.16	0.47	0.09	0.10	0.84	0.01	0.02	-0.07	0.09	0.00	0.01	-0.04	0.04
03_014_001_01	0.77	8	190	-0.11	0.02	-0.25	0.02	0.00	0.00	-0.03	0.03	0.09	0.01	0.04	0.13	0.47	0.03	0.37	0.57	0.01	0.02	-0.06	0.08	0.00	0.01	-0.02	0.03
03_015_001_01	0.96	9.6	190	-0.10	0.05	-0.37	0.19	0.00	0.01	-0.05	0.05	0.09	0.02	-0.02	0.19	0.47	0.06	0.24	0.70	0.01	0.03	-0.12	0.17	0.00	0.01	-0.03	0.04
03_019_001_01	1.5	5.91	100	-0.13	0.04	-0.35	0.00	0.02	0.07	-0.22	0.51	0.09	0.03	-0.08	0.20	0.48	0.06	0.19	0.80	0.01	0.05	-0.18	0.22	0.01	0.07	-0.20	0.41
03_020_001_01	1.5	5.91	190	-0.11	0.02	-0.31	0.00	0.00	0.00	-0.03	0.02	0.09	0.01	0.04	0.13	0.47	0.02	0.40	0.54	0.01	0.01	-0.05	0.06	0.00	0.01	-0.03	0.03
04_010_001_01	1	3.0-16.0	315	-0.13	0.04	-0.29	0.05	0.08	0.02	-0.01	0.19	0.11	0.02	0.02	0.21	0.57	0.22	-0.27	1.39	0.05	0.04	-0.11	0.22	0.00	0.03	-0.13	0.14
04_011_001_01	1	3.0-16.0	45	-0.14	0.04	-0.28	0.02	0.09	0.03	-0.04	0.20	0.10	0.02	0.04	0.18	0.58	0.15	0.00	1.14	0.05	0.04	-0.08	0.18	0.00	0.03	-0.11	0.15
04_015_001_01	0.96	9.6	45	-0.14	0.04	-0.31	0.06	0.09	0.02	-0.02	0.18	0.10	0.03	-0.06	0.24	0.58	0.13	0.02	1.28	0.05	0.04	-0.10	0.20	0.00	0.02	-0.10	0.13
04_016_001_01	1.29	4.4	315	-0.14	0.01	-0.17	-0.10	0.08	0.01	0.05	0.11	0.10	0.01	0.08	0.13	0.57	0.01	0.50	0.63	0.05	0.01	0.01	0.09	0.00	0.01	-0.03	0.03
04_019_001_01	1.5	5.91	315	-0.13	0.02	-0.23	0.00	0.08	0.01	0.00	0.13	0.10	0.01	0.05	0.15	0.57	0.03	0.43	0.74	0.05	0.02	-0.01	0.13	0.00	0.01	-0.06	0.06
04_020_001_01	1.5	5.91	45	-0.13	0.03	-0.23	-0.01	0.09	0.01	0.03	0.15	0.09	0.01	0.04	0.15	0.57	0.03	0.43	0.73	0.05	0.02	-0.01	0.12	0.00	0.01	-0.07	0.06
07_010_001_01	1	3.0-16.0	280	-0.12	0.04	-0.29	0.01	0.03	0.16	-0.45	0.81	0.09	0.10	-0.29	0.43	0.43	0.42	-1.10	2.04	0.04	0.06	-0.21	0.30	-0.01	0.09	-0.36	0.32
07_011_001_01	1	3.0-16.0	10	-0.11	0.03	-0.23	0.01	0.01	0.01	-0.03	0.05	0.10	0.02	0.03	0.17	0.42	0.08	0.10	0.77	0.04	0.02	-0.08	0.13	0.00	0.01	-0.05	0.04
07_012_001_01	1.21	3.8	280	-0.14	0.01	-0.18	-0.11	0.00	0.01	-0.05	0.05	0.09	0.01	0.06	0.12	0.41	0.02	0.30	0.51	0.04	0.01	0.00	0.08	-0.01	0.01	-0.06	0.04
07_013_001_01	1.16	5	10	-0.13	0.01	-0.16	-0.08	0.01	0.00	-0.01	0.03	0.09	0.01	0.06	0.12	0.42	0.01	0.36	0.48	0.04	0.01	-0.01	0.09	-0.01	0.01	-0.04	0.03
07_017_001_01	2	6.63	280	-0.11	0.05	-0.40	0.12	-0.01	0.09	-0.51	0.34	0.09	0.06	-0.19	0.27	0.40	0.12	-0.33	0.88	0.04	0.08	-0.32	0.43	-0.02	0.08	-0.38	0.35
07_019_001_01	1.5	5.91	280	-0.12	0.02	-0.23	-0.03	0.00	0.05	-0.24	0.18	0.09	0.02	-0.04	0.20	0.41	0.06	0.17	0.65	0.04	0.04	-0.13	0.23	-0.01	0.04	-0.18	0.20
07_020_001_01	1.5	5.91	10	-0.09	0.02	-0.16	0.04	0.01	0.01	-0.02	0.05	0.10	0.01	0.04	0.14	0.42	0.02	0.33	0.50	0.04	0.02	-0.03	0.11	0.00	0.01	-0.04	0.04
07_023_001_01	3	7.8	10	0.40	0.40	-1.67	2.29	0.03	0.02	-0.08	0.12	0.08	0.06	-0.16	0.32	0.39	0.07	0.11	0.70	0.04	0.06	-0.24	0.25	-0.04	0.02	-0.13	0.08

TABLE 46 MOTIONS FSRU AND LNGC IN SBS MOORING

MARIN Test No.	Hs	Tp	WaveIncHeading	X_COG_FSRU [m]				Y_COG_FSRU [m]				Z_COG_FSRU [m]				ROLL_FSRU [deg]			
35225_02OB_	[m]	[s]	[deg]	Mean	StdDev	Min	Max	Mean	StdDev	Min	Max	Mean	StdDev	Min	Max	Mean	StdDev	Min	Max
05_010_001_01	1	3.0-16.0	315	-0.05	0.05	-0.24	0.14	0.05	0.03	-0.07	0.17	0.09	0.02	0.00	0.19	0.49	0.10	-0.01	0.93
05_019_001_02	1.5	5.91	315	-0.04	0.05	-0.25	0.24	0.05	0.02	-0.03	0.13	0.09	0.01	0.03	0.13	0.48	0.03	0.35	0.60
06_010_001_01	1	3.0-16.0	280	-0.11	0.05	-0.32	0.09	0.00	0.07	-0.24	0.32	0.07	0.04	-0.08	0.24	0.37	0.38	-1.18	1.93
06_011_001_01	1	3.0-16.0	10	-0.09	0.07	-0.37	0.16	0.01	0.02	-0.10	0.09	0.07	0.02	0.01	0.14	0.37	0.20	-0.40	1.13
06_019_001_01	1.5	5.91	280	-0.12	0.02	-0.22	0.00	-0.01	0.03	-0.15	0.11	0.07	0.02	0.00	0.14	0.36	0.03	0.22	0.50
06_020_001_01	1.5	5.91	10	-0.06	0.11	-0.51	0.54	0.01	0.03	-0.10	0.13	0.09	0.01	0.02	0.14	0.37	0.03	0.24	0.50

MARIN Test No.	PITCH_FSRU [deg]				YAW_FSRU [deg]				X_COG_LNGC [m]				Y_COG_LNGC [m]			
35225_02OB_	Mean	StdDev	Min	Max	Mean	StdDev	Min	Max	Mean	StdDev	Min	Max	Mean	StdDev	Min	Max
05_010_001_01	0.09	0.04	-0.05	0.24	0.00	0.03	-0.15	0.15	-0.05	0.10	-0.48	0.32	-0.03	0.05	-0.25	0.18
05_019_001_02	0.10	0.02	0.02	0.17	0.00	0.02	-0.07	0.07	-0.03	0.17	-0.57	0.49	-0.04	0.06	-0.27	0.20
06_010_001_01	0.04	0.05	-0.13	0.23	-0.01	0.08	-0.32	0.31	-0.12	0.07	-0.39	0.14	-0.06	0.12	-0.46	0.42
06_011_001_01	0.05	0.02	-0.04	0.13	-0.01	0.02	-0.12	0.11	-0.09	0.17	-0.69	0.47	-0.03	0.04	-0.17	0.12
06_019_001_01	0.04	0.01	-0.01	0.10	-0.01	0.02	-0.10	0.07	-0.14	0.12	-0.50	0.31	-0.11	0.11	-0.52	0.28
06_020_001_01	0.04	0.02	-0.06	0.15	-0.01	0.02	-0.11	0.09	-0.06	0.25	-0.92	1.14	-0.01	0.07	-0.25	0.31

MARIN Test No.	Z_COG_LNGC [m]				ROLL_LNGC [deg]				PITCH_LNGC [deg]				YAW_LNGC [deg]			
35225_02OB_	Mean	StdDev	Min	Max	Mean	StdDev	Min	Max	Mean	StdDev	Min	Max	Mean	StdDev	Min	Max
05_010_001_01	0.02	0.02	-0.08	0.10	0.13	0.06	-0.15	0.40	-0.05	0.03	-0.17	0.06	-0.01	0.04	-0.16	0.16
05_019_001_02	0.01	0.01	-0.04	0.07	0.13	0.04	-0.04	0.30	-0.05	0.01	-0.11	0.00	-0.01	0.03	-0.14	0.13
06_010_001_01	-0.02	0.09	-0.39	0.30	0.13	0.13	-0.35	0.64	0.01	0.07	-0.23	0.30	-0.04	0.06	-0.26	0.18
06_011_001_01	-0.02	0.01	-0.08	0.04	0.12	0.05	-0.10	0.31	0.01	0.02	-0.08	0.09	-0.03	0.02	-0.13	0.08
06_019_001_01	-0.02	0.02	-0.09	0.08	0.11	0.08	-0.16	0.44	0.01	0.03	-0.10	0.13	-0.05	0.06	-0.37	0.28
06_020_001_01	0.00	0.01	-0.06	0.05	0.15	0.03	0.00	0.29	0.01	0.02	-0.06	0.08	-0.03	0.04	-0.22	0.14

TABLE 47 RELATIVE WAVEHEIGHTS IN JETTY MOORING

MARIN Test No.	Hs	Tp	WaveIncHeading	REL_01_FSRU [m]				REL_02_FSRU [m]				REL_03_FSRU [m]				REL_04_FSRU [m]				REL_05_FSRU [m]				REL_06_FSRU [m]			
35225_02OB_	[m]	[s]	[deg]	Mean	StdDev	Min	Max	Mean	StdDev	Min	Max	Mean	StdDev	Min	Max	Mean	StdDev	Min	Max	Mean	StdDev	Min	Max	Mean	StdDev	Min	Max
03_010_001_01	1	3.0-16.0	100	0.08	0.40	-1.57	1.72	0.20	0.51	-1.85	2.54	0.10	0.53	-2.24	2.39	0.12	0.59	-2.29	3.16	0.17	0.36	-1.27	1.56	-0.19	0.17	-0.91	0.63
03_011_001_01	1	3.0-16.0	190	0.07	0.30	-1.22	1.44	0.20	0.32	-1.06	1.68	0.07	0.15	-0.51	0.78	0.09	0.13	-0.46	0.68	0.17	0.09	-0.17	0.46	-0.20	0.38	-1.48	1.53
03_014_001_01	0.77	8	190	0.06	0.21	-0.76	0.88	0.19	0.25	-0.69	1.16	0.07	0.10	-0.31	0.48	0.09	0.11	-0.34	0.55	0.17	0.07	-0.12	0.46	-0.20	0.28	-1.25	1.05
03_015_001_01	0.96	9.6	190	0.06	0.30	-1.11	1.52	0.19	0.30	-1.24	1.48	0.07	0.17	-0.52	0.82	0.09	0.14	-0.53	0.67	0.16	0.13	-0.47	0.78	-0.20	0.32	-1.57	1.32
03_019_001_01	1.5	5.91	100	0.06	0.67	-2.85	4.64	0.20	0.80	-2.86	4.28	0.11	0.77	-3.04	4.12	0.15	0.92	-3.70	6.22	0.17	0.49	-2.32	2.31	-0.20	0.08	-0.52	0.13
03_020_001_01	1.5	5.91	190	0.06	0.40	-1.61	1.99	0.19	0.48	-1.71	2.64	0.07	0.18	-0.63	0.84	0.09	0.17	-0.63	0.85	0.17	0.08	-0.21	0.51	-0.20	0.54	-2.05	2.74
04_010_001_01	1	3.0-16.0	315	0.07	0.23	-0.79	1.30	0.22	0.15	-0.33	0.80	0.28	0.13	-0.25	0.87	0.14	0.14	-0.40	0.68	0.17	0.38	-1.22	1.76	-0.21	0.55	-2.43	2.12
04_011_001_01	1	3.0-16.0	45	0.07	0.52	-1.85	2.62	0.22	0.40	-1.29	1.96	0.29	0.52	-1.47	2.43	0.15	0.51	-1.72	2.14	0.17	0.34	-1.06	1.46	-0.22	0.11	-0.69	0.25
04_015_001_01	0.96	9.6	45	0.08	0.39	-1.58	1.62	0.22	0.36	-1.40	1.81	0.29	0.55	-2.19	3.13	0.15	0.41	-1.46	1.84	0.17	0.44	-1.73	2.65	-0.22	0.09	-0.56	0.10
04_016_001_01	1.29	4.4	315	0.07	0.12	-0.35	0.60	0.22	0.08	-0.05	0.51	0.28	0.06	0.03	0.51	0.15	0.07	-0.14	0.44	0.17	0.41	-1.28	2.45	-0.20	0.67	-2.58	3.60
04_019_001_01	1.5	5.91	315	0.07	0.21	-0.75	1.25	0.22	0.10	-0.17	0.61	0.28	0.08	-0.06	0.59	0.14	0.09	-0.22	0.53	0.17	0.55	-1.76	2.70	-0.20	0.86	-4.06	4.87
04_020_001_01	1.5	5.91	45	0.08	0.85	-2.82	3.95	0.22	0.64	-2.23	3.57	0.29	0.80	-3.01	5.25	0.16	0.89	-2.83	4.72	0.16	0.39	-1.59	1.75	-0.22	0.08	-0.54	0.13
07_010_001_01	1	3.0-16.0	280	0.08	0.20	-0.83	1.22	0.18	0.16	-0.47	0.84	0.20	0.14	-0.33	0.77	0.19	0.13	-0.43	0.70	0.15	0.26	-1.01	1.23	-0.18	0.58	-2.61	2.68
07_011_001_01	1	3.0-16.0	10	0.07	0.20	-0.66	0.94	0.18	0.24	-0.85	1.35	0.20	0.37	-1.09	1.83	0.19	0.31	-0.94	1.62	0.15	0.33	-1.28	1.60	-0.20	0.16	-0.85	0.40
07_012_001_01	1.21	3.8	280	0.07	0.15	-0.64	1.63	0.17	0.07	-0.12	0.45	0.19	0.04	0.02	0.37	0.18	0.05	-0.02	0.35	0.14	0.33	-0.86	1.56	-0.16	0.63	-2.36	2.78
07_013_001_01	1.16	5	10	0.07	0.24	-0.93	1.25	0.17	0.26	-0.91	1.41	0.19	0.38	-1.25	2.25	0.18	0.32	-1.03	1.76	0.14	0.29	-1.04	1.54	-0.20	0.18	-1.05	0.76
07_017_001_01	2	6.63	280	0.08	0.44	-1.85	2.67	0.17	0.21	-0.84	1.08	0.19	0.13	-0.36	0.71	0.18	0.13	-0.35	0.64	0.13	0.34	-1.04	1.71	-0.14	1.04	-4.41	5.58
07_019_001_01	1.5	5.91	280	0.08	0.36	-1.26	2.48	0.18	0.15	-0.38	0.75	0.19	0.08	-0.11	0.51	0.18	0.09	-0.14	0.56	0.14	0.32	-0.85	1.60	-0.16	0.79	-3.48	4.11
07_020_001_01	1.5	5.91	10	0.07	0.34	-1.45	1.59	0.17	0.38	-1.44	1.81	0.19	0.54	-1.75	2.54	0.19	0.45	-1.50	2.41	0.14	0.43	-1.69	1.95	-0.20	0.23	-1.28	0.87
07_023_001_01	3	7.8	10	0.08	0.57	-2.44	2.78	0.16	0.66	-2.12	2.83	0.17	0.96	-3.03	4.69	0.16	0.92	-2.83	4.06	0.11	1.03	-3.06	4.62	-0.18	0.46	-2.32	1.75

TABLE 48 RELATIVE WAVEHEIGHTS IN SBS MOORING

MARIN Test No.	Hs	Tp	WaveIncHeading	REL_01_FSRU [m]				REL_02_FSRU [m]				REL_03_FSRU [m]				REL_04_FSRU [m]				REL_05_FSRU [m]				REL_06_FSRU [m]				REL_01_LNGC [m]				REL_02_LNGC [m]			
35225_02OB_	[m]	[s]	[deg]	Mean	StdDev	Min	Max	Mean	StdDev	Min	Max	Mean	StdDev	Min	Max	Mean	StdDev	Min	Max	Mean	StdDev	Min	Max	Mean	StdDev	Min	Max	Mean	StdDev	Min	Max	Mean	StdDev	Min	Max
05_010_001_01	1	3.0-16.0	315	-0.18	0.14	-0.84	0.37	0.19	0.10	-0.23	0.57	0.23	0.12	-0.24	0.70	0.12	0.12	-0.37	0.55	0.16	0.42	-1.43	1.90	-0.21	0.24	-1.17	0.69	0.02	0.22	-0.79	0.99	0.05	0.25	-1.00	0.97
05_019_001_02	1.5	5.91	315	-0.17	0.12	-0.65	0.29	0.19	0.08	-0.16	0.51	0.22	0.10	-0.19	0.66	0.12	0.11	-0.29	0.54	0.15	0.58	-1.78	2.93	-0.22	0.33	-1.59	1.16	0.02	0.34	-1.65	1.75	0.05	0.40	-1.71	2.11
06_010_001_01	1	3.0-16.0	280	0.06	0.20	-0.72	0.93	0.15	0.16	-0.42	0.73	0.17	0.14	-0.53	0.70	0.16	0.18	-0.53	0.87	0.12	0.20	-0.72	0.91	-0.19	0.27	-1.27	1.02	0.05	0.29	-1.11	1.28	0.05	0.26	-1.06	1.21
06_011_001_01	1	3.0-16.0	10	0.06	0.21	-0.71	0.97	0.16	0.24	-0.95	1.31	0.17	0.38	-1.17	1.90	0.16	0.34	-1.09	1.76	0.12	0.34	-1.43	1.61	-0.19	0.57	-2.20	2.49	0.04	0.54	-1.87	2.53	0.05	0.63	-2.23	2.86
06_019_001_01	1.5	5.91	280	0.06	0.15	-0.47	0.85	0.15	0.07	-0.13	0.42	0.17	0.07	-0.10	0.43	0.16	0.07	-0.13	0.46	0.12	0.25	-0.84	1.19	-0.18	0.32	-1.60	1.29	0.04	0.34	-1.26	1.50	0.04	0.33	-1.21	1.45
06_020_001_01	1.5	5.91	10	0.07	0.36	-1.46	1.59	0.16	0.37	-1.30	1.80	0.18	0.56	-1.88	2.60	0.17	0.50	-1.64	2.64	0.12	0.46	-1.74	2.05	-0.19	0.85	-3.28	3.34	0.07	0.80	-2.44	3.51	0.09	1.11	-3.65	5.50

TABLE 49 MAX LINE LOADS IN JETTY MOORING

MARIN Test No.	Hs	Tp	WaveIncHeading	F_01_JET [kN]	F_02_JET [kN]	F_03_JET [kN]	F_04_JET [kN]	F_05_JET [kN]	F_06_JET [kN]	F_07_JET [kN]	F_08_JET [kN]
35225_02OB_	[m]	[s]	[deg]	Max	Max	Max	Max	Max	Max	Max	Max
03_010_001_01	1	3.0-16.0	100	966.37	1165.48	1985.88	401.92	915.50	1155.54	1841.51	1156.47
03_011_001_01	1	3.0-16.0	190	526.14	601.86	987.29	324.40	806.66	616.71	1051.11	749.61
03_014_001_01	0.77	8	190	515.96	593.10	968.45	319.78	835.47	601.48	1047.66	746.34
03_015_001_01	0.96	9.6	190	548.20	627.62	997.27	372.05	881.73	618.25	1102.12	786.61
03_019_001_01	1.5	5.91	100	977.34	1111.91	1748.30	345.77	892.32	842.08	1416.41	944.57
03_020_001_01	1.5	5.91	190	530.03	596.77	961.56	315.68	862.77	602.97	1049.23	747.25
04_010_001_01	1	3.0-16.0	315	615.00	716.08	1187.26	370.79	847.85	707.41	1169.24	830.06
04_011_001_01	1	3.0-16.0	45	599.30	693.17	1151.73	361.02	818.32	695.71	1150.53	812.99
04_015_001_01	0.96	9.6	45	568.98	654.94	1081.88	384.27	846.57	710.01	1197.12	843.00
04_016_001_01	1.29	4.4	315	515.19	593.32	984.82	319.30	773.96	614.60	1046.00	750.56
04_019_001_01	1.5	5.91	315	542.01	622.95	1032.33	346.33	795.13	640.28	1098.61	790.13
04_020_001_01	1.5	5.91	45	538.68	620.02	1040.04	349.08	795.62	650.12	1105.85	786.63
07_010_001_01	1	3.0-16.0	280	714.21	822.99	1352.87	359.48	919.06	1285.32	2039.53	1292.08
07_011_001_01	1	3.0-16.0	10	528.79	599.72	1001.10	330.28	817.68	634.58	1091.42	778.07
07_012_001_01	1.21	3.8	280	523.69	596.26	981.31	297.93	786.76	630.92	1073.83	768.38
07_013_001_01	1.16	5	10	510.62	583.83	965.12	303.16	780.03	609.20	1054.52	756.77
07_017_001_01	2	6.63	280	649.50	730.87	1207.51	368.96	889.39	1018.42	1649.72	1080.45
07_019_001_01	1.5	5.91	280	573.24	648.40	1075.59	324.77	812.53	757.14	1246.59	874.43
07_020_001_01	1.5	5.91	10	524.20	601.55	1001.99	341.38	783.79	623.27	1087.52	782.51
07_023_001_01	3	7.8	10	754.64	700.09	1210.40	1498.15	1674.90	721.08	1864.74	896.69

TABLE 50 MAX LINE LOADS IN SBS MOORING

MARIN Test No.	Hs	Tp	WaveIncHeading	F_01_JET [kN]	F_02_JET [kN]	F_03_JET [kN]	F_04_JET [kN]	F_05_JET [kN]	F_06_JET [kN]	F_07_JET [kN]	F_08_JET [kN]	F_01_SBS [kN]	F_02_SBS [kN]	F_03_SBS [kN]	F_04_SBS [kN]	F_05_SBS [kN]	F_06_SBS [kN]	F_07_SBS [kN]	F_08_SBS [kN]
35225_02OB_	[m]	[s]	[deg]	Max	Max	Max	Max	Max	Max	Max	Max	Max	Max	Max	Max	Max	Max	Max	Max
05_010_001_01	1	3.0-16.0	315	583.33	661.71	1109.75	372.66	841.95	732.79	1196.06	845.99	220.75	273.12	201.87	304.70	272.11	250.72	376.27	189.87
05_019_001_02	1.5	5.91	315	552.76	621.78	1023.45	400.96	834.85	655.37	1109.48	796.16	202.87	316.39	199.61	401.54	313.60	238.29	273.82	188.51
06_010_001_01	1	3.0-16.0	280	768.22	835.84	1321.74	361.53	877.98	967.28	1579.56	1052.63	343.79	1013.04	815.22	287.31	240.24	753.30	907.45	279.92
06_011_001_01	1	3.0-16.0	10	576.39	647.98	1075.90	396.32	876.46	715.29	1243.46	878.39	215.00	264.49	230.45	354.25	255.20	278.78	359.21	181.86
06_019_001_01	1.5	5.91	280	572.92	652.63	1070.51	328.46	805.78	661.61	1130.49	803.17	355.98	557.09	301.58	301.43	272.58	373.22	521.22	214.39
06_020_001_01	1.5	5.91	10	575.34	627.89	1044.52	494.37	945.97	716.86	1251.56	882.87	241.75	449.43	251.88	599.02	331.37	682.81	781.67	308.55

TABLE 51 MAX FENDER LOADS IN JETTY MOORING

MARIN Test No.	Hs	Tp	WaveIncHeading	F_FEN_01_JET [kN]	F_FEN_02_JET [kN]	F_FEN_03_JET [kN]	F_FEN_04_JET [kN]	F_FEN_05_JET [kN]	F_FEN_06_JET [kN]
35225_02OB_	[m]	[s]	[deg]	Max	Max	Max	Max	Max	Max
03_010_001_01	1	3.0-16.0	100	3180.68	3216.05	3005.52	2611.07	2755.46	3015.55
03_011_001_01	1	3.0-16.0	190	1001.39	1167.80	1031.41	997.45	957.78	1122.92
03_014_001_01	0.77	8	190	845.56	870.77	897.06	872.87	859.72	941.90
03_015_001_01	0.96	9.6	190	963.76	1074.88	1015.22	996.04	968.04	1095.13
03_019_001_01	1.5	5.91	100	1816.18	1797.58	1727.86	1548.46	1675.71	2003.48
03_020_001_01	1.5	5.91	190	820.69	876.69	895.23	872.25	854.78	929.17
04_010_001_01	1	3.0-16.0	315	1410.41	1359.06	1293.70	1513.99	1580.69	1844.31
04_011_001_01	1	3.0-16.0	45	1487.11	1466.98	1321.75	1485.60	1517.92	1772.88
04_015_001_01	0.96	9.6	45	1230.47	1275.60	1194.68	1511.10	1586.63	1784.70
04_016_001_01	1.29	4.4	315	878.61	955.27	984.18	905.01	936.83	1068.09
04_019_001_01	1.5	5.91	315	1127.09	1172.08	1175.78	1124.45	1168.83	1384.95
04_020_001_01	1.5	5.91	45	1089.68	1131.93	1059.52	1092.90	1039.68	1208.38
07_010_001_01	1	3.0-16.0	280	2287.98	2364.78	2327.16	3094.18	3064.27	3249.17
07_011_001_01	1	3.0-16.0	10	960.33	999.84	990.10	996.23	899.94	1057.17
07_012_001_01	1.21	3.8	280	986.81	1154.24	1058.11	1211.02	1069.78	1273.93
07_013_001_01	1.16	5	10	742.51	807.47	813.13	980.45	789.95	882.93
07_017_001_01	2	6.63	280	2653.65	2554.02	2545.82	3323.63	3439.80	3576.91
07_019_001_01	1.5	5.91	280	1720.66	1775.71	1798.48	2276.80	2477.35	2515.74
07_020_001_01	1.5	5.91	10	832.19	913.17	889.00	1010.05	875.83	1024.14
07_023_001_01	3	7.8	10	1177.99	1258.48	1146.67	1325.08	1248.92	1366.94

TABLE 52 MAX FENDER LOADS IN SBS MOORING

MARIN Test No.	Hs	Tp	WaveIncHeading	F_FEN_01_JET [kN]	F_FEN_02_JET [kN]	F_FEN_03_JET [kN]	F_FEN_04_JET [kN]	F_FEN_05_JET [kN]	F_FEN_06_JET [kN]	F_FEN_01_SBS [kN]	F_FEN_02_SBS [kN]	F_FEN_03_SBS [kN]	F_FEN_04_SBS [kN]
35225_02OB_	[m]	[s]	[deg]	Max	Max	Max	Max	Max	Max	Max	Max	Max	Max
05_010_001_01	1	3.0-16.0	315	1302.21	1338.98	1282.61	1632.17	1721.27	1939.47	572.62	560.67	617.27	624.04
05_019_001_02	1.5	5.91	315	1123.98	1268.07	1196.29	1265.33	1314.25	1500.68	576.52	536.96	838.96	769.79
06_010_001_01	1	3.0-16.0	280	2077.60	2106.73	1924.66	2197.08	2395.32	2502.88	1236.45	1081.43	940.41	916.65
06_011_001_01	1	3.0-16.0	10	1162.32	1270.66	1188.99	1433.78	1509.46	1533.88	517.34	472.84	570.06	547.14
06_019_001_01	1.5	5.91	280	1402.97	1525.77	1507.26	1623.12	1504.30	1529.26	1084.72	972.53	964.47	921.59
06_020_001_01	1.5	5.91	10	1148.01	1338.51	1231.71	1655.27	1565.85	1709.63	576.91	543.63	632.12	599.80

FIGURES

FIGURE 1 GENERAL LAYOUT FSRU

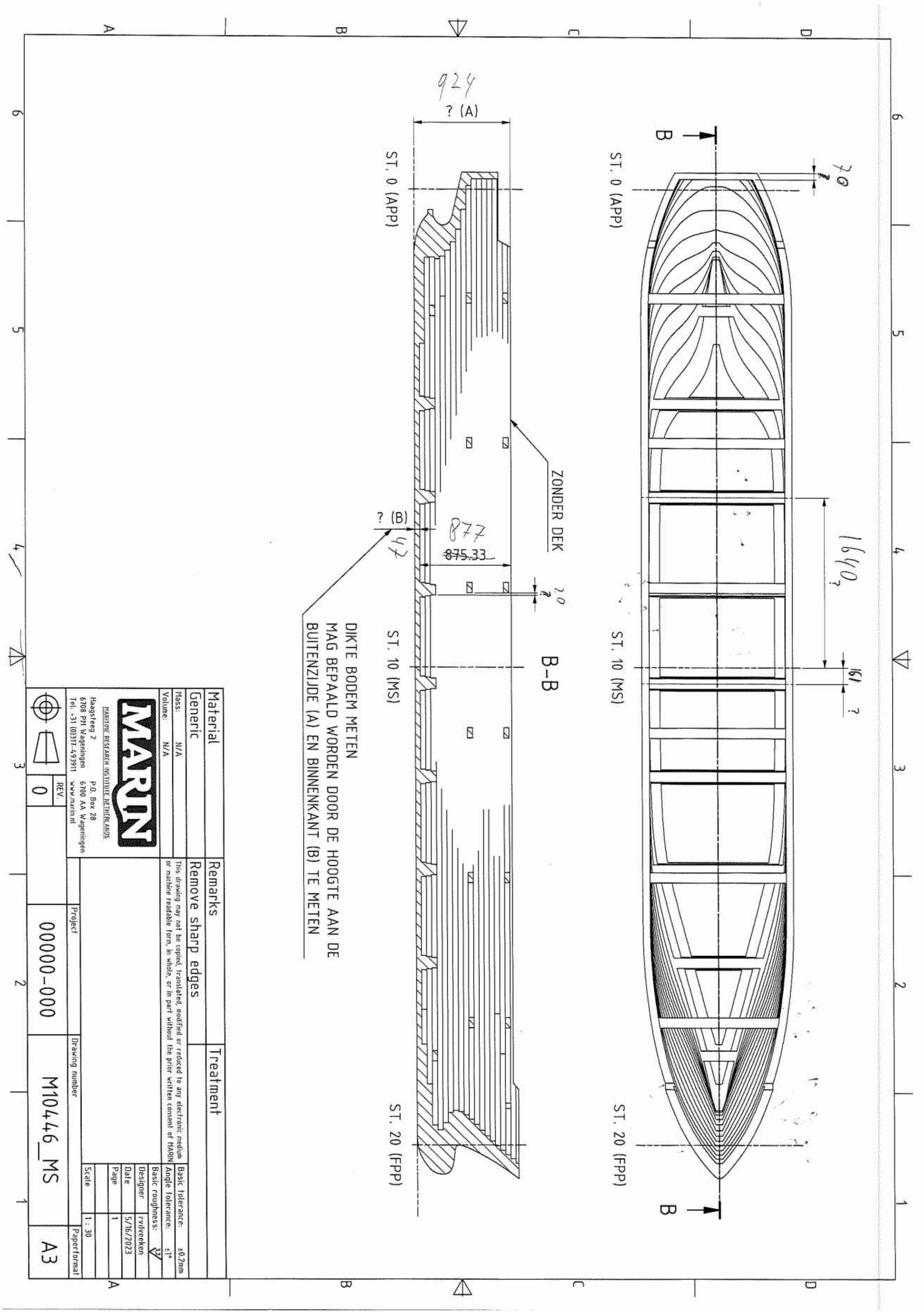

FIGURE 2 GENERAL LAYOUT LNGC

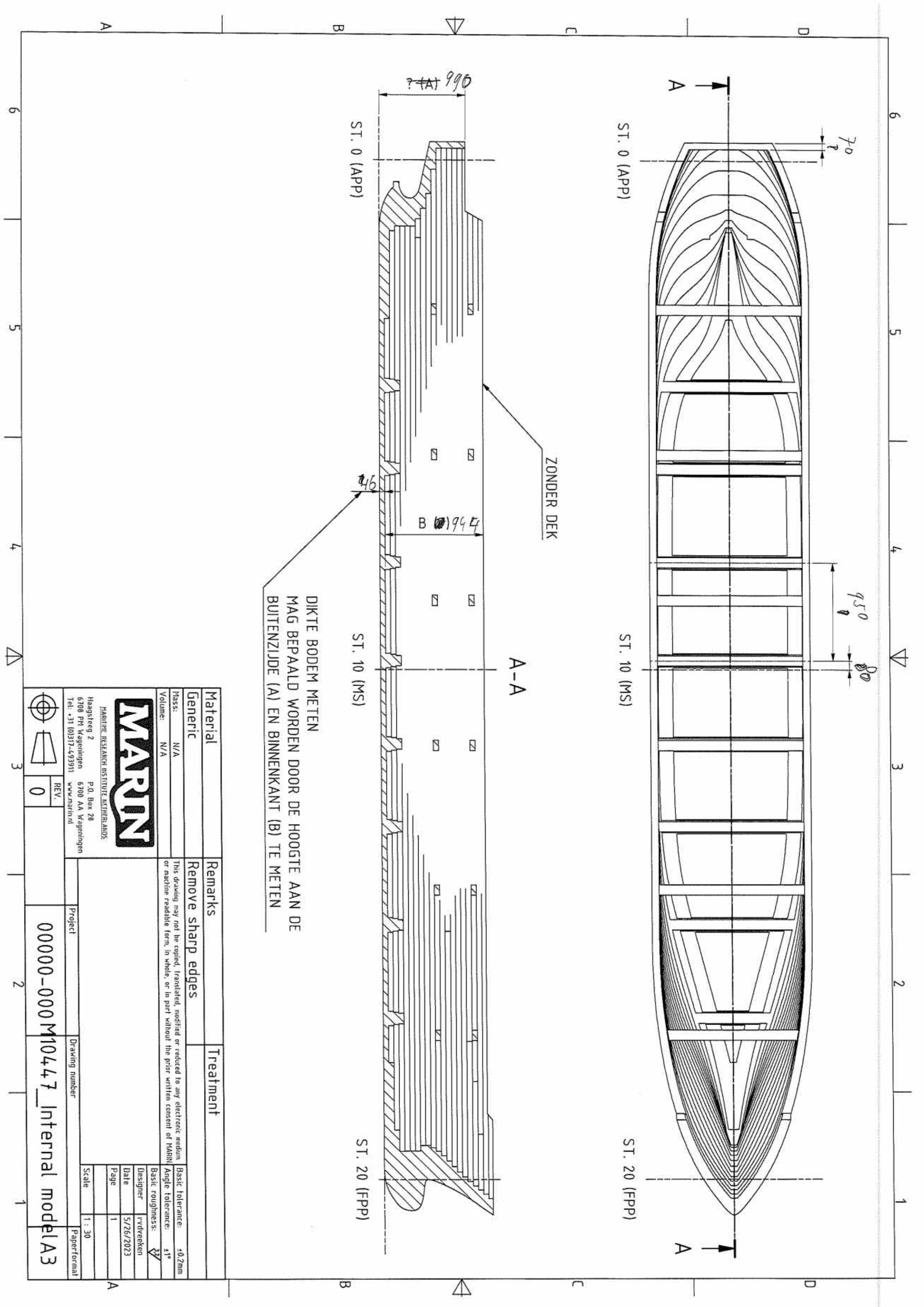

FIGURE 3 JETTY MOORING LAYOUT

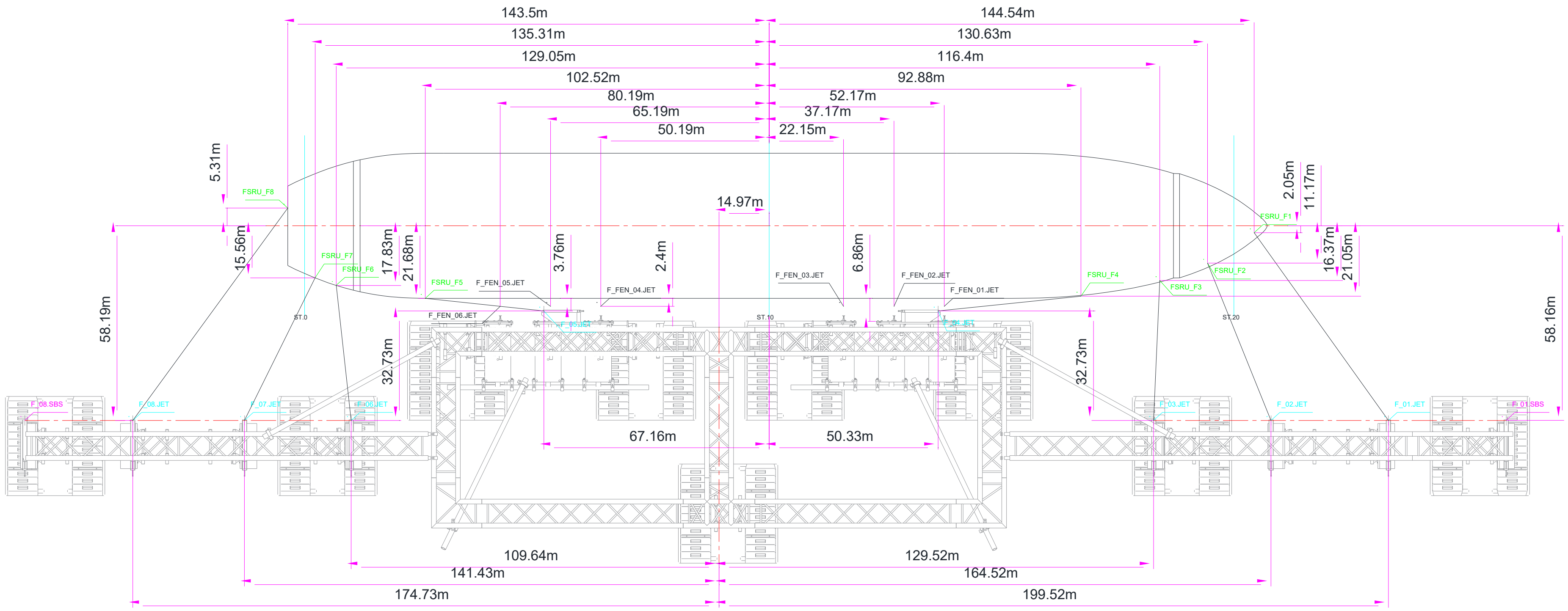

SB-view FSRU

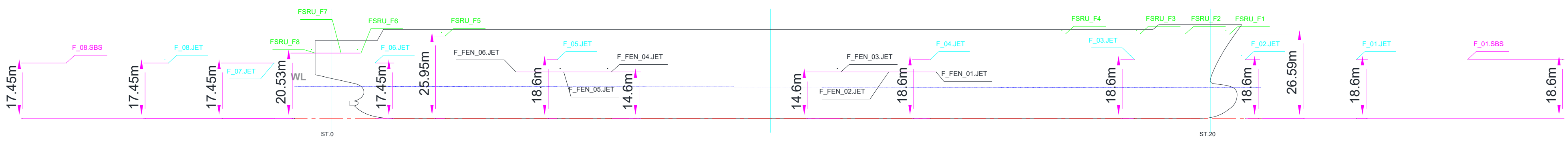

FIGURE 4 SIDE BY SIDE (SBS) MOORING LAYOUT

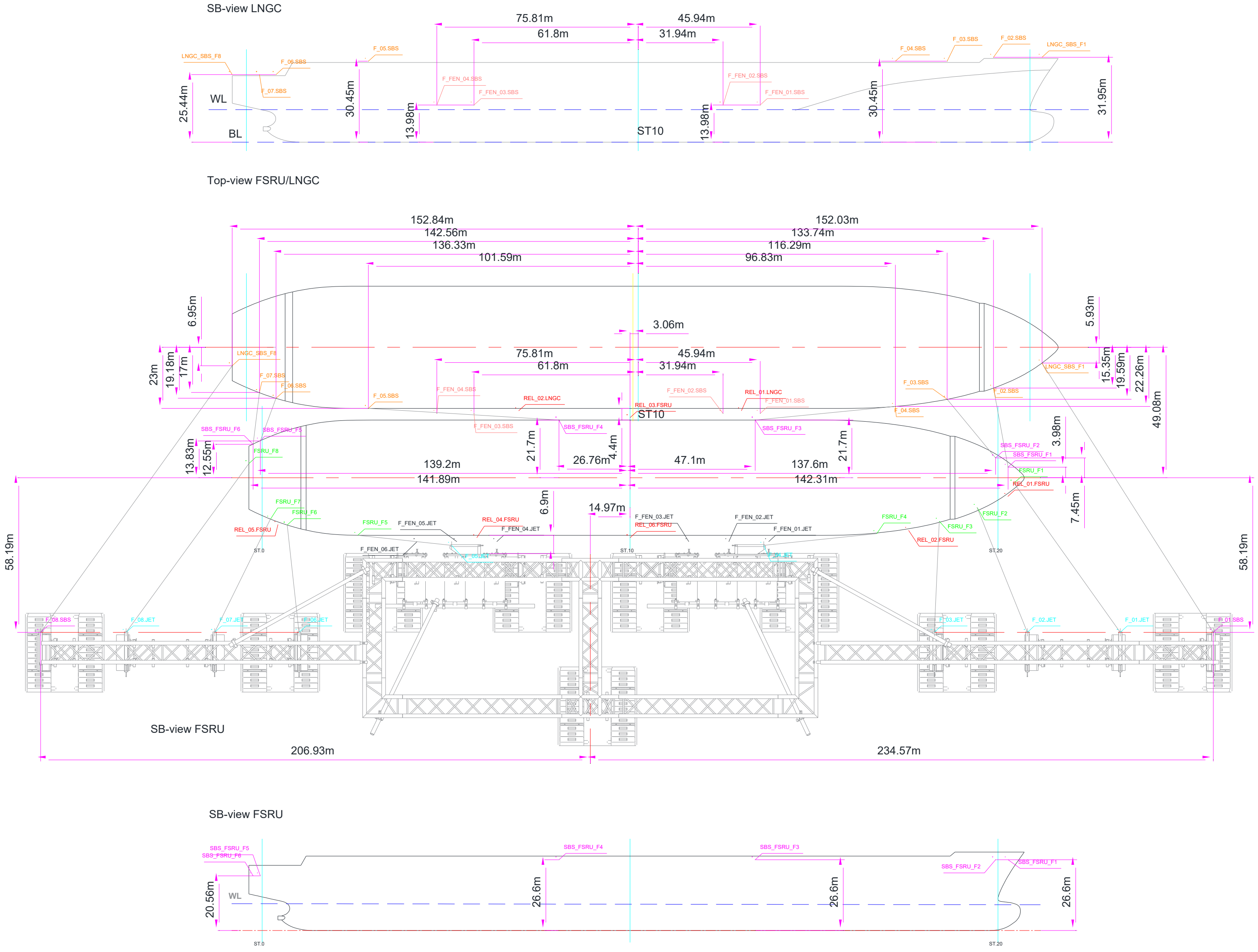

FIGURE 5 JETTY MOORING SETUP IN BASIN HEADING 80 DEGREES

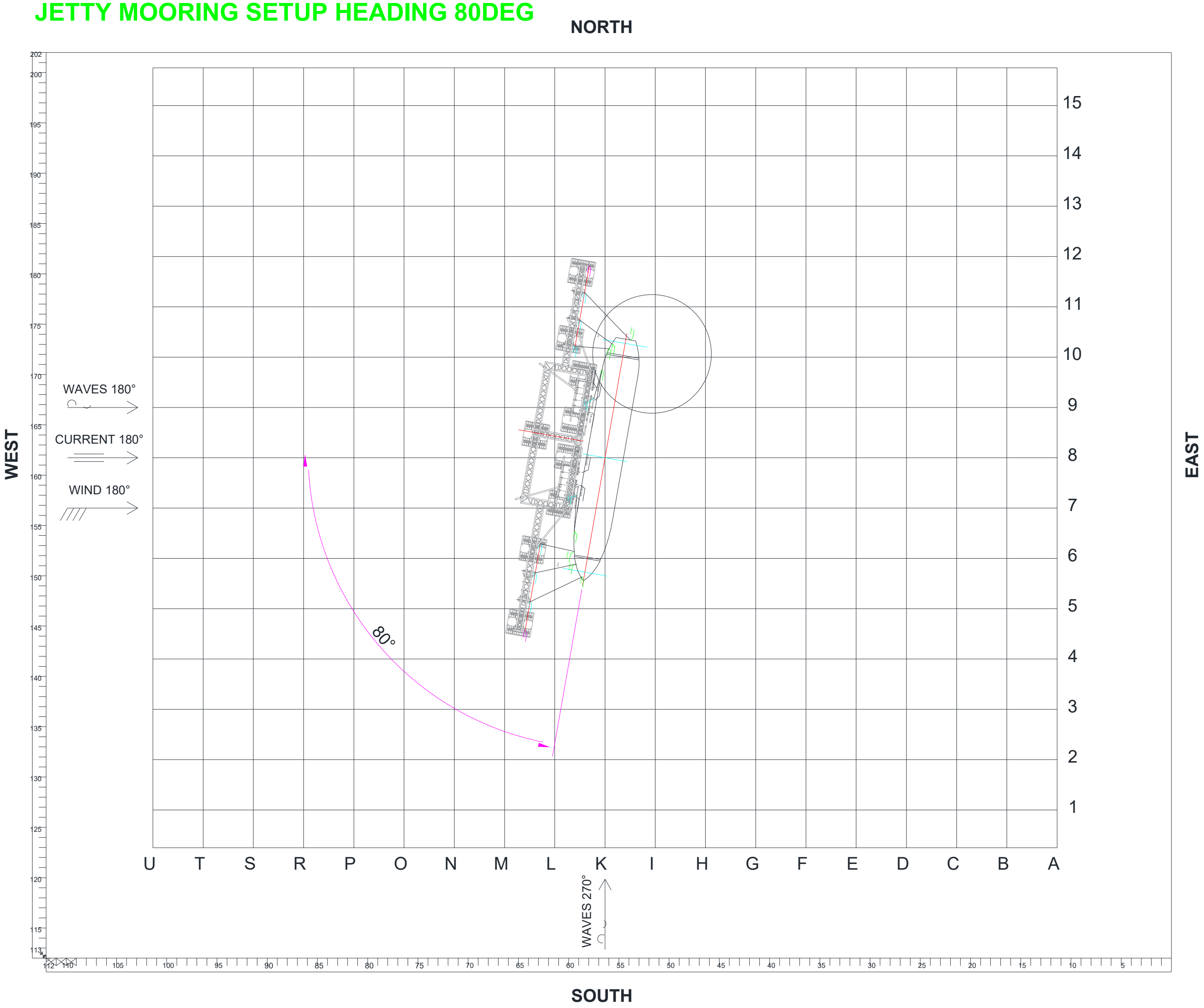

FIGURE 6 JETTY MOORING SETUP IN BASIN HEADING 225 DEGREES

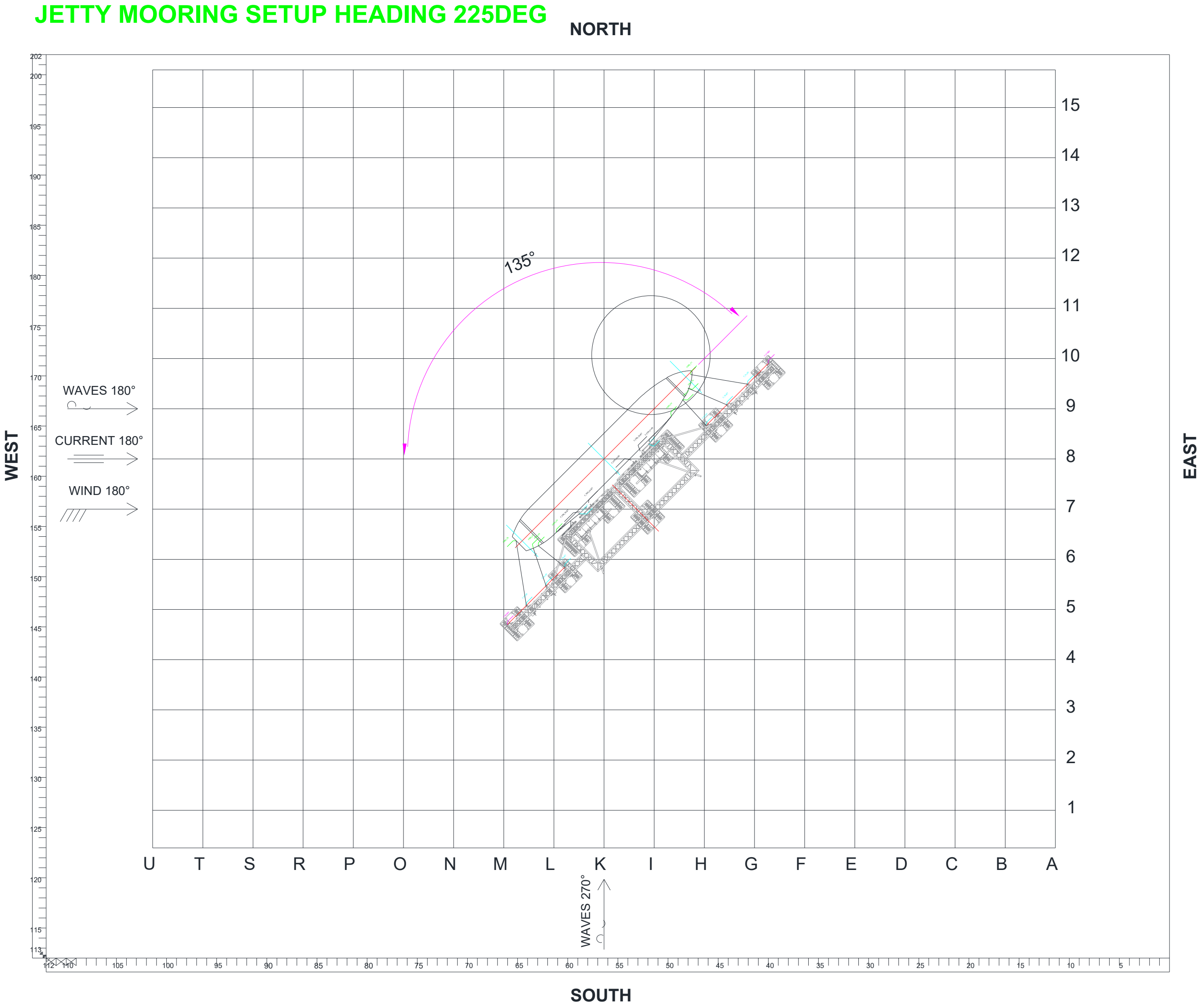

FIGURE 7 JETTY MOORING SETUP IN BASIN HEADING 260 DEGREES

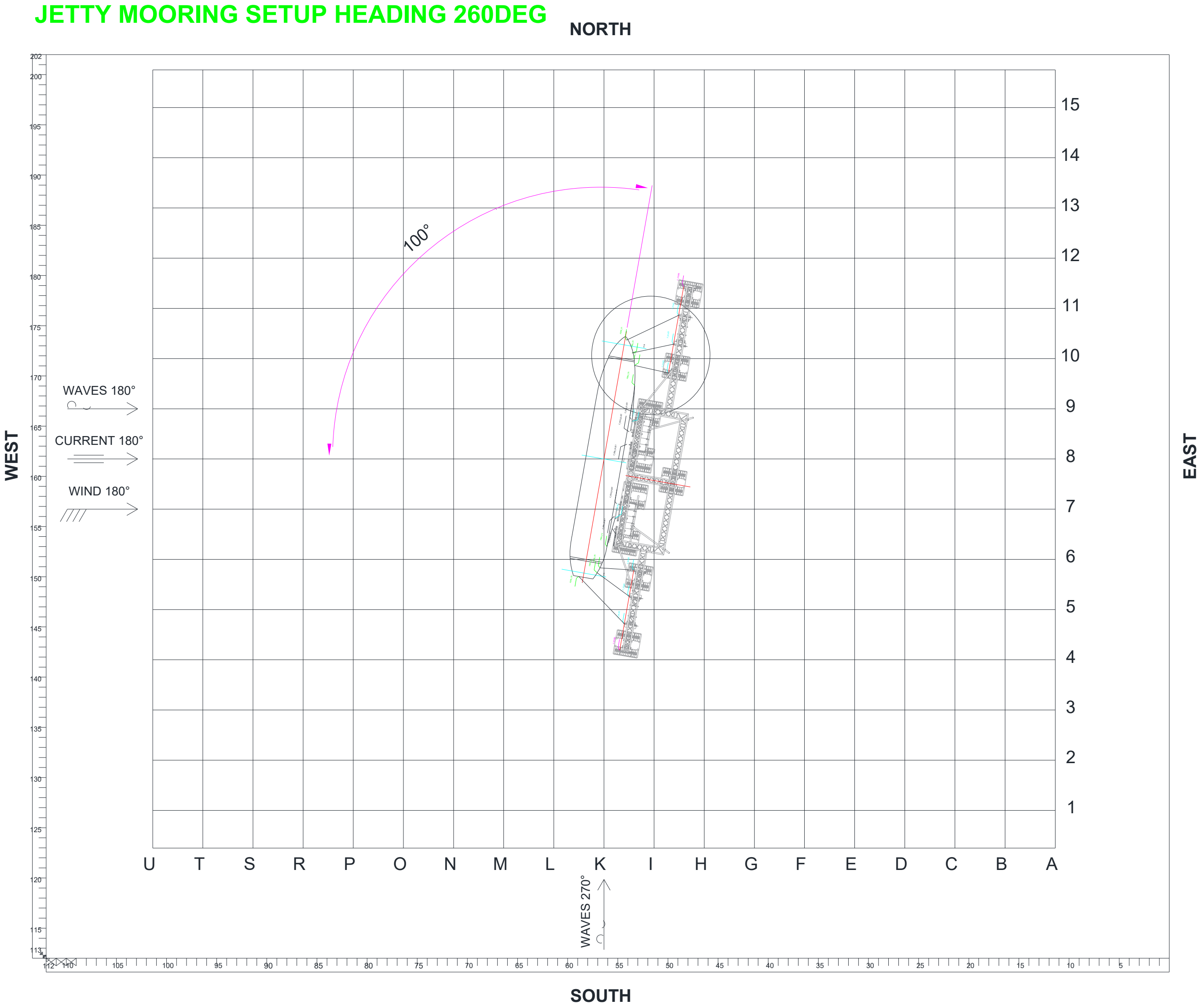

FIGURE 8 SIDE BY SIDE (SBS) MOORING SETUP IN BASIN HEADING 225 DEGREES

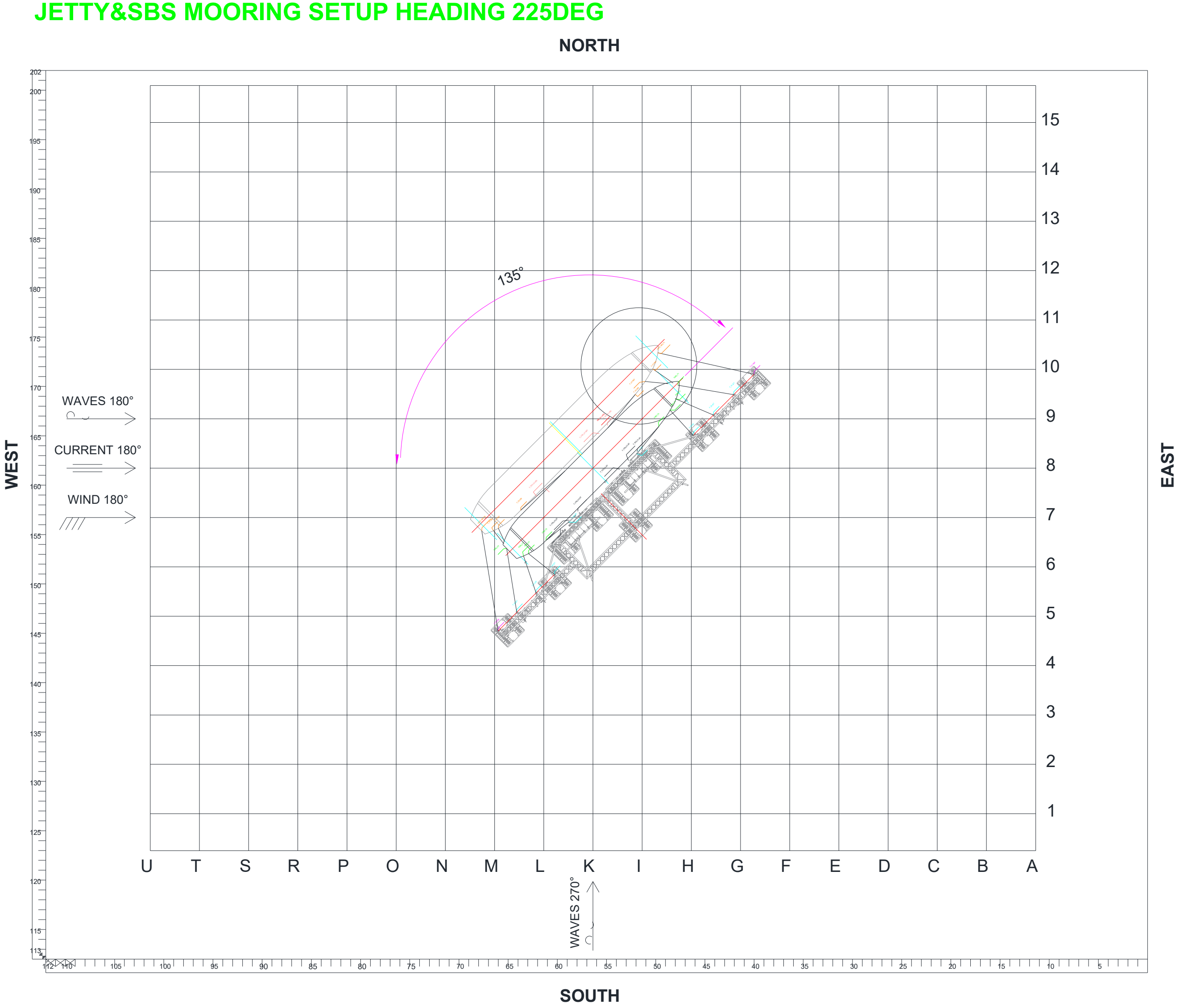

FIGURE 9 SIDE BY SIDE (SBS) MOORING SETUP IN BASIN HEADING 260 DEGREES

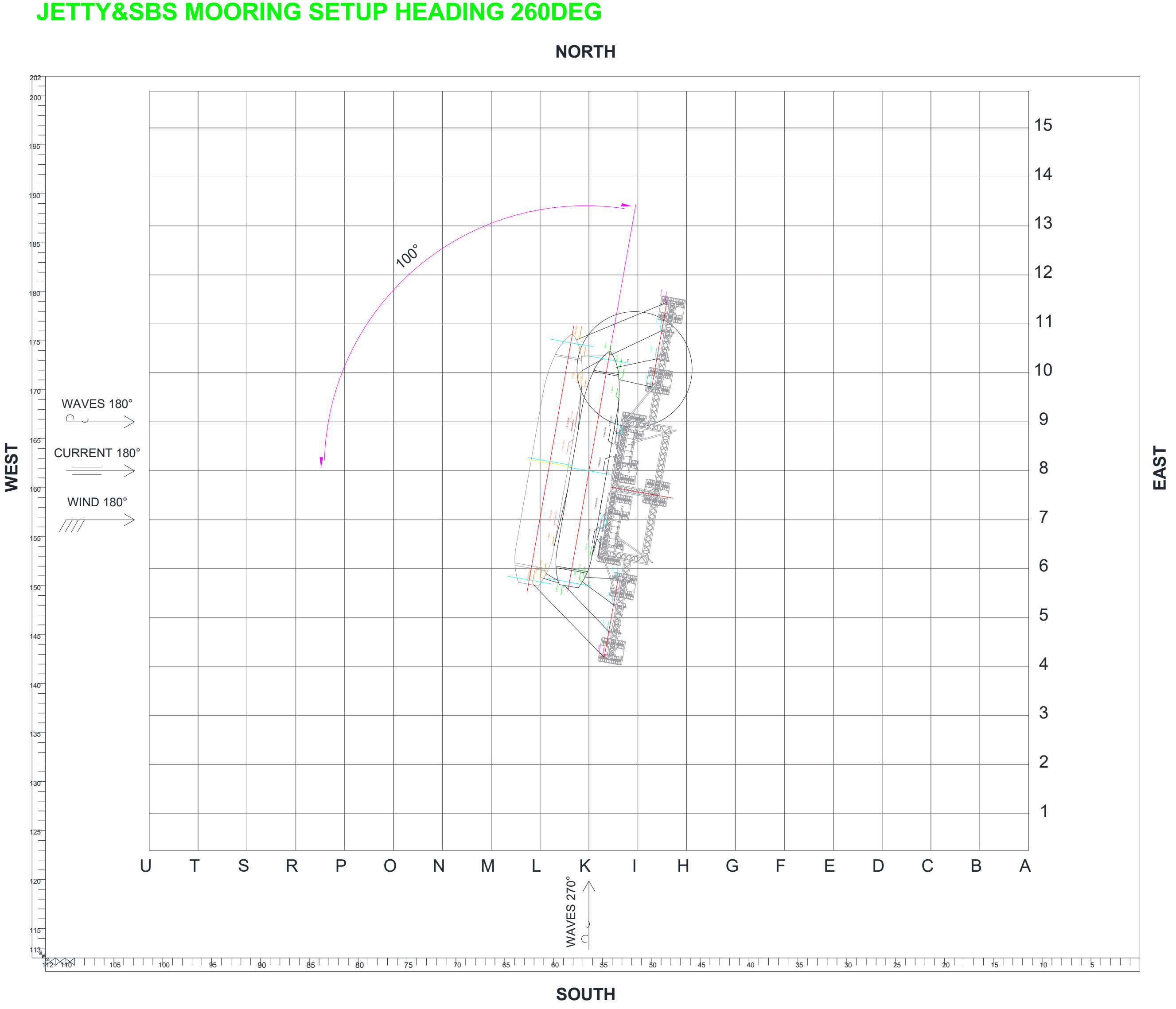

FIGURE 10 WAVE CALIBRATION SETUP 180 DEGREES

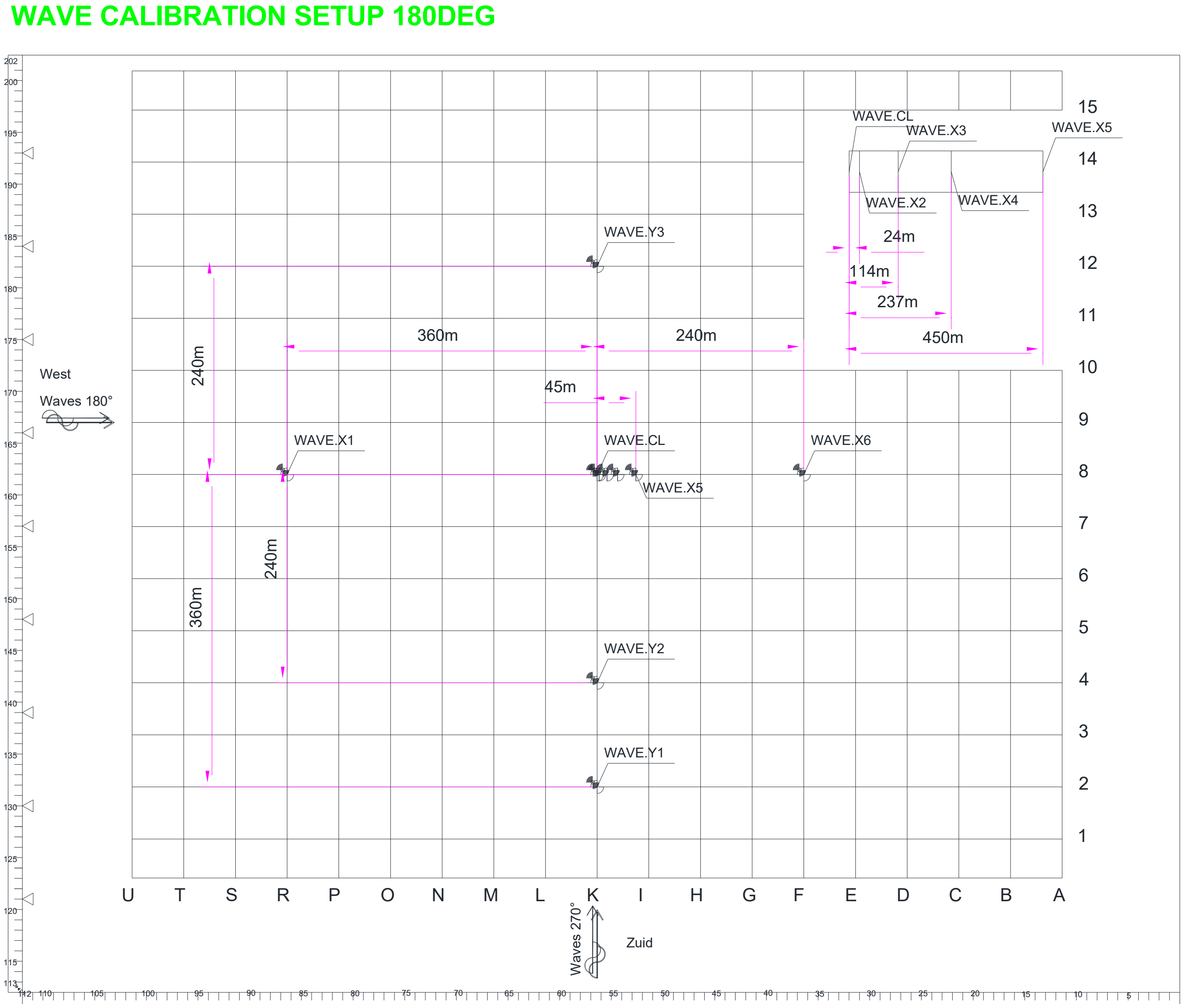

FIGURE 11 WAVE CALIBRATION SETUP 270 DEGREES

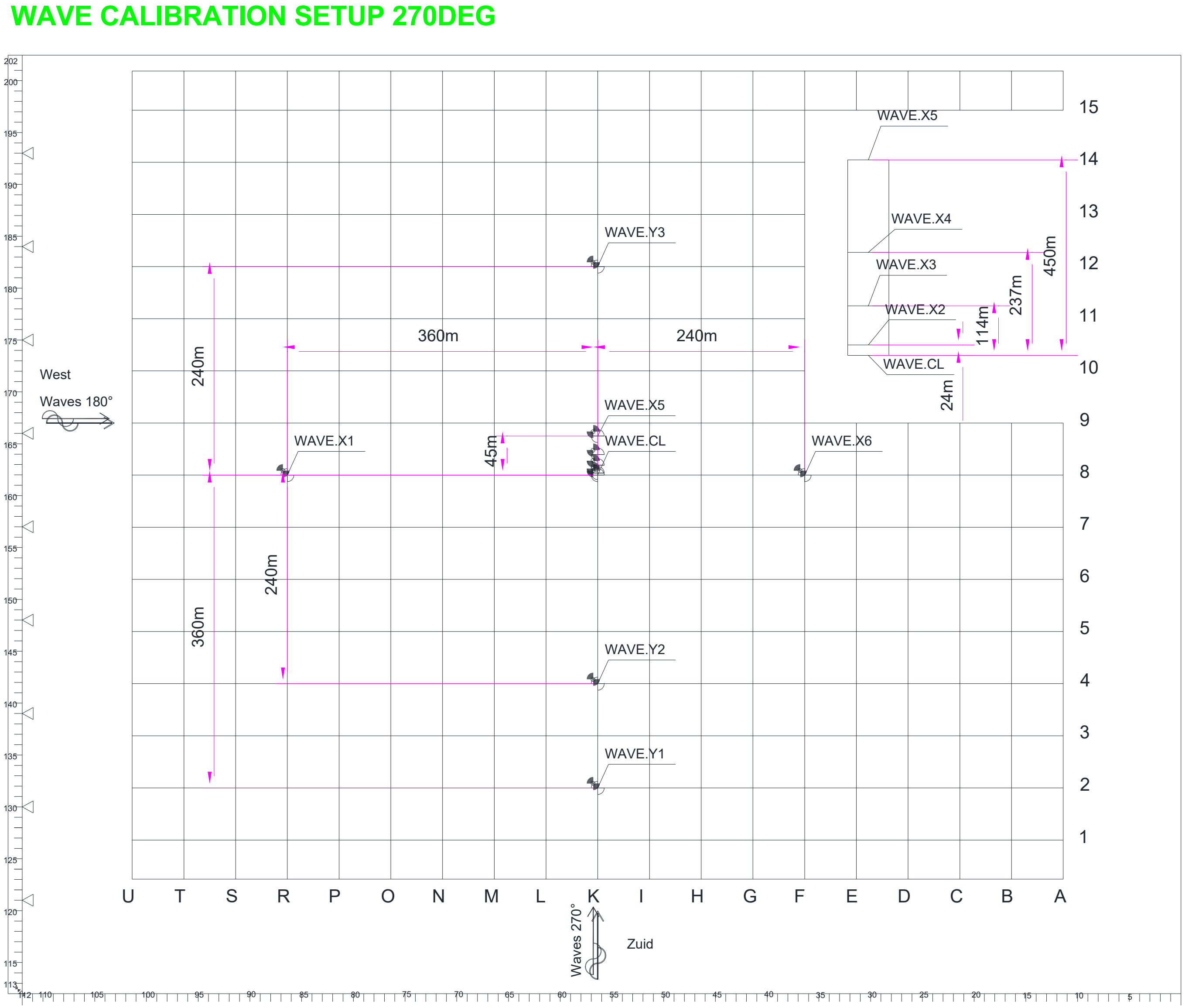

FIGURE 12 JETTY FENDER PLUS DOLPHIN STIFNESS

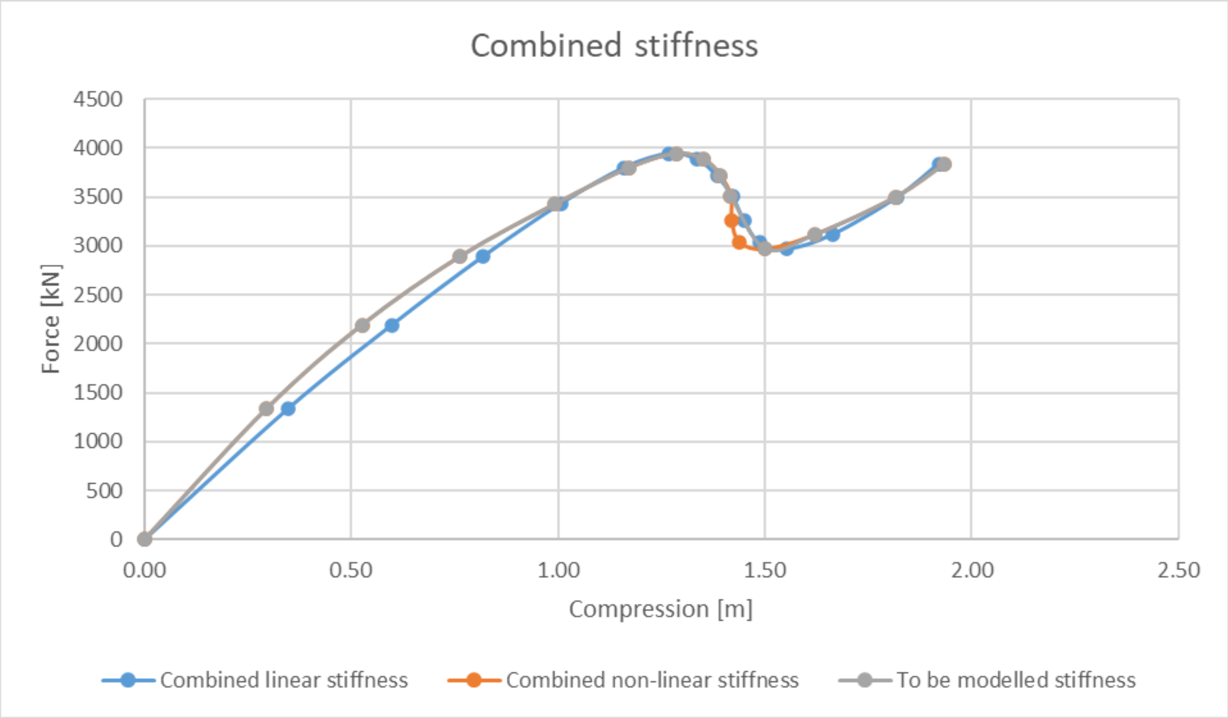

FIGURE 13 JETTY FENDER 01 STIFFNESS CHECK

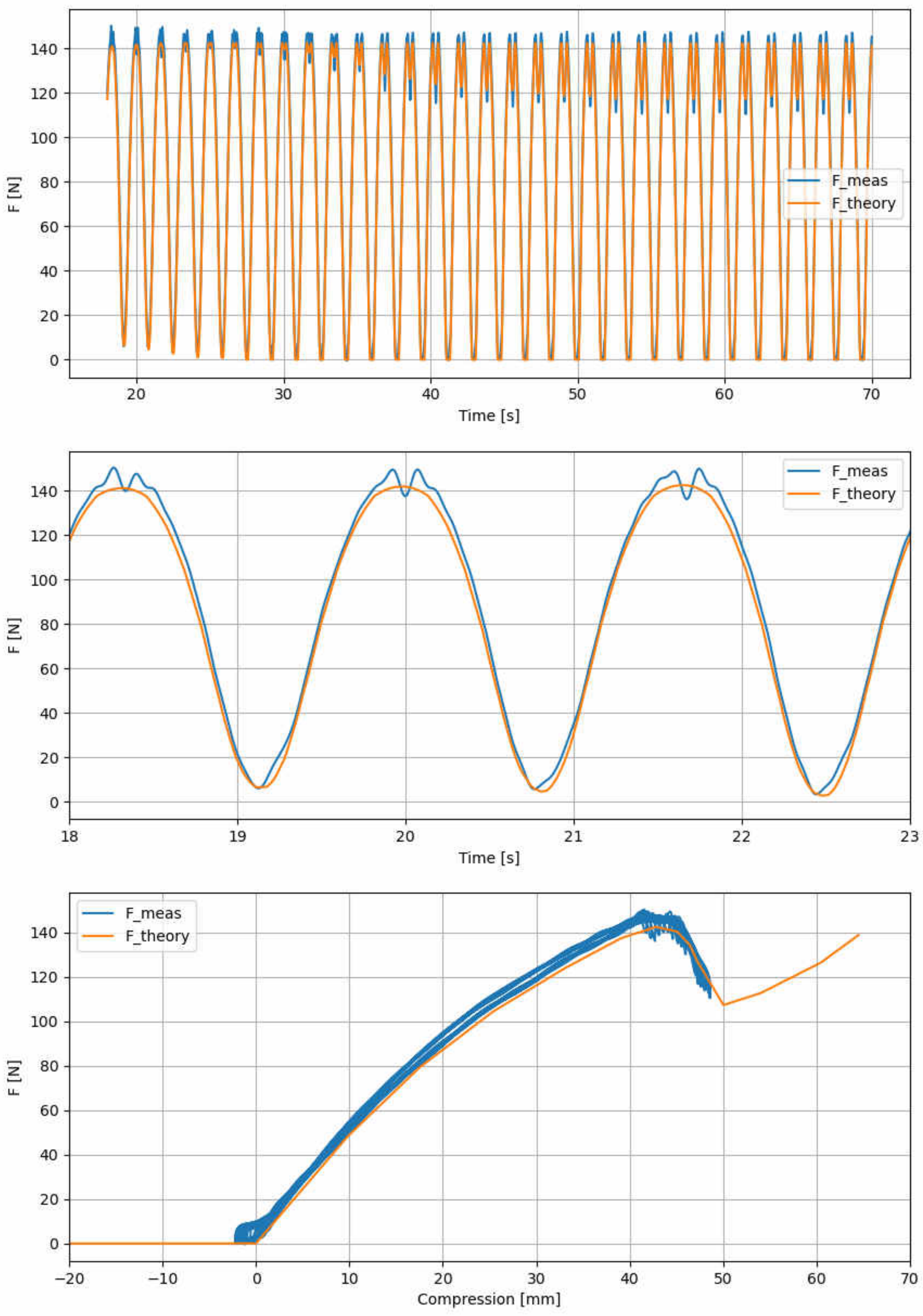

FIGURE 14 JETTY FENDER 02 STIFFNESS CHECK

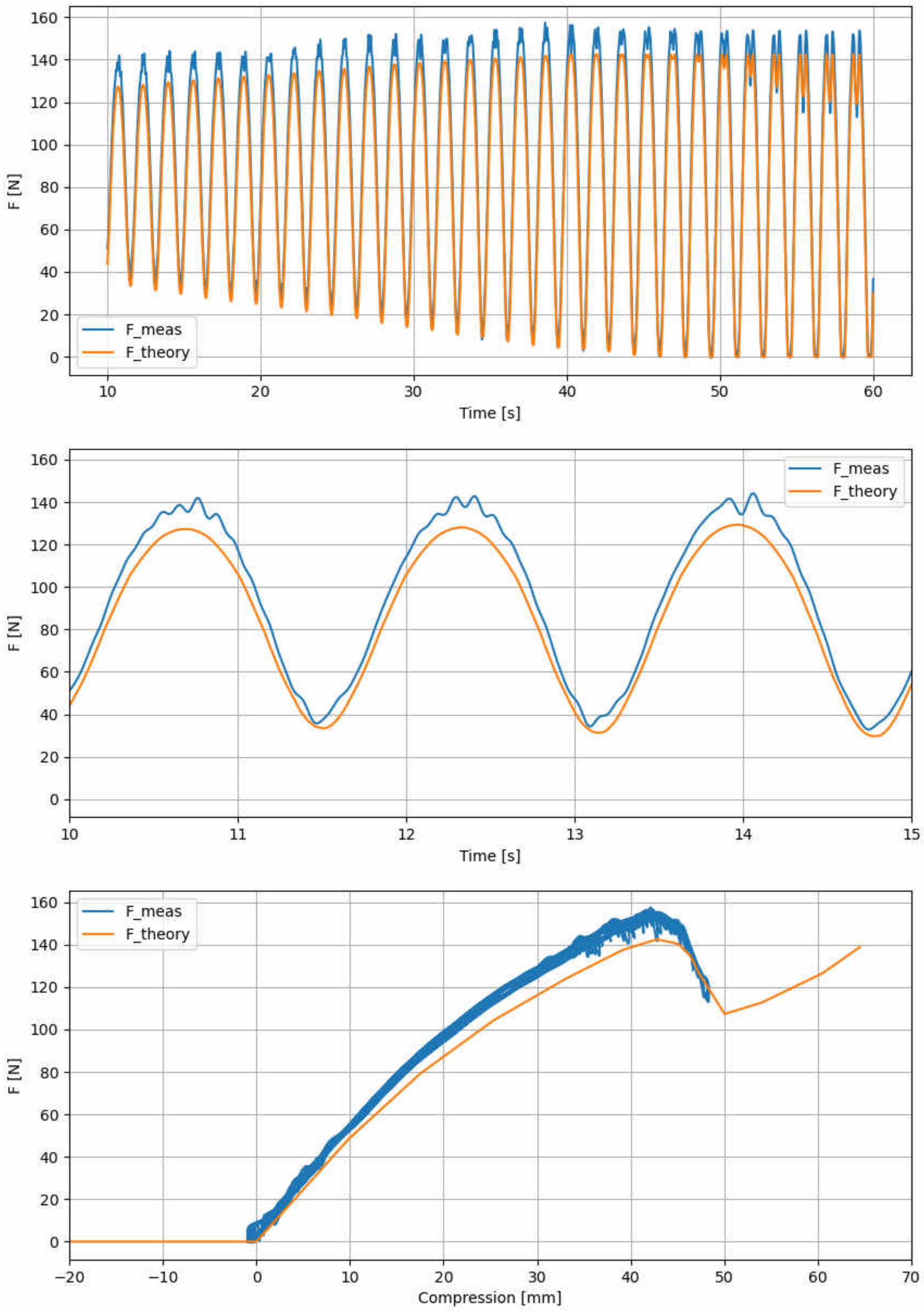

FIGURE 15 JETTY FENDER 03 STIFFNESS CHECK

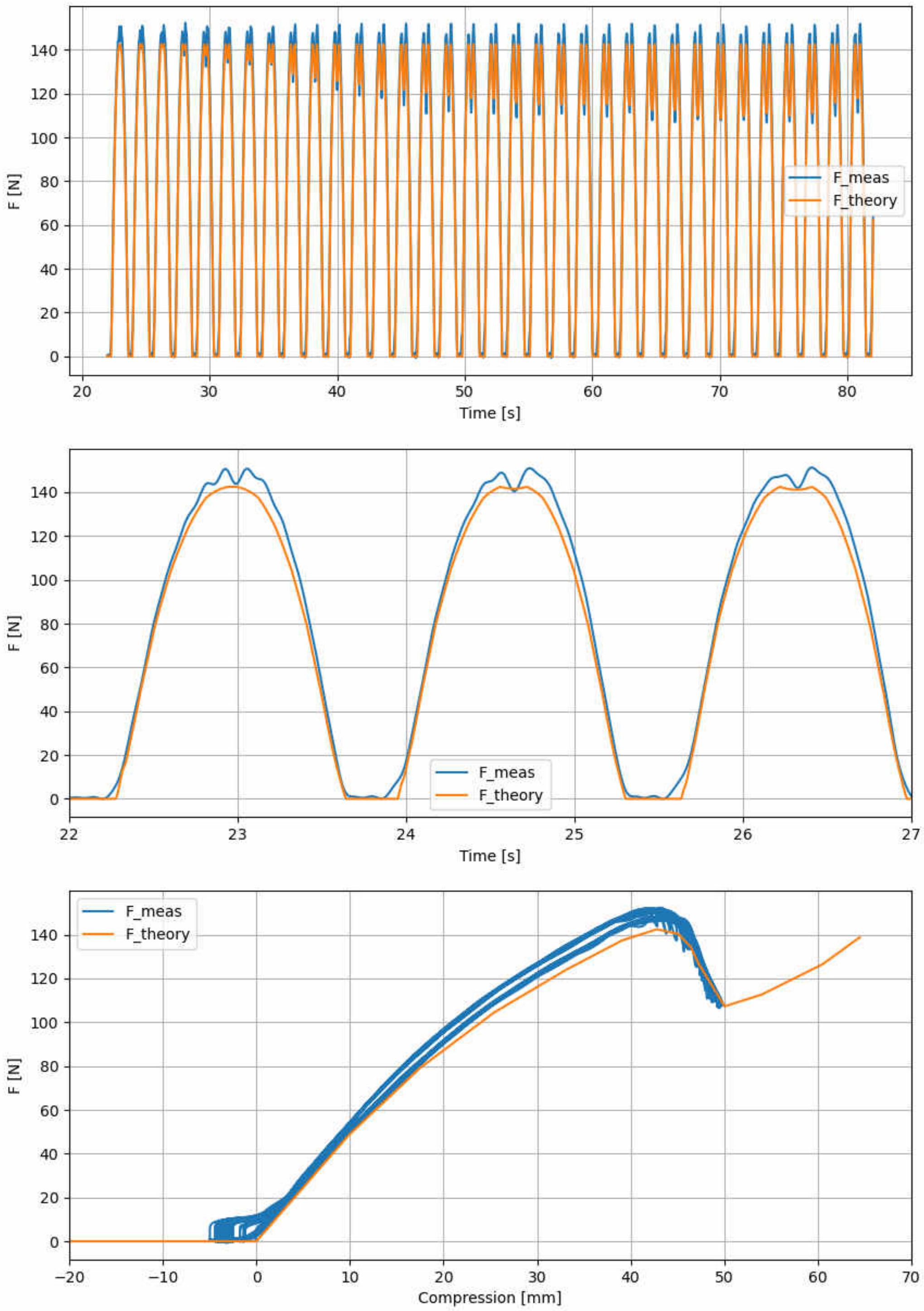

FIGURE 16 JETTY FENDER 04 STIFFNESS CHECK

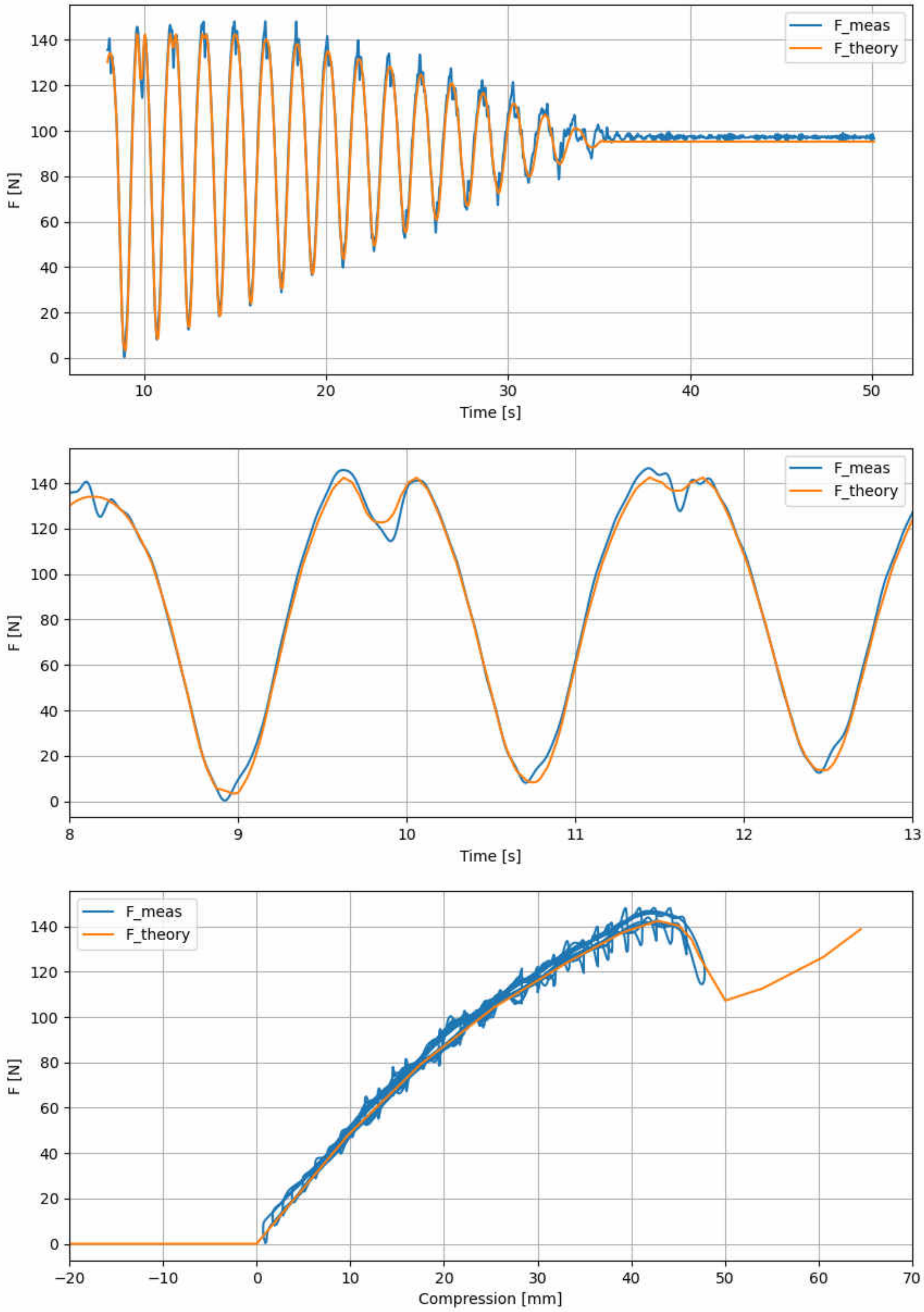

FIGURE 17 JETTY FENDER 05 STIFFNESS CHECK

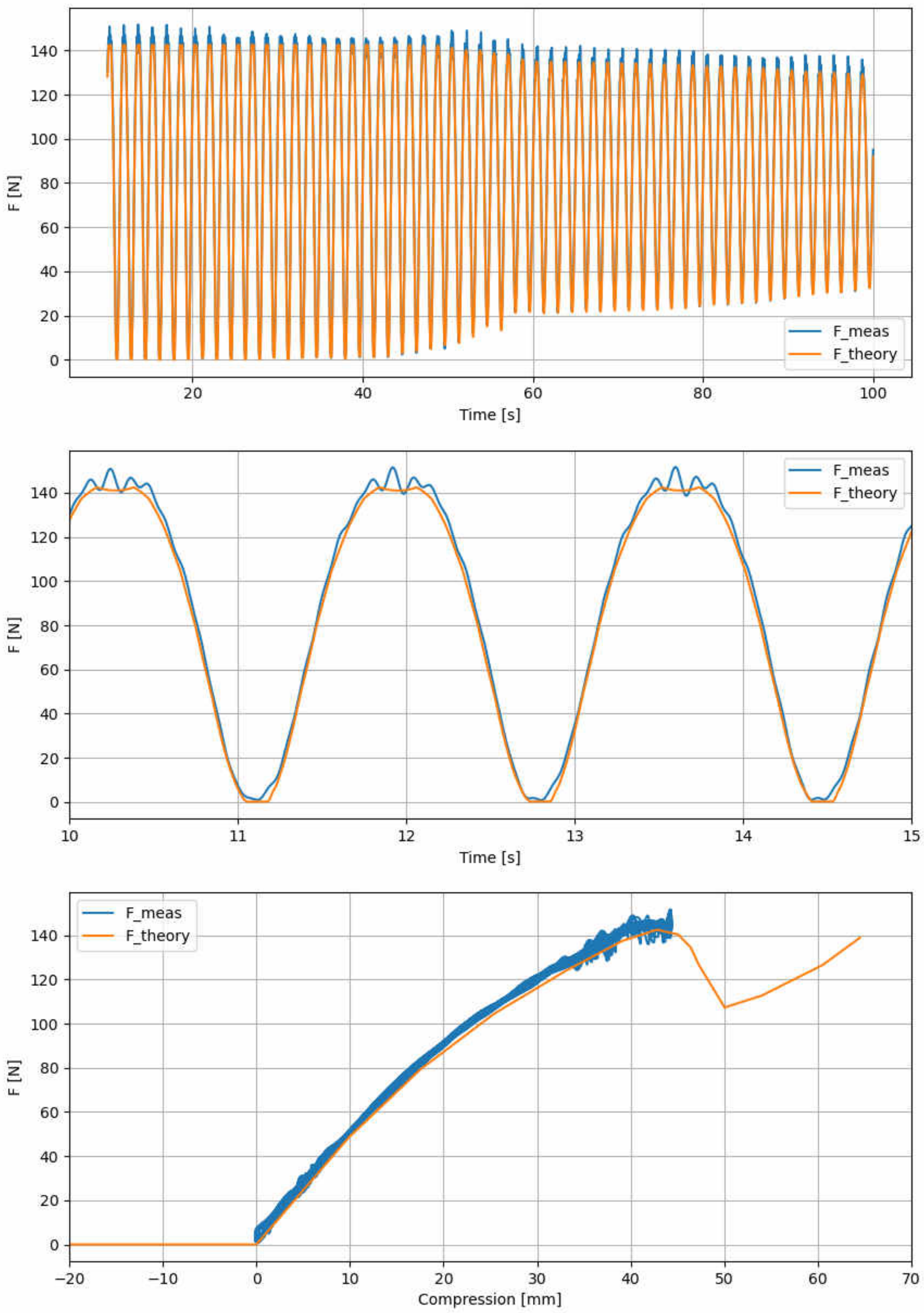

FIGURE 18 JETTY FENDER 06 STIFFNESS CHECK

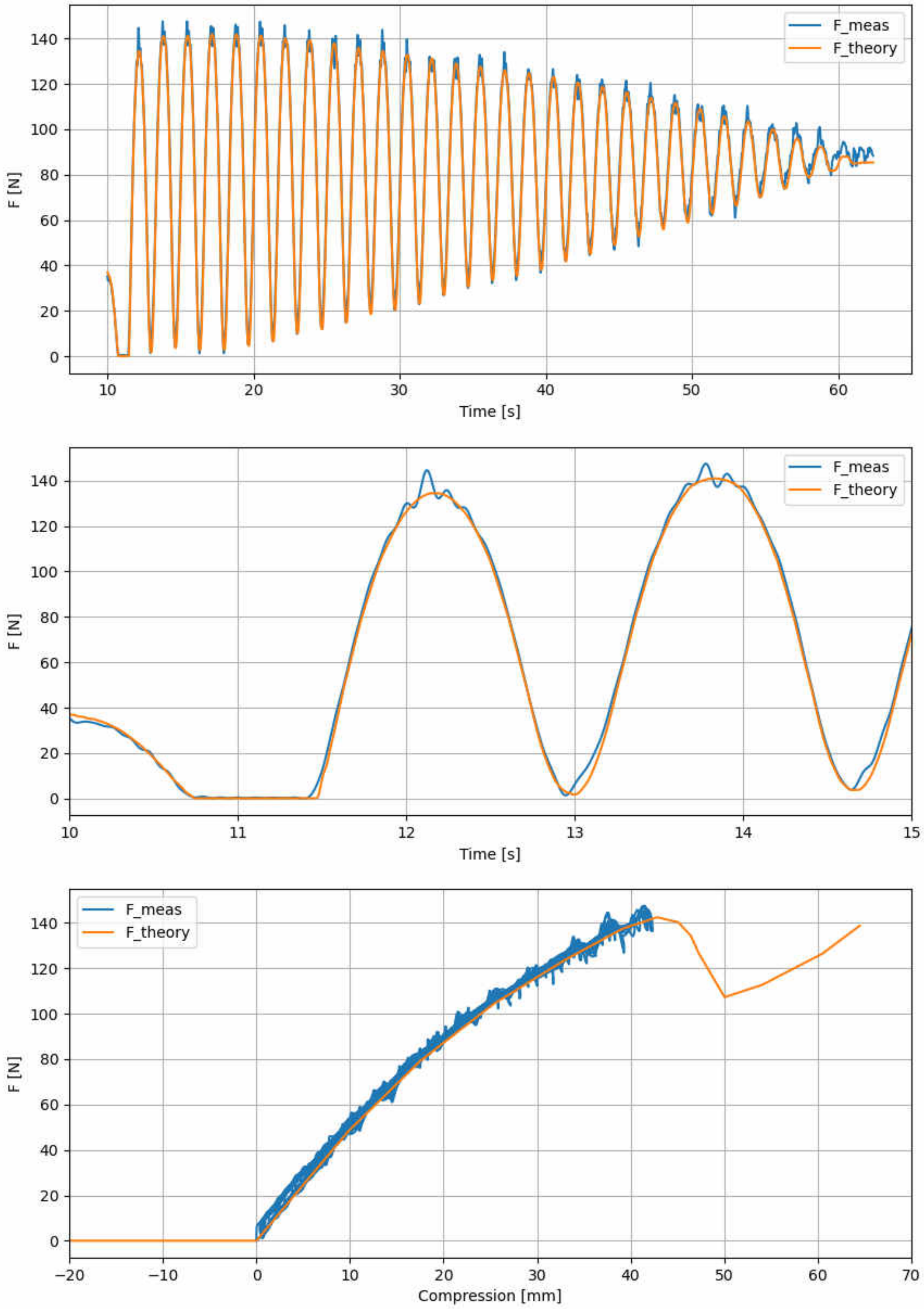

FIGURE 19 SBS FENDERS AS BUILT STIFFNESSES

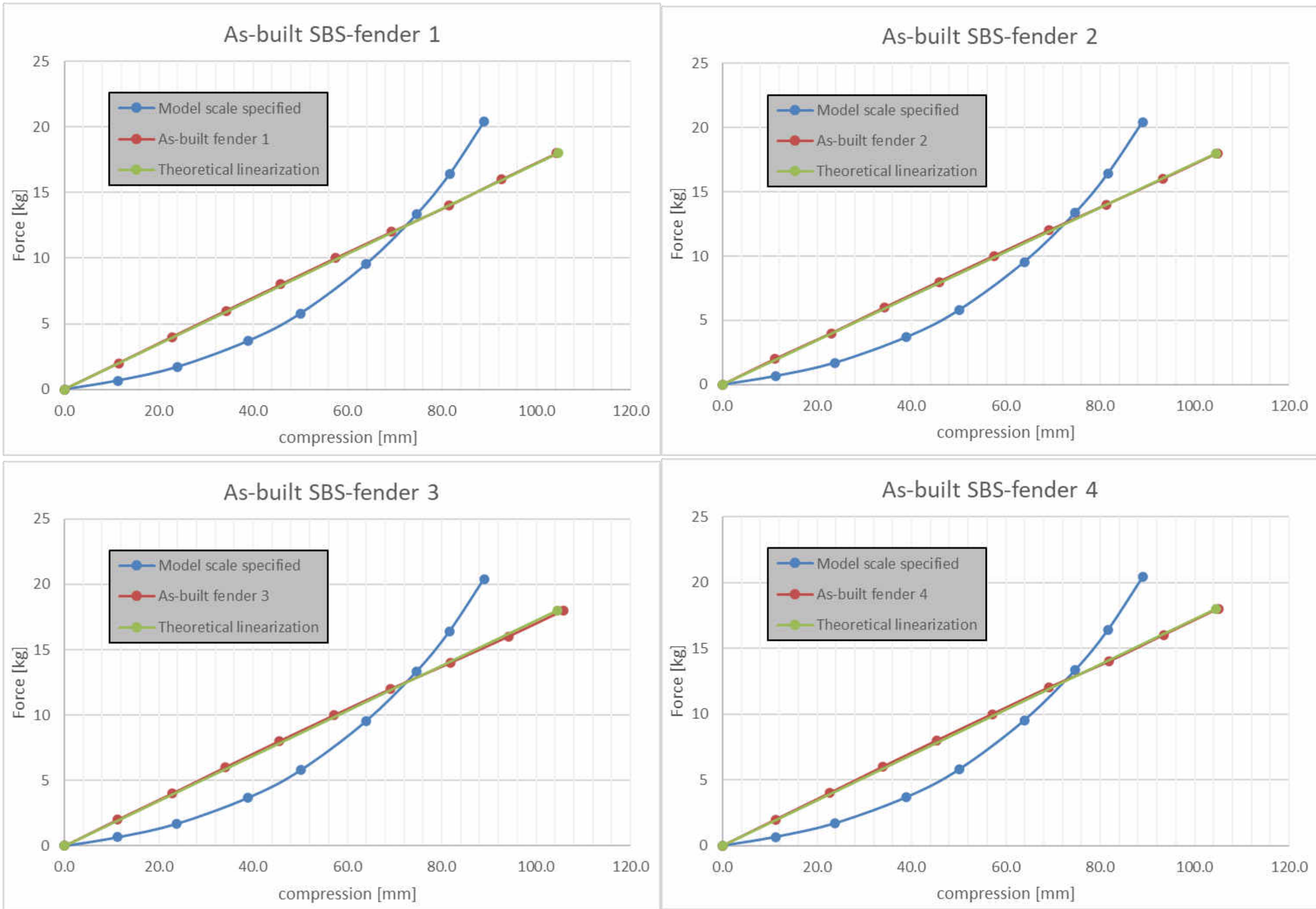

FIGURE 20 THEORETICAL LINE STIFFNESS OF BUNDLED FSRU JETTY LINES

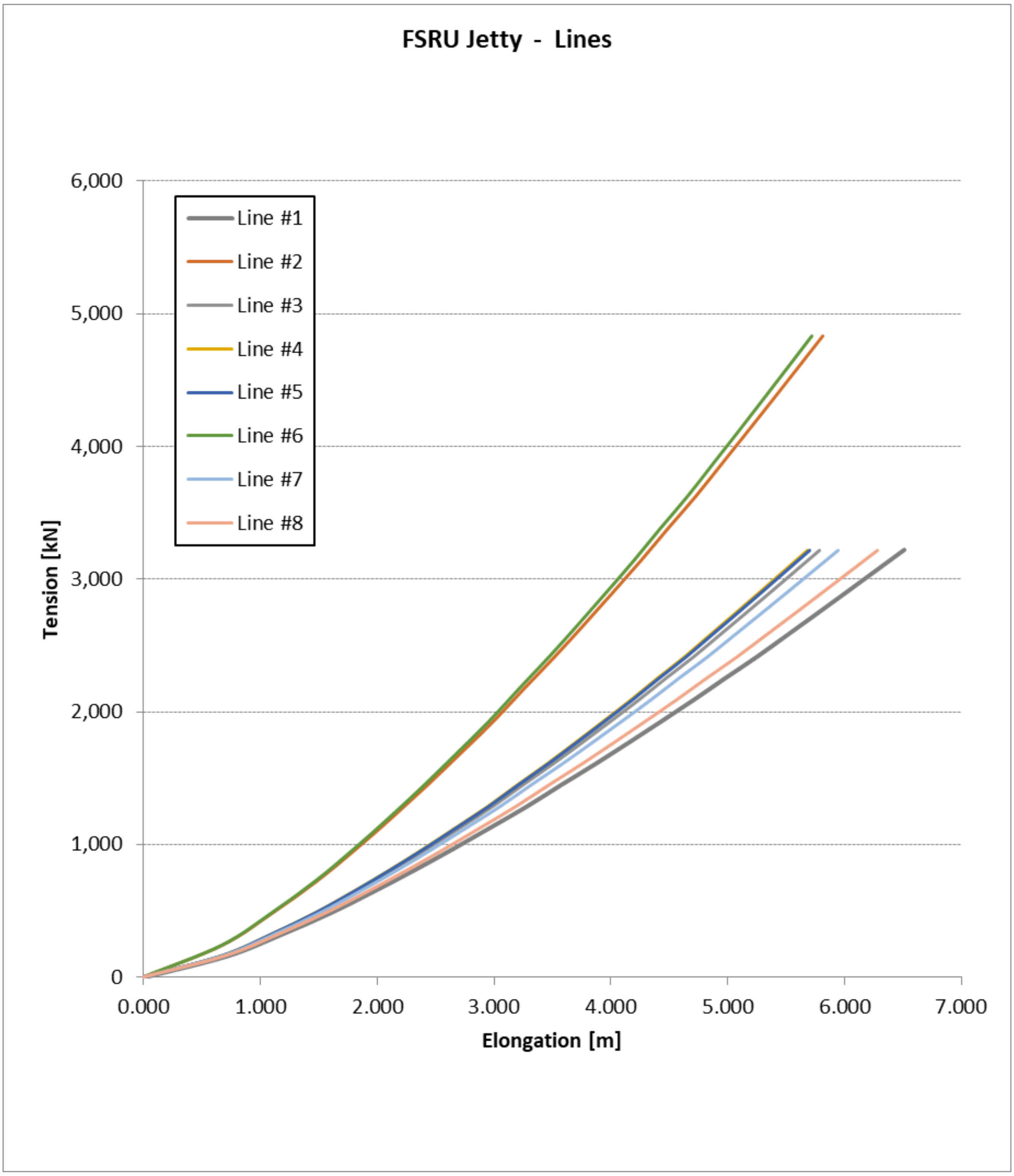

FIGURE 21 THEORETICAL LINE STIFFNESS OF BUNDLED SBS MOORING LINES

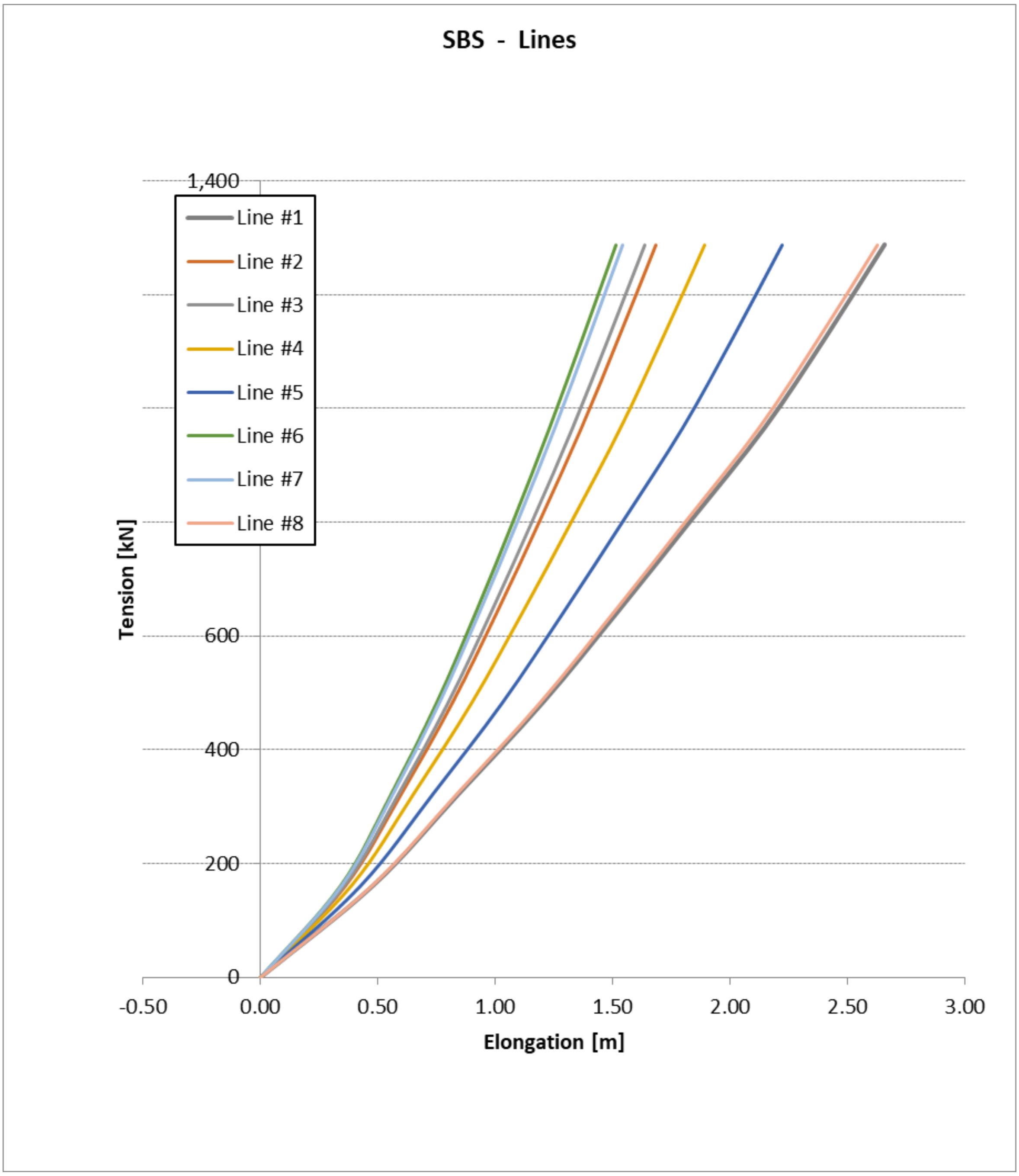

FIGURE 22 THEORETICAL VS BILINEARIZED LINE STIFFNESS OF BUNDLED JETTY MOORING LINES I/II

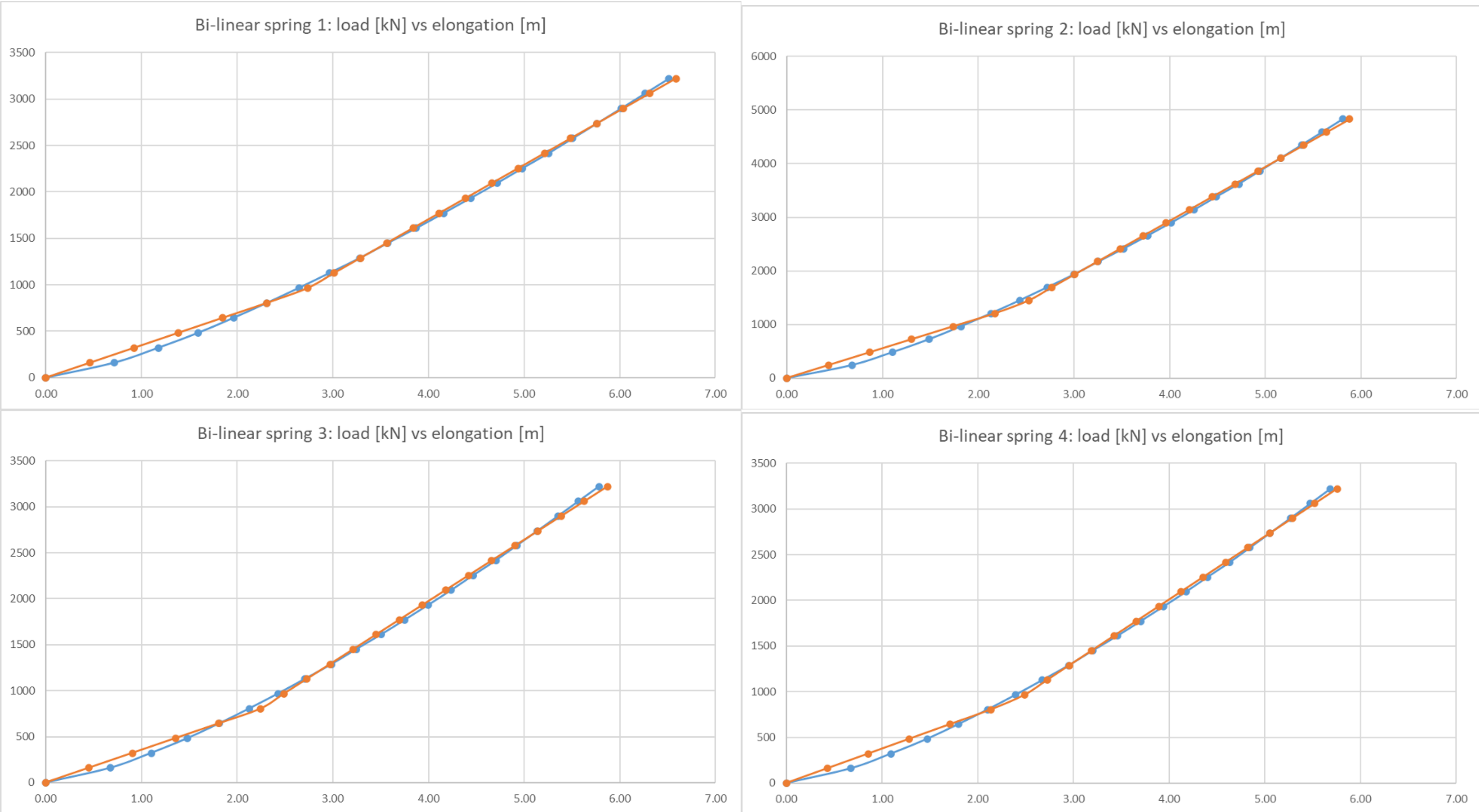

FIGURE 23 THEORETICAL VS BILINEARIZED LINE STIFFNESS OF BUNDLED JETTY MOORING LINES II/II

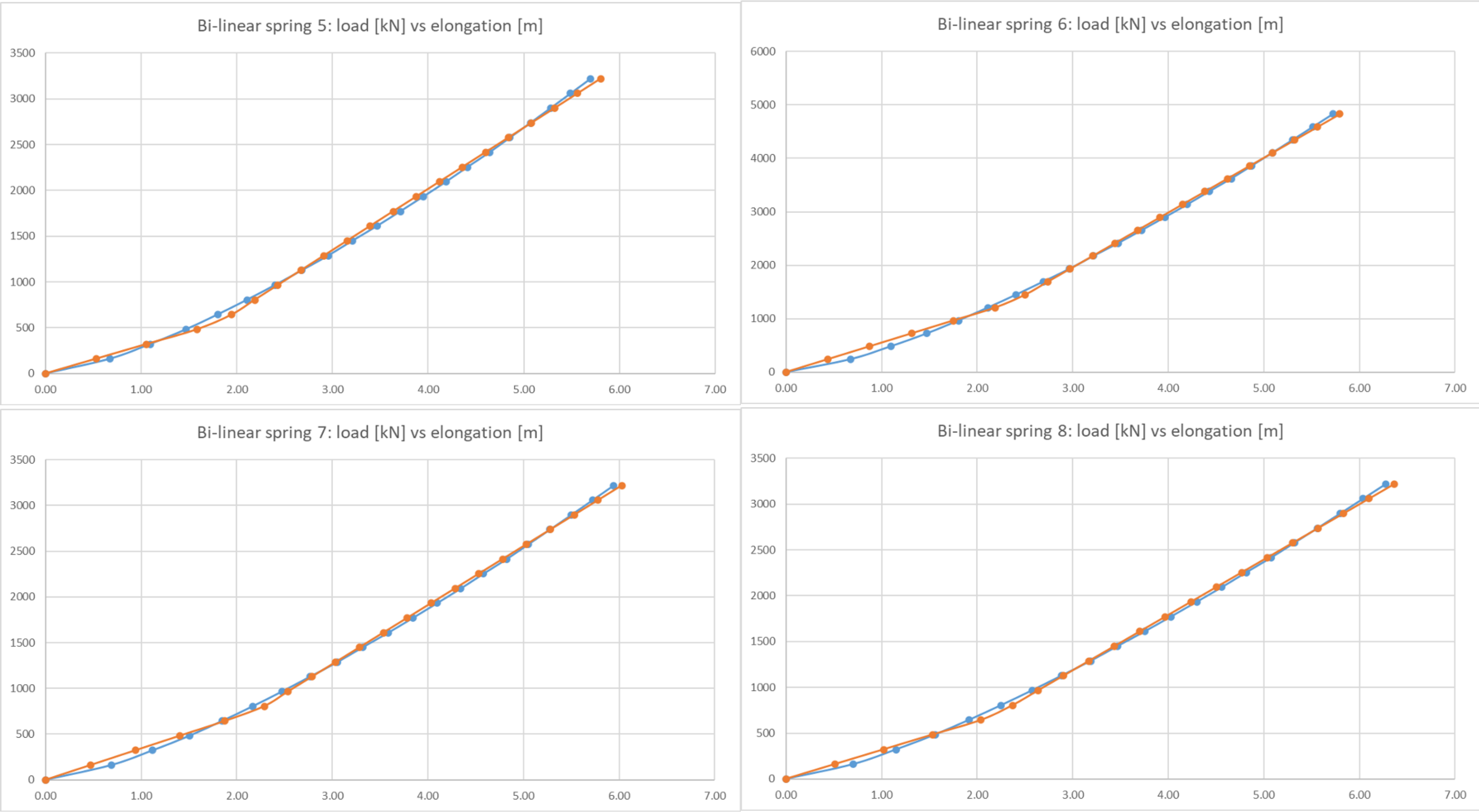

FIGURE 24 THEORETICAL VS BILINEARIZED LINE STIFFNESS OF BUNDLED SBS MOORING LINES I/II

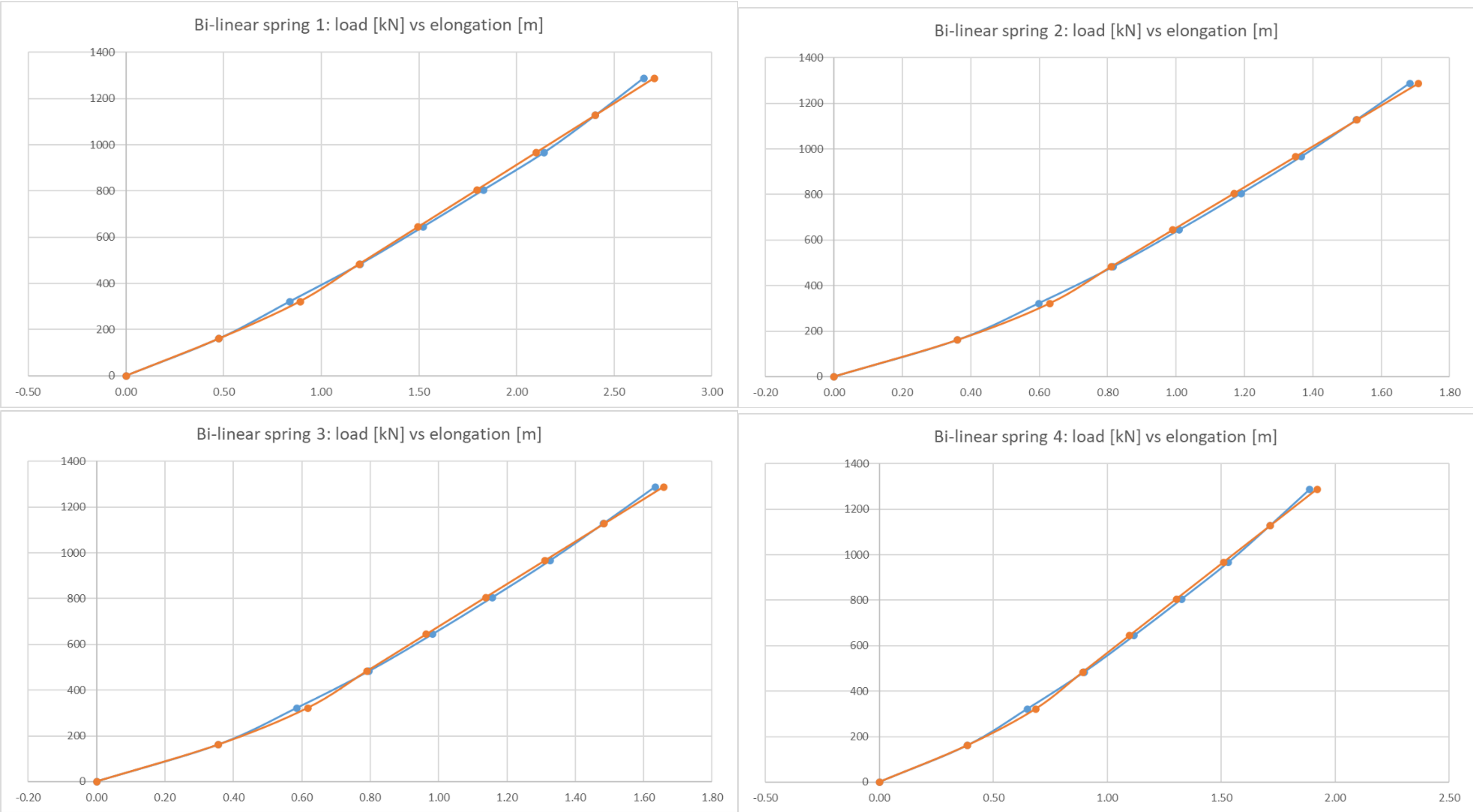

FIGURE 25 THEORETICAL VS BILINEARIZED LINE STIFFNESS OF BUNDLED SBS MOORING LINES II/II

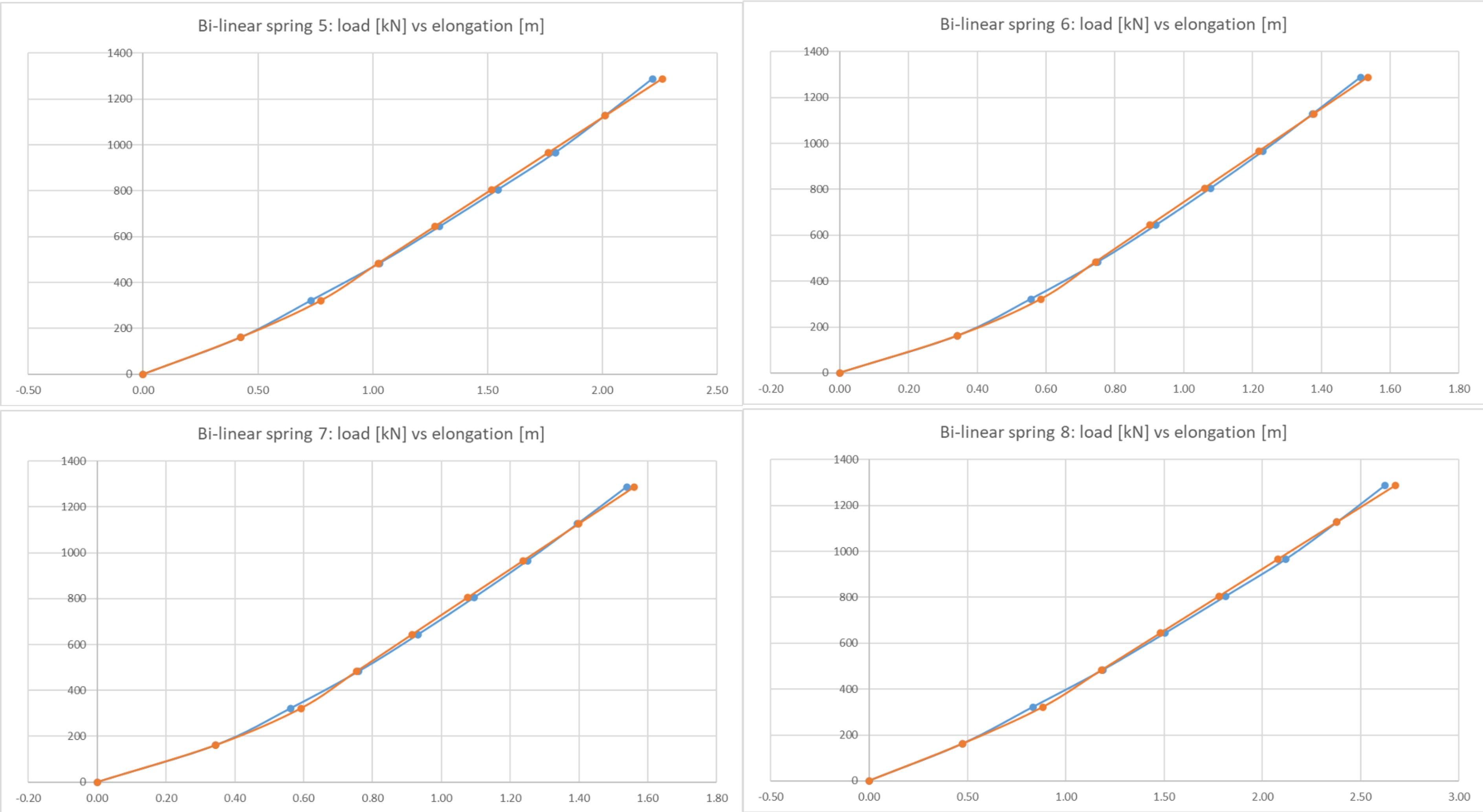

FIGURE 26 MEASURED WAVE SPECTRA - WAVE 10 (LEFT) AND WAVE 11 (RIGHT)
(See table 3 for nomenclature)

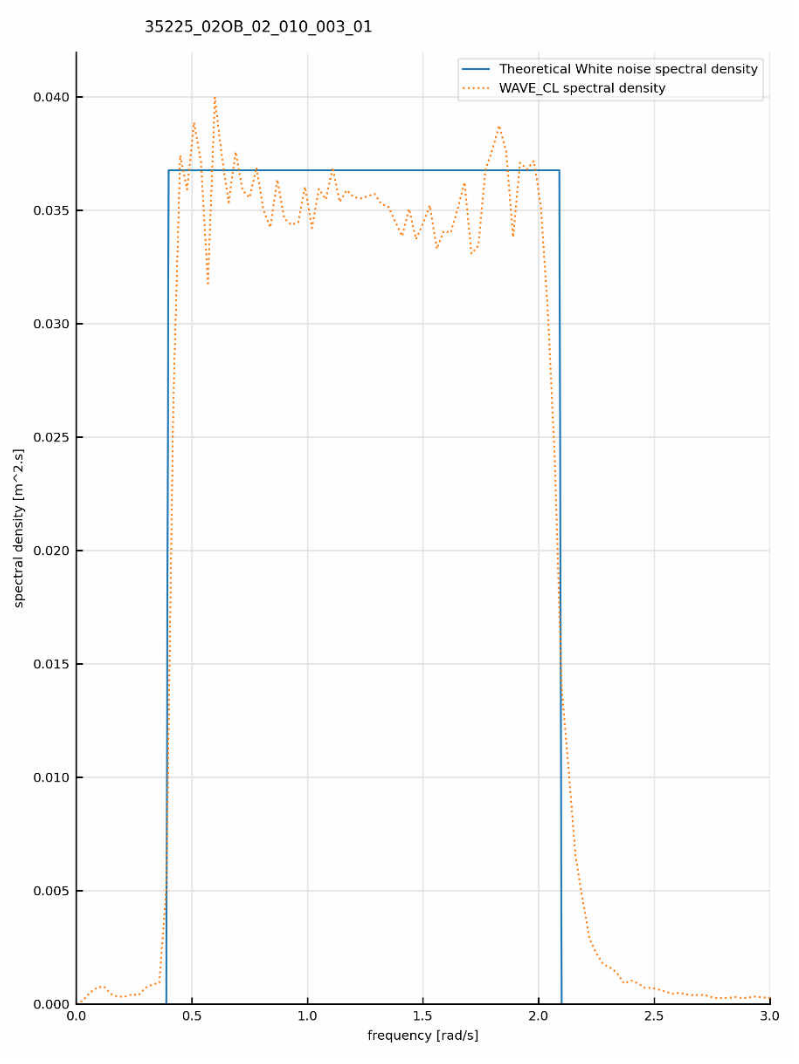

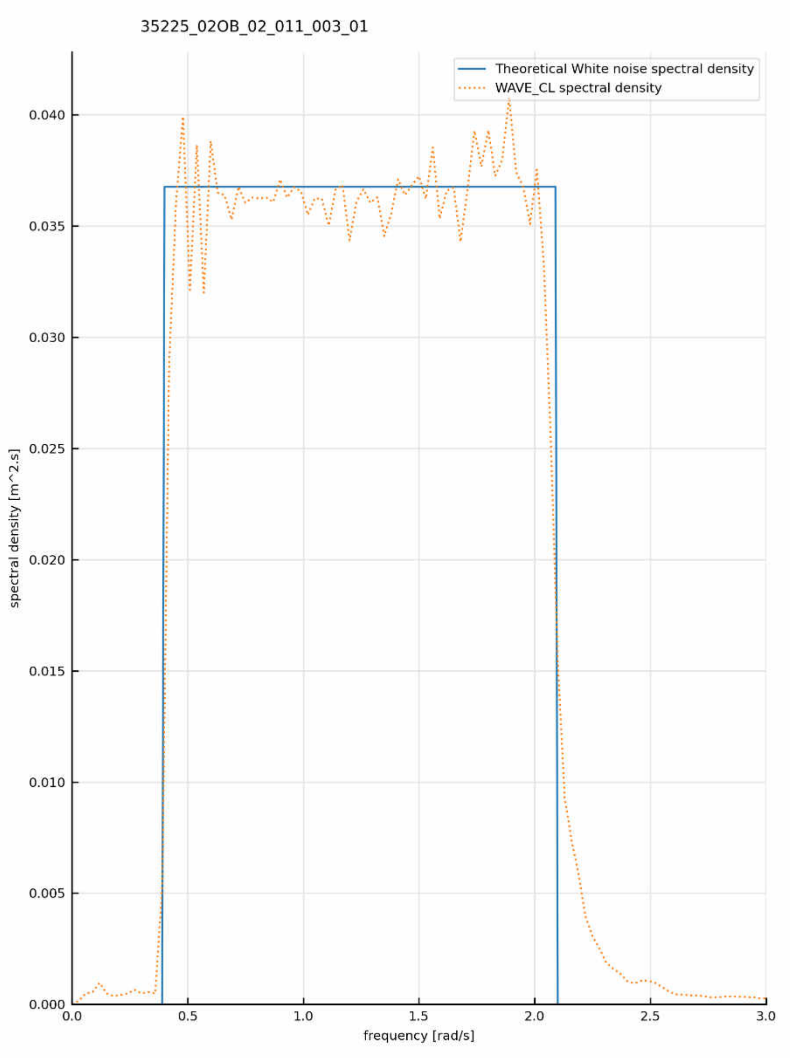

FIGURE 27 MEASURED WAVE SPECTRA - WAVE 12 (LEFT) AND WAVE 13 (RIGHT)
(See table 3 for nomenclature)

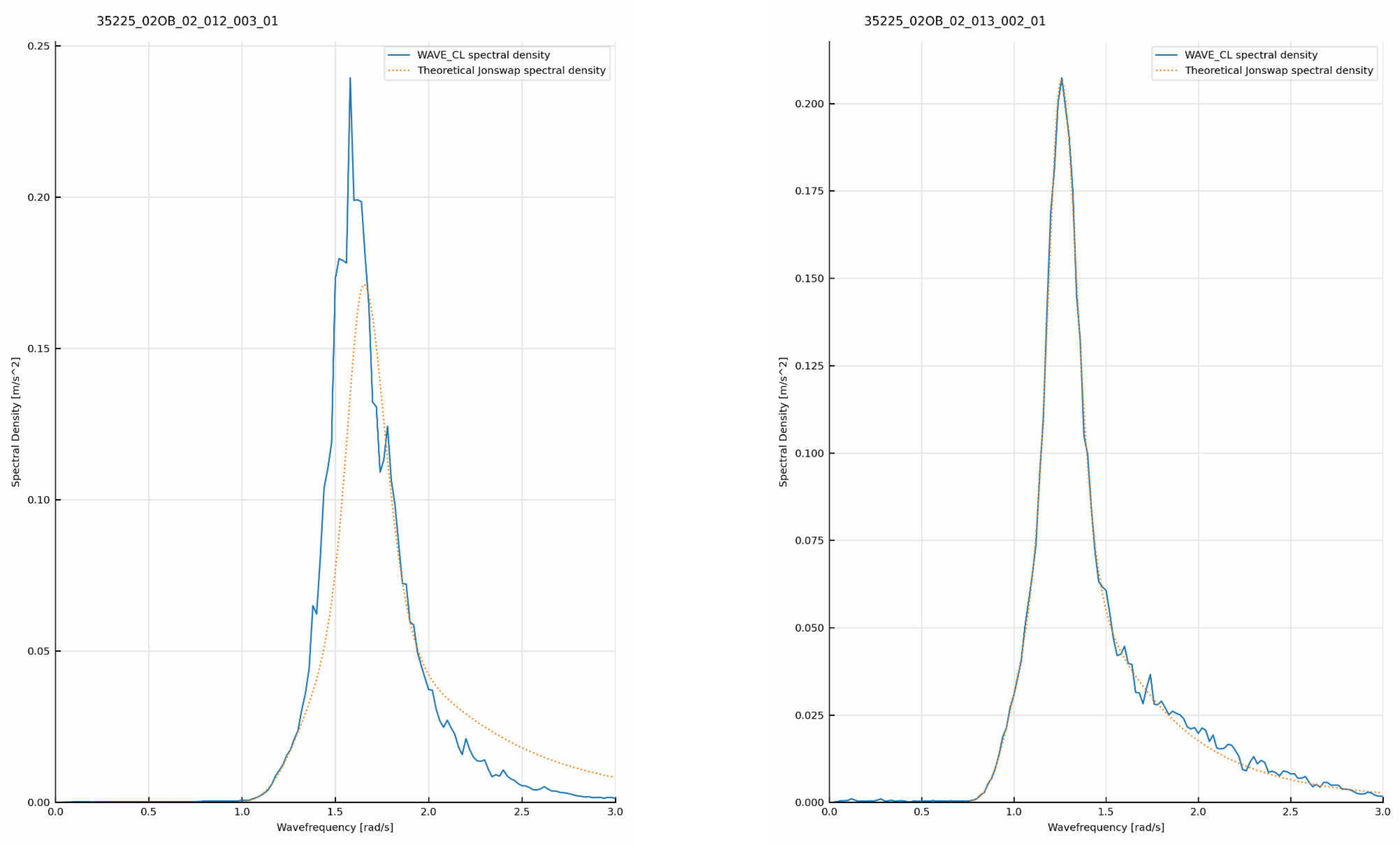

FIGURE 28 MEASURED WAVE SPECTRA - WAVE 14 (LEFT) AND WAVE 15 (RIGHT)
(See table 3 for nomenclature)

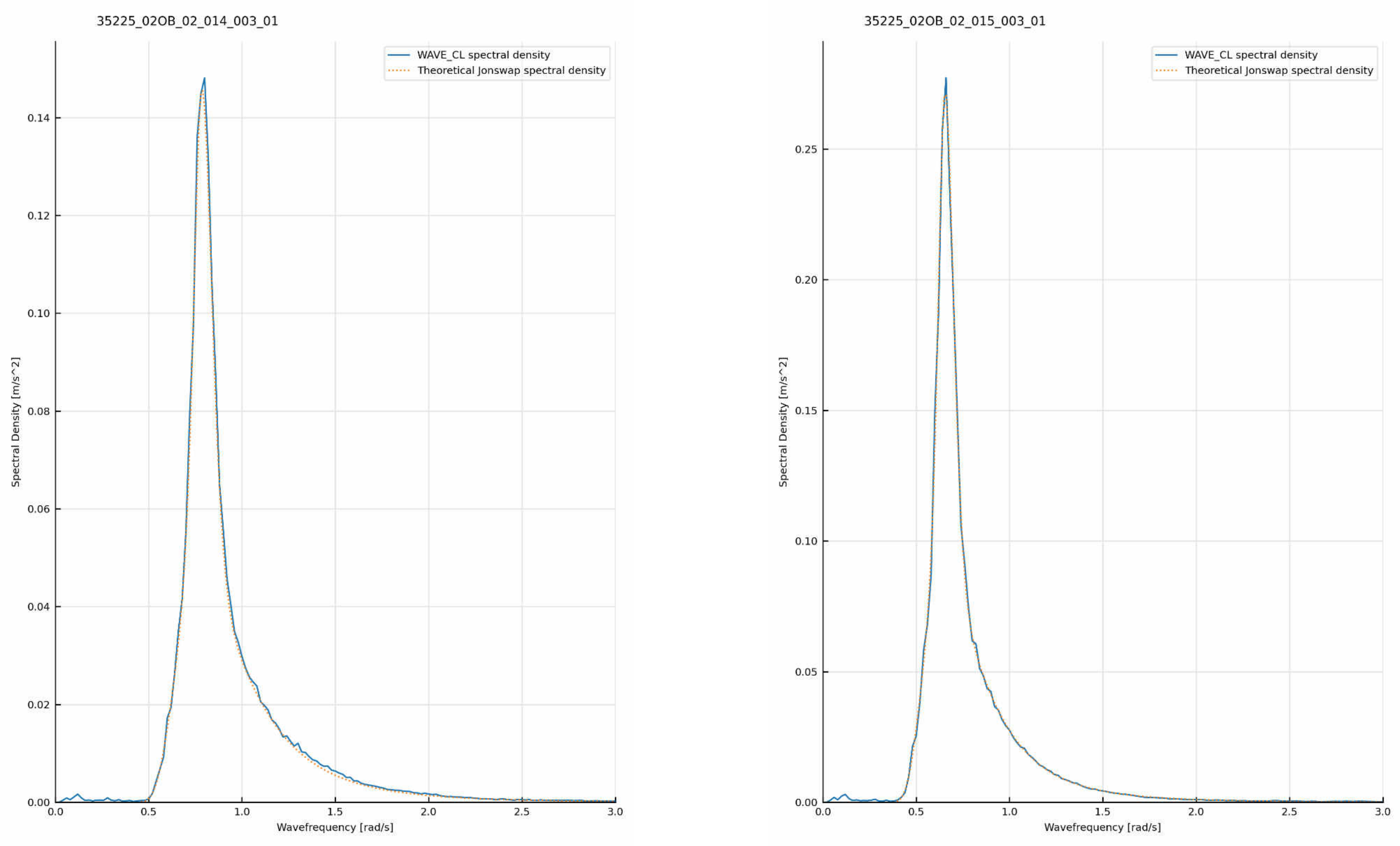

FIGURE 29 MEASURED WAVE SPECTRA - WAVE 16 (LEFT) AND WAVE 17 (RIGHT)
(See table 3 for nomenclature)

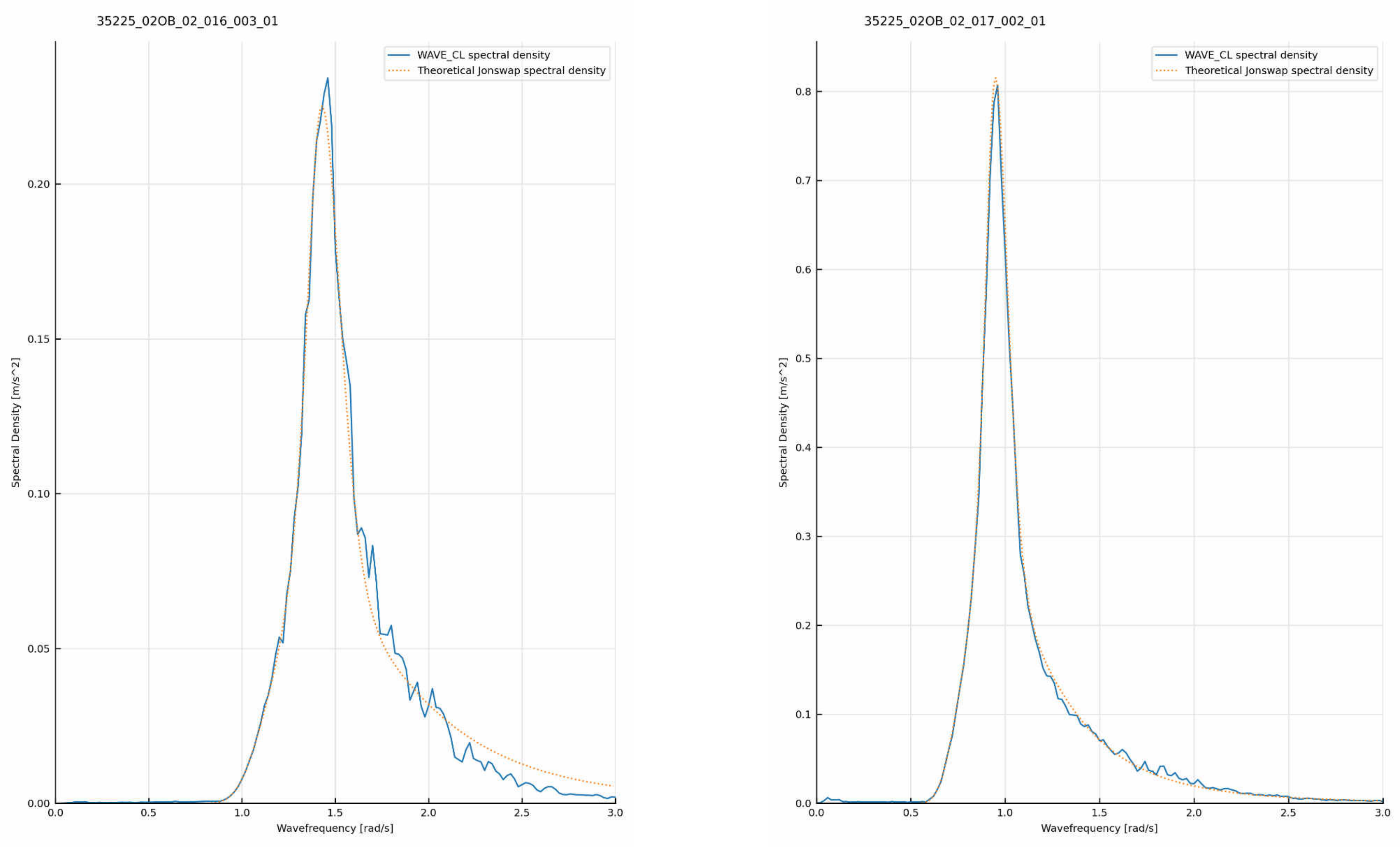

FIGURE 30 MEASURED WAVE SPECTRA - WAVE 18 (LEFT) AND WAVE 19 (RIGHT)
(See table 3 for nomenclature)

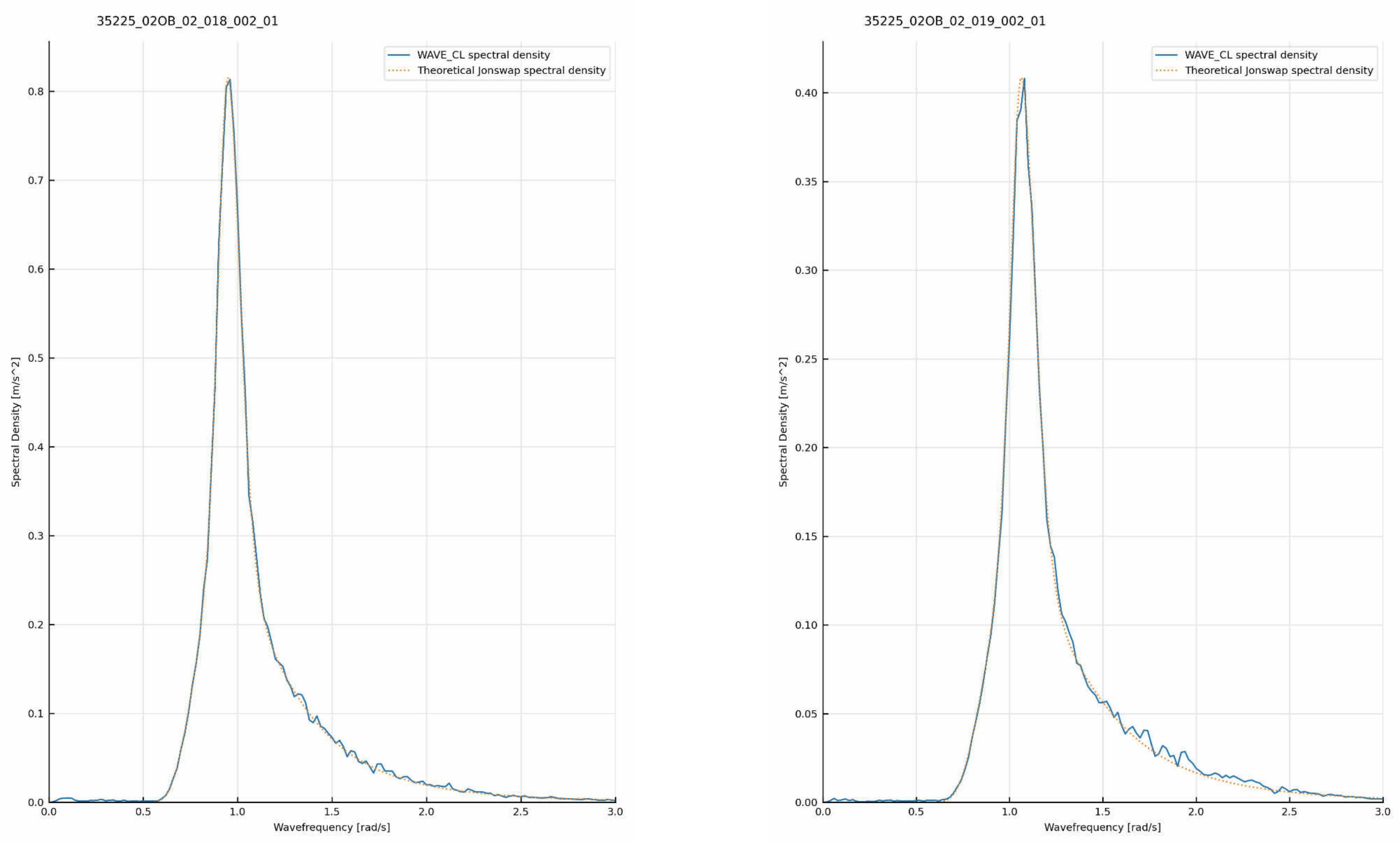

FIGURE 31 MEASURED WAVE SPECTRA - WAVE 20 (LEFT) AND WAVE 21 (RIGHT)
(See table 3 for nomenclature)

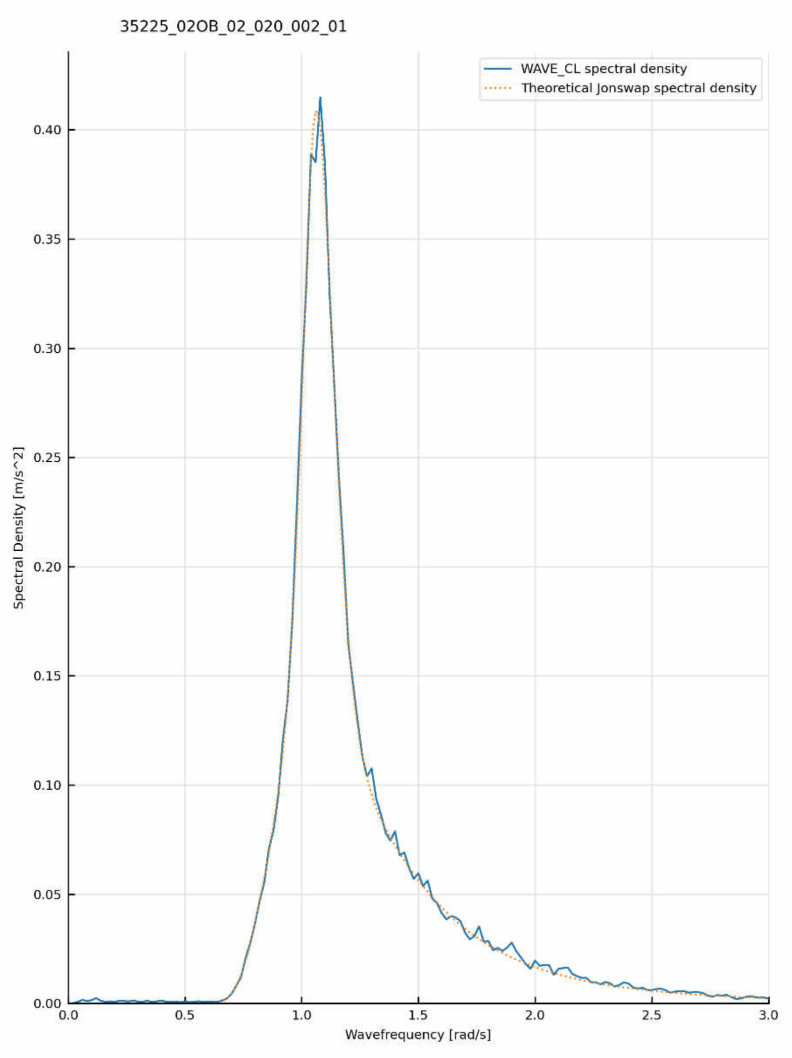

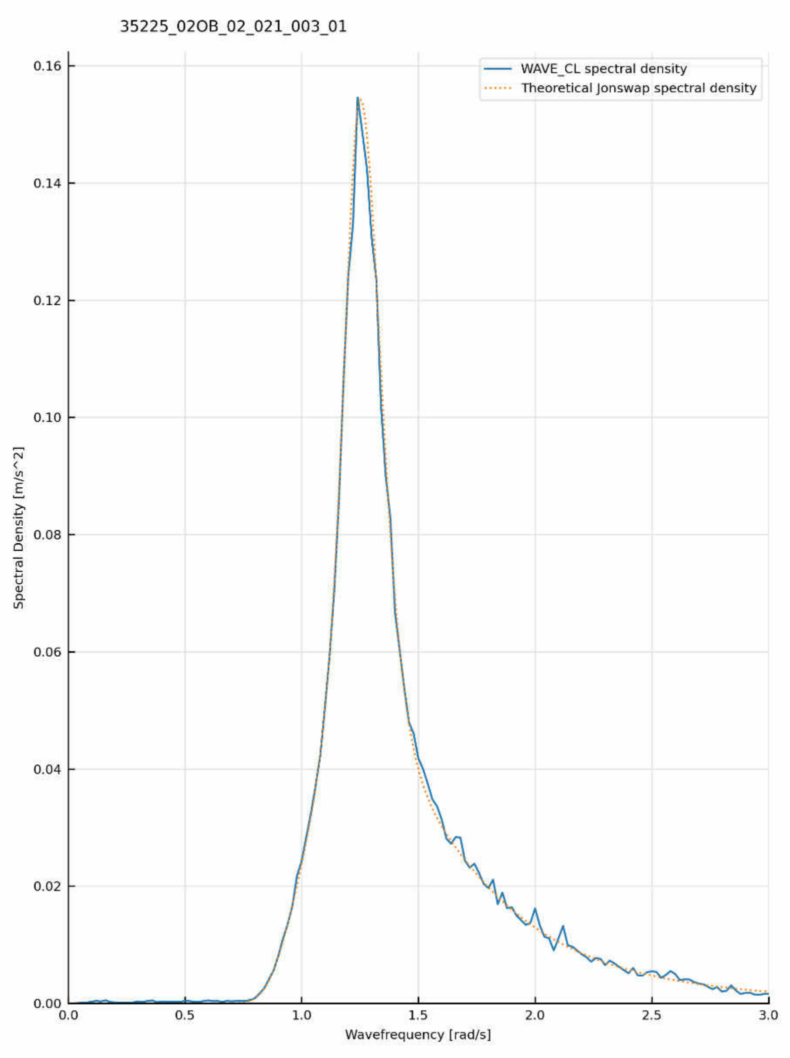

FIGURE 32 MEASURED WAVE SPECTRA - WAVE 22 (LEFT) AND WAVE 23 (RIGHT)
(See table 3 for nomenclature)

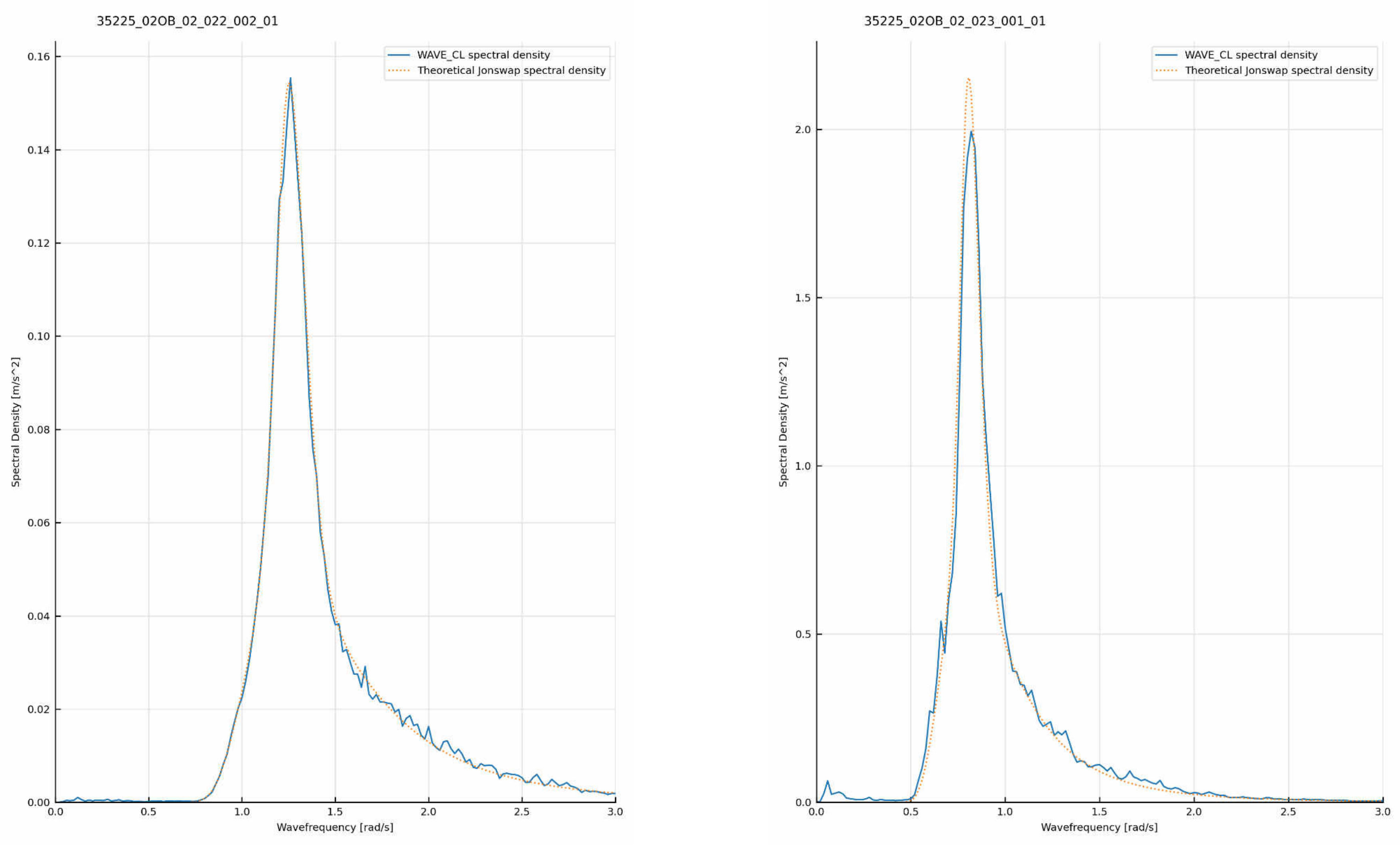

FIGURE 33 MOTION RAOS FSRU - WAVE INCIDENCE ANGLE 10DEGREES (ROTATIONAL)

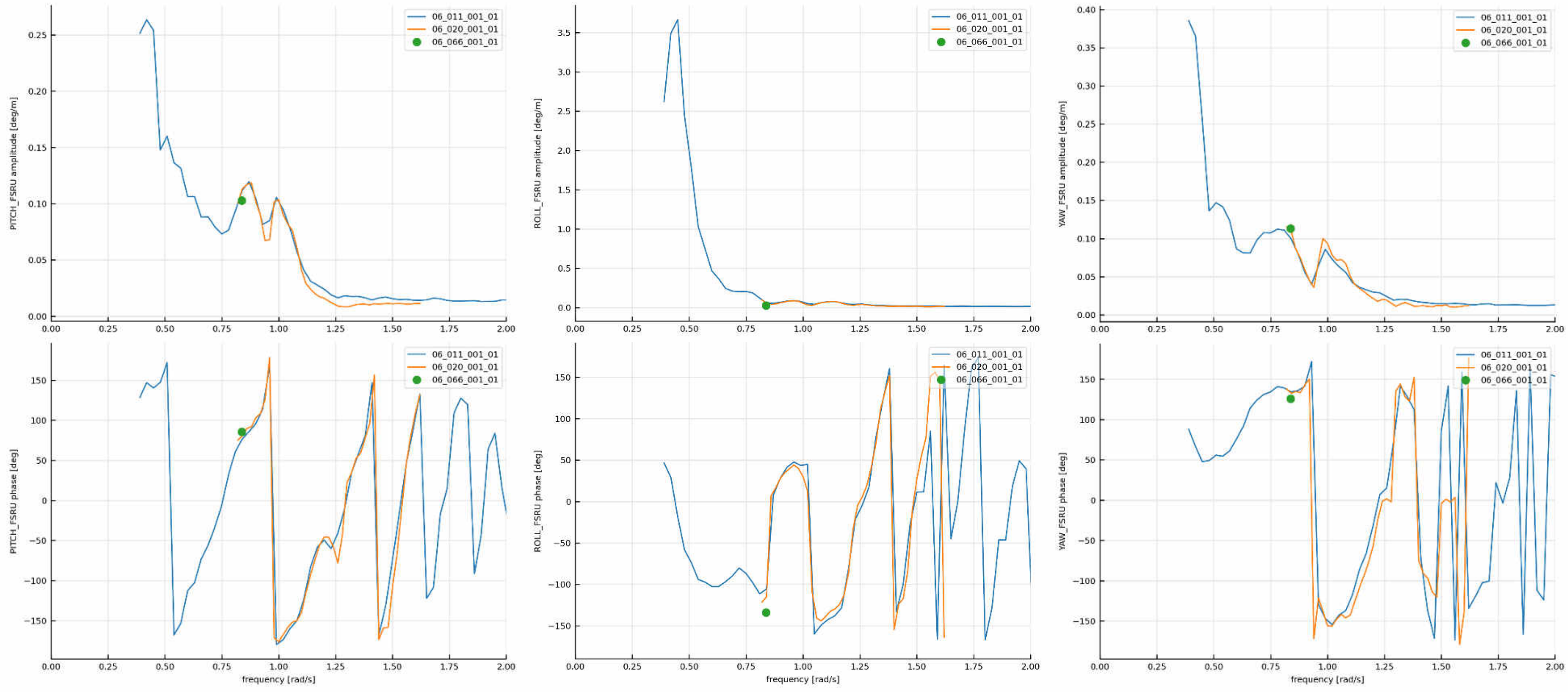

FIGURE 34 MOTION RAOS FSRU - WAVE INCIDENCE ANGLE 10DEGREES (TRANSLATIONAL)

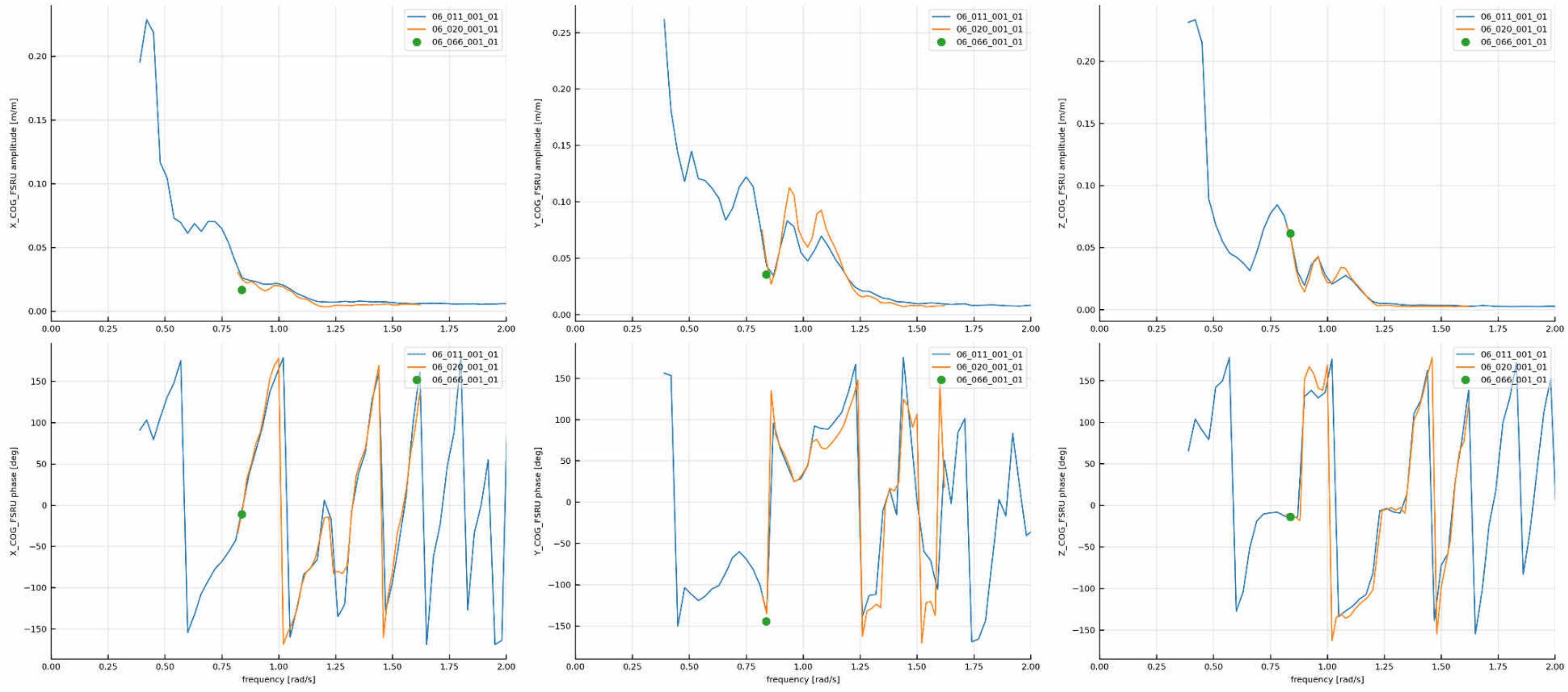

FIGURE 35 MOTION RAOS LNGC - WAVE INCIDENCE ANGLE 10DEGREES (ROTATIONAL)

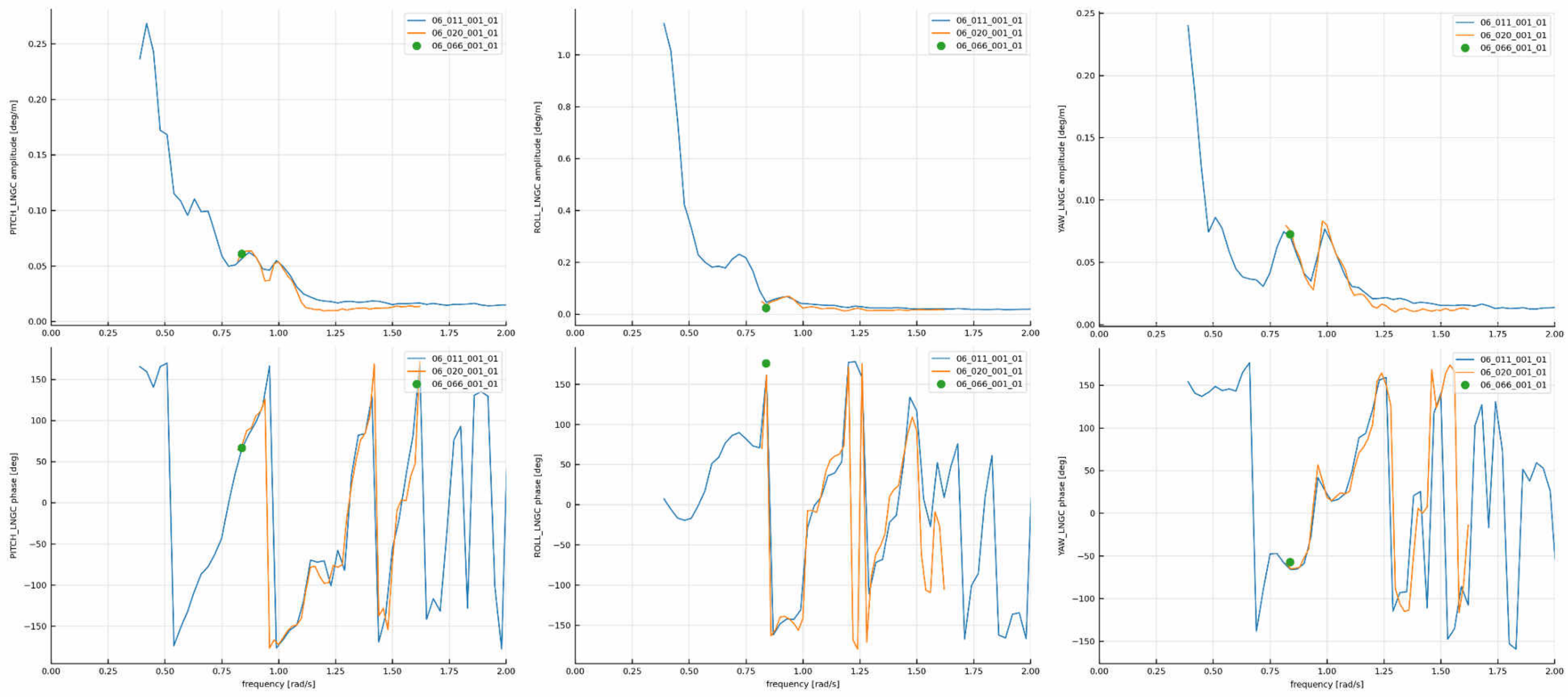

FIGURE 36 MOTION RAOS LNGC - WAVE INCIDENCE ANGLE 10DEGREES (TRANSLATIONAL)

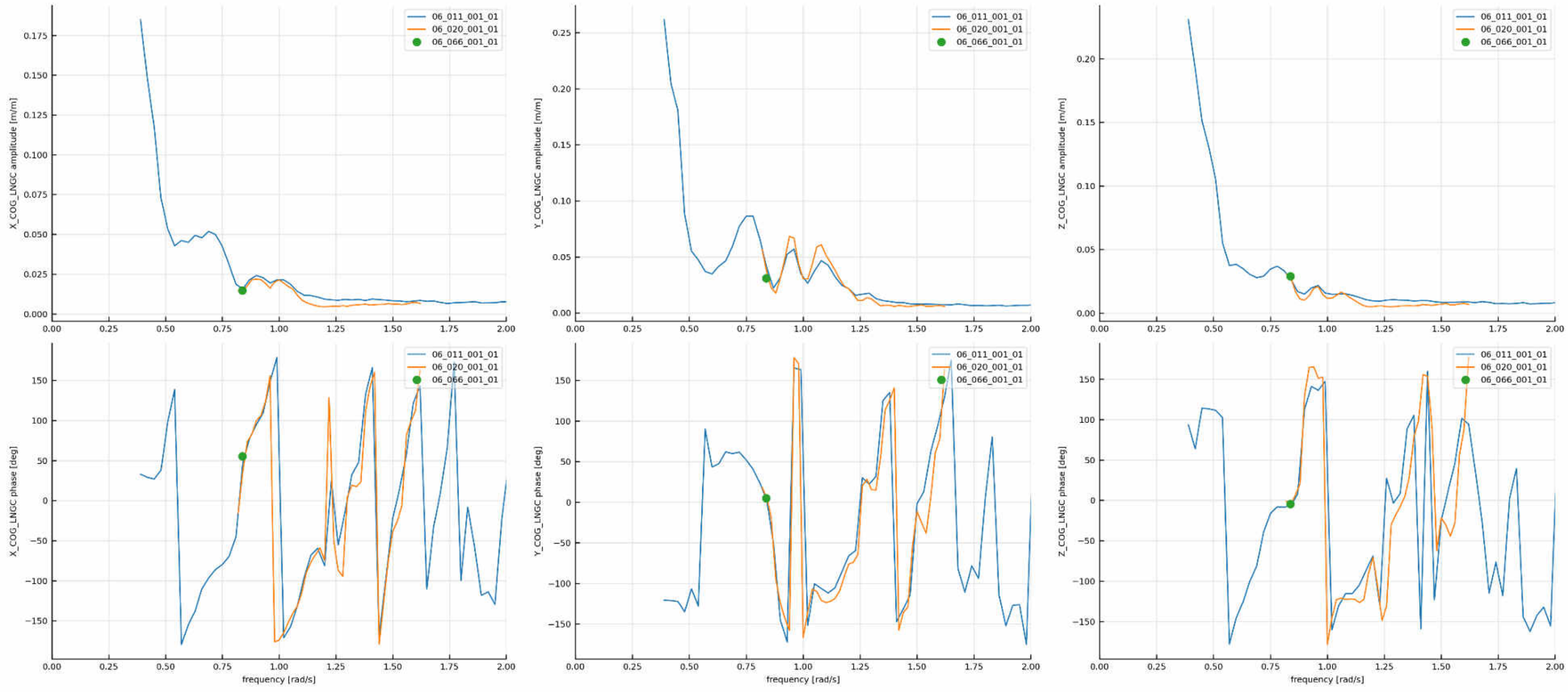

PHOTOGRAPHS

PHOTO 1 WALL PHOTO OF MODEL FSRU (M10446)

PHOTO 2 WALL PHOTO OF PORT FSRU (PARTIAL PORT SIDE FORE)

PHOTO 3 WALL PHOTO OF PORT FSRU (PARTIAL PORT SIDE AFT)

PHOTO 4 CLOSE UP OF MODEL FSRU: STERN

PHOTO 5 CLOSE UP OF MODEL FSRU (STARBOARD AFT)

PHOTO 6 CLOSE UP OF MODEL FSRU (PORT SIDE AFT)

PHOTO 7 CLOSE UP OF MODEL FSRU (PORT SIDE VIEW OF SKEG)

PHOTO 8 CLOSE UP OF BILGE KEELS FSRU

PHOTO 9 CLOSE UP OF BOW FSRU

PHOTO 10 WALL PHOTO OF MODEL LNGC (M10447)

PHOTO 11 WALL PHOTO OF MODEL STARBOARD LNGC (PARTIAL STARBOARD AFT)

PHOTO 12 WALL PHOTO OF MODEL STARBOARD LNGC (PARTIAL STARBOARD FORE)

PHOTO 13 CLOSE UP OF MODEL LNGC: BOW

PHOTO 14 CLOSE UP OF MODEL LNGC: STERN

PHOTO 15 BILINEAR SPRING MOUNT FOR SPRING LINE SBS MOORING

PHOTO 16 BILINEAR SPRING MOUNTS AFT LNGC

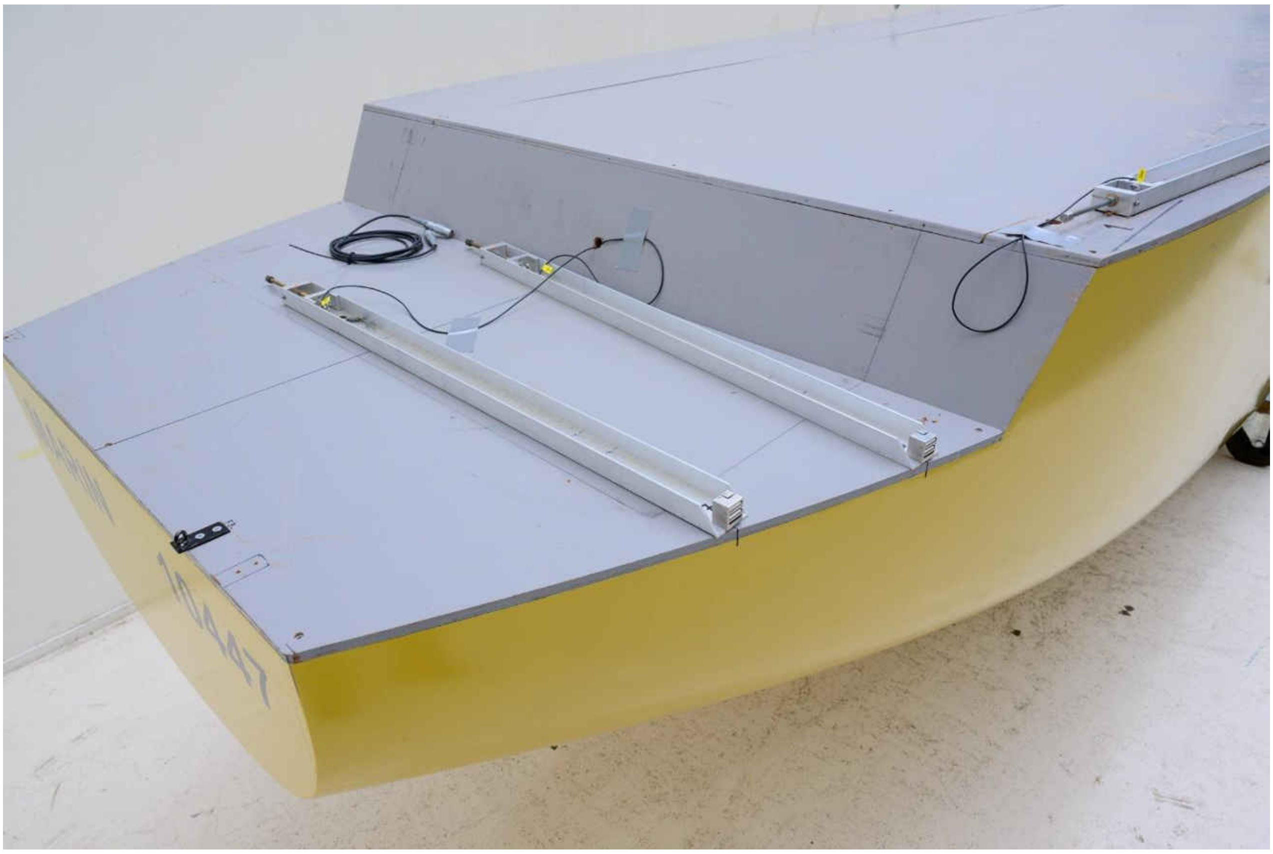

PHOTO 17 CLOSE UP OF BILINEAR SPRING MOUNT

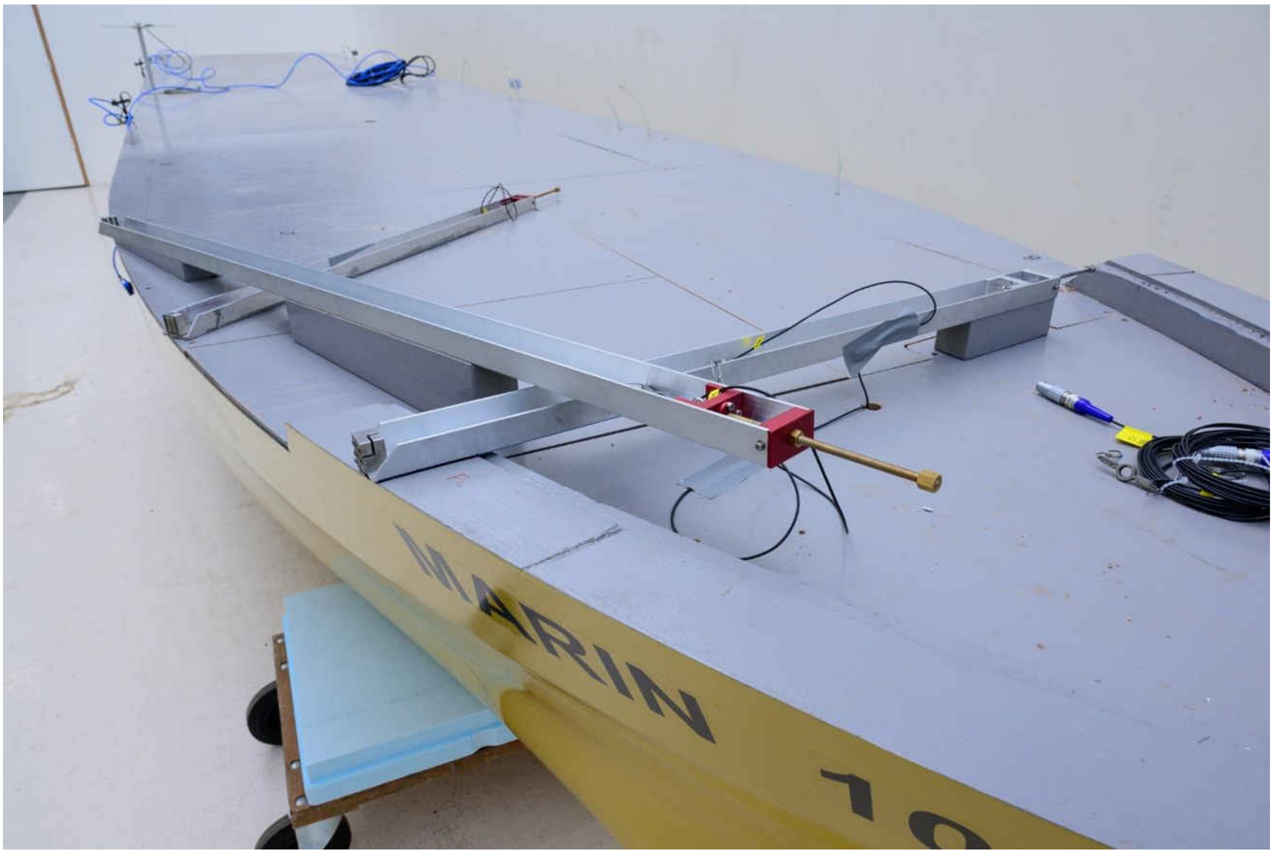

PHOTO 18 CLOSE UP OF BILINEAR SPRING MOUNT ON BOW LNGC

PHOTO 19 SBS FENDER ROD WITH AIR BEARING BUILT INTO LNGC

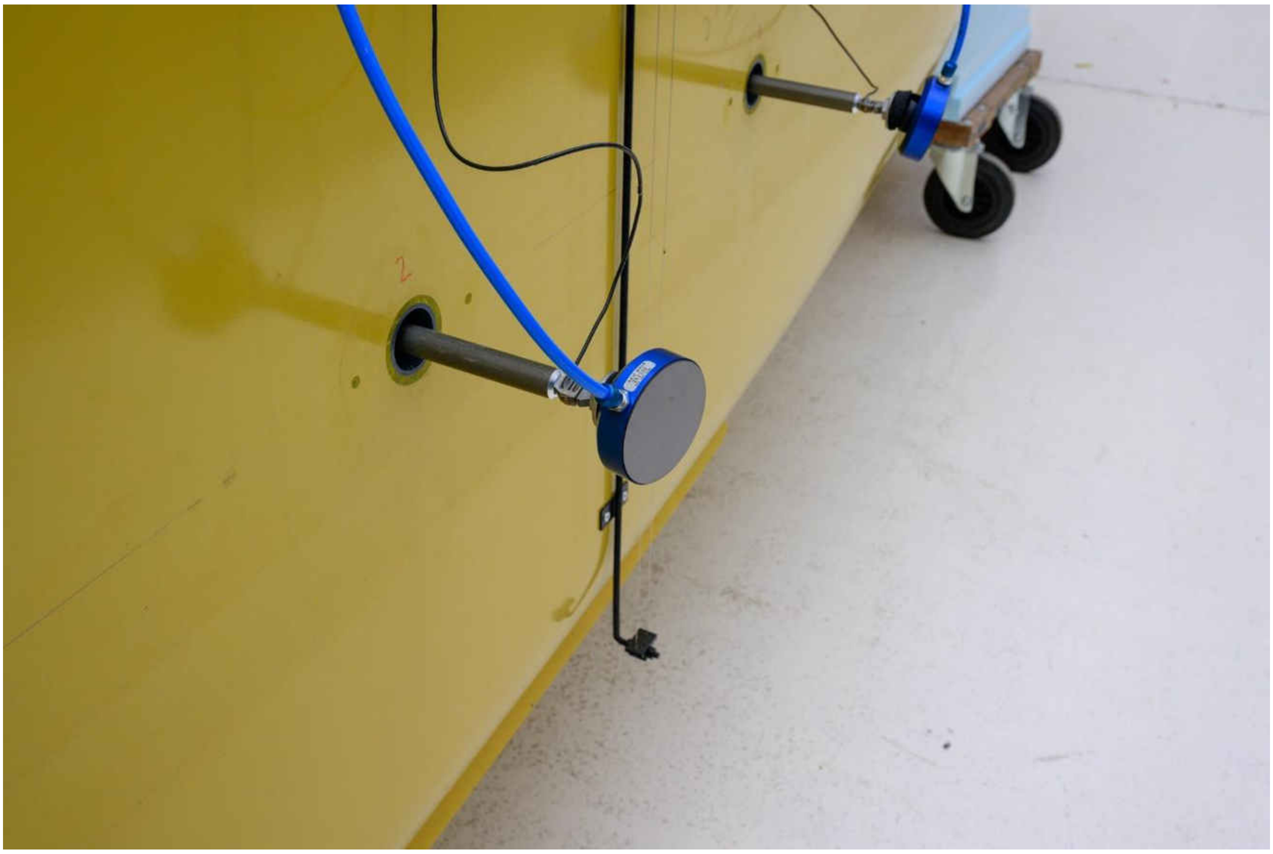

PHOTO 20 OVERVIEW OF STARBOARD SIDE LNGC WITH SBS FENDERS

PHOTO 21 AFT SBS FENDERS

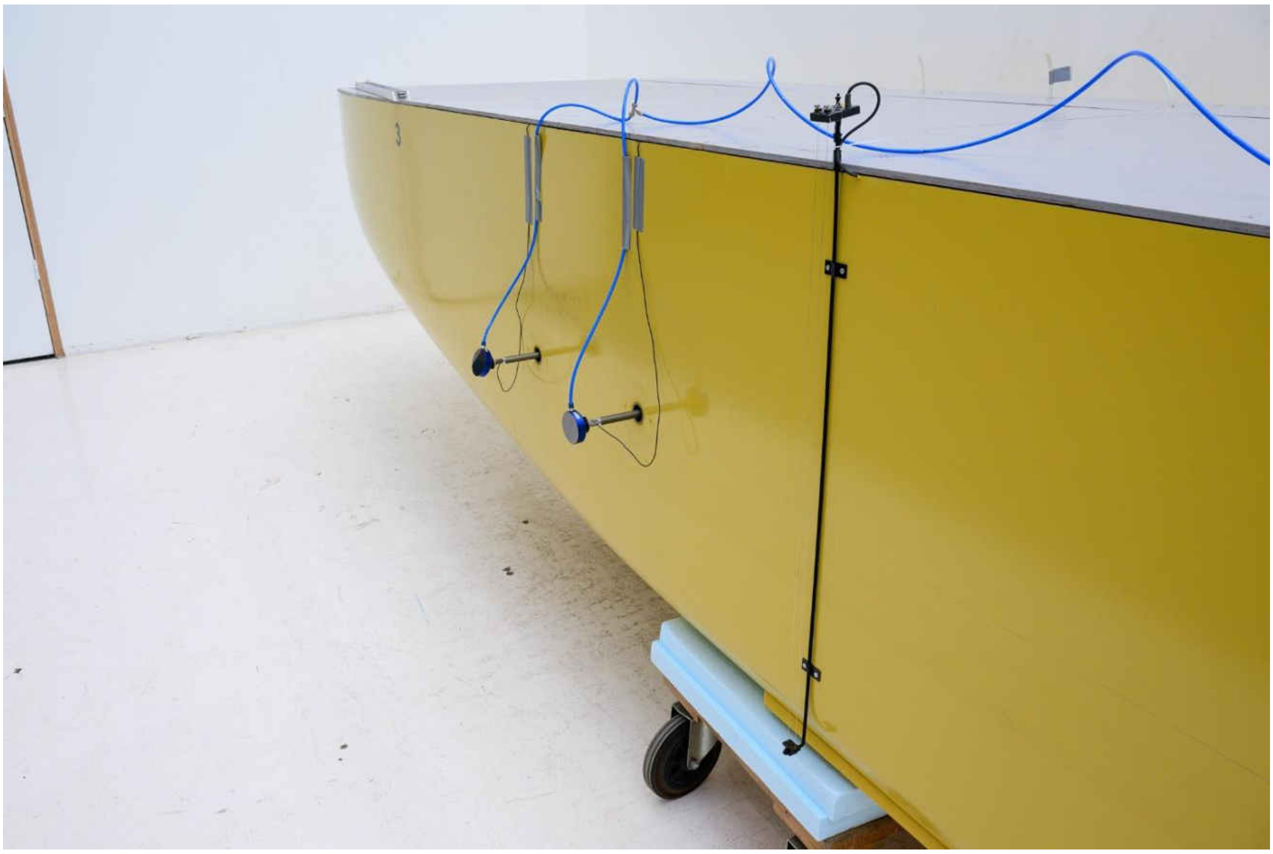

PHOTO 22 SBS MECHANICAL FENDER SPRINGS MOUNTED IN LNGC

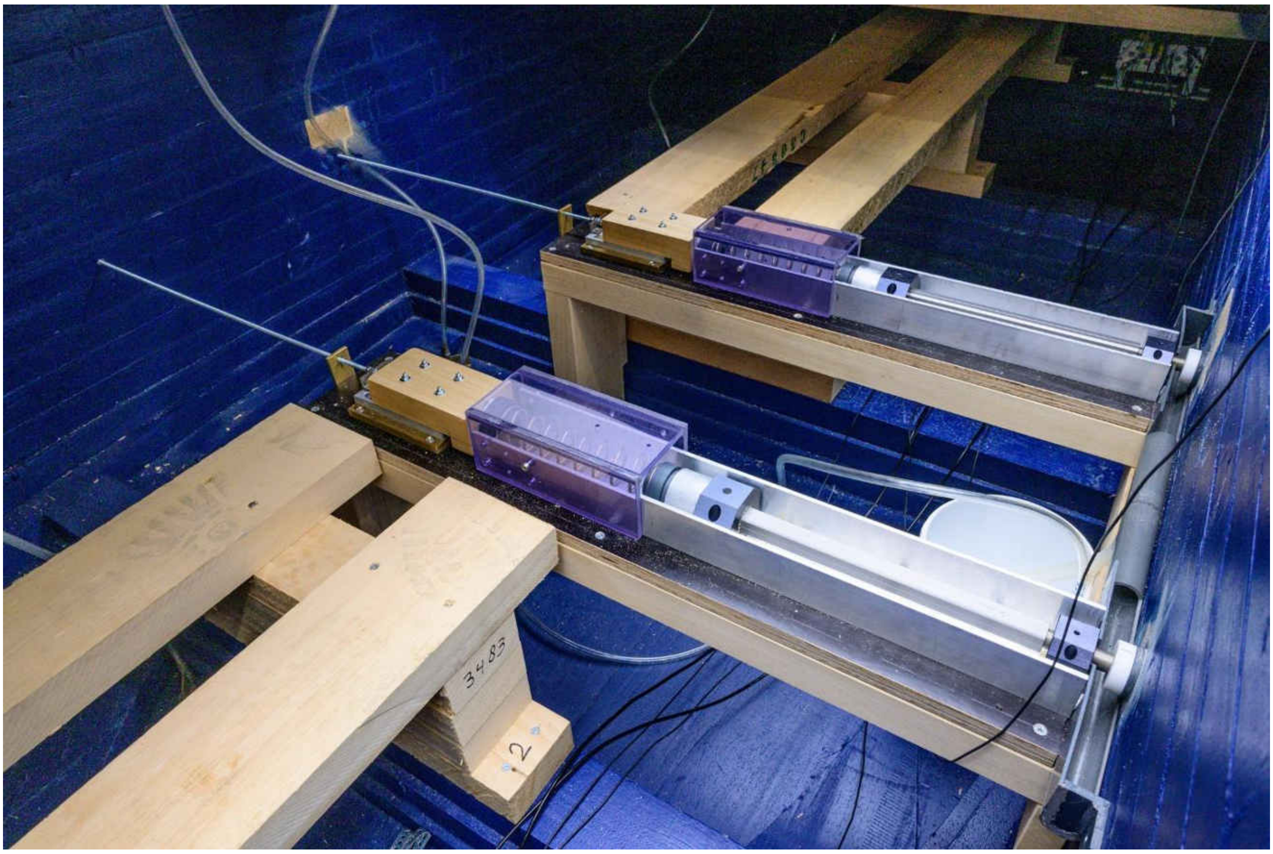

PHOTO 23 JETTY FENDER ACTUATOR DURING CALIBRATION

PHOTO 24 JETTY FENDER ACTUATOR RODS AND AIR BEARINGS IN TEST SETUP

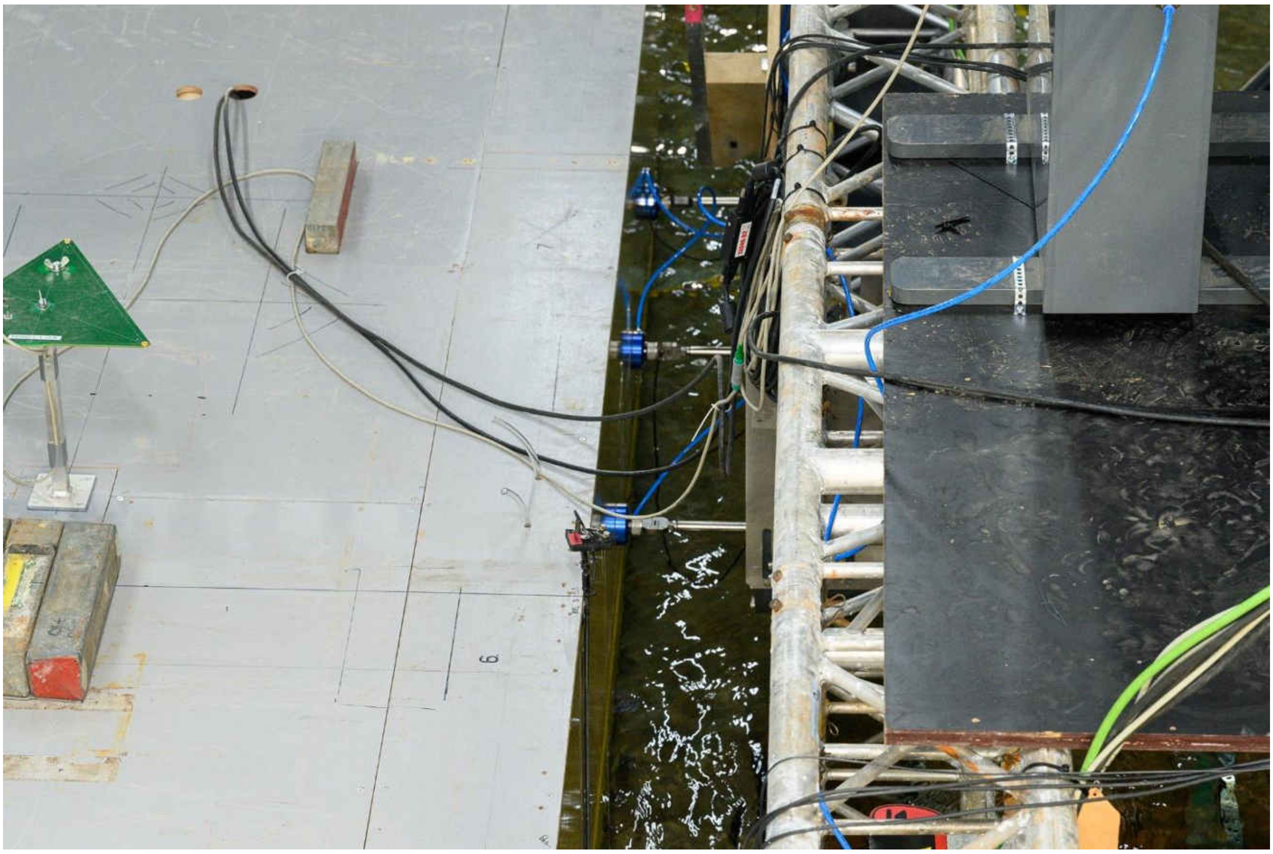

PHOTO 25 JETTY FENDERS WITH CASINGS ON JETTY IN TEST SETUP

PHOTO 26 OVERVIEW OF JETTY IN 80 DEGREES HEADING

PHOTO 27 FSRU IN JETTY MOORING

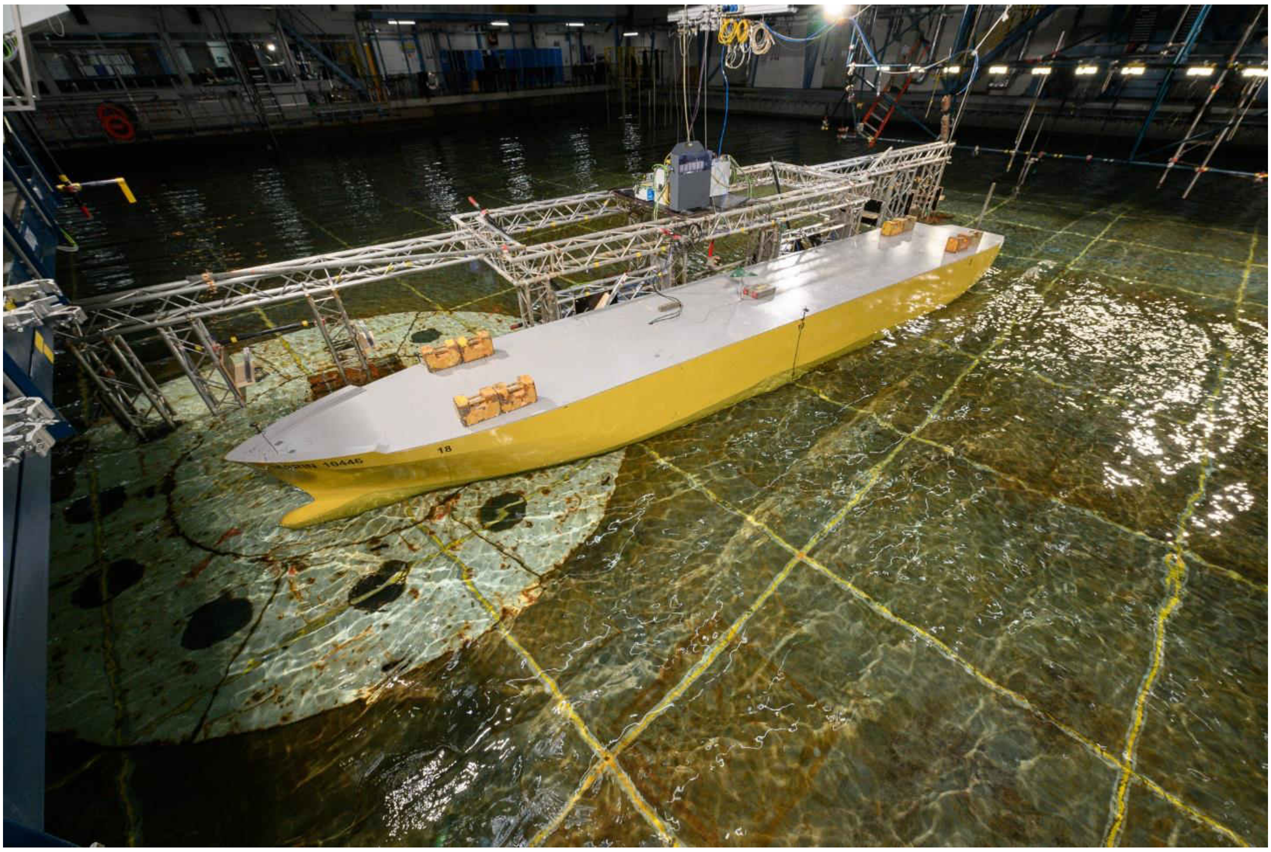

PHOTO 28 FSRU IN JETTY MOORING: GAP BETWEEN JETTY AND FSRU

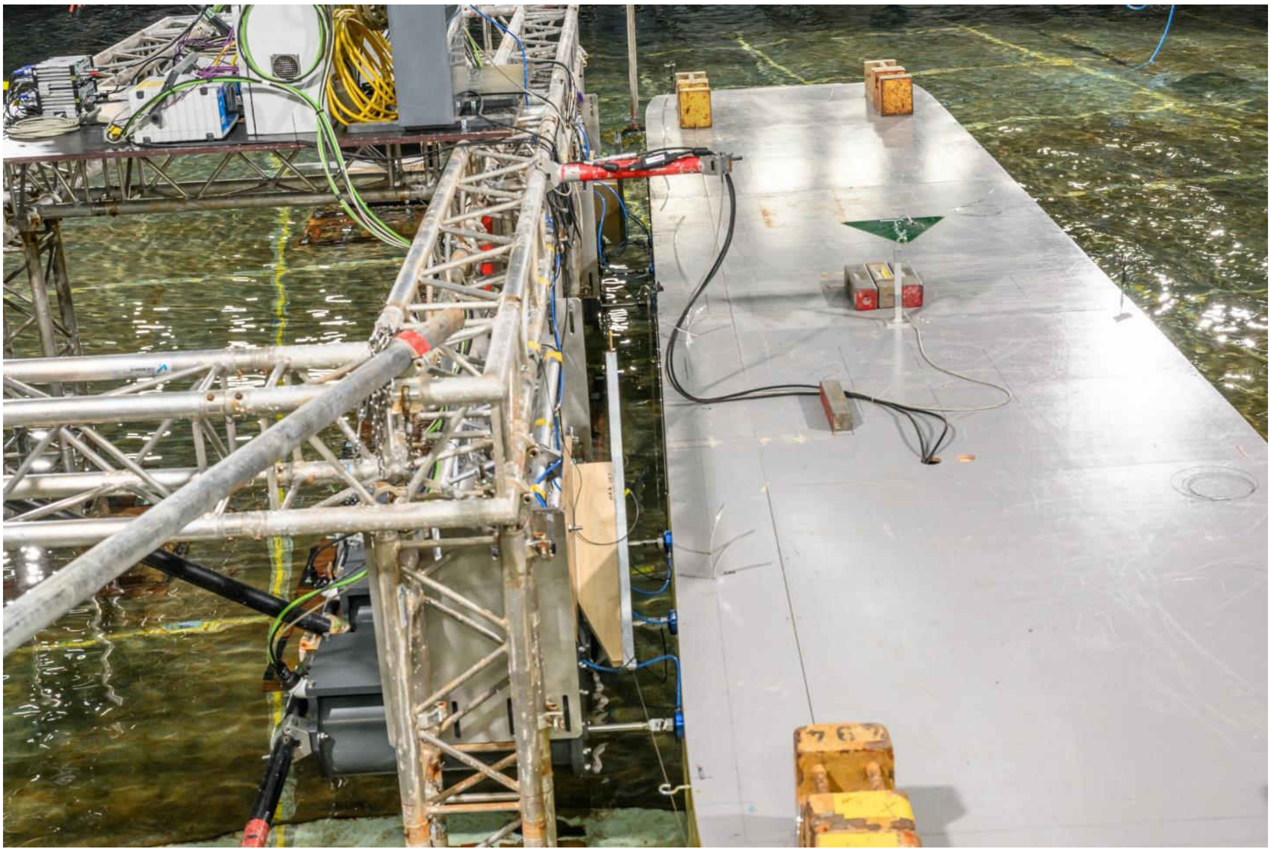

PHOTO 29 FSRU IN JETTY MOORING: REAR VIEW

PHOTO 30 FSRU IN JETTY MOORING: FRONT VIEW

PHOTO 31 FSRU IN JETTY MOORING: TOP VIEW

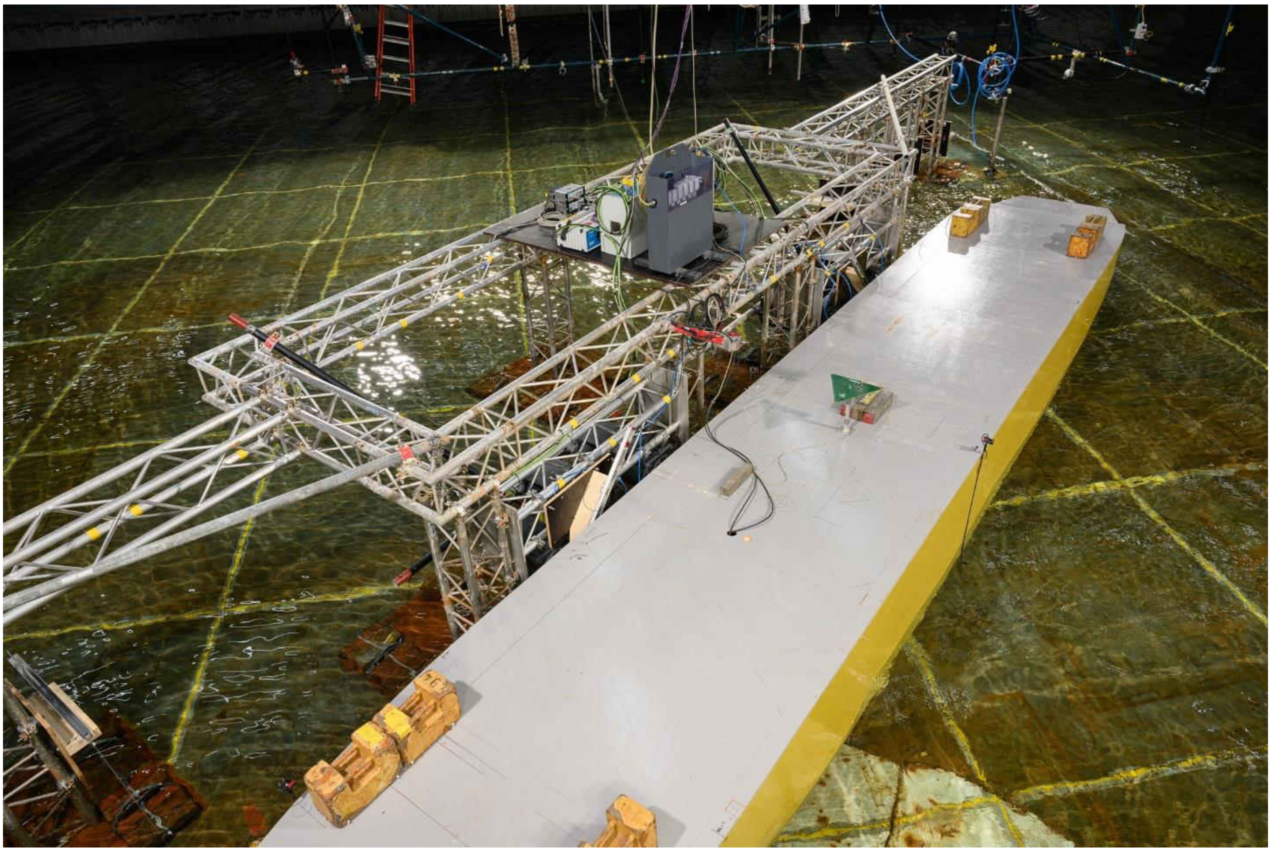

PHOTO 32 FSRU AND LNGC IN SBS JETTY MOORING

PHOTO 33 FSRU AND LNGC IN SBS JETTY MOORING: FRONT VIEW

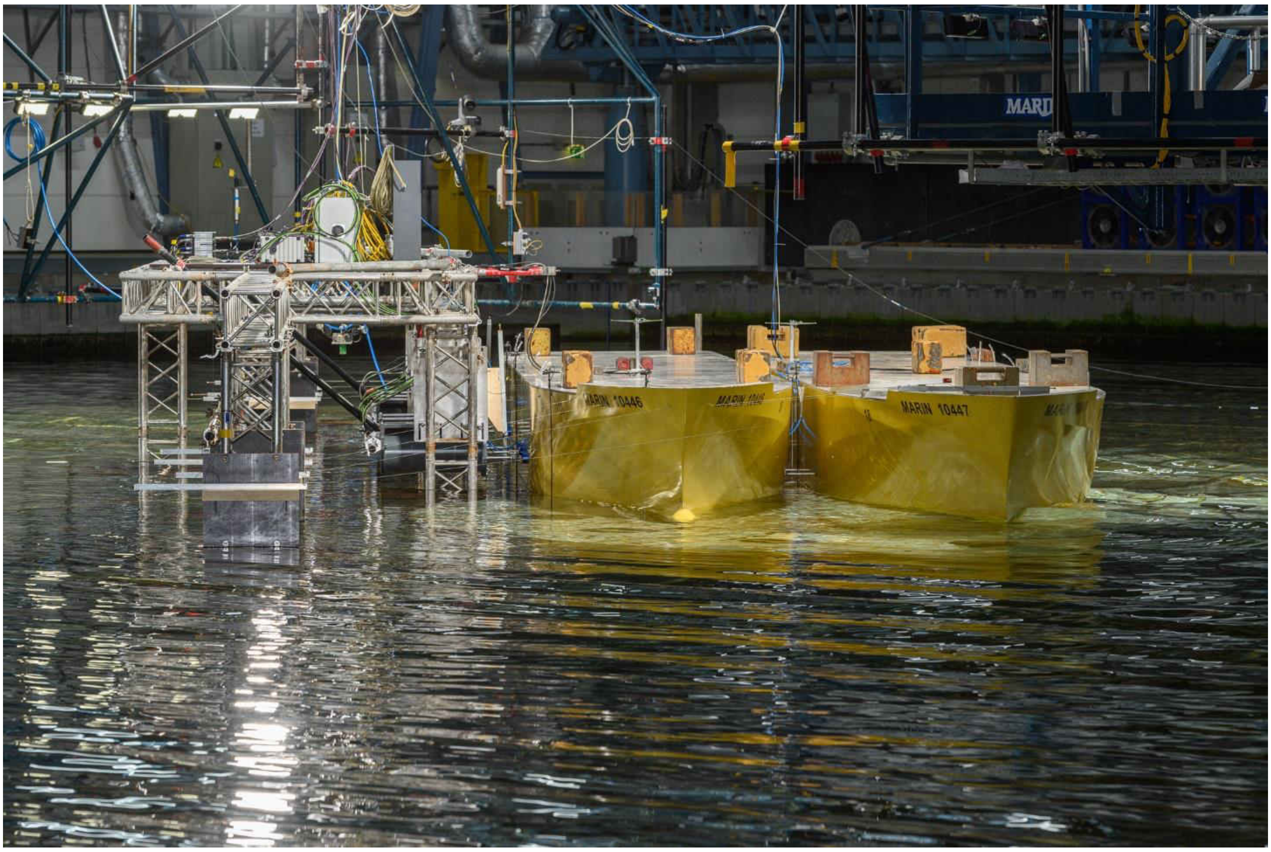

PHOTO 34 FSRU AND LNGC IN SBS JETTY MOORING: TOP VIEW BOWS

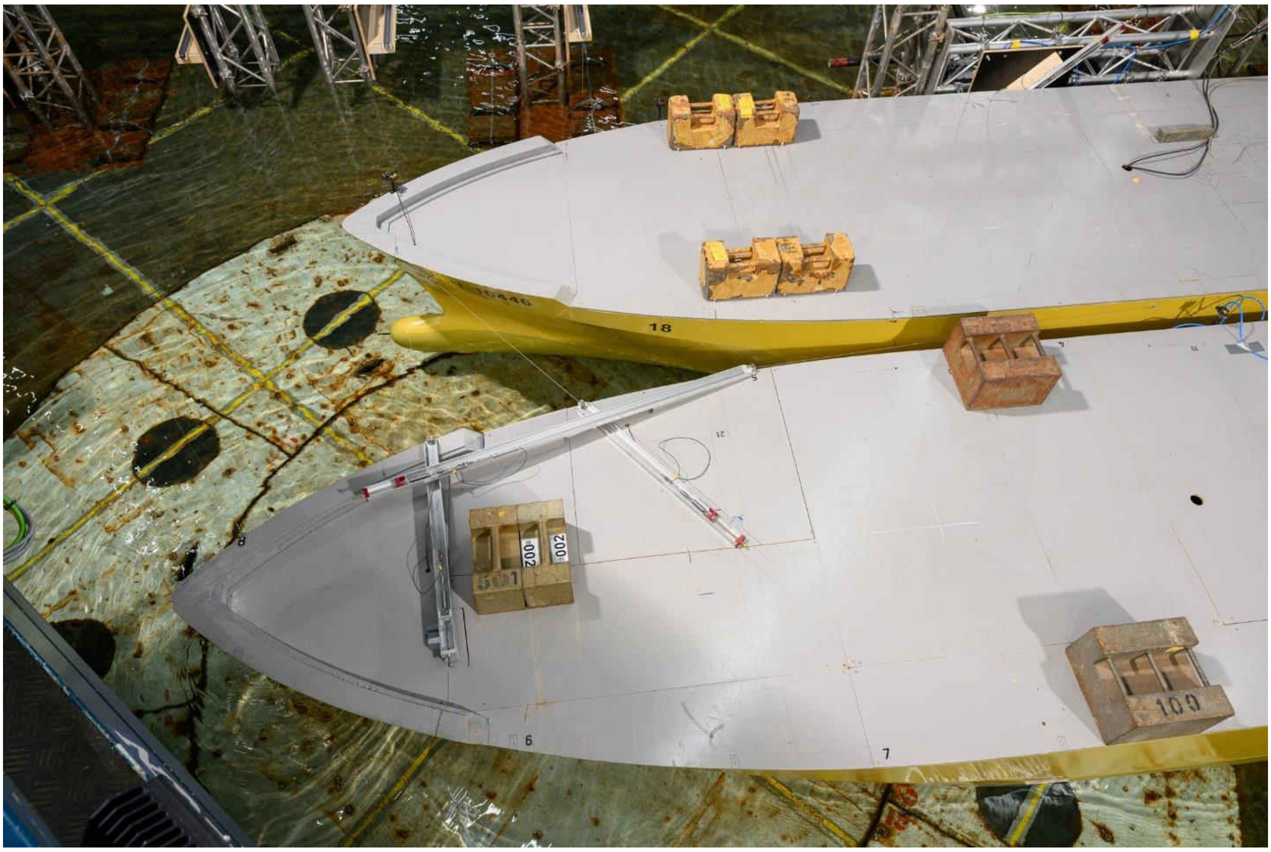

PHOTO 35 FSRU AND LNGC IN SBS JETTY MOORING: TOP VIEW

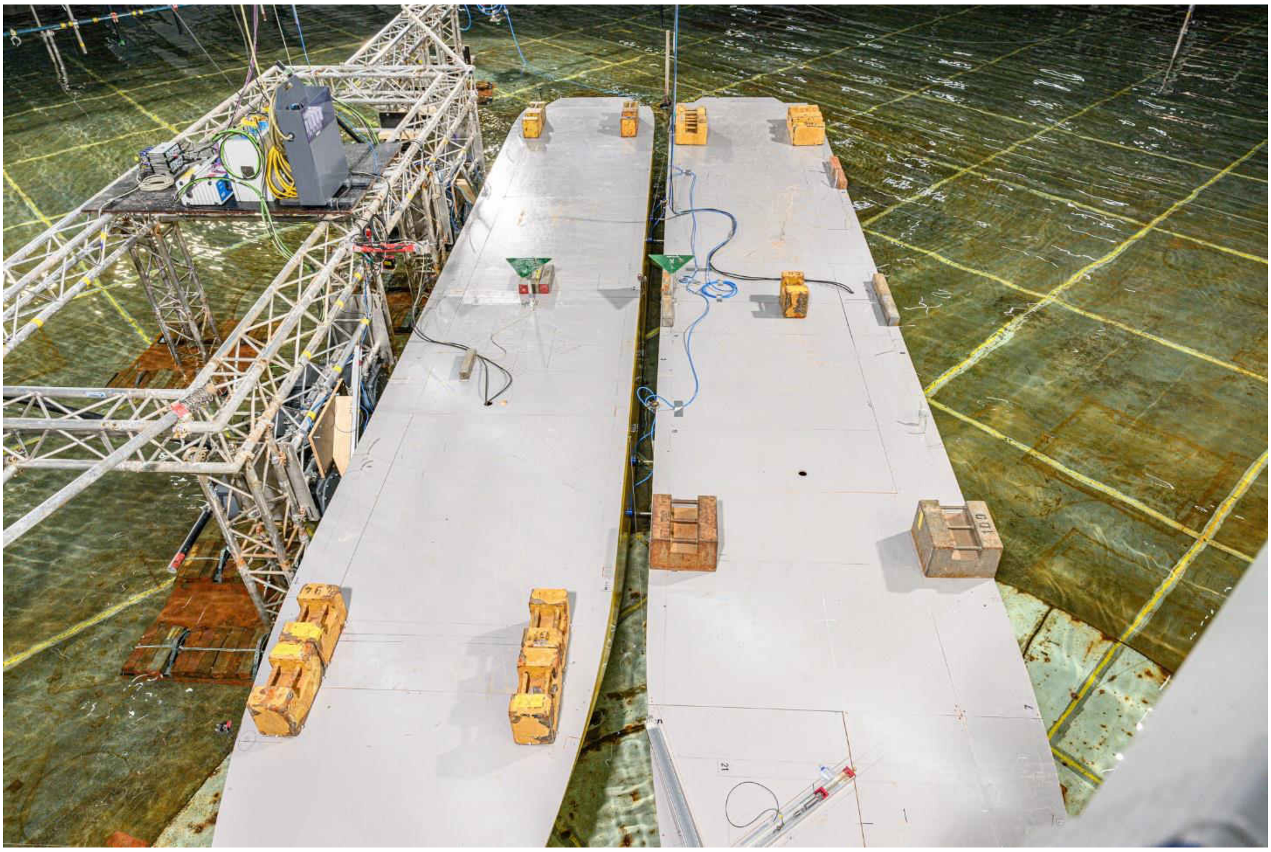

APPENDICES

APPENDIX D01

Methods to Determine Damping Coefficients from the Results of Motion Decay Tests

Revision	Date	Description of revision	Author
0	September 10, 2009	First version of the appendix	JH
1	February 24, 2010	Minor corrections in wording and equations	JvdB
2	January 28, 2011	Units and eq. damping formulation added	JJS
3	September 13, 2017	Typo's corrected	FJ
4	November 12, 2018	Adjusted to SHARK	AN

DECAY TESTS, DETERMINING DAMPING AND PERIODICITY

Decay/free extinction tests are performed to determine the damping coefficients, damped period and natural period of a floater or system. Decaying signals are characterised by a decaying oscillation around a mean value, with an approximately constant period. An example of a decaying signal is shown below:

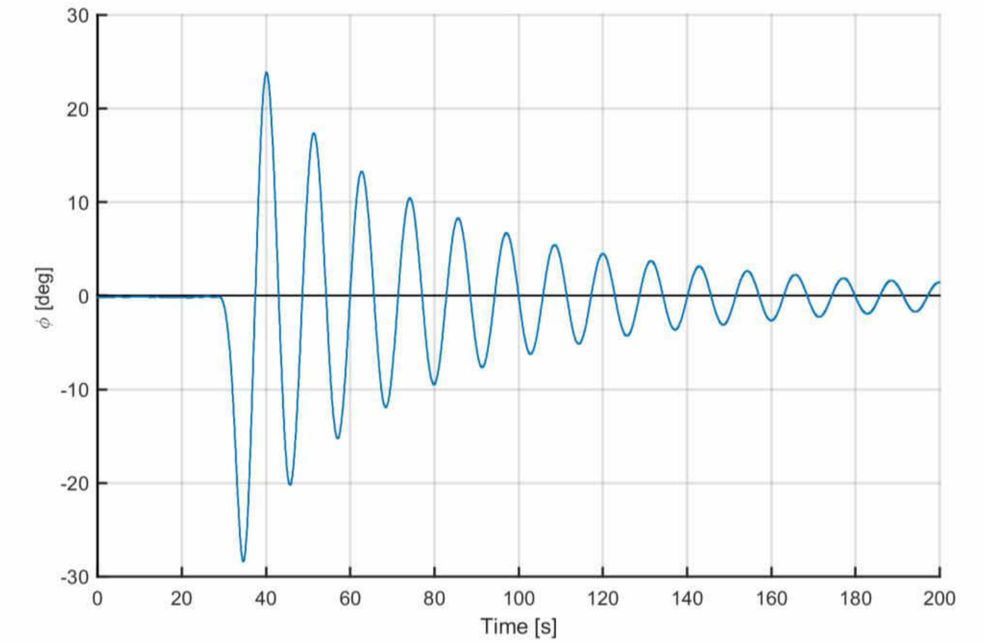

Time series of decaying roll signal

It is assumed that the decaying system can be accurately described by the following equation:

$$a\ddot{x} + b(\dot{x}) + cx = 0 \qquad (1)$$

Where:

- x is a motion signal (e.g. roll, pitch or heave)
- $\dot{x}$ is the first derivative of the motion signal (e.g. roll velocity)
- $\ddot{x}$ is the second derivative (e.g. roll acceleration)
- *a* is the mass or inertia of the floater (including added mass or added inertia)
- *c* is the restoring term of the floater
- *b()* is the damping function

The damping function can have various terms. The following terms are implemented for analysis at MARIN:

$$b(\dot{x}) = B_1\dot{x} + B_2\dot{x}|\dot{x}| + B_3\dot{x}^3 \qquad (2)$$

Where:

- B_1 is the linear damping coefficient
- B_2 is the quadratic damping coefficient
- B_3 is the cubic damping coefficient

Solving only for B_1 is called the "first order solution", solving for B_1 and B_2 is called the "second order solution" and solving for B_1, B_2 and B_3 is called the "third order solution". In very rare cases B_1 and B_3 can be determined while leaving B_2 zero. This is called the "13 order solution". Usually the second order solution is used. Only when a damping test clearly shows cubic behaviour is the third term determined as well.

Analysis of a motion signal alone does not provide absolute damping coefficients; it only provides relative damping coefficients in the form *B/c*. An absolute value of *c* has to be provided before an absolute value of *B* can be found. As an example, *c* can be defined as *g*   *GM* for a roll decay.

The relative damping can be analysed by three methods. First, Equation 1 can be solved by inserting the measured motion, velocity and acceleration and solving in a least squared sense. This is called the "least squares fit". Secondly, classic "PQ analysis" can be performed. PQ analysis sets out all individual crests and troughs as a function of amplitude and fits a polynomial through. The polynomial coefficients are denoted by *P* and *Q* (and *R* in the cubic damping case). Lastly, the motion signal itself can be fit in an optimal sense by varying the relative damping and natural period of the system until an optimum is found. This is called "motion optimised".

All three methods determine the same relative damping values, but with different approaches to what is optimal. The classic PQ analysis works very well for lightly damped systems, but has difficulties to provide accurate values for highly damped systems (e.g. ships sailing at speed). The least squares fit and motion optimised methods are closely related. The motion optimised method actually removes the need for fitting velocity and acceleration in the system of equations, which sometimes caused irregularities in the fitting.

The decay analysis results can be verified using a PQ-diagram, a recalculation of the time series and via a plot of the damped period per oscillation.

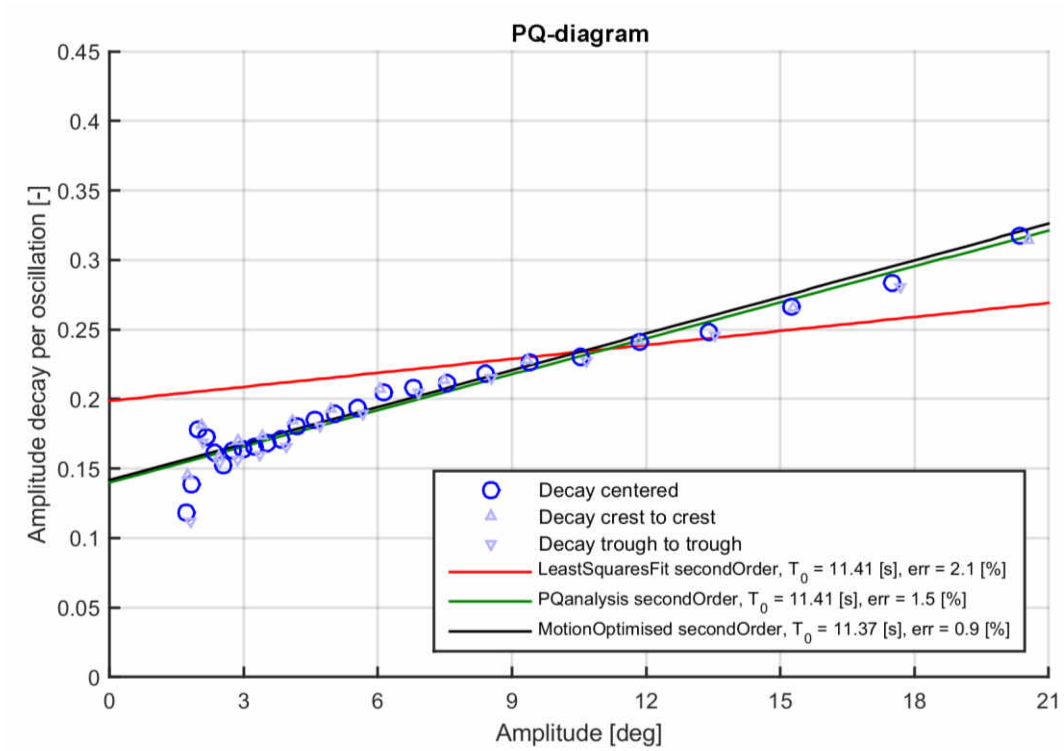

Example of a PQ-diagram showing all three methods

The PQ-diagram shows the decay of the crests and troughs in three ways. “Decay centred” shows the amplitude decay calculated as the difference between two consecutive crest-trough differences or trough-crest differences. This method is not sensitive to offsets in the signal. These values are also used in the PQ analysis method. The “crest to crest” and “trough to trough” decays are provided to indicate offsets and other irregularities in the signal. Ideally all three should coincide. In this case the second order results of all three fitting methods are indicated. Normally the best fitting method is used and the others are not shown.

The damping coefficients B_1, B_2, B_3 and P, Q, R values translate into one another as follows; see also “Slingergedrag van Schepen” door Ir J.J.W. van der Vegt, “KIVI-zeegangsdag”, March 1 1984:

$$\frac{B_1}{c} = \frac{PT_0}{2\pi^2}$$
$$\frac{B_2}{c} = \frac{3QT_0^2}{32\pi^2} \qquad (3)$$
$$\frac{B_3}{c} = \frac{RT_0^3}{6\pi^4}$$

Where:

- P, Q and R are the zeroth, first and second order polynomial components of the fit of crest and trough decay
- T_0 is the natural or undamped period of the system

Ideally the natural period can be expressed as:

$$T_0 = 2\pi\sqrt{\frac{a}{c}} \qquad (4)$$

The damped period T_d is the observed period and can change slightly with oscillation amplitude. In the case of an ideal linear damped system the damped and natural periods are related via:

$$T_0 = T_d\sqrt{1-\zeta^2}$$
$$\zeta = \frac{B_1}{2\sqrt{ac}} \qquad (5)$$

Where:

- ζ is the damping ratio

T_d and hence T_0 is (initially) determined from the mean crossings of the signal; however, it is further optimised when the motion optimised method is used.

The error mentioned in the legend of the PQ-diagram is actually the error function used in the motion optimised method, which is the L2-norm of the difference between the measured motion and the recalculated motion after fitting. An example of the recalculation is shown in the next figure:

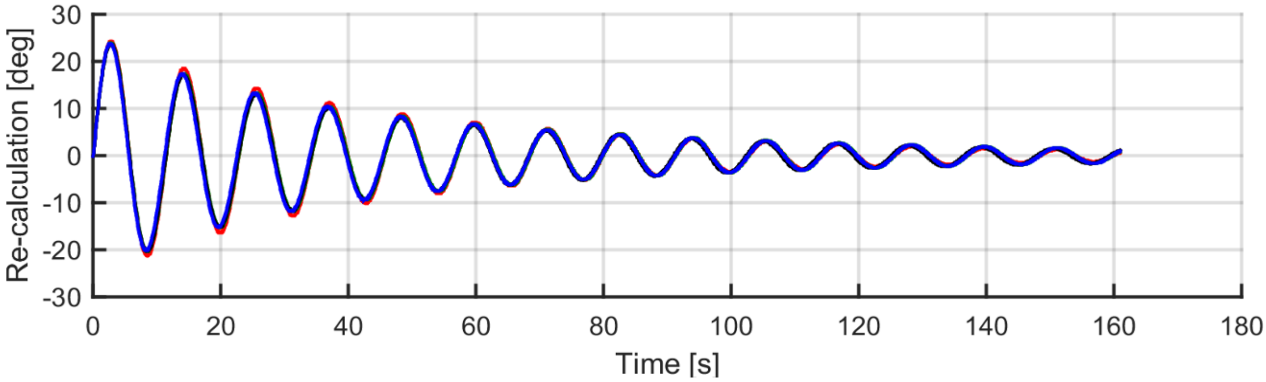

Example of a recalculation showing all three methods; the original signal is shown in blue

The recalculation diagram can be used to check whether the periods found and damping actually match with the measured signal. In this case the red line of the least square fit method shows too little damping at the beginning of the time series at large oscillation amplitudes and somewhat too much damping at the end of the time series. This was also indicated in the PQ-diagram. The other methods fit relatively accurate to the measured data.

The behaviour of the damped period is shown as a function of the number of oscillations as shown below:

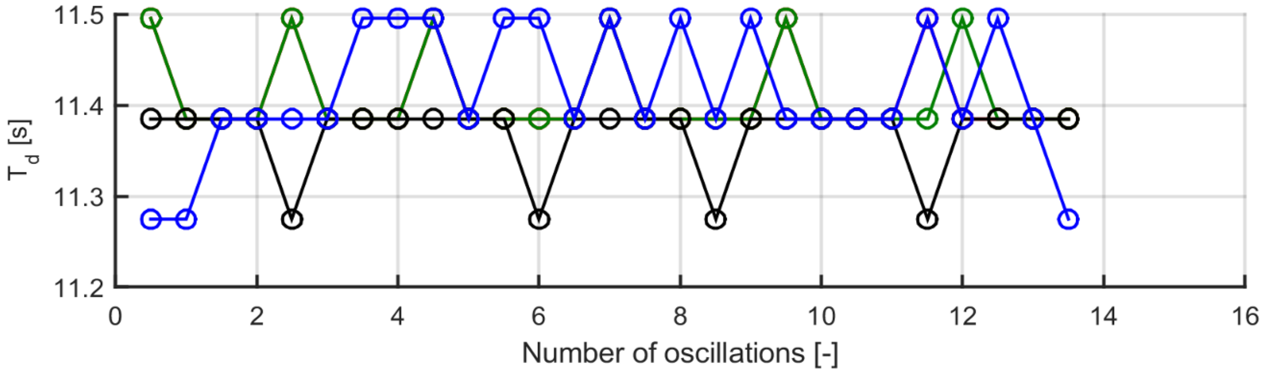

Example of a period overview; the original signal is shown in blue

This plot can be used to check for errors in the mean crossings (e.g. when a poorly conditioned signal has erratic mean crossings the average period estimate will be too small). In this case both the original signal and the three methods are in agreement and show a very constant damped period.

APPENDIX D02

Mathematical Description of Irregular Phenomena

Revision	Date	Description of revision	Author
0	May 19, 2009	First version of the appendix	JLC

Mathematical Description of Irregular Phenomena

General

A quantity x, varying irregularly in time or space is called a stochastic variable. The stochastic variables that are most interesting in the field of seakeeping are varying in time and can each be described by a distribution function of the probability that x fulfils a certain condition. Examples of such distribution functions are (see Figure A):

1. The probability distribution for the period of time that the value x lies between a and b.
2. The probability distribution of amplitudes of x lying between a and b.

Figure A

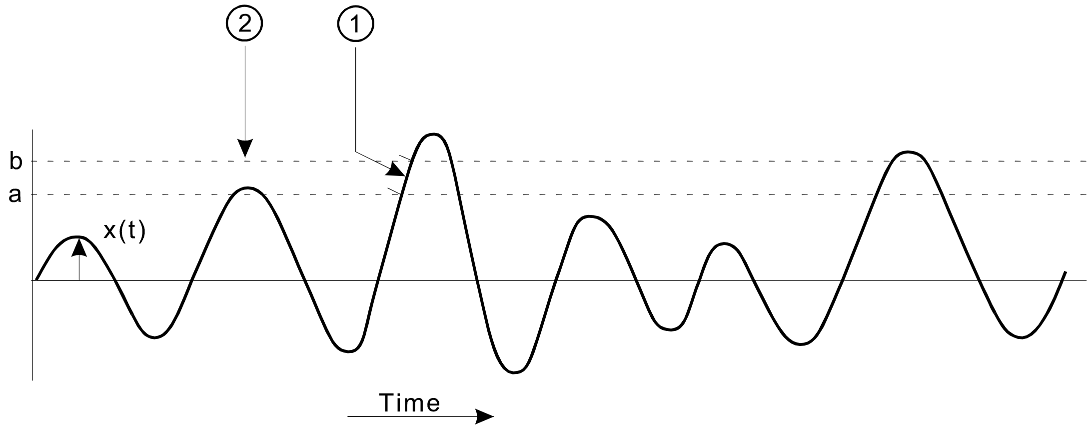

These various descriptions are discussed under the following subheadings. Before doing so, it is necessary to mention a few characteristics to classify random processes.

A process, described by a stochastic variable x, is completely defined if all statistical properties are known, or to be precise, when the expectation values E[x], E[x^2], E[x^3], ... are all known. In general this is not the case.

Processes can be classified by certain properties of their statistics. If for a process all statistical properties are invariant with respect to time shifts, the process is called ***stationary***. This means, for example, that:

$$E[x(t)] = E[x(t+\tau)] \qquad -\infty < \tau < \infty \tag{1}$$

E[x] is the ***mean value*** of x, also denoted by $\bar{x}$.

The statistical properties of a random process can be measured in several ways, depending on the character of the process. For instance, assume a sea with a large number of wave height measuring buoys of the same type, measuring simultaneously. The mean value of the wave elevations is established as the average of the registration of all buoys at time t = t_m. Now, the actual waves at sea are a weakly stationary process; in case of long periods of time the expectation values are not time invariant, but for practical purposes the wave elevation (and as a result: ship motions) can be considered as stationary processes.

A stationary process is called ergodic when it is allowed to replace the averaging over space by an averaging over time and to use the registration of one single buoy for the characterization of the sea state, as described above, or to use one ship model to measure its motions.

Probability distribution of x(t)

The wave elevations are a continuous function of time (see Figure A) and the probability that $a \le x \le b$ is given by the probability density function $p_x(y)$ in such a way that:

$$P[a \le x \le b] = \int_a^b p_x(y)\, dy$$

where:

$$\int_{-\infty}^{\infty} p_x(y)\, dy = 1 \qquad (2)$$

If the process has a normal (Gaussian) distribution the probability density function is:

$$p(x) = \frac{1}{\sigma_x \sqrt{2\pi}} . \exp\left[- \frac{(x - \bar{x})^2}{2\sigma_x^2} \right] \qquad (3)$$

in which:

$\bar{x}$	=	E[x], the mean value, and
σ_x	=	the standard deviation of the process

The standard deviation is defined as the root of the variance and:

$$\sigma_x^2 = VAR. = E[x - E[x]]^2 = E[x^2] - (E[x])^2 \qquad (4)$$

Now it is possible to calculate for a normal distributed stochastical variable x the probability that, for instance, $(\bar{x} + \frac{n}{2}\sigma_x) \le x \le (\bar{x} + \frac{n+1}{2}\sigma_x)$ for several values of n. The result is shown in the histogram in Figure B on the next page. Note that the mean value not necessarily coincides with the point of reference in the measuring system, so in the above definition of a Gaussian distribution x is given relative to $\bar{x}$.

Figure B: Normalised Gaussian distribution

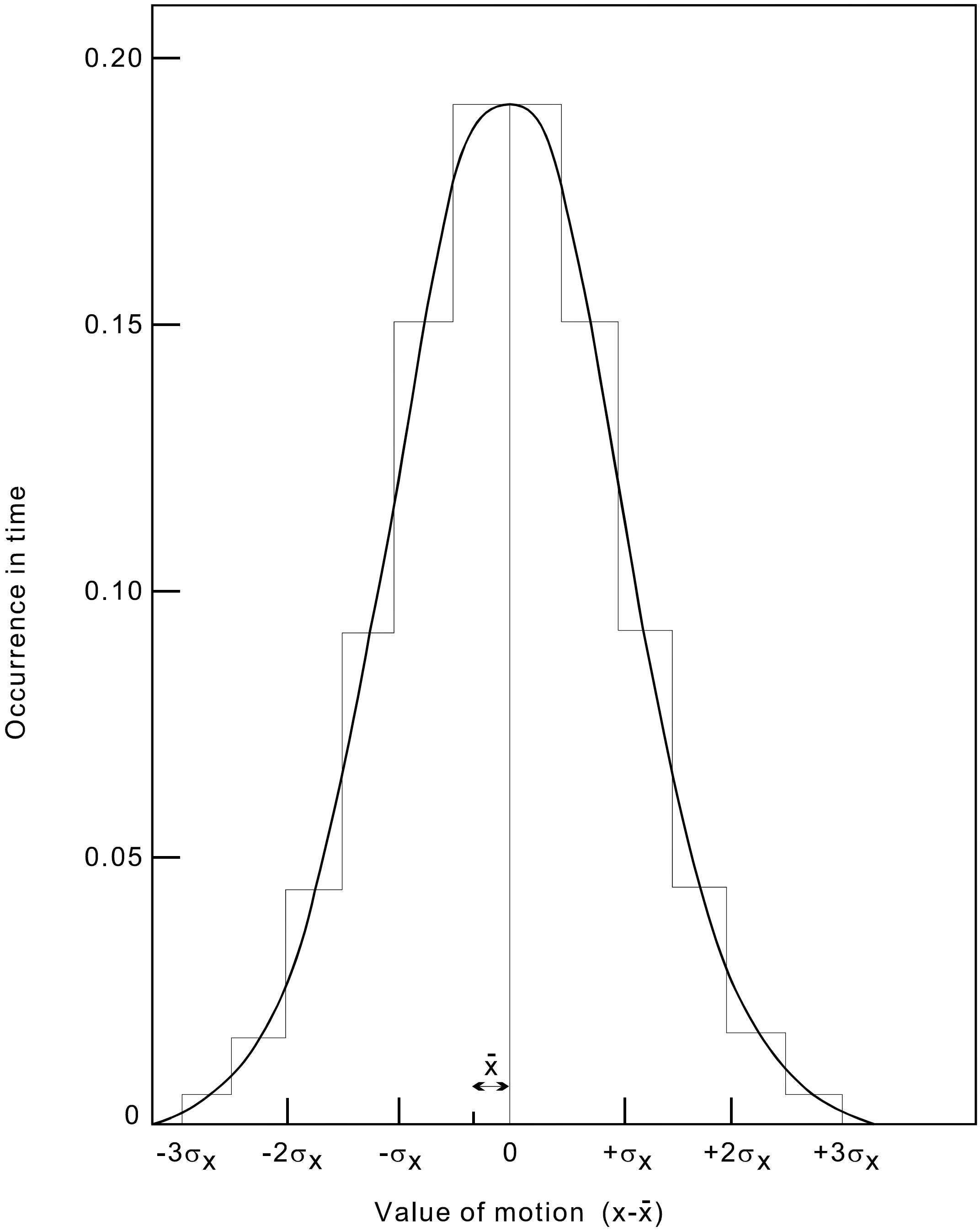

NOTE: width of the columns in the histogram = $\frac{1}{2}\sigma_x$

σ_x = standard deviation of the variable x

The probability that the value for $(x - \bar{x})$ exceeds a certain level x_m can be expressed as:

$$P[x_m \leq (x - \bar{x}) < \infty] = \int_{x_m + \bar{x}}^{\infty} p_x(y)\,dy \qquad (5)$$

Using (3), (4) and (5) the following table gives results for several values of x_m.

x_m	Probability percentage $P[x_m \leq x < \infty]$	Probability percentage $P[-\infty < x \leq x_m]$
$\bar{x} - 3\sigma_x$	99.87	0.13
$\bar{x} - 2\sigma_x$	97.72	2.28
$\bar{x} - 1\sigma_x$	84.10	15.90
$\bar{x} + 1\sigma_x$	15.90	84.10
$\bar{x} + 2\sigma_x$	2.28	97.72
$\bar{x} + 3\sigma_x$	0.13	99.87

Probability distribution of amplitudes of x(t)

Additionally, the stochastic variable x can be described by the distribution of the amplitudes (= peak values) of x. When x has a normal distribution, the amplitudes follow a Rayleigh distribution. As regards these amplitudes, which are the most interesting quantities in the measurement of ship motions, several stochastic quantities can be defined. When:

- x_a ≡ the amplitude of $[x - \bar{x}]$, then:
- $x_{a\,1/3}$ ≡ the mean of the highest one-third of the amplitudes of x_a, or as it is often called: the significant single amplitude of x;
- $2x_{a\,1/3}$ ≡ mean of the highest one-third of the maximum to minimum values of x_a, often called: the significant double amplitude of x

Then the most probable maximum value $2x_{a\,max.}$ (double amplitude) of the variable x depends on the number of oscillations N_o, as calculated by Longuet-Higgins[2)].

$$2x_{a\,max.} = 2\sigma_x \sqrt{2\theta} \qquad (6)$$

with:

$$\theta = \ln N_o - \ln\left[1 - \frac{1}{2\theta}(1 - e^{-\theta})\right] \qquad (7)$$

2) Longuet-Higgins, M.S.; “On the Statistical Distribution of the Heights of Sea Waves”, Journal of Marine Research 1952, Number 3.

For large values of N_o it can be shown that:

$$2x_{a\,max.} = 2\sigma_x \sqrt{2 \ln N_o} \tag{8}$$

In actual measurements, the registration of x over a period of time is used. This period of time has to be long enough to give a reliable estimate of the statistical properties of the variable x as well as for the above introduced stochastical variables $x_{a1/3}$ and $2x_{a1/3}$. (It is generally accepted to be sufficient when this period corresponds to half an hour real time or includes at least 180 oscillations). Then, the mean value is given by:

$$E[x] = \bar{x} = \frac{1}{T}\int_{t_1}^{t_2} x(t)\,dt \qquad \text{with } T = t_2 - t_1$$

and the standard deviation is:

$$\sigma_x = \sqrt{\frac{1}{T}\int_{t_1}^{t_2} [x(t) - \bar{x}]^2\,dt}$$

The observed processes are stationary - or at least weakly stationary - and ergodic. So the above described simplifications for the establishment of $\bar{x}$ and σ_x are allowed. When the duration of the measurement is sufficiently long, the difference between the standard deviation of the sample and the standard deviation of the actual density function can be neglected. The probability functions actually found from sampling an experiment generally conform very well with the theoretical distributions for x-values in the vicinity of $\bar{x}$. Due to the limited sample size the agreement at x-values far from $\bar{x}$ is hard to prove.

Spectral density of x

When the stochastic quantity x, varying irregularly in time t ($0 \le t < T$ with $T \to \infty$), is plotted as a function of time and its variations between t and $t + \Delta t$ are bounded for $\Delta t \to 0$, then x(t) can be represented by an infinite number of harmonic components with arbitrary phase angles:

$$x(t) = x_0 + \sum_{n=1}^{\infty} x_n \cos(\omega_n t + \varepsilon_n) \qquad \text{(Fourier series)} \tag{9}$$

in which:

x_n = the amplitude of harmonic component n
ε_n = phase angle of the n-th component
ω_n = $n\omega_1$ = angular frequency of the n-th harmonic component
ω_1 = $2\pi/T$ (T = measuring time)

and so: $x_0 = \bar{x}$ the mean value of x.

Now, suppose there is a stationary, ergodic process, described by the stochastic variable $x_T(t)$ of which the observation takes place over a time interval ($-T < t < T$, $T \rightarrow \infty$), as shown in Figure C.

Figure C

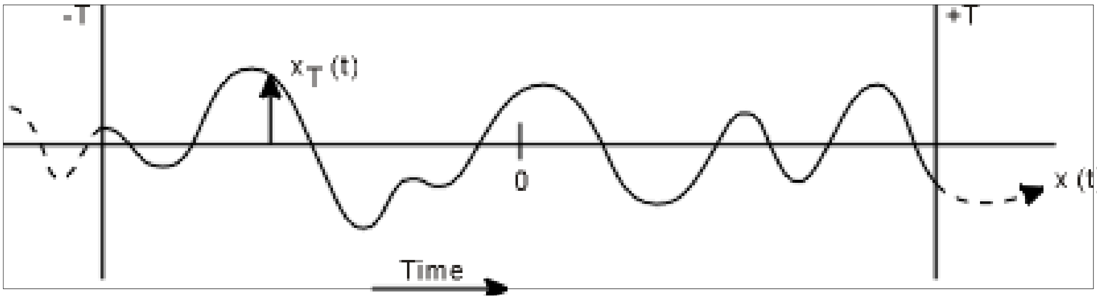

Then the Fourier series can be replaced by the Fourier transformation and the following relations result:

$$X_T(\omega) = \int_{-\infty}^{\infty} x_T(t)\, e^{-i\omega t}\, dt = \int_{-T}^{T} x(t)\, e^{-i\omega t}\, dt \tag{10}$$

$$x_T(t) = \frac{1}{2\pi} \int_{-\infty}^{\infty} X_T(\omega)\, e^{+i\omega t}\, d\omega \quad \text{(inverse Fourier transformation)}$$

The mean value and mean square value (= standard deviation when $\bar{x}$ = 0) are defined as follows:

$$\bar{x} = \lim_{T \rightarrow \infty} \frac{1}{2T} \int_{-\infty}^{\infty} x_T(t)\, dt = \lim_{T \rightarrow \infty} \frac{1}{2T} \int_{-T}^{T} x(t)\, dt \tag{11}$$

$$\bar{M}_x = \lim_{T \rightarrow \infty} \frac{1}{2T} \int_{-\infty}^{\infty} \{x_T(t)\}^2\, dt = \lim_{T \rightarrow \infty} \frac{1}{2T} \int_{-T}^{T} \{x(t)\}^2\, dt \tag{12}$$

The spectral density function $S_{xx}(\omega)$ of the random process $x_T(t)$ can be proven to be[3)]:

$$S_{xx}(\omega) = \lim_{T\to\infty} \frac{1}{2\pi T} |X_T(\omega)|^2 \tag{13}$$

Using Parceval's theorem on Fourier transformations[4)], the mean square can be expressed in terms of frequency:

$$\bar{M}_x = \lim_{T\to\infty} \frac{1}{2T} \left\{ \frac{1}{2\pi} \int_{-\infty}^{\infty} |X_T(\omega)|^2 \, d\omega \right\} = \frac{1}{2} \int_{-\infty}^{\infty} S_{xx}(\omega)\, d\omega \tag{14}$$

The spectral density function can be related to the energy W which will be clarified in the following discussion. The Fourier transformation $X_T(\omega)$ is the continuous representation of the amplitudes x_n in the Fourier series of $x_T(t)$. Now, the potential energy E_n of the component with frequency ω_n is proportional with $(x_n)^2$ and analogously the potential energy in the frequency range of $\omega_i \le \omega \le \omega_j$ is:

$$W(\omega_i \le \omega \le \omega_j) \_ \int_{\omega_i}^{\omega_j} |X_T(\omega)|^2 \, d\omega$$

and the average potential energy over a period of time is, using (13):

$$W \sim \lim_{T\to\infty} \frac{1}{T} [W(\omega_i \le \omega \le \omega_j)] = \int_{\omega_i}^{\omega_j} S_{xx}(\omega)\, d\omega \tag{15}$$

So, the average potential energy of $x_T(t)$, associated with the frequency band $\omega_i \le \omega \le \omega_j$ is given by the integral of $S_{xx}(\omega)$ over the frequency interval and hence $S_{xx}(\omega)$ may be called the ***energy spectral density function.***

---

3) Therefore use is made of the auto-covariance function $R_{xx}(\tau)$, defined as:

$$R_{xx}(\tau) = E[\{x(t) - E[x(t)]\} . \{x(s) - E[x(s)]\}]$$

with $\tau = s - t$. In the representation of this section, with $\bar{x} = 0$, is:

$$R_{xx}(\tau) = \lim_{T\to\infty} \frac{1}{2T} \int_{-\infty}^{\infty} x_T(t)\, x_T(t+\tau)\, dt$$

Now, $S_{xx}(\omega)$ is defined as the Fourier transformation of the auto-covariance function:

$$S_{xx}(\omega) = \frac{1}{\pi} \int_{-\infty}^{\infty} R_{xx}(\tau)\, e^{-i\omega\tau}\, dt$$

4) This theorem states that:

$$\int_{-\infty}^{\infty} \{x(t)\}^2 \, dt = \frac{1}{2\pi} \int_{-\infty}^{\infty} |X(\omega)|^2 \, d\omega$$

The concept of response

Mechanical and physical systems may be interpreted as a transducer transmitting energy from the input x(t) towards the output or response y(t). Suppose the output is uniquely determined in terms of the input: y(t) = L[x(t)], then the system is completely defined if the nature of the operator L is known. The spectral density representation of a stochastic variable allows an output density function $S_{yy}(\omega)$ to the input density $S_{xx}(\omega)$ by means of a frequency response function, provided that the observed system is linear[5)]. Consider the situation where the unit impulse, described by the Dirac delta function[6)] $\delta(t - t_0)$, is applied at time $t = t_0$ to a linear system and let $h(t - t_0)$ be the response of the system: $L[\delta(t - t_0)] = h(t - t_0)$. Because such an input-output system is causal, $h(t - t_0)$ does not exist for $t_0 > t$. Now, an arbitrary input x(t) can be expressed as a sum of impulses, that is:

$$x(t) = \int_{-\infty}^{t} x(t_0)\,\delta(t - t_0)\,dt_0 \qquad (16)$$

5) A system is linear if the response characteristics are additive and homogeneous:

$L[x_1(t) + x_2(t)] = L[x_1(t)] + L[x_2(t)] = y_1(t) + y_2(t)$

$L[ax(t)] = aL[x(t)] = ay(t)$ (a = constant).

6) The Dirac function or "unit impulse function" is an infinitely sharp peak function with the following character:

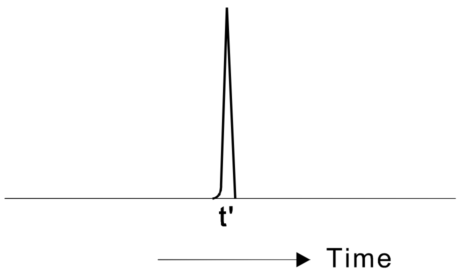

$\delta(t - t') = 0$ for $t \neq t'$

and:

$$\int_{t'-\varepsilon}^{t'+\varepsilon} \delta(t - t')\,dt = 1 \quad \text{for } \varepsilon \to +0$$

and:

$$\int_{-\infty}^{\infty} x(t)\,\delta(t - t')\,dt = x(t').$$

in which case, assuming that L is time-invariant:

$$y(t) = L[x(t)] = \int_{-\infty}^{t} x(t_0)\, L[\delta(t-t_0)]\, dt_0 = \int_{-\infty}^{t} x(t_0)\, h(t-t_0)\, dt_0 =$$

$$= \int_{0}^{\infty} x(t-\tau)\, h(\tau)\, d\tau$$

where: $t - t_0 = \tau$ was substituted.

For the truncated variables $x_T(t)$ and $y_T(t)$ as used before, with their Fourier transformations $X_T(\omega)$ and $Y_T(\omega)$ it is thus found that:

$$y_T(t) = \int_{0}^{\infty} x_T(t-\tau)\, h(\tau)\, d\tau \tag{17}$$

and:

$$\begin{aligned} Y_T(\omega) &= \int_{-\infty}^{\infty} e^{-i\omega t} \left[\int_{0}^{\infty} x_T(t-\tau)\, h(\tau)\, d\tau \right] dt \\ &= \int_{0}^{\infty} h(\tau) \left[\int_{-\infty}^{\infty} e^{-i\omega t}\, x_T(t-\tau)\, dt \right] d\tau \\ &= \int_{0}^{\infty} h(\tau) \left[\int_{-\infty}^{\infty} x_T(u)\, e^{-i\omega u} du \right] e^{-i\omega\tau}\, d\tau \\ &= X_T(\omega) \int_{0}^{\infty} h(\tau)\, e^{-i\omega\tau}\, d\tau \\ &\equiv X_T(\omega)\, H(\omega) \end{aligned} \tag{18}$$

in which $u = t - \tau$.

$H(\omega)$ is the Fourier transformation of $h(t)$ and is called the frequency response function. Using the definition for the spectral density function (13), it follows that for real processes $x_T(t)$ and $y_T(t)$:

$$S_{yy}(\omega) = \lim_{T\to\infty} \frac{1}{2\pi T} |Y_T(\omega)|^2 = \lim_{T\to\infty} \frac{1}{2\pi T} |X_T(\omega)|^2 |H(\omega)|^2$$

and thus:

$$S_{yy}(\omega) = S_{xx}(\omega) |H(\omega)|^2 \tag{19}$$

So, the relation is derived that the output spectral density function is equal to the product of the input spectral density function and the square of the frequency response function.

In a graphic representation:

Figure D

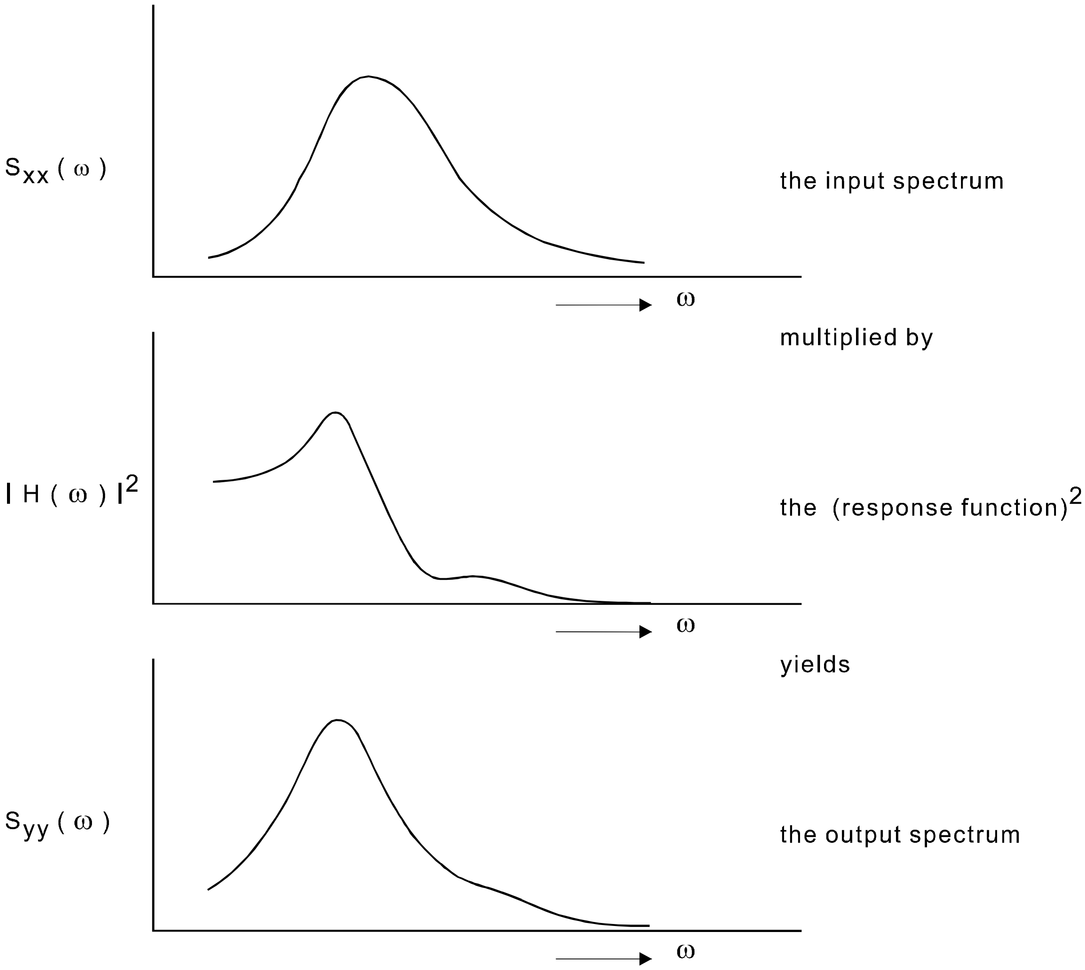

Some relations

The following quantities can now be calculated with use of the spectral density function:

$$m_{x0} = \int_0^\infty S_{xx}(\omega)\,d\omega \tag{20}$$

and

$$m_{x1} = \int_0^\infty S_{xx}(\omega)\,\omega\,d\omega \tag{21}$$

For a stochastic variable x, describing a stationary ergodic process, is:

$$\overline{M}_x = \frac{1}{2}\int_{-\infty}^{\infty} S_{xx}(\omega)\,d\omega \tag{14}$$

When $S_{xx}(\omega)$ is an even, real function and x has a narrow spectrum and zero mean value, it follows that:

$$\overline{M}_x = \int_0^\infty S_{xx}(\omega)\,d\omega = m_{x0}$$ (= area under the spectrum)

and:

$$\sigma_x = \sqrt{\overline{M}_x} = \sqrt{m_{x0}} \tag{22}$$

$$T_1 = 2\pi\frac{m_{x0}}{m_{x1}} \tag{23}$$

When x follows a normal distribution, then it can be calculated that:

$$4\sigma_x = 2x_{a1/3} \quad \text{(significant double amplitude)} \tag{24}$$

Irregularity of waves

Since it is known that the distributions of the wave elevations at sea are approximately normal, all formulae mentioned earlier are valid to describe irregular sea conditions. To judge the behaviour of vessels at sea, irregular seas are assumed to have energy spectral density functions - or power spectra - that can be described by:

$$S_{\zeta\zeta}(\omega) = A \,.\, \omega^{-r} \,.\, e^{-B \,.\, \omega^{-s}} \tag{25}$$

Formula (25) represents the hypothetical spectra, similar to the Pierson-Moskowitz[7)] spectra for fully developed seas when:

r = 5,
s = 4,
A = 172.8 $(\zeta_{w1/3})^2 \, (T_1)^{-4}$
B = 691.0 $(T_1)^{-4}$

Assuming that the wave height is a random variable with a narrow band normal distribution and zero mean value one arrives at (see also (24) and (23)):

$$\zeta_{w1/3} \simeq 4\sqrt{m_{\zeta 0}}$$

$$T_1 \simeq 2\pi \frac{m_{\zeta 0}}{m_{\zeta 1}}$$

where $\zeta_{w1/3}$ is the significant wave height and T_1 the average wave period.

In relating the spectra (25) to observations, the average observed wave height ζ_w is assumed to coincide with the significant wave height $\zeta_{w1/3}$. The average observed period T is assumed to coincide with the average calculated period T_1. So, observed sea conditions can be represented by means of a spectrum, as shown in Figure E, where the observations of H.U. Roll on the North Atlantic Ocean are represented in Pierson-Moskowitz spectra.

7) Pierson, W.J. and Moskowitz, L.; “A Proposed Spectral Form for Fully Developed Wind Seas Based on Similarity Theory of S.A. Kitaigorodskii”, Journal of Geophysical Research, Vol. 69, December 1964.

Figure E

PIERSON-MOSKOWITZ SPECTRA
(s = 4) and (r = 5)
Significant wave height $\zeta_{w1/3}$ and average period T_1
according to Roll for the North Atlantic Ocean
$T_1 = 2\pi\ (m_{\zeta 0}/m_{\zeta 1})$

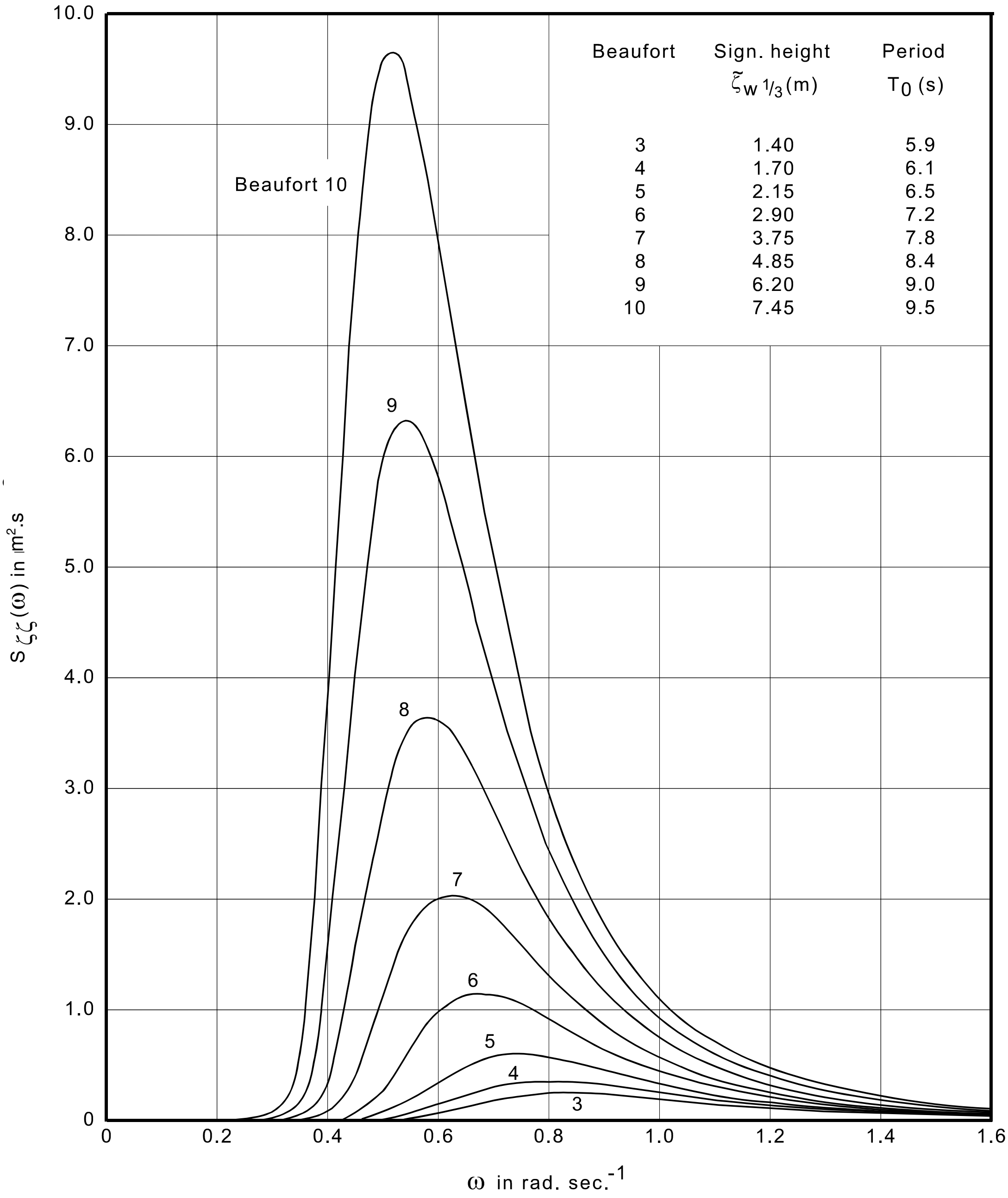

Irregularity of waves

Since it is known that the distributions of the wave elevations at sea are approximately normal, all formulae mentioned earlier are valid to describe irregular sea conditions. To judge the behaviour of vessels at sea, irregular seas are assumed to have energy spectral density functions - or power spectra - that can be described by the JONSWAP[8)] formula:

$$S_{\zeta\zeta}(\omega) = \alpha \,.\, g^2 \,.\, \omega^{-5} \,.\, \exp\left[-1.25\,(\omega/\omega_0)^{-4}\right] . \gamma^{\exp\left[-(\omega-\omega_0)^2/(2\sigma^2 \,.\, \omega_0^2)\right]} \tag{26}$$

$$\sigma = \begin{cases} \sigma_a \text{ for } \omega \leq \omega_0 \\ \sigma_b \text{ for } \omega > \omega_0 \end{cases}$$

in which:

ω	=	circular frequency
ω_0	=	spectral peak frequency
g	=	acceleration due to gravity

The dimensionless shape parameters α, γ, σ_a and σ_b are generally taken as:

$\alpha = 0.0989$; $\gamma = 3.3$; $\sigma_a = 0.07$; $\sigma_b = 0.09$

Assuming that the wave height is a random variable with a narrow band normal distribution and zero mean value one arrives at (see also (24) and (23)):

$$\zeta_{w1/3} \simeq 4\sqrt{m_{\zeta 0}}$$

$$T_1 \simeq 2\pi \frac{m_{\zeta 0}}{m_{\zeta 1}}$$

where $\zeta_{w1/3}$ is the significant wave height and T_1 the average wave period.

In relating the spectra (26) to observations, the average observed wave height ζ_w is assumed to coincide with the significant wave height $\zeta_{w1/3}$. The average observed period T is assumed to coincide with the average calculated period T_1. So, observed sea conditions can be represented by means of a spectrum, as shown in Figure F, for a range of Beaufort numbers.

---

8) Hasselman, K. et al.; “Measurement of Wind-wave Growth and Swell Decay During the Joint North Sea Wave Project (JONSWAP)”, Deutsches Hydrographisches Institut Hamburg, 1973.

NOTE: The relation between the average period T_1 and the peak period T_0 for the JONSWAP type spectra is $T_0/T_1 = 1.20$.

Figure F

JONSWAP SPECTRA

Significant wave height $\zeta_{w1/3}$ and peak period T_0 according to Roll for the North Atlantic Ocean

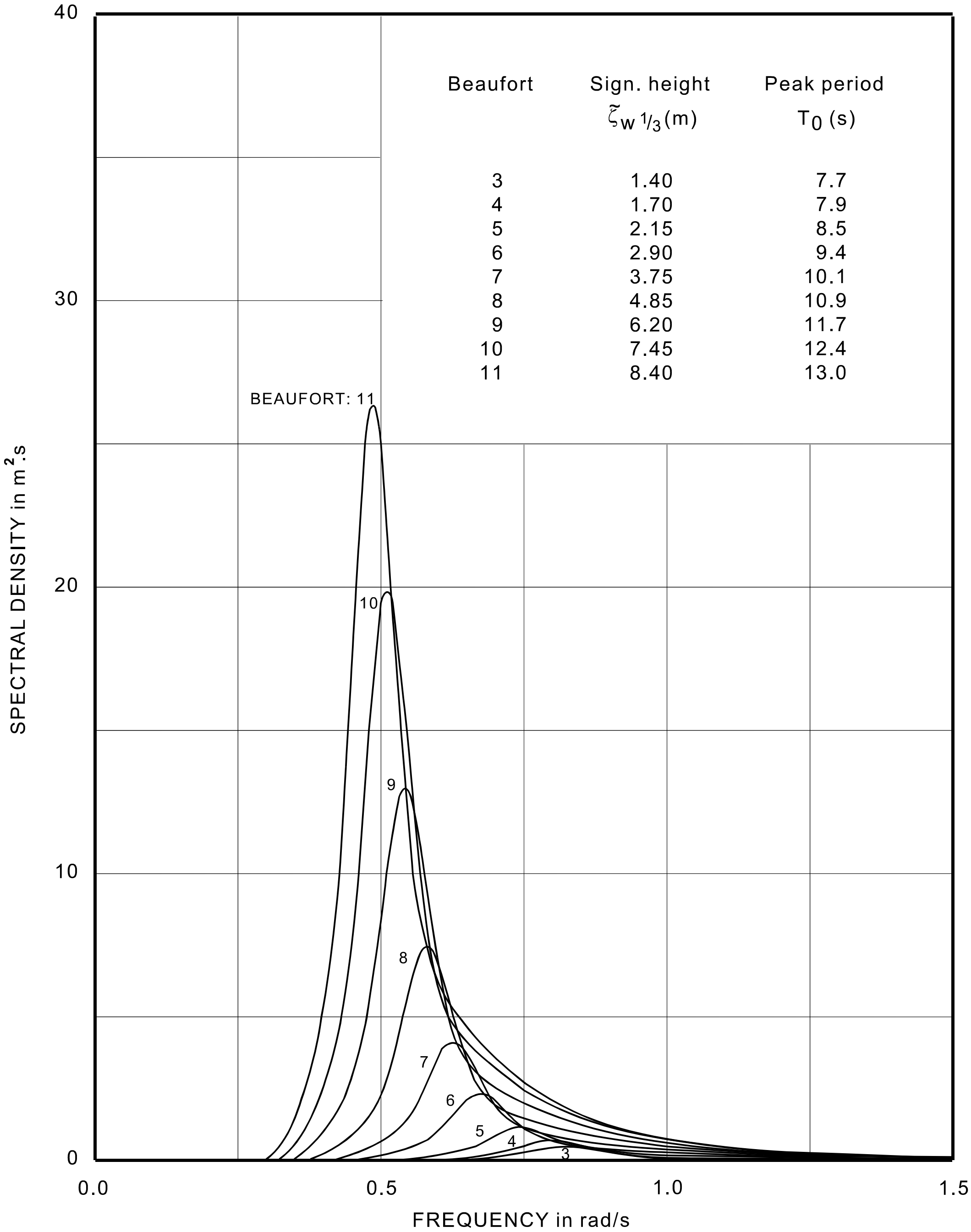

APPENDIX D03

Statistical Analysis

Revision	Date	Description of revision	Author
0	September 10, 2009	First version of the appendix.	JLC
1	February 26, 2010	Review and up-date of the text.	JLC
2	September 1, 2010	Remark on extremes in STATAN added.	JH/JJS
3	April 11, 2018	Adjusted to SHARK	JvdB

Statistical Analysis

The data analysis of the model tests or simulations includes a statistical analysis of the recorded time signals. Two types of statistical analysis are available, being “BasicStatistics” and “ExtendedStatistics”. The “BasicStatistics” tables contain a limited statistical analysis. The “ExtendedStatistics” tables contain a more detailed statistical analysis. The statistical quantities included in both analysis methods are listed below.

BasicStatistics tables

The following quantities are determined for the measured and calculated time signals.

1. *Mean value*: $\bar{u}$ (MEAN)

   $$\bar{u} = \frac{1}{N}\sum_{n=1}^{N} u_n \quad (N = \text{number of samples})$$

2. *Standard deviation*: σ_u (ST.DEV)

   $$\sigma_u = \sqrt{\frac{1}{N}\sum_{n=1}^{N}(u_n - \bar{u})^2}$$

3. *Maximum value*: A MAX +
   Highest crest value.

4. *Maximum value*: A MAX -
   Highest trough value.

ExtendedStatistics tables

The following quantities are determined for the measured and calculated time signals.

5. *Maximum value*: A MAX +
   Highest crest value.

6. *Maximum value*: A MAX -
   Highest trough value.

7. *Maximum double amplitude*: 2A MAX
   This is the maximum crest to trough value.

8. *Significant peak value*: A 1/3 +
   This is the mean of the highest one-third zero to crest values.

9. *Significant trough value*: A 1/3 -
   This is the mean of the highest one-third zero to trough values.

10. *Significant double amplitude*: 2A 1/3
    This is the mean of the highest one-third crest to trough values.

11. *Number of oscillations*: NO
    This is the total number of oscillations in the record.

APPENDIX D05

Description of the 3-Parameter Weibull Fit

Revision	Date	Description of revision	Author
0	September 10, 2009	First version of the appendix	JH
1	February 1, 2010	Review and up-date of the text	JLC

Description of the 3-Parameter Weibull Fit

The values “A MAX. +” and “A MAX. -” presented in the tables with statistical output represent the measured maximum and minimum values, as observed during the test or simulation. For design purposes, however, the so-called “most probable maximum” (MPM-) value is often applied. This is a statistically more reliable maximum value. The most probable maximum is defined as follows:

$$P(X > X_{MPM}) = \frac{1}{N} \cdot 100\%$$

in which:

P	=	probability of exceedance, [-]
X	=	variable, e.g. the turret motion
X_{MPM}	=	“most probable maximum” (MPM-) value for variable X
N	=	number of oscillations in duration for which the value of X_{MPM} is determined

The MPM-value is the extreme value with the probability to occur once during the duration of the storm (P = 1/N). The MPM-value, therefore, will depend on the storm duration or the number of oscillations N; a longer storm duration will lead to a higher most probable maximum. The number of oscillations N is counted for each signal and can be found in the tables with the results of the statistical.

From the test or simulation results MPM-values can be determined using the distribution of the extremes plotted on Weibull paper. Because the highest measured maximum is deleted from Weibull plots (for this value no probability of exceedance can be determined), the most probable maximum with the same probability is determined based on an extrapolation of the upper part of the curve of the Weibull plots.

The 3-parameter Weibull fit is defined as follows:

$$P(x) = e^{-\left(\frac{x-\theta}{\alpha}\right)^{\beta}}$$

in which:

P(x)	=	probability of exceedance of value x
α	=	scale parameter
β	=	shape parameter
θ	=	location parameter

On Weibull paper the 3-parameter Weibull fit is a straight line.

The values of α, β and θ are determined using a least-squares fitting procedure through the peak values obtained from the recorded signal. The calculated values for α, β and θ can be found at the top of the Weibull plots.

The formulation on the previous page can be used to determine the probability of exceedance P for a given peak value x. Alternatively, the 3-parameter Weibull distribution can be represented as follows:

$$x(P) = \theta + \alpha \cdot \sqrt[\beta]{-\ln(P)}$$

This formulation can be used to determine the peak value for a given probability of exceedance. The MPM-value is defined as the peak value with a probability to occur once during the storm duration (or: P = 1/N). Therefore, if a 3-parameter Weibull fit is available, the MPM-value can then be calculated as follows:

$$x_{MPM} = \theta + \alpha \cdot \sqrt[\beta]{-\ln\left(\frac{1}{N}\right)} \quad \text{for maxima}$$

$$x_{MPM} = \theta - \alpha \cdot \sqrt[\beta]{-\ln\left(\frac{1}{N}\right)} \quad \text{for minima}$$

in which:

α,β,θ	=	Weibull fit parameters
N	=	number of peaks in the signal

The calculated MPM values are shown at the top of the Weibull plots with a fitted line. They are shown next to the calculated α, β and θ values.

Remark

It should be noted that an MPM-value determined from the fitted line in the Weibull distribution depends on the values of the parameters α, β and θ and may be affected by the selection of peaks used in the least-squares fit. Typically, the 25% or 50% highest peaks are included in the analysis, but the selected percentage is more or less arbitrary. In sensitive cases, it is therefore recommended to also determine the MPM-value using e.g. the highest 10%, 25%, 50% and 75% of the peaks in order to check the robustness of the determined MPM-value.

Furthermore, it must be noted that the quality of the MPM-value depends on the distribution function of the analyzed signals. Some signals show only one or two extreme peaks (very low probability of exceedance), while the rest of the peaks show a closer agreement with the distribution function. This behaviour depends on the applied wave realisation and non-linear effects. Due to the combination of a low probability of exceedence of the single peak and the Weibull fit based on the majority of the peaks the MPM-value can show a large deviation from the maximum value.

APPENDIX D06

Determination of Response Functions on basis of Cross-correlation Method

Revision	Date	Description of revision	Author
0	May 19, 2009	First version of the appendix	JLC
1	April 18, 2017	Update Jaap de Wilde	JdW

Determination of Response Functions on Basis of Cross-correlation Method

Introduction

This appendix describes the relation between two processes x(t) and y(t) being the input and output signal respectively of a physical system.

x(t) → System → y(t)

For instance: the input signal can be an irregular wave and the output signal the resulting motion of a floating structure.

It will be assumed that the signals discussed are realisations of random processes being stationary and ergodic. Stationary means that the statistical properties of the realisations are independent of time, while ergodicity indicates that one single realisation of the process determines the statistical properties of the process completely.

Characterisation of input-output system in frequency domain

For a description of the input-output system in the frequency domain use can be made of the so-called cross-spectral density function being defined as the Fourier transform of the cross-correlation function:

$$S_{xy}(\omega) = \frac{1}{\pi} \int_{0}^{+\infty} R_{xy}(\tau)\, e^{-i\omega\tau}\, d\tau \qquad (2)$$

Since the cross-correlation function $R_{xy}(\tau)$ is not an even function its Fourier transform has the complex form. The cross-spectral density function consists therefore of a real and an imaginary part or an amplitude and a phase part:

$$S_{xy}(\omega) = A_{xy}(\omega) e^{-i\phi_{xy}(\omega)} \qquad (3)$$

Frequency response functions

If a system with an input signal x(t) and output signal y(t) is linear, an impulse response function h(t) can be defined so that:

$$y(t) = h(t) * x(t) = \int_{-\infty}^{+\infty} h(\tau)\, x(t-\tau)\, d\tau \qquad (4)$$

,where $*$ denotes a convolution.

Transformation to the frequency domain yields:

$$Y(\omega) = H(\omega)\, X(\omega) \qquad (5)$$

,where $X(\omega)$, $Y(\omega)$ and $H(\omega)$ are the Fourier transforms of x(t), y(t) and h(t) respectively.

The quantity $|H(\omega)|$ is called the frequency response function and $\phi_H(\omega)$ is the phase response function.

$$H(\omega) = |H(\omega)| e^{-i\phi_H(\omega)} \tag{6}$$

From (12) it can be found that:

$$|H(\omega)| = \sqrt{\frac{S_{yy}(\omega)}{S_{xx}(\omega)}} \tag{7}$$

in which $S_{xx}(\omega)$ and $S_{yy}(\omega)$ are the scalar spectra of the signals x(t) and y(t), being defined as the Fourier transform of the auto-correlation functions $R_{xx}(\tau)$ and $R_{yy}(\tau)$ respectively:

$$S_{yy} = \frac{1}{2\pi} \int_{-\infty}^{+\infty} R_{yy}(\tau) e^{-i\omega\tau} d\tau \tag{8}$$

$$S_{yy} = \frac{1}{2\pi} \int_{-\infty}^{+\infty} R_{yy}(\tau) e^{-i\omega\tau} d\tau \tag{9}$$

If both the amplitude and the phase response function are required use has to be made of the cross-spectral density functions $S_{xy}(\omega)$ and the scalar spectral density function of the input $S_{xx}(\omega)$ as is shown below:

$$\begin{aligned} R_{xy}(\tau) &= \lim_{T\to\infty} \frac{1}{2T} \int_{-T}^{T} x_r(t)\, y_r(t+\tau)\, d\tau = \\ &= \lim_{T\to\infty} \frac{1}{2T} \int_{-T}^{T} \left\{ x_r(t) \int_{-\infty}^{+\infty} h(\theta)\, x_r(t+\tau-\theta) d\theta \right\} dt = \\ &= \int_{-\infty}^{+\infty} h(\theta) R_{xx}(\tau-\theta) d\theta \end{aligned} \tag{10}$$

The Fourier transform yields:

$$\begin{aligned} S_{xy}(\omega) &= \frac{1}{2\pi} \int_{-\infty}^{+\infty} e^{-i\omega\tau} \left\{ \int_{-\infty}^{+\infty} h(\theta) R_{xx}(\tau-\theta)\, d\theta \right\} d\tau \\ &= \frac{1}{2\pi} \int_{-\infty}^{+\infty} \left\{ h(\theta) e^{-i\omega\theta} \int_{-\infty}^{+\infty} R_{xx}(\tau-\theta)\, e^{-i\omega(\tau-\theta)} d\tau \right\} d\theta \\ &= \left\{ \int_{-\infty}^{+\infty} h(\theta)\, e^{-i\omega\theta}\, d\theta \right\} S_{xx}(\omega) \\ &= H(\omega)\, S_{xx}(\omega) \end{aligned} \tag{11}$$

This shows that:

$$H(\omega) = \frac{S_{xy}(\omega)}{S_{xx}(\omega)} \tag{12}$$

in which $H(\omega)$ and $S_{xy}(\omega)$ have the complex form.

The amplitude response function $|H(\omega)|$ is given by:

$$|H(\omega)| = \frac{|S_{xy}(\omega)|}{S_{xx}(\omega)} = \frac{A_{xy}(\omega)}{S_{xx}(\omega)} \tag{13}$$

and the phase response function by:

$$\phi_H(\omega) = \arg \frac{S_{xy}(\omega)}{S_{xx}(\omega)} = \phi_{xy}(\omega) \tag{14}$$

In addition to the given variables the coherency function $\gamma^2_{xy}(\omega)$ can be defined as:

$$\gamma^2_{xy}(\omega) = \frac{|S_{xy}(\omega)|^2}{S_{xx}(\omega)\,S_{yy}(\omega)} \tag{15}$$

The coherency function is defined to be a measure for the linear dependence or the correlation between the frequency components of the two processes.

For a purely linear system the coherency function becomes unity. For completely uncorrelated input and output processes the coherency function becomes zero.

Usually the coherency will be between these two extremes:

$$0 \le \gamma^2_{xy}(\omega) \le 1 \tag{16}$$

due to one or more of the following reasons:

- insufficient accurate spectral estimates for S_{xx}, S_{yy} and S_{xy};
- the presence of noise in either one or both of the records;
- non-linear effects.

In summary we have seen that the amplitude response function can be obtained in two different ways, respectively:

$$|H(\omega)|_{(1)} = \sqrt{\frac{S_{yy}(\omega)}{S_{xx}(\omega)}}$$

and

$$|H(\omega)|_{(2)} = \frac{|S_{xy}(\omega)|}{S_{xx}(\omega)}$$

References

[1] Newland, D.E.; "An Introduction to Random Vibrations and Spectral Analysis", Longman Scientific & Technical, Second edition, 1984.

APPENDIX D09

Review of Theory of Harmonic Analysis

Revision	Date	Description of revision	Author
0	May 19, 2009	First version of the appendix	JLC
1	December 11, 2009	Added amplitude and phase determination	JvdB
2	January 26, 2010	Added small revisions	AK

Review of the Theory of Harmonic Analysis

A regular signal f(t) can be represented as a sum of sines and cosines (Fourier series):

$$f(t) = \sum_{k=0}^{k=\infty} (a_k \cos kt + b_k \sin kt)$$

in which the first term (k=0) represents the mean value and the other terms represent the particular harmonic component. The coefficient a_k can be obtained by multiplying the above equation with cos (nt) and integrating over the interval 0 to 2π:

$$\int_0^{2\pi} f(t)\cos nt\,dt = \sum_{k=0}^{\infty}\left(a_k \int_0^{2\pi}\cos kt\cos nt\,dt + b_k \int_0^{2\pi}\sin kt\cos nt\,dt\right)$$

All terms of the sum yield the result 0, except the term:

$$\int_0^{2\pi}\cos kt\cos nt\,dt \qquad \text{for } n=k$$

from which a_n can be determined:

$$a_n = \frac{1}{\pi}\int_0^{2\pi} f(t)\cos nt\,dt$$

The coefficients b_n can be obtained in an equivalent way by multiplying with sin (nt) and integrating:

$$b_n = \frac{1}{\pi}\int_0^{2\pi} f(t)\sin nt\,dt$$

The solution of above integrals is performed in a numerical way by integrating over the complete measuring time:

$$a_k = \frac{2}{N}\sum_{n=1}^{N} f_n \cos kt \qquad \text{and} \qquad b_k = \frac{2}{N}\sum_{n=1}^{N} f_n \sin kt$$

in which f_n is the magnitude and N is the number of samples used for the numerical integration. The coefficients a_k and b_k determine the amplitude and the phase of each component k:

$$amp_k = \sqrt{a_k^{\,2} + b_k^{\,2}} \qquad \text{and} \qquad \varepsilon_k = a\tan\left(\frac{-b_k}{a_k}\right)$$

By comparing the amplitude and phase information of a signal s_1 to a lead signal s_0, an RAO can be determined.

APPENDIX D12

Calculation of Derived Quantities

Revision	Date	Description of revision	Author
0	June 22, 2015	First version of the appendix	FJ
1	July 23, 2015	Description of force frame added	FJ
2	October 4, 2017	Derived Quantities of Wind Calibration Added	AN
3	November 16, 2018	Several improvements & additions	AN
4	August 30, 2023	Improvements to inertia correction	JvdZ

Calculation of Derived Quantities

This appendix describes how the derived quantities are calculated from the signals measured in the basin. The description of the following derived quantities are included in this Appendix:

- Motions of the model
- Accelerations of the model

MOTIONS OF THE MODEL

Earth fixed motions of the model

During the tests the motions of the measuring target were measured. The location of the target during the model test programme is listed in TABLE 5 and TABLE 6. For the calculation of the earth-fixed motions at a point P (e.g. the centre of gravity) from the measured motions the formulas below were used.

$$\begin{pmatrix} x_e \\ y_e \\ z_e \end{pmatrix} = \begin{pmatrix} x_{meas} \\ y_{meas} \\ z_{meas} \end{pmatrix} + \begin{pmatrix} D_{11} & D_{12} & D_{13} \\ D_{21} & D_{22} & D_{23} \\ D_{31} & D_{32} & D_{33} \end{pmatrix} \cdot \begin{pmatrix} A \\ B \\ C \end{pmatrix}$$

in which:

x_{meas}	=	measured X-translation of measurement point in earth fixed system
y_{meas}	=	measured Y-translation of measurement point in earth fixed system
z_{meas}	=	measured Z-translation of measurement point in earth fixed system
ϕ	=	measured roll motions
θ	=	measured pitch motions
ψ	=	measured yaw motions
A	=	ship fixed X-co-ordinate of point P from measurement point
B	=	ship fixed Y-co-ordinate of point P from measurement point
C	=	ship fixed Z-co-ordinate of point P from measurement point

and

$$D_{11} = \cos(\psi)\cdot\cos(\theta) - 1$$
$$D_{12} = -\sin(\psi)\cdot\cos(\varphi) + \cos(\psi)\cdot\sin(\theta)\cdot\sin(\varphi)$$
$$D_{13} = \sin(\psi)\cdot\sin(\varphi) + \cos(\varphi)\cdot\cos(\psi)\cdot\sin(\theta)$$

$$D_{21} = \sin(\psi)\cdot\cos(\theta)$$
$$D_{22} = \cos(\psi)\cdot\cos(\varphi) + \sin(\psi)\cdot\sin(\theta)\cdot\sin(\varphi) - 1$$
$$D_{23} = -\cos(\psi)\cdot\sin(\varphi) + \cos(\varphi)\cdot\sin(\psi)\cdot\sin(\theta)$$

$$D_{31} = -\sin(\theta)$$
$$D_{32} = \cos(\theta)\cdot\sin(\varphi)$$
$$D_{33} = \cos(\theta)\cdot\cos(\varphi) - 1$$

In this way the motions at several locations as listed in TABLE 11 and TABLE 12 were calculated.

Relative motions at the manifold location

The relative motions at the manifold location is calculated as follows:

REL_MAN_X_FSRU_JETTY = X_MAN_JETTY + 0.0
REL_MAN_Y_FSRU_JETTY = Y_MAN_JETTY + 6.87 (gap between the side of the FSRU and the jetty)
REL_MAN_Z_FSRU_JETTY = Z_MAN_JETTY + 0.0

REL_MAN_X_FSRU_LNGC = X_MAN_LNGC – X_MAN_FSRU + 0.0
REL_MAN_Y_FSRU_LNGC = Y_MAN_LNGC – Y_MAN_FSRU + 4.596 (gap between the side of the FSRU and the LNGC)

REL_MAN_Z_FSRU_LNGC = Z_MAN_LNGC – Z_MAN_FSRU + 0.0

ACCELERATIONS OF THE MODEL

The linear accelerations were calculated at the Centre of Gravity listed in TABLE 11 and TABLE 12 based on the accelerations measured at four locations on the model as listed in TABLE 5 and TABLE 6. As a cross check, the accelerations at the COG were derived from the motions measured by the optical measurement system and compared to the accelerations derived from the accelerometers. The accelerations were calculated using the formulas below.

First the angular accelerations are calculated, using the formulas below.

Roll acceleration : $A\varphi = \frac{(Az,ps - Az,sb)}{Y}$

Pitch acceleration : $A\theta = \frac{(Az,aft - Az,fore)}{X}$

Yaw acceleration : $A\psi = \frac{(Ax,sb - Ax,ps)}{Y}$

In which:
Az,ps = Accelerations in Z direction at portside, [m/s^2]
Az,sb = Accelerations in Z direction at starboard, [m/s^2]
Ax,ps = Accelerations in X direction at portside, [m/s^2]
Ax,sb = Accelerations in X direction at starboard, [m/s^2]
X = Distance in X-direction between the aft and both portside and starboard transducers, [m]
Y = Distance in Y-direction between both portside and starboard transducers, [m]

Subsequently, the linear accelerations in any point on the model were calculated using the following formulas.

$$\begin{pmatrix} D_{ax} \\ D_{ay} \\ D_{az} \end{pmatrix} = \begin{pmatrix} A_x \\ A_y \\ A_z \end{pmatrix} + \begin{pmatrix} 0 & -A_\psi & A_\theta \\ A_\psi & 0 & -A_\varphi \\ -A_\theta & A_\varphi & 0 \end{pmatrix} \cdot \begin{pmatrix} C_x \\ C_y \\ C_z \end{pmatrix}$$

In which:
D_A = Acceleration at derived location, x, y & z, [m/s^2]
A_{xyz} = Measured translational accelerations at source location, [m/s^2]
$A_{\varphi\theta\psi}$ = Calculated rotational accelerations at source location, [rad/s^2]
C = Coordinates of derived location, x, y & z relative to the source location, [m]

APPENDIX E01

Description of the Offshore Basin wind, wave and current generation systems

Revision	Date	Description of revision	Author
0	May 27, 2009	First version of the appendix	JH

Description of the Offshore Basin wind, wave and current generation systems

The model tests in combined environments will be carried out in MARIN's Offshore Basin (OB). This basin offers a number of unique possibilities for the modelling of current, waves and wind.

The figure below shows a cross section of the Offshore Basin.

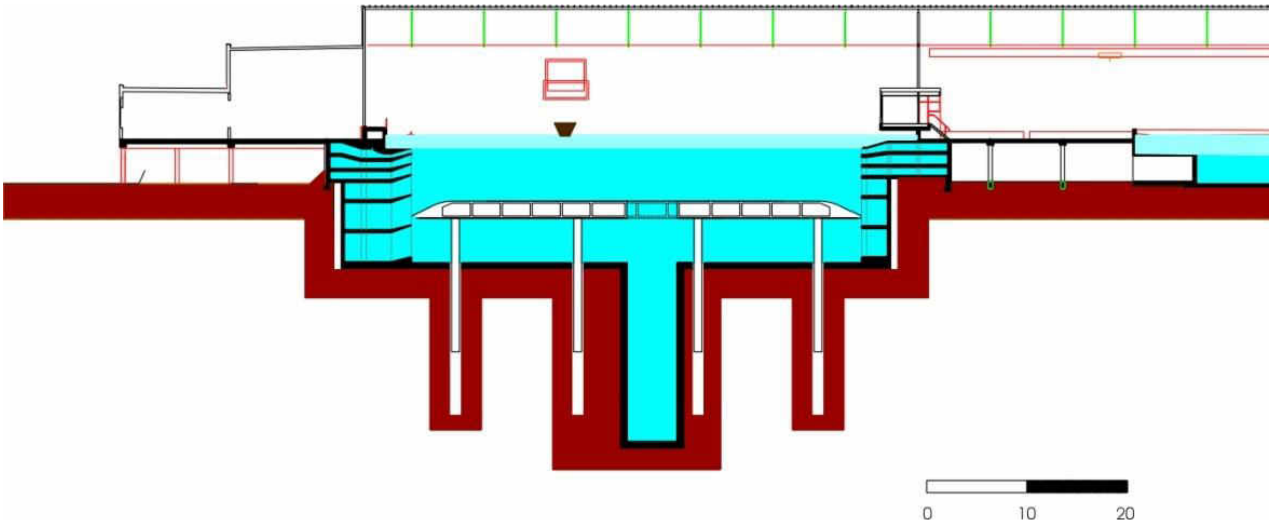

The basin measures 46 m * 36 m and has a movable floor (dimensions 36.35 m * 31.6 m), which is used to adjust the water depth. The maximum water depth measures 10.2 m at model scale. The basin also has a deep pit, with a maximum depth of 30 m.

The current generation system consists of 6 separate layers, each equipped with its own pump. Current can be generated over the full depth of 10.2 m. The water is re-circulated through a system of channels outside the basin, in order to avoid re-circulation in the basin itself. This current generation system enables the adjustment of vertical current profiles. The picture below shows a cross section of the 6 current layers at the current inflow openings into the basin.

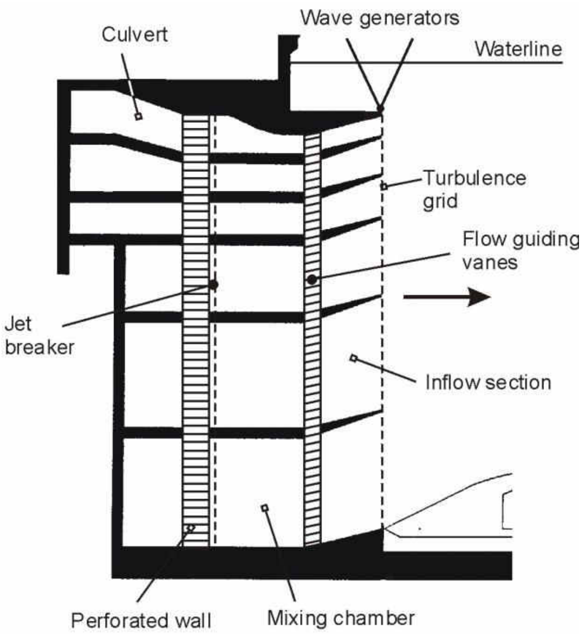

The uppermost layer is directly located under the 1.2 m high wave generators. The uniformity of the flow in the basin is obtained by flow distributing in- and outflow culverts.
To measure and adjust vertical current profiles, an electro-magnetic speed (EMS) probe mounted on a vertical traversing system is used. The EMS probe is an ellipsoidal probe for high spatial resolution and minimum disturbance. It is able to measure biaxial current velocities. Two types of measurements are carried out::

- Sweep measurements with a small constant vertical velocity of the probe to determine the vertical profile
- Stationary measurements a certain depths to determine the behaviour of the current in time (turbulence levels).

The figure below shows an example of a modelled vertical current profile. A sweep measurement was taken (low velocity carriage travelling along tension leg type vertical support wires) as well as stationary measurements at 4 depths.

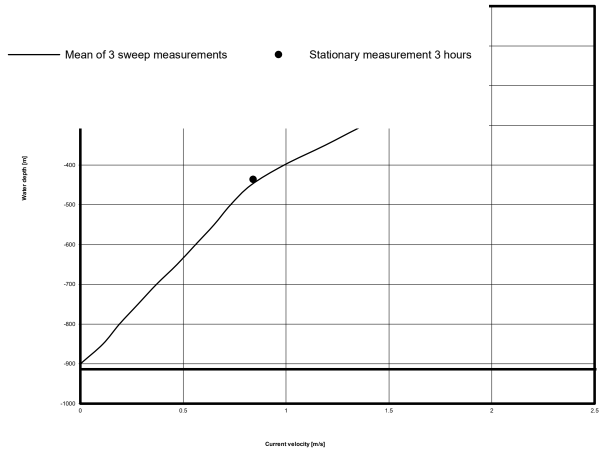

The next figure shows the time traces of the 4 stationary measurement points: 2 in the upper constant part, 2 in the sheared current part.

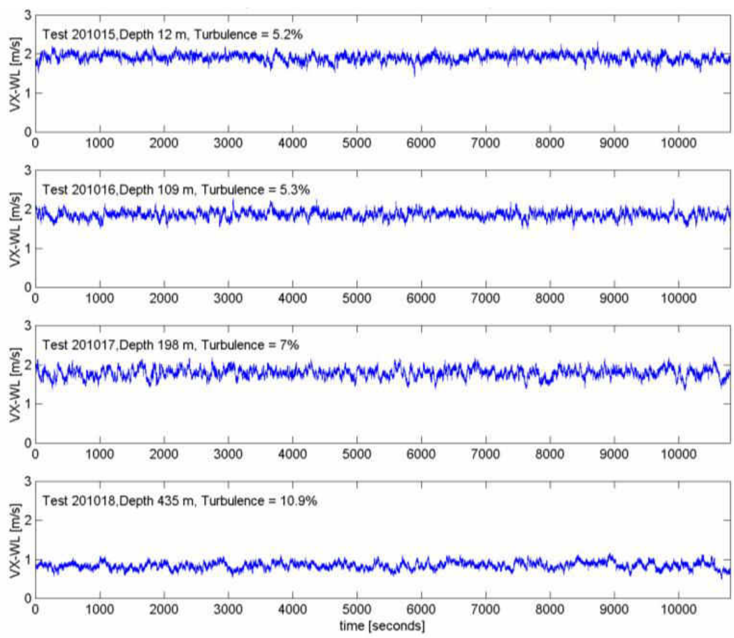

In the constant upper part the variation is very low (Turbulence level=5%), in the sheared current the variation is slightly higher (Turbulence level=7% and 10.9%) but this is a result of the natural processes in sheared current. For the present project it is recommended to keep the current constant over the entire low depth. A constant current guarantees the modelling of a realistic current load and a correct wave-current interaction.

Irregular waves are generated by a system of approximately 200 oscillating flaps. The wave flaps are shown in the picture below, showing an overview of the Offshore Basin. Each of these wave flaps is controlled individually with full control over stroke and period. This wave generation system can generate long-crested irregular seas, irregular seas with directional spreading and combinations of irregular waves and swell, each with their own direction of propagation. Wave absorbing beaches are present opposite to the wave generators.

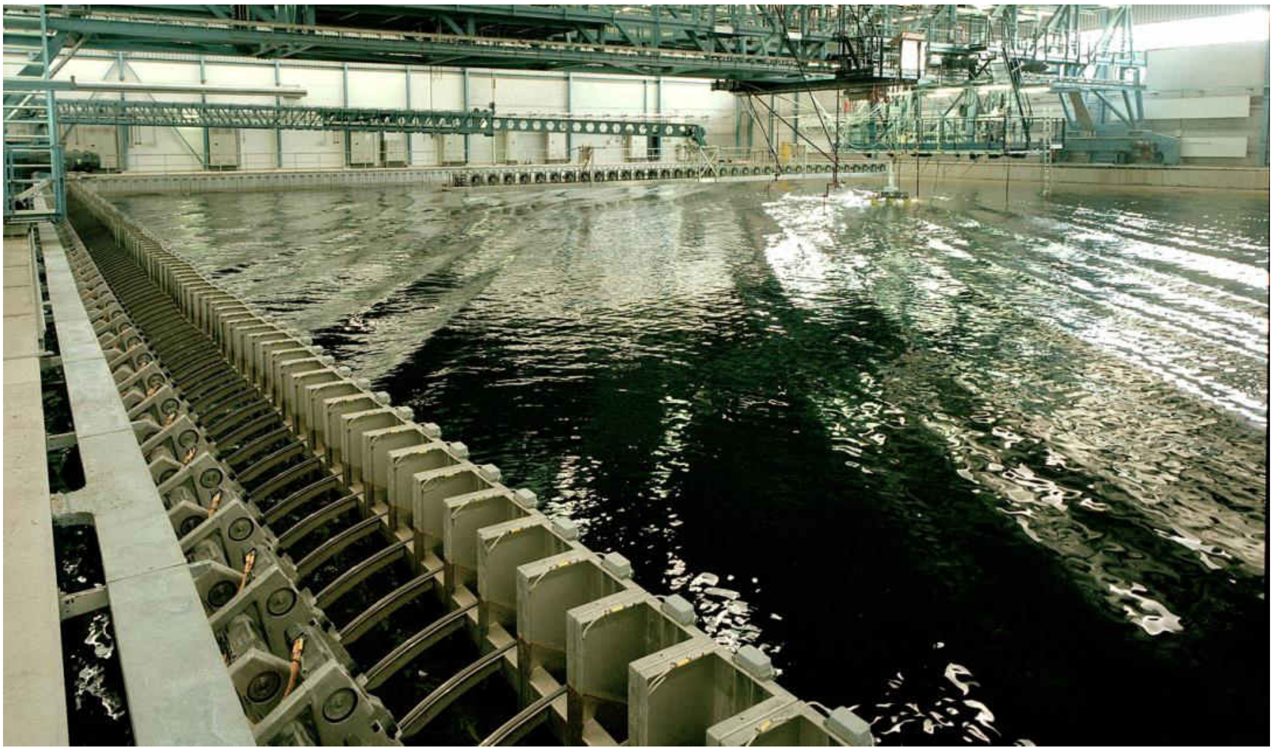

The movable floor is curved on its sides so optimize the current inflow. However, at the sides this means that the waves start to diffract in shallow water due to the difference in depth, rotating them onto the basin floor under the wrong angle. Therefore, we do not use the wave flaps in the corners anymore. The consequence is that we can only make waves perpendicular to the wave generators on both sides: either parallel with the current or perpendicular to the current.

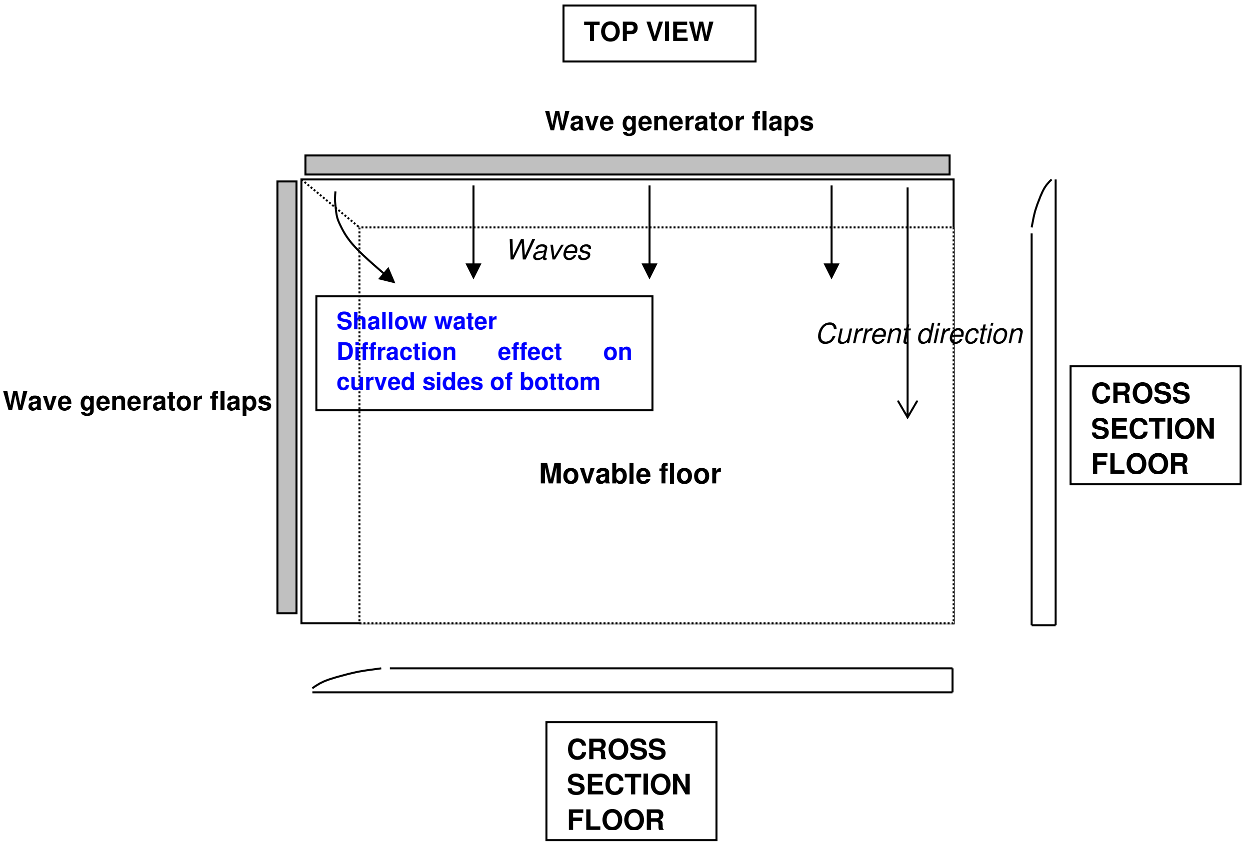

Wind is generated by a large number of wind fans. Together they form a wind field of 24 m width, as shown in the picture below. This ensures a constant wind field over the full measurement area, even when using a large test set-up. Constant wind as well as gusting and squall winds can be generated.

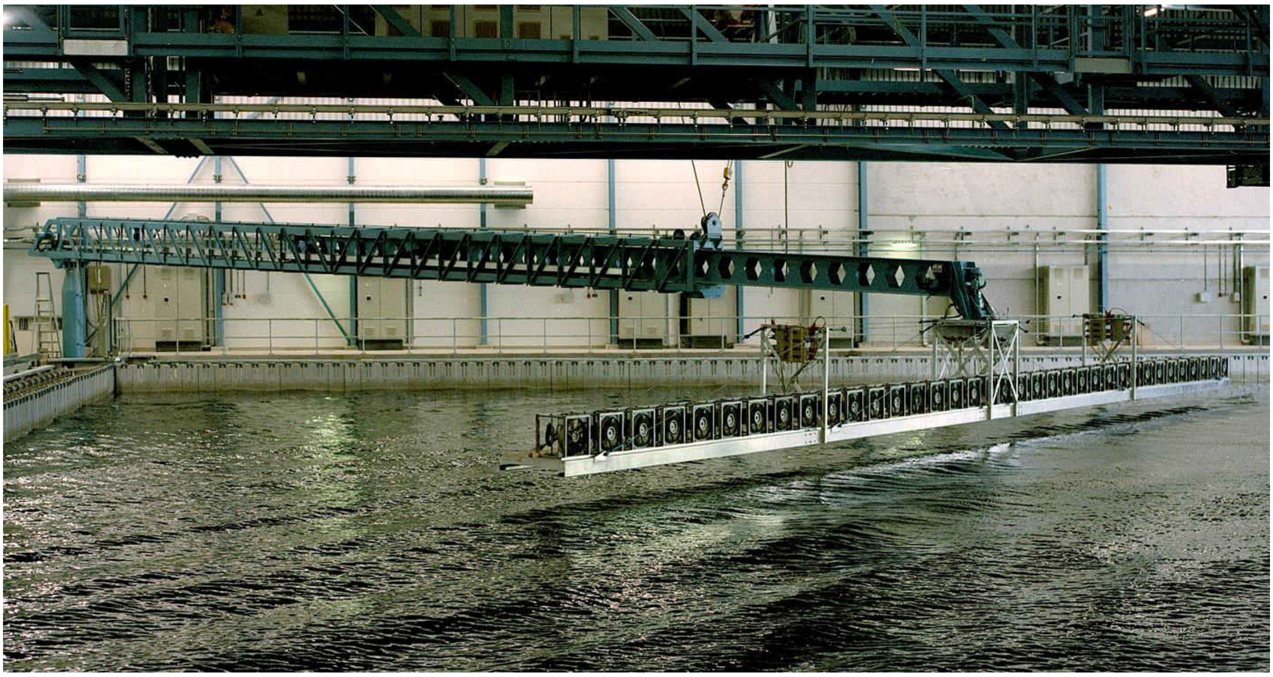

The relative angles of wind, waves and current as requested can be simulated, as shown in the figure below:

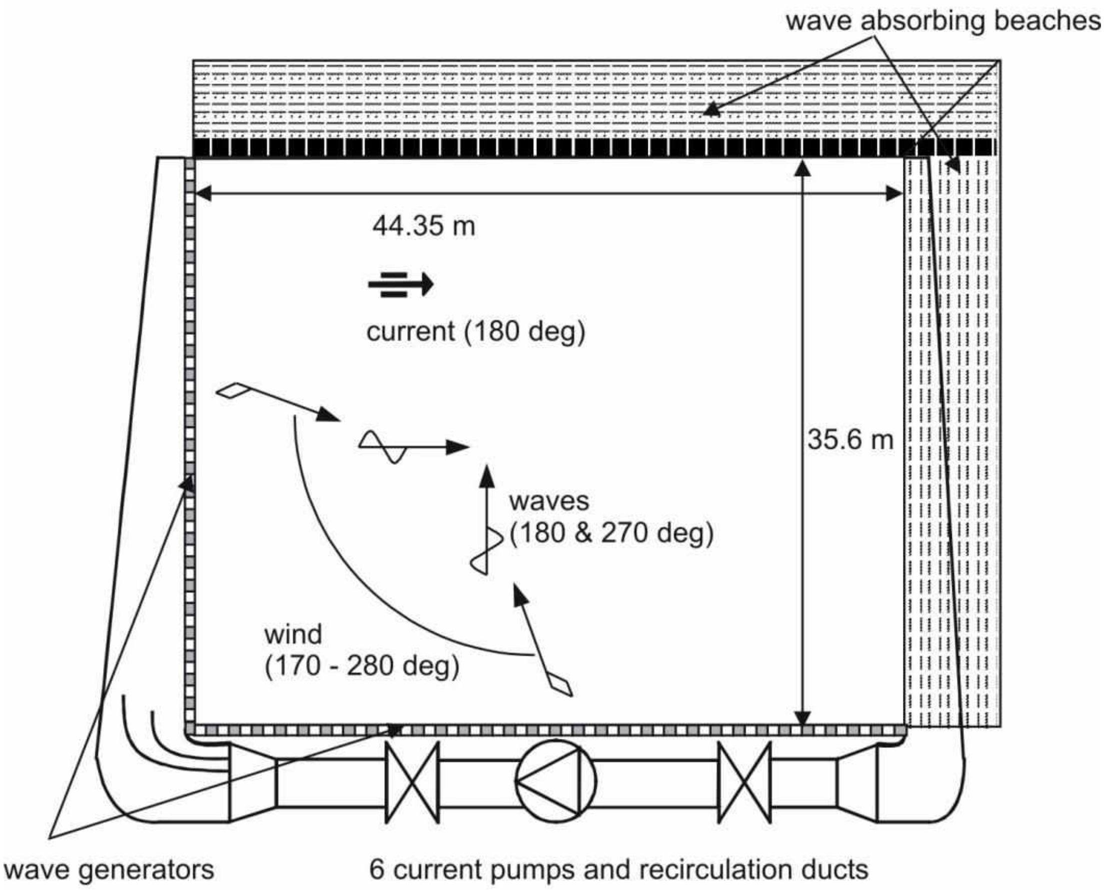

APPENDIX E03

Wave Spectrum Formulations

Revision	Date	Description of revision	Author
0	May 19, 2009	First version of the appendix	JLC

Wave Spectrum Formulations

In this appendix the mathematical formulation of a number of wave spectra used in offshore model testing is presented. Descriptions of the following spectra are included:

1. Pierson Moskowitz wave spectrum
2. JONSWAP wave spectrum
3. TMA wave spectrum
4. Gaussian spectrum
5. Ochi-Hubble wave spectrum
6. White noise spectrum
7. Some remarks on wave and group spectra

The spectral formulations are described based on the wave period and the significant wave height. In order to define the spectra $S_\zeta(\omega)$, the following definitions are required.

$H_s = 4\sqrt{m_0}$ = Significant wave height, [m]

$m_0 = \int_0^\infty S_\zeta(\omega)\cdot d\omega$ = Area under the wave spectrum or zeroth moment, [m^2]

$\omega_p = \frac{2\pi}{T_p}$ = Frequency at which the maximum energy is found, [rad/s]

T_p = Peak period, [s]

$T_1 = 2\pi\cdot\frac{m_0}{m_1}$ = Mean wave period or first period, [s]

$T_2 = 2\pi\cdot\sqrt{\frac{m_0}{m_2}}$ = Mean zero-upcrossing wave period or second period, [s]

$m_1 = \int_0^\infty \omega\cdot S_\zeta(\omega)\cdot d\omega$ = First moment, [m^2/s]

$m_2 = \int_0^\infty \omega^2\cdot S_\zeta(\omega)\cdot d\omega$ = Second moment, [m^2/s^2]

The bandwidth of a spectrum influences the time intervals between wave crests:

$$T_m = 2\pi\sqrt{\frac{m_2}{m_4}}$$ (Rice; 1944, 1945)

T_m is the mean period between wave crests. The ratio T_m/T_2 is related to the width of the spectrum. For each of the spectra the relationships between T_p, T_1 and T_2 are stated in a table in this appendix.

Pierson-Moskowitz wave spectrum (1964)

Among the wave spectra the Pierson-Moskowitz spectrum [1] is the most frequently applied one for fully developed seas. Pierson and Moskowitz have derived the wave spectral formulation for fully developed seas from analysis of wave spectra measured on the North Atlantic Ocean:

$$S_\zeta(\omega) / (H_{1/3})^2 \cdot T_1 = \frac{172.8}{(T_1 \cdot \omega)^5} \cdot e^{-\frac{691}{(T_1 \cdot \omega)^4}}$$

$$S_\zeta(\omega) / (H_{1/3})^2 \cdot T_2 = \frac{124}{(T_2 \cdot \omega)^5} \cdot e^{-\frac{496}{(T_2 \cdot \omega)^4}}$$

By means of numerical integration the following relationships between various wave periods valid for the Pierson-Moskowitz spectrum can be derived, see the table below:

Example: $T_2 = 0.71\ T_p$	T_1	T_p	T_2
Average wave period $T_1 =$	1	0.77	1.086
Period of the spectral component associated with maximum wave energy (peak period) $T_p =$	1.296	1	1.408
Mean zero-upcrossing period $T_2 =$	0.92	0.71	1

According to Reference [2] the following relationship between various wave heights exist for fully developed seas:

Example: $H_{1/10} = 1.27\ H_{1/3}$	$H_{1/1}$	$H_{1/3}$	$H_{1/10}$
Average wave height $H_{1/1}$	1	0.63	0.49
Significant wave height $H_{1/3}$	1.59	1	0.78
$H_{1/10}$	2.03	1.27	1

Here, $H_{1/n}$ is the mean of the wave height of the n^{th} highest part of the wave height distribution.

JONSWAP wave spectrum (1973)

An extensive wave measurement program known as the Joint North Sea Wave Project (JONSWAP) was carried out in 1968 and 1969 along a line extending over 100 miles (160 km) into the North Sea from Silt Island. From the analysis of the measured spectra, a JONSWAP wave spectral formulation was derived which is representative of wind- generated seas with a fetch limitation, see Reference [3].

The JONSWAP spectrum, based on a period and the significant wave height, can be expressed using the formulation below. This formulation is based on a Pierson-Moskowitz type spectrum, with a "peak enhancement" factor to modify its shape.

$$S_\zeta(\omega) = \alpha \cdot g^2 \cdot \omega^{-5} \cdot \exp\left[-1.25\,(\omega/\omega_0)^{-4}\right] \cdot \gamma^{\exp\left[-(\omega-\omega_0)^2/(2\sigma^2 \cdot \omega_0^2)\right]}$$

$$\sigma = \begin{bmatrix} \sigma_a \text{ for } \omega \le \omega_0 \\ \sigma_b \text{ for } \omega > \omega_0 \end{bmatrix}$$

in which:

$S_\zeta(\omega)$	=	spectral density at wave frequency ω, [m^2s]
ω	=	wave frequency, [rad/s]
ω_0	=	spectrum peak frequency, [rad/s]
g	=	gravitational acceleration, [m/s^2], g = 9.81 m/s^2

A definition sketch of the parameters for the description of the JONSWAP spectrum is given in the figure below:

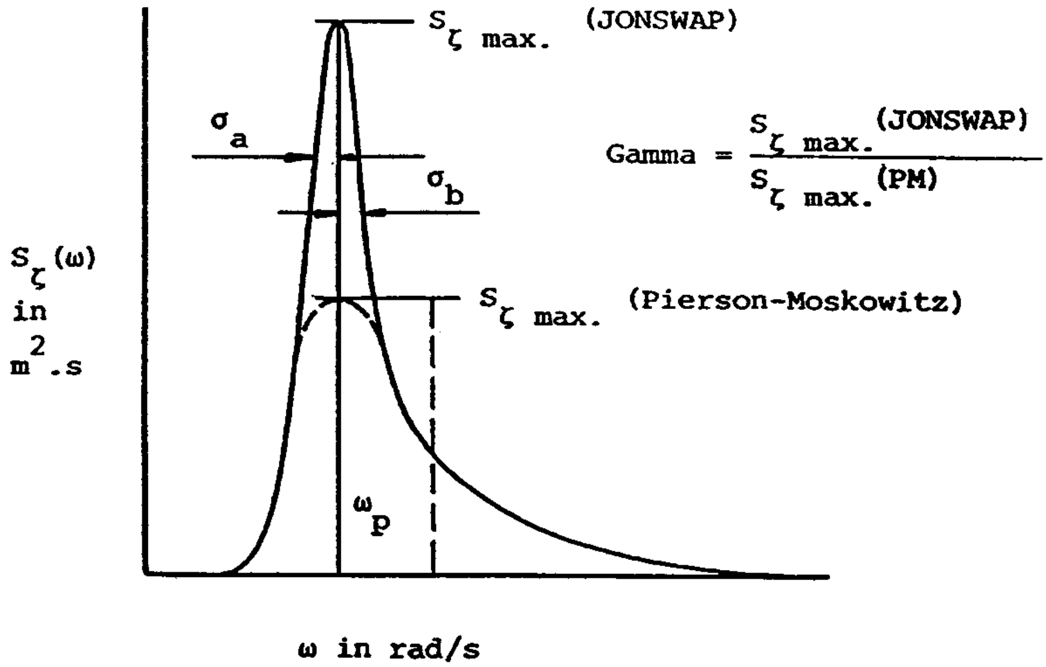

For the mean JONSWAP spectrum the authors of Reference [3] found the following values for the dimensionless spectral shape parameters σ_a, σ_b and γ.

γ = 3.0
σ_a = 0.07
σ_b = 0.09

In the case that only the significant wave height $H_{1/3}$ and the average period T_1 are known, the following procedure can be applied when using the JONSWAP spectrum:

- For the shape parameters σ_a and σ_b the default values are selected (see above).
- By means of numerical integration the following relation between T_p, T_1, T_2 for the JONSWAP spectra (σ_a = 0.07 and σ_b = 0.09) as a function of γ-value was established.

γ	T_p/T_1	T_p/T_2	T_1/T_2
1.0 (P.M.)	1.296	1.408	1.086
2.0	1.240	1.338	1.079
3.0	1.206	1.295	1.073
3.3 (mean)	1.198	1.285	1.072
4.0	1.183	1.264	1.069
5.0	1.165	1.240	1.065
6.0	1.151	1.221	1.061

Using the appropriate value from the table above at a chosen γ-value in combination with the given average wave period T_1 the period of the spectral component associated with the maximum energy T_p can be calculated.

- Finally, the factor α is chosen such, that the following relation is fulfilled.

$$H_{1/3} = 4\sqrt{\int_0^{\infty} S_{\zeta}(\omega)\cdot d\omega} = 4\sqrt{m_{\zeta 0}}$$

in which:

$H_{1/3}$ = significant wave height, [m]
$m_{\zeta 0}$ = area beneath the wave spectrum, [m^2]

TMA wave spectrum

In shallow water conditions, instead of the JONSWAP spectrum the so-called TMA spectrum can be applied. “TMA” is an abbreviation for “Texel-Marsen-Arsloe”. It is a JONSWAP spectrum modified by a term accounting for the actual water depth, see Reference [6]:

$$S_{TMA}(\omega) = S_J(\omega)\cdot\phi(\omega)$$

$$\phi(\omega) = \frac{\omega^5 \frac{\partial k}{\partial \omega}}{2g^2k^3}$$

$$\omega^2 = gk\tanh(kd); \quad \frac{\partial k}{\partial \omega} = \frac{2\omega}{\frac{\omega^2}{k} + \frac{gkd}{\cosh^2(kd)}}$$

where

$S_J(\omega)$ = JONSWAP spectral density as given above at wave frequency ω, [m^2s]
$\phi(\omega)$ = depth function at wave frequency ω, [-]
ω = wave frequency, [rad/s]
k = wave number, [rad/m]
g = gravitational acceleration, [m/s^2], g = 9.81 m/s^2
d = water depth, [m]

Comparing TMA and JONSWAP spectra for the same significant wave height, peak period, peak enhancement factor and shape parameters, in the TMA spectrum energy is shifted to higher frequencies, see figure below for 20 m water depth:

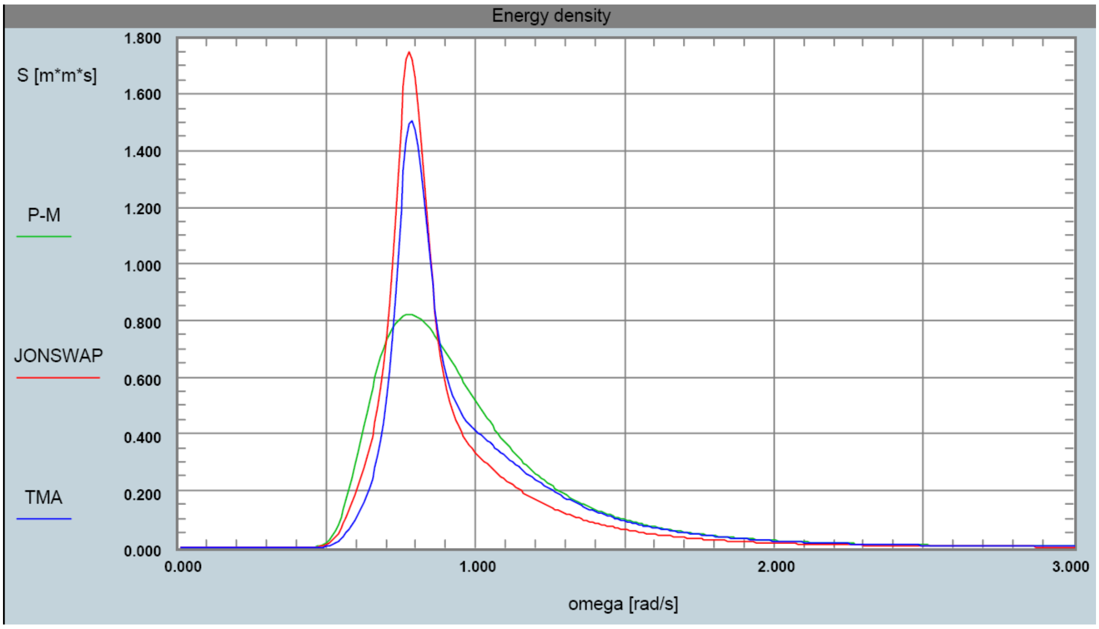

Gaussian swell spectrum

The Gaussian distribution function can be used to describe the spectrum of a swell wave. In this case, the spectral formulation is as follows:

$$S_\zeta(\omega) = \left(\frac{H_{1/3}}{4}\right)^2 \cdot \frac{1}{\sigma \cdot \sqrt{2\pi} \cdot \omega_0} \cdot \exp\left[-\frac{(\omega - \omega_0)^2}{2 \cdot \sigma^2 \cdot \omega_0^2}\right]$$

in which:

ω_0 = Spectrum peak frequency, [rad/sec]
σ = Dimensionless shape parameter, [-]
$H_{1/3}$ = Significant wave height, [m]

The Gaussian spectrum is symmetrical and therefore $T_0 = T_1 = T_2 = T_p$.

Ochi-Hubble wave spectrum

The Ochi-Hubble wave spectrum has two peaks, representing a long-period swell and short-period wind seas. The parameters defining the Ochi-Hubble wave spectrum include two values for the significant wave height H_s (one for the swell and one for the wind seas), two values for the peak period T_p (same) and two values for an enhancement factor λ (same).

The Ochi-Hubble wave spectrum can be formulated as follows:

$$S_\zeta(\omega) = \frac{1}{4} \cdot \sum_{j=1}^{2} \frac{\left[\left(4\lambda_j + 1\right)\omega_{p,j}^4/4\right]^{\lambda_j}}{\Gamma(\lambda_j)} \cdot \frac{H_{s,j}^2}{\omega^{\left(4\lambda_j+1\right)}} \cdot \exp\left[-\left(\frac{4\lambda_j+1}{4}\right)\left(\frac{\omega_{p,j}}{\omega}\right)^4\right]$$

in which:

j	=	Wave component index [-], j=1 (swell), j = 2 (sea)
$H_{s,j}$	=	Significant wave height of wave component j, [m]
$\omega_{p,j}$	=	Spectrum peak frequency, [rad/sec]
λ_j	=	Dimensionless shape parameter, [-]
Γ	=	Gamma function, [-]

White noise spectrum

The white noise spectrum has a constant energy distribution over a range of wave frequencies. This spectrum can be formulated as follows:

$$S_\zeta(\omega) = \begin{cases} 0 & \text{for } \omega \leq \omega_b \\ \dfrac{(H_{1/3}/4)^2}{(\omega_e - \omega_b)} & \text{for } \omega_b < \omega \leq \omega_e \\ 0 & \text{for } \omega > \omega_e \end{cases}$$

in which:

ω_b	=	Lowest wave frequency, [rad/sec]
ω_e	=	Highest wave frequency, [rad/sec]

Some remarks on wave and wave group spectra

In the foregoing the different wave spectrum formulations are reviewed. The wave spectral components of the spectrum will cause, according to the linear theory, the wave exciting forces and moments on the moored vessel and mooring system inducing the wave frequency motions and forces in the mooring system. The spectral shape involved, however, will not only affect the high frequency behaviour of the system. In Reference [4] it is shown that from the normal wave spectrum $S_\zeta(\omega)$ the spectrum of the square of the wave envelope can be derived theoretically. This feature is important because of the analogy which exists between the low frequency wave drifting forces and the low frequency part of the square of the heights of the incident waves, see Reference [5].

The wave elevation is written as:

$$\begin{aligned}\zeta(t) &= \sum_{i=1}^{2} \zeta_i \sin(\omega_1 t + \varepsilon_1) \\ &= \zeta_1 \sin(\omega_1 t + \varepsilon_1) + \zeta_2 \sin(\omega_2 t + \varepsilon_2)\end{aligned}$$

For small differences between ω_1 and ω_2 a schematic representation of the wave train is shown in the figure below. Such a wave train will be called a regular wave group. This type of wave train is characterized by a periodic variation of the wave envelope. The frequency associated with the envelope is equal to $\mu = \omega_2 - \omega_1$ being the difference frequency of the regular wave components.

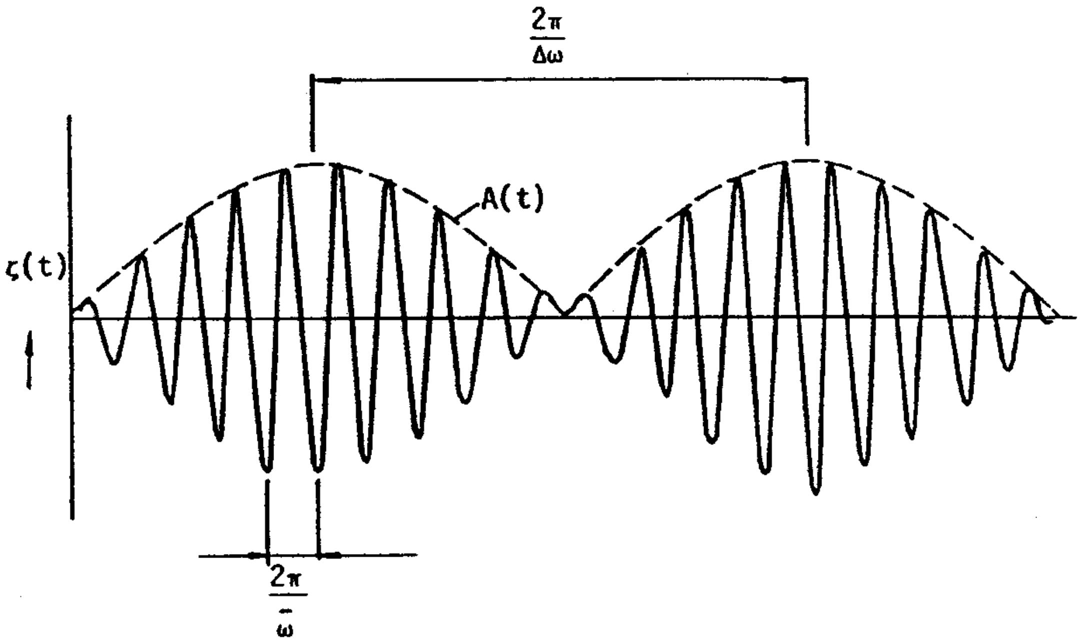

The wave elevation in amplitude modulated form can be written as:

$$\zeta(t) = A(t)\sin(\bar{\omega}t + \bar{\varepsilon})$$

in which:

$$\bar{\omega} = (\omega_1 + \omega_2)/2$$
$$\bar{\varepsilon} = (\varepsilon_1 + \varepsilon_2)/2$$

It can be shown that the envelope becomes:

$$A(t) = \left[\sum_{i=1}^{2}\sum_{i=1}^{2} \zeta_1 \zeta_j \cos\left((\omega_i - \omega_j)t + (\varepsilon_i - \varepsilon_j)\right)\right]^{1/2}$$

The square of the envelope is:

$$A^2(t) = \sum_{i=1}^{2}\sum_{i=1}^{2} \zeta_1 \zeta_j \cos\left((\omega_i - \omega_j)t + (\varepsilon_i - \varepsilon_j)\right)$$

or

$$A^2(t) = \zeta_1^2 + \zeta_2^2 + 2\zeta_1\zeta_2 \cos\mu t$$

in which: $\mu = \omega_2 - \omega_1$

Note that (see figure below):

$\zeta_1 = 1/2\, A^2$ in which: ζ_1 = low frequency part of the squared wave height $\zeta(t)$.

In accordance with the definition of a spectrum the spectral densities are:

$S_\zeta(\omega)\, d\omega \quad = \quad 1/2\, \zeta_a^2$

$S_{A2}(\mu)\, d\omega \quad = \quad 1/2\, p^2$ in which $p = A^2$

In accordance with the definition of a spectrum the spectral densities of the square of the wave envelope will be:

$S_{A2}(\mu)\, d\omega = 1/2\, (2\zeta_1\, (\omega_1)\, \zeta_2\, (\omega_1 + \mu))^2$

which will yield for the regular wave group with $\zeta(\omega_1)$ and $\zeta_2(\omega_2)$:

$$\begin{aligned} S_{A2}(\mu)\, d\omega &= 2\, (\zeta_1\, (\omega_1)\, \zeta_2\, (\omega_1 + \mu))^2 \\ &= 2\{2\, S_{\zeta 1}\, (\omega_1)\, d\omega\, 2\, S_{\zeta 2}\, (\omega_1 + \mu)\, d\omega\} \end{aligned}$$

or for all the wave groups with the frequency-difference μ in a wave spectrum:

$$S_{A2}(\mu) = 8 \int_0^\infty S_\zeta(\omega)\, S_\zeta\, (\omega + \mu)\, d\omega$$

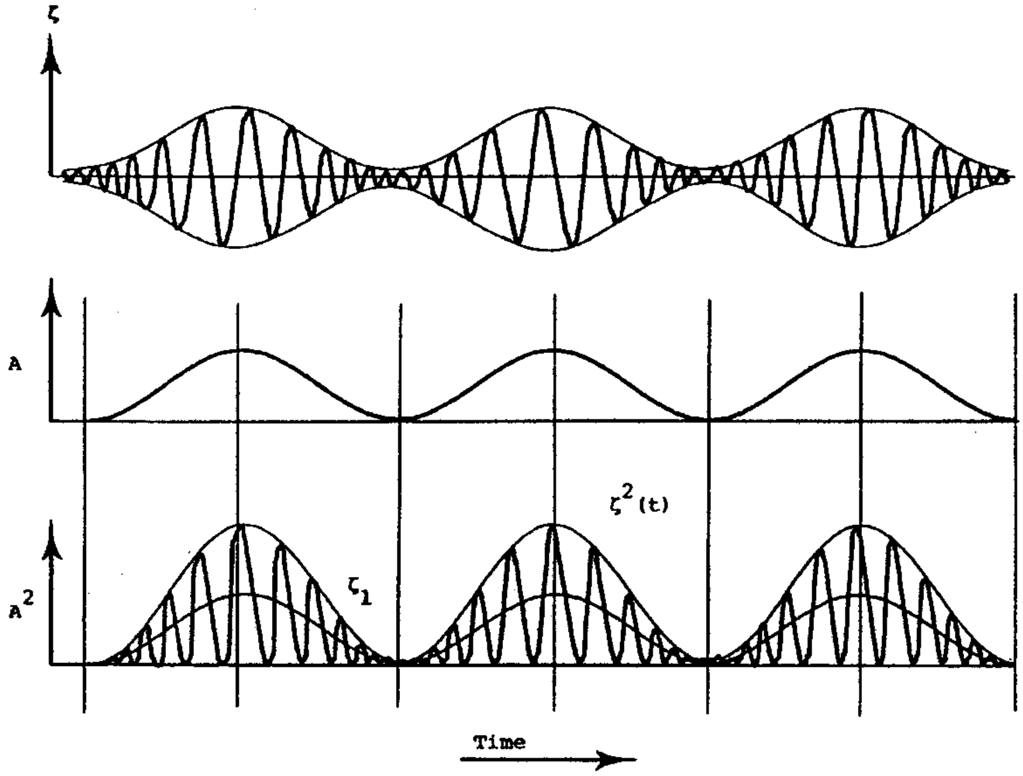

The distribution function of $A^2(t)$ is, for a narrow band spectrum:

$$P(A^2) = \frac{1}{2m_0} \cdot e^{-\frac{A^2}{2m_0}}$$

where:

$$m_0 = \int_0^\infty S_\zeta(\omega) \cdot d\omega$$

From the above, it follows that knowledge of $S_\zeta(\omega)$ and the assumption that the wave elevation is normally distributed is sufficient to calculate the spectral density and distribution function $A^2(t)$.

From the foregoing it follows that the spectral density and distribution may also be calculated from the low frequency part of the square of the record of the wave height measured in the basin. If the waves are completely random then the spectral density and distribution obtained from and based on the normal (first) spectrum of the waves should correspond with the spectral density and distribution of $2.\zeta_1^2$ calculated directly from the wave record.

The distribution function $P(A^2)$ and $p(2.\zeta_1^2)$ and the spectral density of the waves and of A^2 and $2.\zeta_1^2$ are shown in Figures A and B on the next page, respectively for an irregular wave train generated in a basin of MARIN.

As mentioned, the wave envelope is related to the low-pass filtered square of the wave elevation:

$$A(t) = \sqrt{2 \cdot \overline{\zeta_1^2(t)}}$$

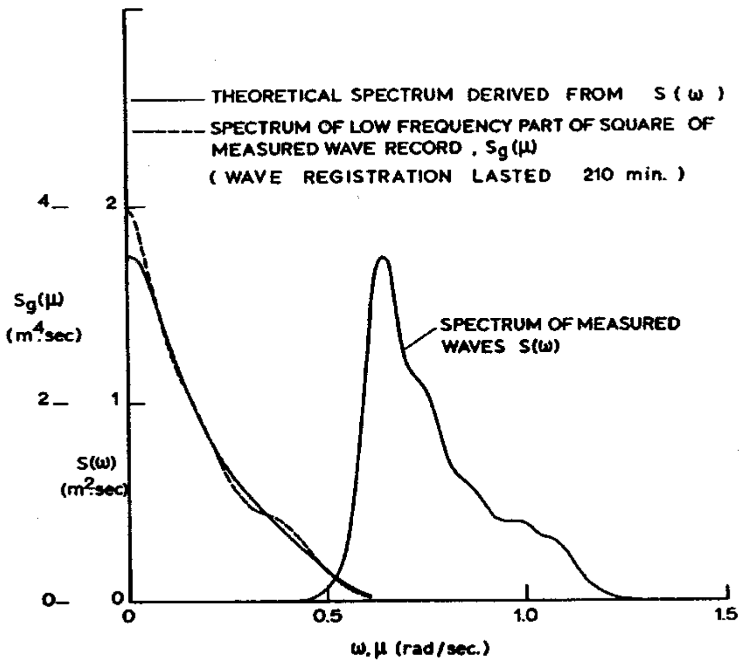

Figure A: Spectra of waves and low frequency part of the square of a wave record

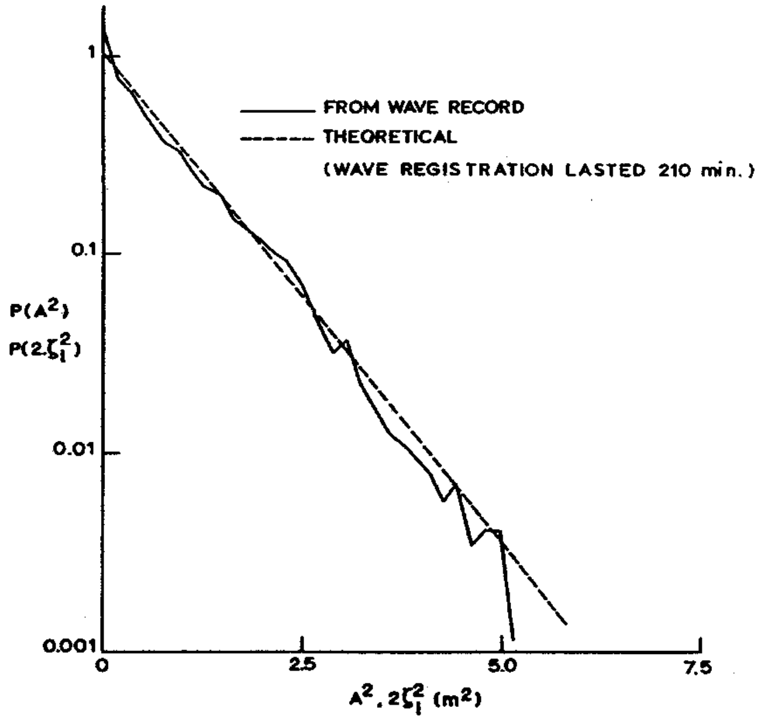

Figure B: Distribution function of the low frequency part of the square of a wave record

In order to show that this operation does indeed represent the wave envelope, results of an analyzed irregular wave train are plotted in the figure below showing the wave elevation ζ (t) and the corresponding wave envelope A (t).

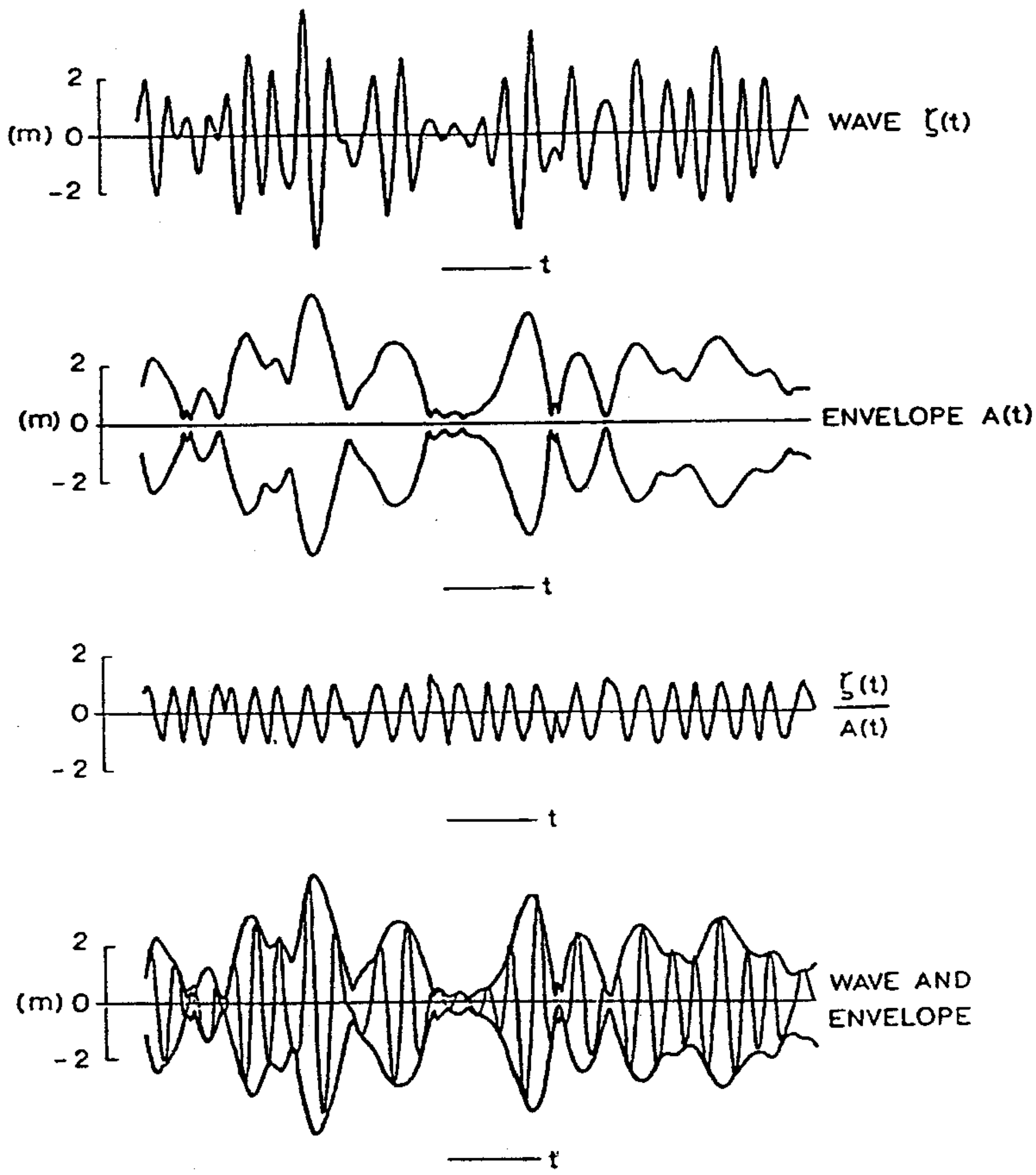

Using the spectral density formulation of A^2 (t), which means the spectrum of the square of the wave envelope or the wave group spectrum according to:

$$S_g(\mu) = 8 \int_0^\infty S_\zeta(\omega)\, S_\zeta(\omega+\mu)\, d\omega$$

Computations have been carried out on the different afore-mentioned wave spectrum formulations.

In the figure below the wave group spectra have been computed for 5 different wave spectrum formulations each having the same significant wave height $\zeta_{w1/3}$ = 5.5 m and the same average period T_1 = 11.50 s.

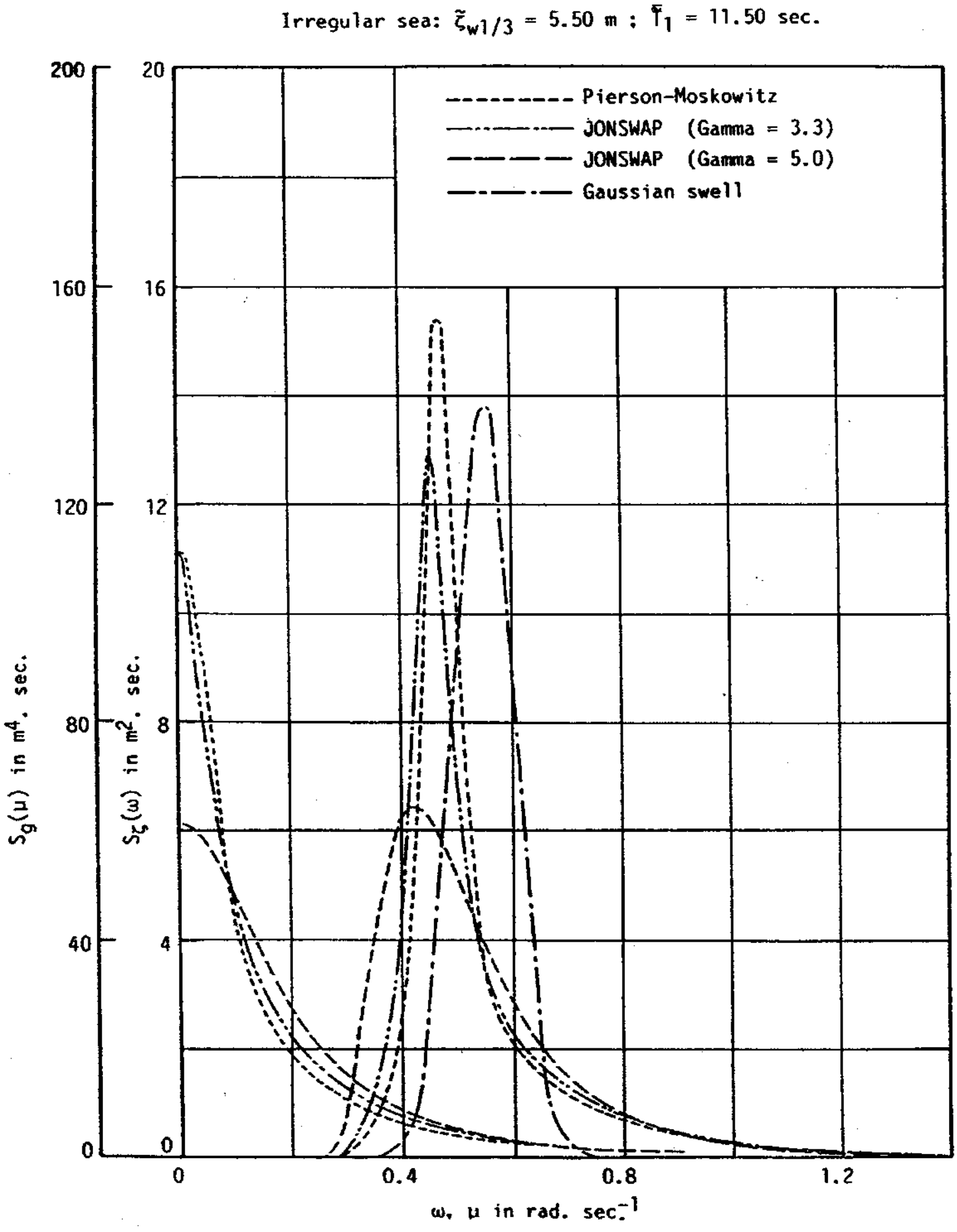

Spectra of waves and the square of the wave envelope

In the figure below the wave group spectra have been computed for 5 different wave spectrum formulations each having the same significant wave height $\zeta_{w1/3}$ = 5.5 m and the same peak period T_p = 14.9 s.

Irregular sea: $\tilde{\zeta}_{w1/3}$ = 5.50 m ; T_p = 14.90 sec.

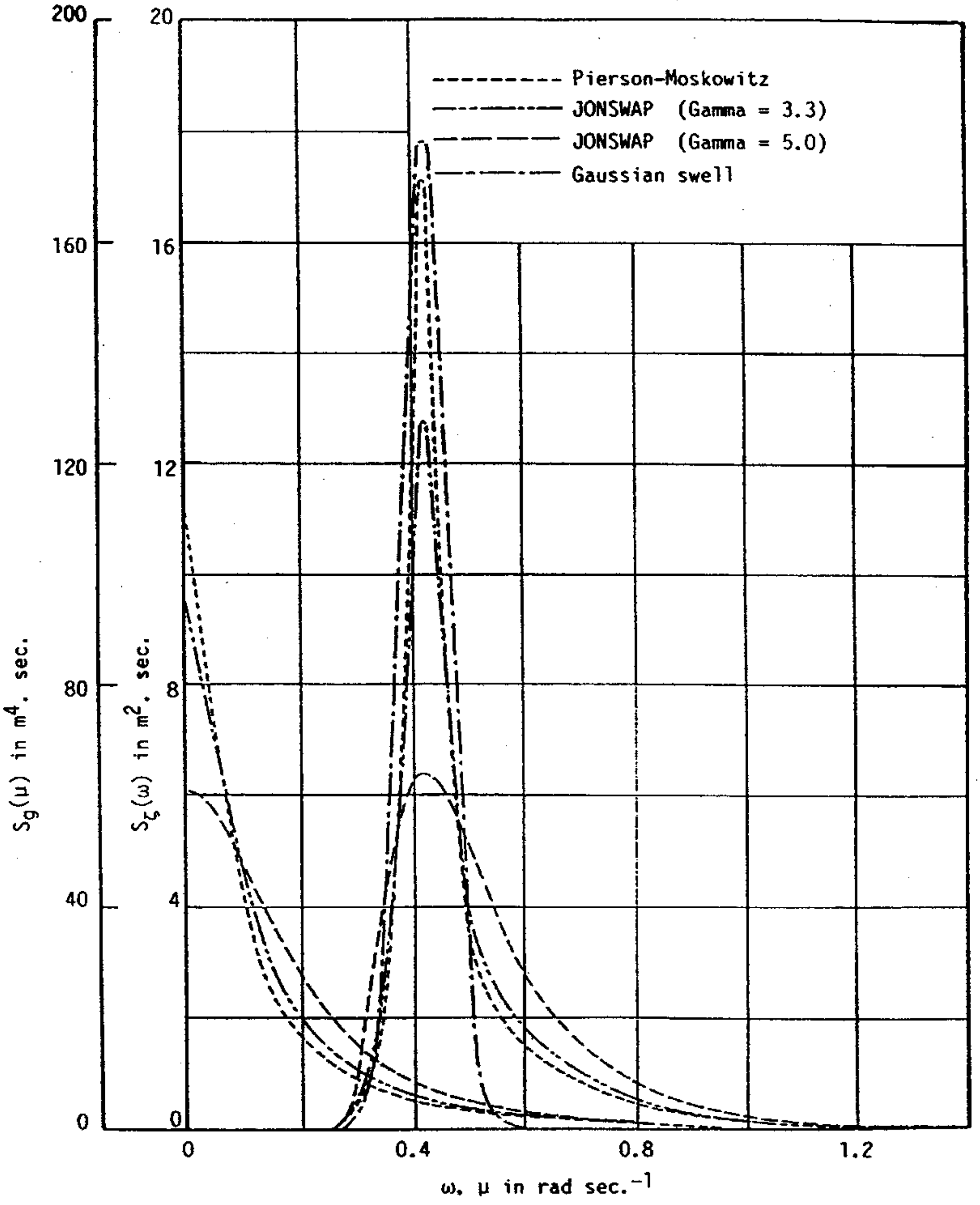

Spectra of waves and the square of the wave envelope

From the results it can be concluded that the spectral density of the square of the wave groups will be substantially influenced by the shape of the chosen wave spectrum.

References

1. Pierson, W.J. and Moskowitz, L.; “A Proposed Spectral Form for Fully Developed Wind Seas Based on the Similarity Theory of S.A. Kitagorodskii”, Journal of Geoph. Res., 69, No. 2, Dec. 1964.

2. Pierson, W.J., Neumann, G. and James, R.W.; “Practical Methods for Observing and Forecasting Ocean Waves by Means of Wave Spectra and Statistics”, H.O. Pub. No. 603, Hydrographic Office, U.S. Navy, 1955.

3. Hasselmann, K. et al.; “Measurements of Wind and Wave Growth and Swell Decay during the Joint North Sea Wave Project (JONSWAP)”, Ergänzungsheft Nr. 12, Reihe A, Deutsche Hydrographischen Zeitschrift 1973.

4. Pinkster, J.A.; “Low Frequency Second Order Wave Exciting Forces on Floating Structures”, Doctoral Thesis, Delft University of Technology, 1980.

5. Wichers, J.E.W.; “Simulation Model for a Single Point Moored Tanker”, Doctoral Thesis, Delft University of Technology, 1988.

6. Nestegård, A., Ronœss, M., Hagen, Ø., Ronold, K.O. and Bitner-Gregersen, E. (Det Norske Veritas); “New DNV Recommended Practice DNV-RP-C205 on Environmental Conditions and Environmental Loads”, Proceedings of the Sixteenth International Offshore and Polar Engineering Conference, 2006.

APPENDIX E04

Wave Calibration Procedure in the Offshore Basin (OB)

Revision	Date	Description of revision	Author
0	May 27, 2009	First version of the appendix	JH
1	February 25, 2010	Review and up-date of the text	JLC

Wave Calibration Procedure in the Offshore Basin (OB)

The requested irregular wave conditions are calibrated prior to the actual model tests, without the model(s) present in the basin. The wave elevations are measured by means of resistance wire wave probes, placed at the centre of the test set-up and at additional (typically 2) reference positions. The reference wave probes remain at their location in the test set-up for the entire duration of the model test project. The irregular waves are calibrated for a duration of 1 hour or 3 hours (prototype value).

The irregular waves are calibrated through the following procedure.

1. The correct current profile is generated in the basin.

2. The required wave spectrum is specified in the wave generation software. Based on this input the software calculates a control file for the wave generators. This file contains motion control information for all individual wave flaps in the basin.

3. After the current has become stationary, the irregular seas are generated, measured and analysed. The measured wave spectrum at the zero position (centre of the test set-up) is compared with the required wave spectrum.

4. If necessary, a correction for the wave generator control file is calculated. This correction is based on the (frequency-by-frequency) ratio between the measured and required spectrum at the zero position. After applying correction to the control file, the sea state is generated, measured and analysed again, until a sufficiently close correspondence is found between the measured and the required wave spectrum. Depending on the spectral shape, this iterative process typically takes 2 or 3 attempts to generate the wave spectrum at the required accuracy.

5. The final version of the wave generator control file is stored, in order to be able to exactly reproduce the calibrated sea state at any time during the project.

APPENDIX E05

Estimation of the Reflection Coefficients of the Beaches in the Offshore Basin, Based on the Results of Regular and Irregular Wave Measurements

Revision	Date	Description of revision	Author
0	September 10, 2009	First version of the appendix	JLC
1	April 12, 2011	Figures and reference included	JLC

Estimation of the Reflection Coefficients of the Beaches in the Offshore Basin, Based on the Results of Regular and Irregular Wave Measurements

This appendix describes the results of wave measurements that were carried out in MARIN's Offshore Basin. The objective of these tests was to determine the reflection coefficients of the wave absorbing beaches in the basin. In this document, the set-up used in the measurements is described, the analysis method to determine the wave reflection coefficients is discussed and the result of the measurements are presented.

Test set-up and measurements

During a previous research project in the Offshore Basin, a total of 9 additional wave probes was placed in the basin during (regular) wave calibrations, besides the usual wave probes "WAVE CL", "WAVE 180" and "WAVE 270". The additional wave probes were placed in a line along the direction of propagation of the waves, which is shown in the figures below, for 180 and 270 deg wave directions.

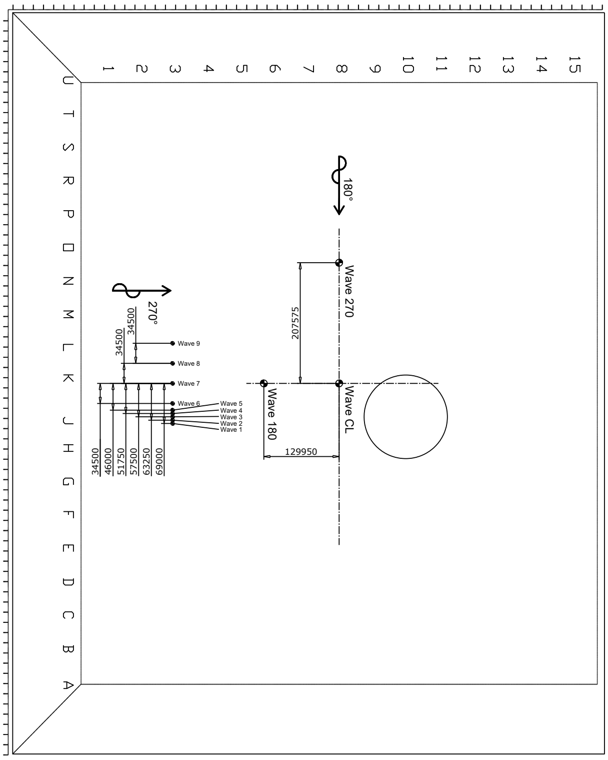

Wave Probe Set-up - 180 deg Waves

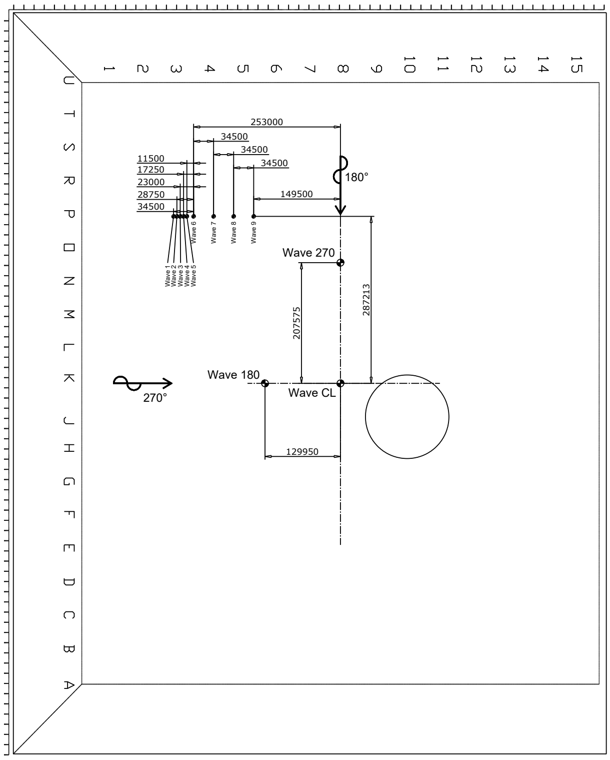

Wave Probe Set-up - 270 deg Waves

The purpose of the wave elevations measured with these 9 additional probes was to quantify the reflection of the waves from the wave absorbing beaches. The amplitudes of the wave components propagating towards the beach (generated wave) and coming from the beach (reflected wave) were determined from the wave elevations measured during the (regular) wave calibrations. The reflection coefficient of the wave absorbing beaches is a function of the wave frequency and amplitude and is defined as the ratio between the amplitudes of the incoming and the reflected waves. Both regular and irregular wave conditions were investigated. The applied analysis method is further described in the following section.

Theory of the analysis of the reflection coefficient

Consider a wave ζ_G travelling from the wave generator (hence the index) towards the beach and a second reflected wave ζ_R travelling in the opposite direction, so in the +X direction. The equations governing the time and spatial wave elevations are:

$$\zeta_G(t) = \zeta_{GA} \cdot \cos(\omega t + \kappa x + \varepsilon_1)$$
$$\zeta_R(t) = \zeta_{RA} \cdot \cos(\omega t - \kappa x + \varepsilon_2)$$

in which:

ζ_{GA}	=	Amplitude of the wave generated by the wave maker, [m]
ζ_{RA}	=	Amplitude of the wave reflected by the beach, [m]
ω	=	Wave frequency, [rad/s]
κ	=	Wave number, [m^{-1}], for deep water $\kappa = \omega^2 \cdot g^{-1}$
ε	=	Unknown phase angle, [rad]

If the wave elevation is measured with a wave gauge on a distance $x = x_1$ from the beach, the measurement will be the sum of the two waves.

$$\zeta_M = \zeta_{MA} \cos(\omega t + \varepsilon_M) = \zeta_{GA} \cos(\omega t + \kappa x_1 + \varepsilon_1) + \zeta_{RA} \cos(\omega t - \kappa x_1 + \varepsilon_2)$$

This equation can be re-arranged as follows to bring the amplitude and the phase angle in an explicit form.

$$\zeta_{MA} = \sqrt{\zeta_{GA}^2 + \zeta_{RA}^2 + 2\zeta_{GA}\zeta_{RA} \cos(2\kappa x_1 + \varepsilon_1 - \varepsilon_2)}$$

$$\tan \varepsilon_M = \frac{\zeta_{GA} \sin(2\kappa x_1 + \varepsilon_1) - \zeta_{RA} \sin(2\kappa x_1 - \varepsilon_2)}{\zeta_{GA} \cos(2\kappa x_1 + \varepsilon_1) + \zeta_{RA} \cos(2\kappa x_1 - \varepsilon_2)}$$

In theory the 4 unknowns ζ_{GA}, ζ_{RA}, ε_1 and ε_2 can be derived from the two amplitudes and 2 phase angles obtained from measurements at two points. In practice, however, the accuracy will then be insufficient. There is a frequency dependent optimum distance between the two measurement points. For this reason 9 wave probes were used, to cover a sufficiently large range of frequencies with sufficient accuracy of the analysis. The positions of the 9 additional wave probes are shown in the figure on page 2 of this appendix. The separation between these gauges was based on the required frequency range for the tests. The applied theory for determining the reflection coefficients is discussed in more detail in Reference [1], which has been included in this appendix.

A purpose made FORTRAN program has been used to analyse the results and to find an optimum fit through the measurement points. The program uses a least squares method to minimise the error in the real and imaginary part of estimated wave for each measurement location. Because of the behaviour of the functions of Y_{MA} and ε_M with a lot of local maxima and minima, a rather robust approach has been used; the program calculates the error for a large range of values of the four variables, considering all possible combinations. If a minimum is found on the border, the grid is re-located; if it is somewhere inside the grid, the steps are made smaller until sufficient accuracy is obtained. The program appeared to work sufficiently quick to run on a PC (on a 200 MHz Pentium PC it takes about 1 minute).

Results of the wave reflection analysis

The reflection coefficient of the wave absorbing beaches is defined as the ratio between the amplitudes of the incoming and the reflected waves. The reflection coefficient generally depends on the wave period and the wave height.

In the figure below the wave reflection coefficients, as measured in the Offshore Basin, are shown. The results of regular (points) and irregular waves (lines) are plotted together. In this particular figure the reflection coefficient is based on the wave energy.

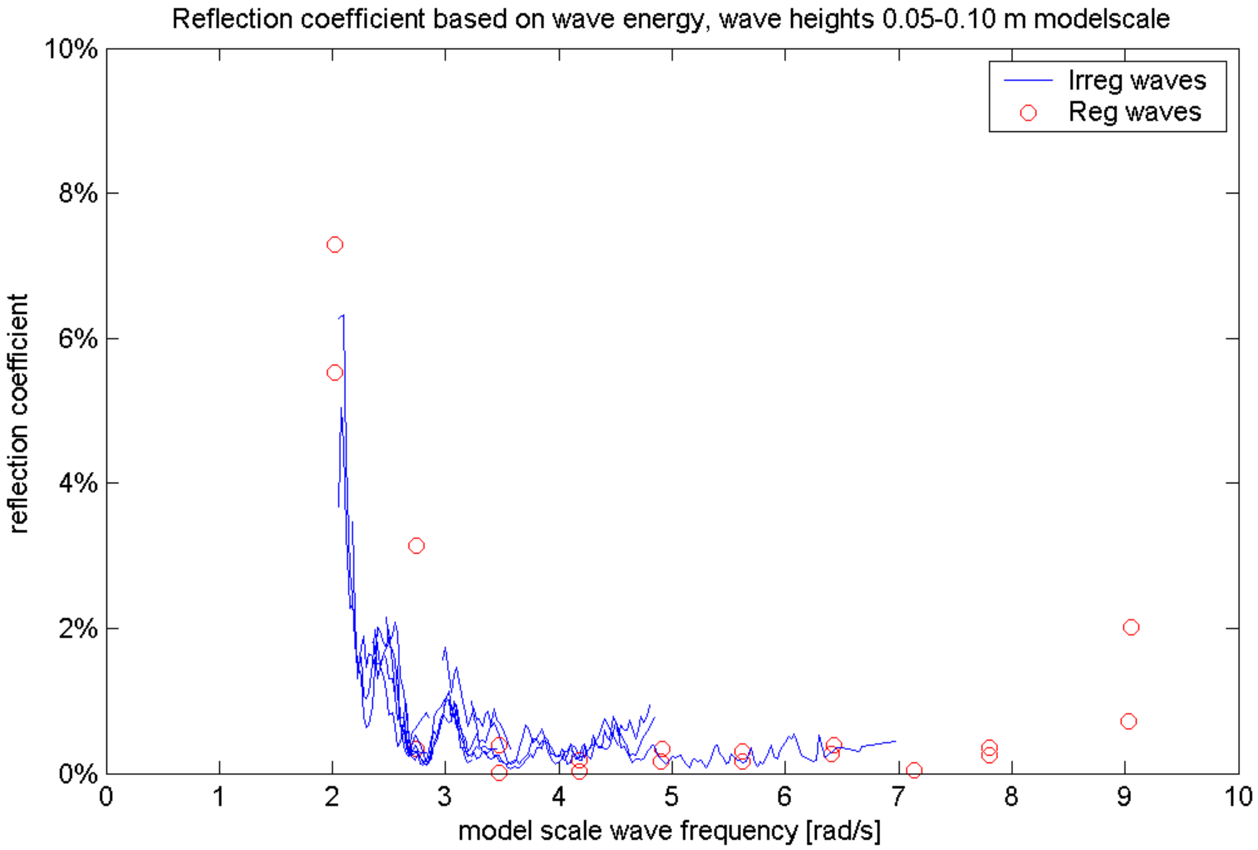

The above results show that the wave reflection is very low for wave frequencies between 3 and 8 rad/s (model scale values). For very long waves (below 3 rad/s) and for very short waves (above 8-9 rad/s) the reflection coefficient increases. The orbital motions of the very long waves extend below the depth of the beaches, limiting the wave absorbing properties for these frequencies. For very short waves, the efficiency of the beaches decreases.

References

[1] Kyung Doug Suh, Woo Sun Park, Beom Seaok Park; “Separation of Incident and Reflected Waves in Wave-Current Flumes”, page 149-159, Coastal Engineering 43, Elsevier Science B.V., 2001.

APPENDIX F01

Offshore Basin (OB)

Revision	Date	Description of revision	Author
0	March 27, 2017	First version of the appendix	JJS

Offshore Basin (OB)

General

In the Offshore Basin (OB) irregular long and short crested waves can be generated. The OB is 45 m long, 36 m wide and has an adjustable water depth with a maximum of 10 m. The basin is mainly designed for testing models of offshore structures which are fixed, moored or controlled by dynamic positioning, in waves, wind and current.

Figure F01-1: Overview of the offshore basin

Sign convention

The figure shows the possible directions of current, swell, local waves and wind that can be modelled in MARIN's Offshore Basin. All directions are defined in the basin-fixed system of axes.

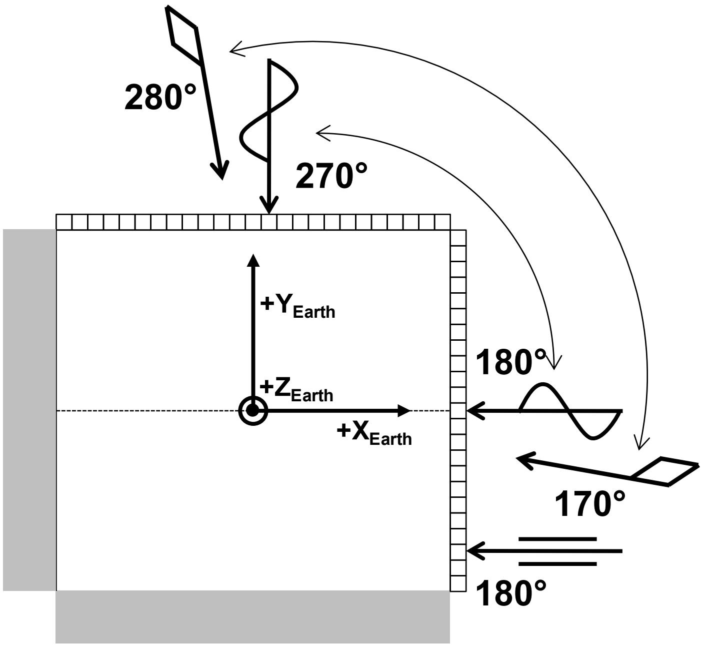

Figure F01-2: Representation of the Basin Fixed Coordinate System (BFCS) in the OB

Wave generation

At two adjacent sides of the basin, segmented wave generators consisting of hinged flaps are installed. This implies that waves can be generated in any direction ranging between head seas and beam seas (180 - 270 deg, defined in the basin fixed system of axes). Wave directions between following seas and beam seas can be modeled by changing the vessel heading. Opposite the 270 deg wave generator, passive sinkable wave absorbers are installed.

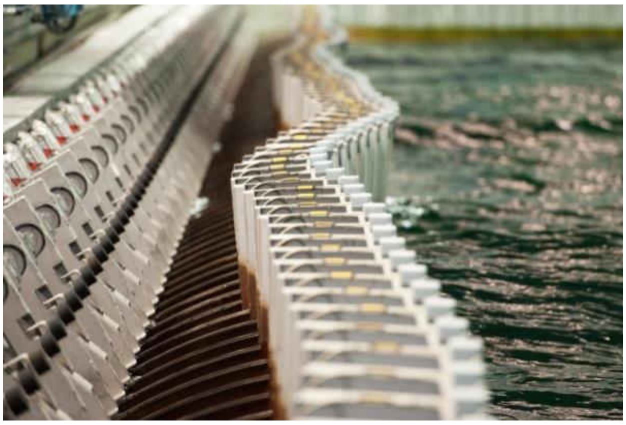

Figure F01-3: Overview of the wave flaps (left) and absorbing beaches (right)

The wave generator system is equipped with higher order wave synthesis techniques. The beaches of the OB are designed to minimize wave reflections, even for long period swells. For the generation of irregular seas the wave generator flaps perform (pre-calculated) irregular motions. The signal of the wave flap motions is non-repetitive and contains the same range of frequencies present in the irregular seas to be generated. Each flap is controlled separately by a driving motor and has a width of 40 cm.

The capability of the wave flaps is limited due to power, wave flap angles or wave breaking criteria. Therefore, it may be difficult to calibrate wave spectra which contains energy at low periods, high periods, or with a too high significant wave height. Figure F01-4 shows the wave generation capability at model scale. The plot shows the capability of long crested waves from the 180 deg and 270 deg wave maker. The horizontal axis represents the peak period of the wave spectrum in [s] at model scale. The vertical axis represents the significant wave height in [m] at model scale. It should be noted that these plots are indicative and depend on many parameters (spectrum enhancement factor, current, wave direction…).

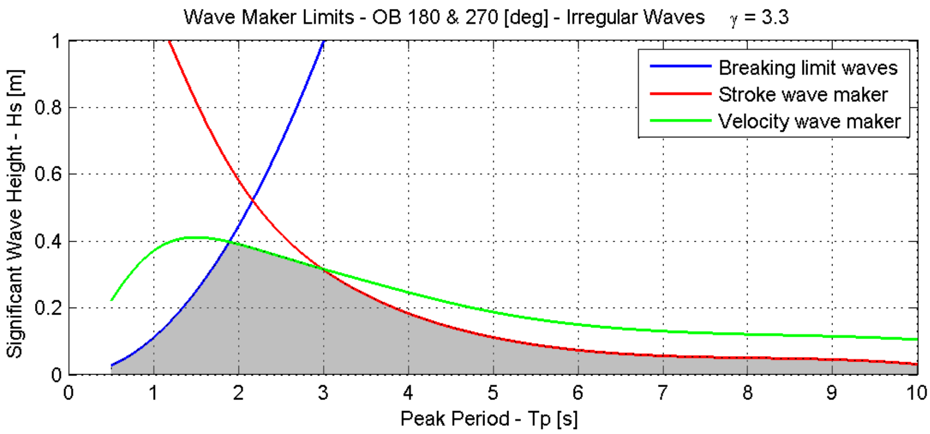

Figure F01-4: Wave generation capability in the OB

Wind generation

Wind can be generated by a large number of wind fans. Together they form a wind field of 20 m width. This ensures a constant wind field over the full measurement area, even when using a large test set-up, e.g. in case of tandem offloading tests. Constant wind as well as gusting and squall wind can be generated. It is noted that the wind forces to be modelled will be an important factor to take into account in the choice of the scale, as the maximum wind speed that can be reached in the basin is approximately 6.5 m/s.

Figure F01-5: Overview of the wind fans used in the Offshore Basin

As an alternative to the wind fans, the wind forces can be modelled using a dynamic winch. This is a good option for spread mooring systems as the model heading is relatively constant during a test, which means that a fixed attachment point can be used.

Current generation

The current generation system in the Offshore Basin consists of 6 separate layers, each equipped with its own pump. Current can be generated over the full depth of 10.0 m. The water is re-circulated through a system of channels outside the basin, in order to avoid recirculation in the basin itself. This current generation system enables the adjustment of vertical current profiles with constant speeds. The water is flowing into the basin from one side and flowing out on the opposite side over the full basin width. The water is re-circulated outside the basin through a system of large channels, in order to avoid re-circulation in the basin itself. On Figure F01-6 and Figure F01-7 both the inlet (left) and the outlet (right) of the six current layers are displayed.

Figure F01-6: Current inlet

Figure F01-7: Current outlet

The turbulence intensity in the current flow in the Offshore Basin is generally very low (around 5%). However, the turbulence may be somewhat larger in case of a strongly sheared current profile (current profiles with a strong variation in velocity over the water depth). This can be explained as follows. In the Offshore Basin the current is adjusted in 6 separate layers (each with their actual heights) and the natural shear in the current flow will prevent sharp steps in current speed between the different layers. In case of a very high surface current and small (or even zero) velocity for larger depths a strong current gradient may cause an increase in turbulence, which is a natural phenomenon. Therefore, no guarantee can be given about the turbulence that will be measured in the basin.

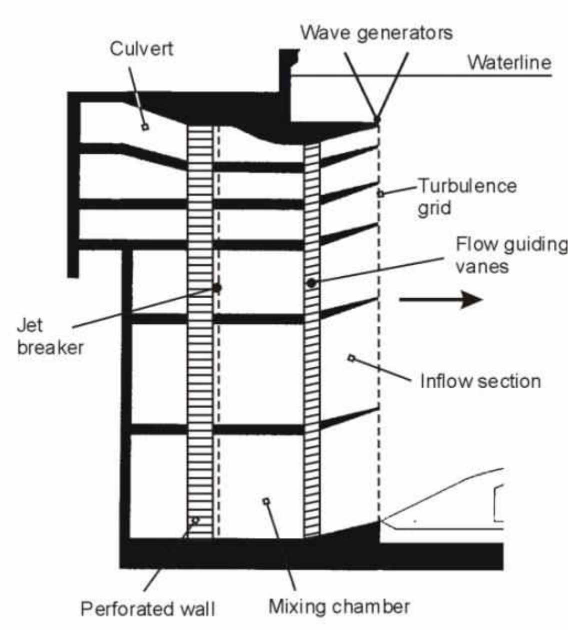

Figure F01-8: Side view of the current pump system

Figure F01-9 shows the capability of the current generation system. The minimum and maximum current speeds that can be achieved are represented as a function of the basin depth. Model scale values are shown on this Figure. Also, this Figure shows that the current generation system of the Offshore Basin is designed to standard current profiles, i.e. the deeper the water, the lower the current speed. For particular current profiles, the calibration in the bottom layers parts may be more difficult.

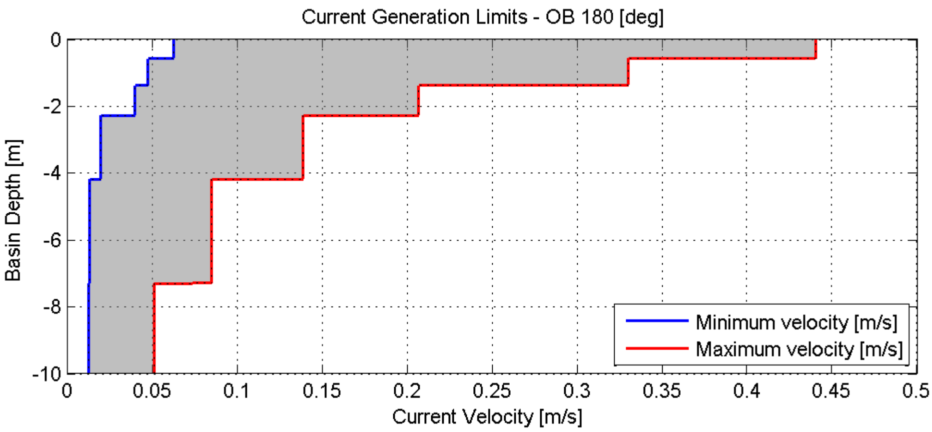

Figure F01-9: Capability of the current generation in the OB

APPENDIX I02

Instrumentations

Revision	Date	Description of revision	Author
0	December, 2016	First version of the appendix	JT/DB
1	Augustus, 2018	Pressure sensor added	JSt/JD

Tension ring load cell

Measurand [Unit]	:	Force [Newton]
Function	:	Measuring tension loads
Measurement principle	:	Strain gauges in full Wheatstone bridge
Typical application	:	Tension measurement in anchor lines
Manufacturer	:	MARIN
Typical dimensions	:	53 x 14 x 4 mm
Mass	:	1-3 g
Material	:	Titanium, Hardened Stainless Steel
Water resistance	:	Submersible

Available types

MARIN type	Maximum measuring value E_{max} [1]) [N]
140,141	30
142	60
143,145	100
144,146	300

1) Model scale values

Example uncertainty calculation:

- Measured full scale value $F = 490.0\ \text{kN}$
- Model scale = 30 and sensor 140 $\Rightarrow E_{max} = 810\ \text{kN}$
- $F/E_{max} = 60\% \Rightarrow U_F/E_{max} = 0.49\%$
- Uncertainty $U_F = 4.0\ \text{kN} \Rightarrow F = (490.0 \pm 4.0)\ \text{kN}$

Tension ring load cell

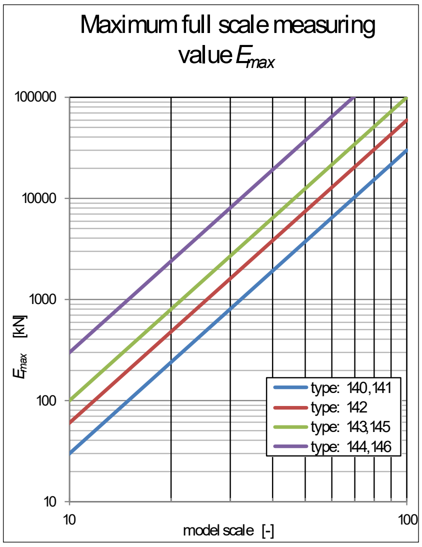

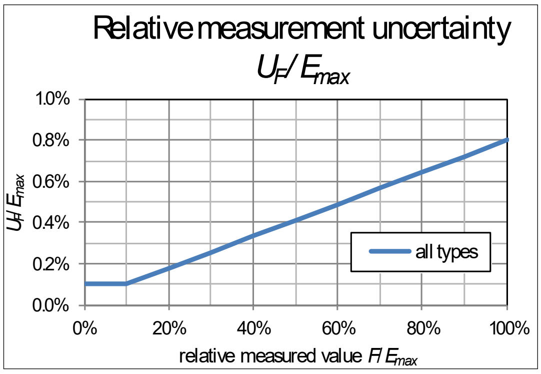

Tension-compression ring load cell

Measurand [Unit]	:	Force [Newton]
Function	:	Measuring compression and tension loads
Measurement principle	:	Strain gauges in full Wheatstone bridge
Typical application	:	Force measurement in small multi component frames
Manufacturer	:	MARIN
Typical dimensions	:	5.5 x 9 x 25 mm
Mass	:	3-15 g
Material	:	Stainless Steel
Water resistance	:	Submersible

Available types

MARIN type	Maximum measuring value E_{max} [1]) [N]
161	40
162	125
163	250
164	300

1) Model scale values

Example uncertainty calculation:

- Measured full scale value $F = 648.0$ kN
- Model scale = 30 and sensor 161 $\Rightarrow E_{max} = 1080$ kN
- $F/E_{max} = 60\% \Rightarrow U_F/E_{max} = 0.32\%$
- Uncertainty $U_F = 3.5$ kN $\Rightarrow F = (648.0 \pm 3.5)$ kN

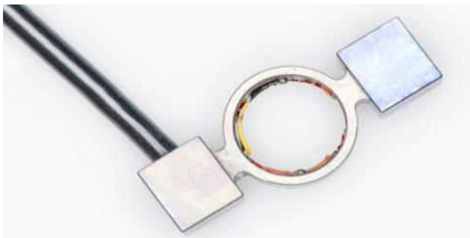

Tension-compression ring load cell

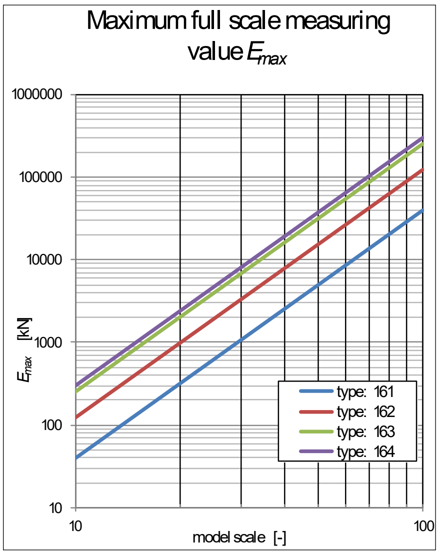

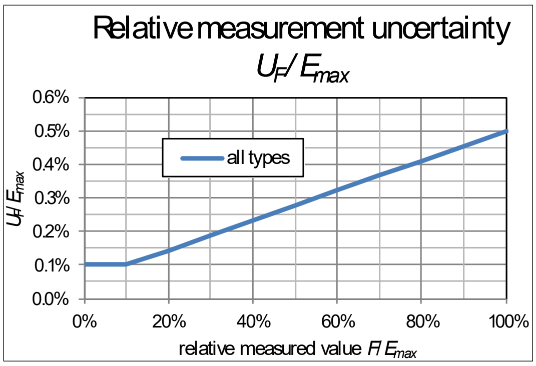

S beam shear load cell

Measurand [Unit]	:	Force [Newton]
Function	:	Measuring positive and negative loads in one direction
Measurement principle	:	Strain gauges in full Wheatstone bridge with remote sense
Typical application	:	One component tension and compression measurement, transducer in multi component force frames
Manufacturer	:	MARIN
Typical dimensions	:	40 x 21 - 26 x 12 mm
Mass	:	34 - 80 g
Material	:	Titanium, Hardened Stainless Steel
Water resistance	:	Submersible

Available types

MARIN type	Maximum measuring value E_{max} [1]) [N]
109	100
110,111	200
112	400
113	800
114	1400
115	2000

1) Model scale values

S beam shear load cell

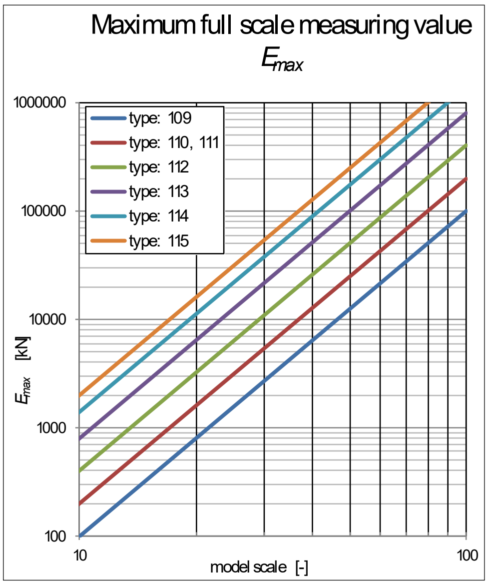

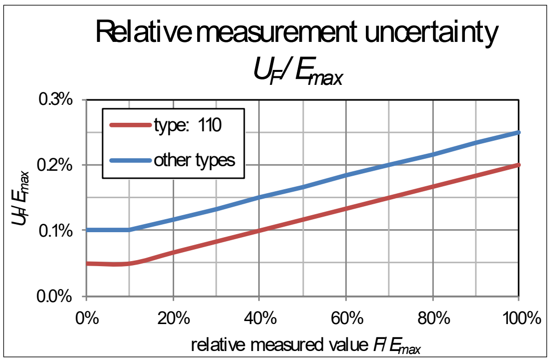

S-beam type load cell

MARIN type name : Wybertje
Measurand & Unit Force & Newton
Description : Measuring positive and negative loads in one direction
Measurement principle : Strain gauges in full Wheatstone bridge with remote sense
Usage : One component tension and compression measurement, transducer in multi component force frame
Manufacturer : MARIN
Dimensions : 40 x 26 x 12 mm
Mass : 50 -90 g
Material : Hardened Stainless Steel, Titanium
Water resistance : IP68, 1000 hours, 30m, tap water

Available types

MARIN type number	Typical maximum measuring limit [N][1]	Typical uncertainty[2] [N]
109	100	0.02% Measured value +0.050
111	200	0.02% Measured value +0.10
112	400	0.02% Measured value +0.20
113	750	0.02% Measured value +0.38
114	100	0.02% Measured value +0.05

1 Model scale values.
2 Corresponding confidence level: 95%

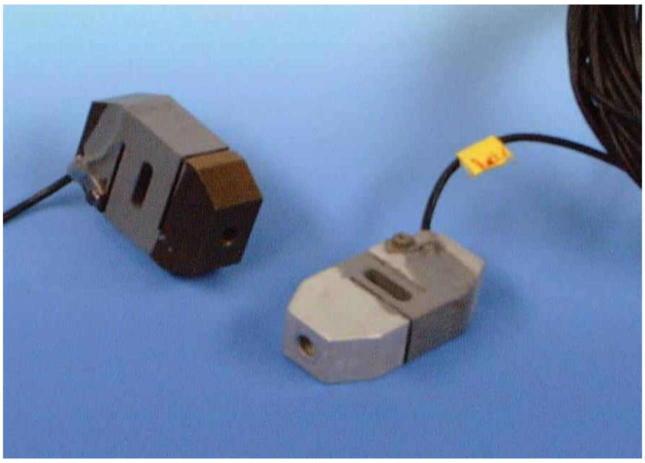

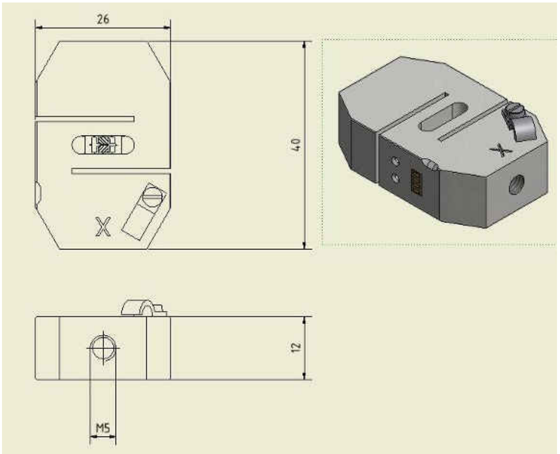

Double bending beam load cell

Measurand [Unit]	:	Force [Newton]
Function	:	Measuring compression and tension loads
Measurement principle	:	Strain gauges in full Wheatstone bridge
Typical application	:	Measurement of 'green water' impact
Manufacturer	:	MARIN
Typical dimensions	:	10 x 10 x 24 mm
Mass	:	10-12 g
Material	:	Stainless Steel
Water resistance	:	Submersible

Available types

MARIN type	Maximum measuring value E_{max} [1]) [N]
131	15
132	30
133	70

1) Model scale values

Example uncertainty calculation:

- Measured full scale value $F = 243.0\ \text{kN}$
- Model scale = 30 and sensor 131 $\Rightarrow E_{max} = 405\ \text{kN}$
- $F/E_{max} = 60\% \Rightarrow U_F/E_{max} = 0.43\%$
- Uncertainty $U_F = 1.7\ \text{kN} \Rightarrow F = (243.0 \pm 1.7)\ \text{kN}$

Double bending load cell

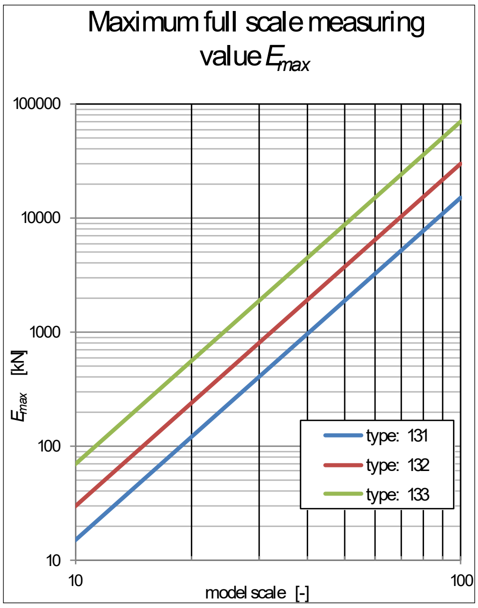

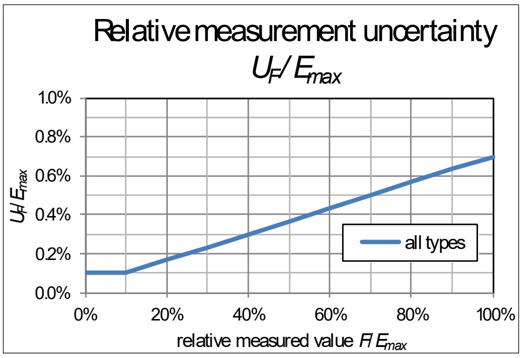

Wave height probe

Measurand [Unit]	:	Water level *h* [m]
Function	:	Measuring the relative water level in time
Measurement principle	:	Electrical resistance between two wires
Typical application	:	Wave field around a ship model
Manufacturer	:	MARIN
Length	:	Up to 0.9 m
Max. wave frequency	:	30 Hz
Calibration uncertainty	:	0.0015 m
Material (wires)	:	RVS

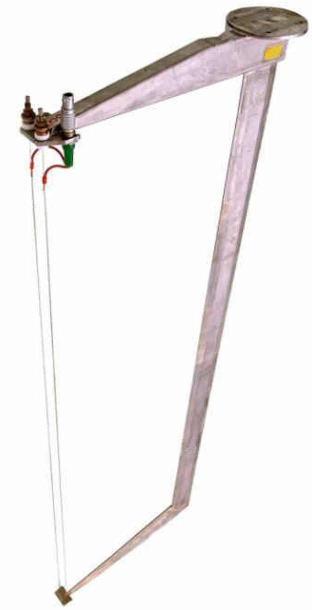

Single resistance wave height probe

Relative single resistance wave height probe (mounted at ship model)

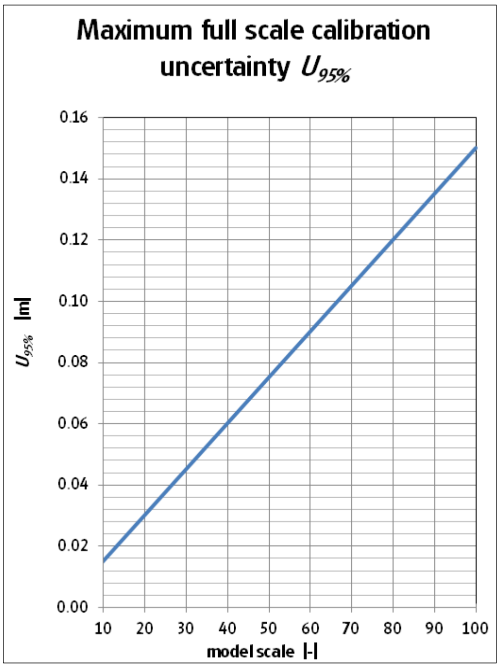

Slamming Pressure Transducer Marin

Measurand [Unit]	:	Pressure P [Pa]
Function	:	Measuring the relative pressure in time
Measurement principle	:	Piezoresistive strain gauge bridge
Typical application	:	Relative pressure field around submerged objects, slamming loads
Typical dimensions	:	20x36mm, with diameter active sensor surface of 2 mm
Minimum spacing	:	centre to centre spacing between these sensors is 25 mm
Measuring range	:	-30 - 30 kPa; Gauge pressure (relative to ambient pressure), This sensor can be used in depressurized tunnels at environmental pressures down to 25 mbar
Frequency response	:	The resonance frequency is 50 kHz. The bandwidth ranges from 0 to 10 kHz (-3 dB).
Sensitivity ambient light	:	2% of Full Scale Output, Stroboscopic flashes may appear in het output signals as sharp peaks. Ambient light from high speed video lighting may result in sudden shifts of the zero level.
Temperature shock sensitivity	:	10° Celcius shock response does not exceed 1% of Full Scale Output
Total error (CNL&H)	:	60 Pa (= 0.1% of Full Scale measuring Range)

The pressure sensor showing the active measuring area in the centre of the flush diaphragm

APPENDIX I05

Sign Convention

Revision	Date	Description of revision	Author
0	May 16, 2017	First version of the appendix	AN
1	December 12, 2017	Added SEMI LCS figure	AN
2	November 3, 2023	Basin Fixed Coordinate System added	JJS

Sign Convention

Units

The following metric (SI) units are used throughout this report unless otherwise stated:

- Motions and dimensions are given in metres [m]
- Angles are given in degrees [deg]
- Masses are given in 1,000 kg [tonnes]
- Forces are given in 1,000 Newtons [kN]
- Moments are given in 1,000 Newton metres [kNm]

Ship-Fixed / Local Coordinate System (LCS)

The Ship-Fixed coordinate system is the coordinate system of each vessel. The applied sign convention and coordinate system are in accordance with the OCIMF [1] standard. An overview of this standard is given in the figure below. The origin of the Local Coordinate System (LCS) is located at the intersection of the keel, centreline and Frame 0. A right handed coordinate system is applicable. The order of rotations is Yaw-Pitch-Roll.

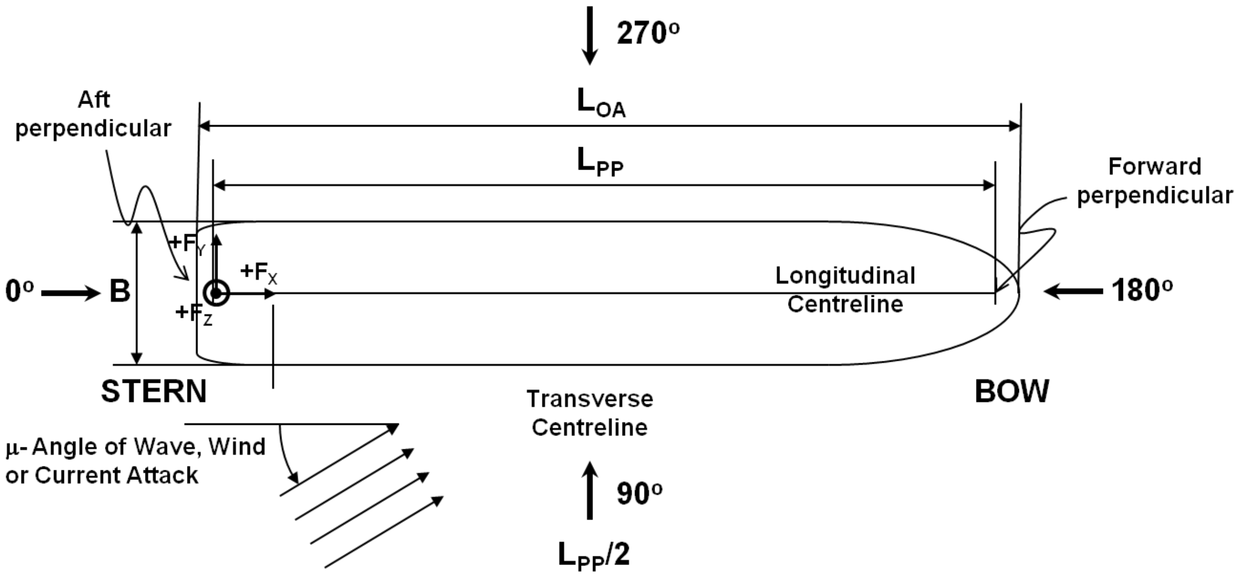

General OCIMF convention

The motions are positive in the following directions:

positive surge	(x)	:	towards the bow
positive sway	(y)	:	towards port side
positive heave	(z)	:	upwards
positive roll	(ϕ)	:	starboard side down
positive pitch	(θ)	:	bow down
positive yaw	(ψ)	:	bow towards port side

The forces and moments are positive in the following directions:

positive longitudinal force	(F_x)	:	towards the bow
positive lateral force	(F_y)	:	towards port side
positive vertical force	(F_z)	:	upwards
positive roll moment	(M_x)	:	starboard side down
positive pitch moment	(M_y)	:	bow down
positive yaw moment	(M_z)	:	bow towards port side

The relative environmental headings are defined as follows:

0 degree heading	:	stern on
90 degrees heading	:	starboard side on
180 degrees heading	:	bow on
270 degrees heading	:	port side on

Global Coordinate System (GCS)

The origin of the Global Coordinate System (GCS) is located in the Still Water Line (SWL). A right handed coordinate system is used. All environmental conditions are specified with respect to the GCS.

Basin-Fixed coordinate system (BFCS) in the Offshore Basin

In the model test basin the environmental directions are defined with respect to the Basin Fixed coordinate system (BFCS). The origin is selected at K8 in the basin, see Figure Io5-2, and the directions are defined as follows:

- The Offshore Basin uses a “going to” definition for the wind, waves and current with 180° for waves travelling from the short side wave makers (Basin West) to the short side beaches (Basin East). The basin wave angles increase in Counter Clockwise (CCW) direction.
- The model orientation in the BFCS is defined Counter Clockwise (CCW) direction with 0° towards Basin West.

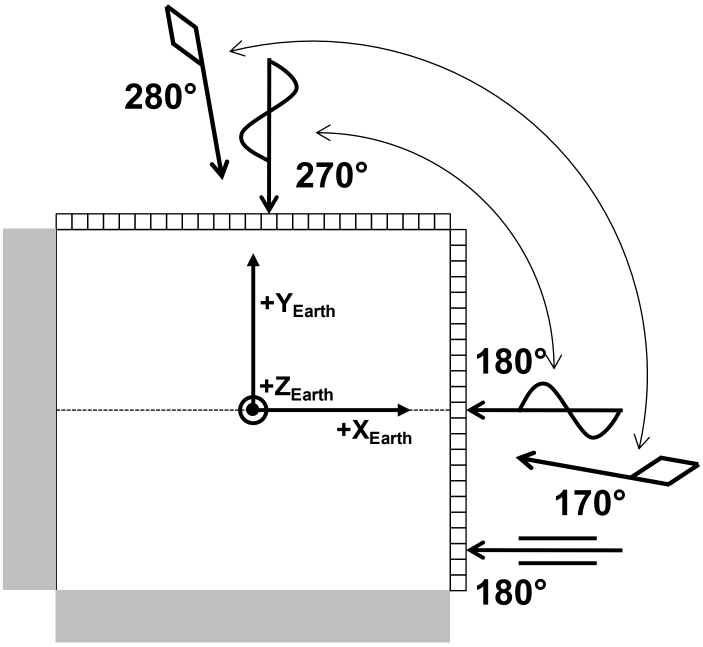

Figure I05-2: Representation of the Basin Fixed Coordinate System (BFCS) in the OB

The following relation applies between the BF environmental direction, SF environmental direction and the orientation of the vessel:

$$\mu_{SF} = \mu_{BF} - \Psi_{BF}$$

in which:

μ_{SF} = environmental direction in the Ship Fixed Coordinate System
μ_{BF} = environmental direction in the Basin Fixed Coordinate System
Ψ_{BF} = orientation of the vessel in the Basin Fixed (BF)

APPENDIX M01

Calibration of Model Weight Distribution

Revision	Date	Description of revision	Author
0	May 19, 2009	First version of the appendix	JLC
1	January 31, 2010	Reviewed and up-dated text and figures.	JLC
2	July 11, 2012	Description of double pendulum method instead of bifilar swing method	JJS

Calibration of Model Weight Distribution

Prior to the start of the model tests, the weight distributions of the scale models are adjusted. This includes the model mass, the position of the CoG and the radii of inertia about the principal axes. The following procedure is applied.

1. The model including as much measurement equipment, instrumentation and topsides as practically possibly is suspended in air and weighed by means of load cells in the wire.
2. The position of the centre of gravity is determined by means of differences in the loads measured in the wires (LCG) and static inclination tests in air (KG).
3. The oscillating periods are measured in 3 degrees of freedom.
4. The inertia I_{xx}, I_{yy} and I_{zz} of the model is determined based on the measured mass (step 1), the position of the COG (step 2) and the measured natural periods (step 3) and the geometry of the wires.

   The set-up of the measurements is shown in the sketch below.

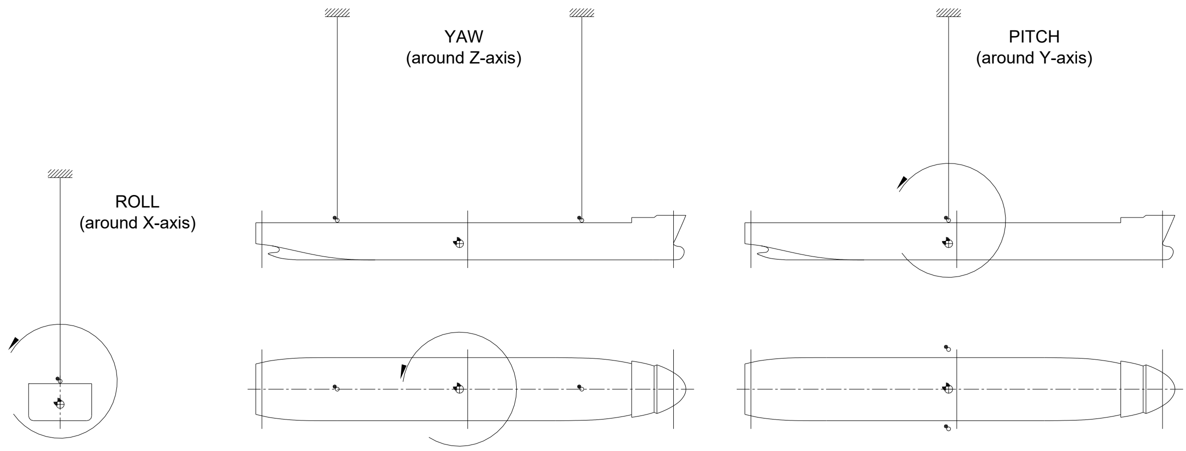

5. The weight and positions of all instrumentation, ballast weights and other elements to be included in the model is determined. The necessary amount of ballast weight inside the model is calculated to obtain the correct total model mass. The positions of these ballast weights are selected such, that the correct total weight distribution is achieved after placing the weights inside the model. The weight distribution is made symmetrical as much as possible, in order to avoid any undesired couplings between the different modes of motion (e.g. pitch induced roll).
6. The model, including instrumentation and all its ballast weights, is placed in the basin. The model draft and trim are checked by the draft marks on the hull.
7. The model GM value is determined by means of a heeling test.
8. The vessel roll natural period is determined in a roll decay test. When necessary, the ballast weight positions are modified to achieve the required roll period. The final positions of the ballast weights inside the model are marked and the modelled weight distribution is documented in the model test report.

APPENDIX M05

Calibration of Model Weight Distribution using Resonic

Revision	Date	Description of revision	Author
0	October 19, 2017	First version of the appendix	JLC
1	October 20, 2017	Reviewed and up-dated	JLC + RvdV
2	October 26, 2017	Measurement accuracies added	JLC

Calibration of Model Weight Distribution using Resonic

Prior to the start of the model tests, the weight distributions of the scale models are calibrated. The calibrated properties include the model mass, the position of the CoG and the moments of inertia about the principal axes. Measurements are performed using a Resonic[9] oscillation table, as shown in the photo below.

Resonic 2000F Oscillation Table

The following weight calibration procedure is applied:

9. The mass of the completed empty model (including all top-sides, instrumentation, cables, measurement equipment and thrusters, but without ballast weights) is carefully measured and the model is placed on the Resonic oscillation table. After the measurement software is started a number of passive oscillations is performed. This process is fully automated. The software derives the inertia properties of the model, based on the measured natural frequencies. The output of the analysis includes the position of the center of gravity (x, y, z) and the moments inertia around the principal axes (I_{xx}, I_{yy}, I_{zz}).

[9] Resonic GmbH, http://www.resonic.de/

10. The weight and positions of all ballast weights to be included in the model are determined. This is than such, that the correct total mass, CoG position and moments of inertia are achieved. In order to avoid any undesired couplings between the different modes of motion, the so-called products of inertia (I_{xy}, I_{xz}, I_{yz}), the ballast weights are placed symmetrical as much as possible.

11. The complete model (including all ballast weights) is placed in the water in the basin harbour. The model draft and trim are checked by the draft marks on the hull. The model GM value is checked by means of a heeling test. The vessel roll period is determined in a roll decay test. If necessary, the position of the ballast weights is changed to achieve the required GM value or roll period. The final positions of the ballast weights inside the model are marked and the modelled weight distribution is documented in the model test report.

12. The complete model is lifted from the water and placed on the Resonic oscillation table. The inertia measurement process is repeated to obtain the inertia properties of the model as it will be used in the model tests. The results are included in the model test report.

13. The model is placed in the water in the model basin. Here, in the test set-up, the final measurements of the GM value and roll natural period are carried out. The results of these measurements are included in the model test report.

Remark

For typical size models used in offshore model tests, the following measurement accuracies are achieved with the Resonic 2000F oscillation table.

Measured Property	Measurement Accuracy
Model Mass (M)	+/- 0.5 kg
Position of CoG (x, y, z)	+/- 2 mm
Main diagonal moments of inertia (I_{xx}, I_{yy}, I_{zz})	+/- 1%
Cross moments of inertia (I_{xy}, I_{xz}, I_{yz})	+/- 1% of largest principal moment

APPENDIX P03

Experimental procedure for motion decay tests

Revision	Date	Description of revision	Author
0	May 27, 2009	First version of the appendix	JH
1	February 1, 2010	Review and up-date of the text	JvdB
2	September 19,2014	Pumping method is added	FJ

Experimental procedure for motion decay tests

The purpose of the motion decay tests is to determine the natural periods and the damping levels for the various modes of motion of the vessel model. Two different methods can be used to performed the decay tests. On one hand, the held-over decay starts with the model at rest and in calm water. On the other hand, the decay with pre-oscillations starts with building up the motion amplitude before releasing the model. The objective is to take into account eventual memory effects due to the presence of vortices generated during the pre-oscillations. These vortices are not present when the decay is started with a static offset. The test procedure applied for the motion decay tests is described below.

Method 1 – Held over decays

1. The vessel model is completely at rest in its equilibrium position in calm water. The model is at the correct draft and correct trim with a zero heel angle.

2. The measurement is started.

3. The model is given an offset by manually moving it away from its equilibrium position in the desired mode of motion (e.g. surge, or roll). Then the model is released.

4. The model motions are measured and recorded. The recorded time traces are analysed using the methods described in Appendix D01.

Method 2 – Decays with pre-oscillations

1. The vessel model is completely at rest in its equilibrium position in calm water. The model is at the correct draft and correct trim with a zero heel angle.

2. The measurement is started.

–

3. The model is excited manually at its natural period for a given degree of freedom (e.g. roll, pitch). The motion is built up on a few periods till a pre-defined amplitude is reached.

4. The model is released.

5. The model motions are measured and recorded. The recorded time traces are analysed using the methods described in Appendix D01.

APPENDIX P04

Experimental procedure for model tests in (current, wind and) waves

Revision	Date	Description of revision	Author
0	May 27, 2009	First version of the appendix	JH
1	June 11, 2010	Reviewed and up-dated text	JLC

Experimental procedure for model tests in (current, wind and) waves

The model tests in environments of combined current, irregular waves and wind are performed according to the procedure described below.

1. The model is completely at rest in its zero position in calm water. The model is at the correct draft and correct trim with a zero heel angle.

2. The signals of all quantities are set to zero. This means that all quantities are measured relative to their values in the equilibrium position. In the data analysis, the mooring line pretensions are again added, so the mooring line tensions can be regarded as absolute tensions (in other words; zero tension is a slack line).

3. The current pumps are started and set at the correct RPMs (if applicable). After approximately 20 minutes (model scale value) the current has become stationary.

4. The wind fans are started and set at the correct RPMs (if applicable). The wind flow is stationary within a few minutes.

5. The wave generators are started, together with the measurement system. The first 30 minutes (1,800 s) of irregular seas are generated to let possible transient phenomena vanish ("start-up time"). Subsequently, irregular seas are generated for the actual duration of the model test (e.g. 3 hours / 10,800 s).

6. The model motions, line tensions, accelerations and all other signals are measured and recorded.

APPENDIX P08

Experimental Procedure for Side-by-Side Mooring System

Revision	Date	Description of revision	Author
0	May 15, 2014	First version of the appendix	FJ
1	May 21, 2014	Review and update of the text	WP

Experimental Procedure for Side-by-Side Mooring System

Prior to performing the side-by-side tests, the pretension in the side-by-side lines and fenders is adjusted. Furthermore, the measured equilibrium position is measured and compared to the expected equilibrium position. The following procedure is applied to setup the side-by-side mooring arrangement:

1. The pretension in the fenders is pre-adjusted outside the basin. A dedicated component with a force transducer is used. The dimension between the transducer and the FLNG corresponds to the distance between the FLNG and the LNGC in the equilibrium position. The pretension in adjusted by adjusting the position of the fenders.

2. The FLNG is connected to the carriage using stiff rods to lock the FLNG position in the basin.

3. The LNGC is positioned next to the FLNG at the correct (equilibrium) position. This is done by tensioning steel wires between the FLNG and the LNGC. Steel rings installed on the models are used to connect these steel wires. On the other hand, stiff separators are used to temporarily lock the LNGC position at the specified distance from the FLNG.

4. The pretension in the fenders are checked and adjusted to the specified values if necessary. The pretension in the side-by-side lines is adjusted to the specified values.

5. The motion signals are zeroed, and the stiff separators installed between the FLNG and the LNGC are removed. It is noted that all signals are measured with respect to the relative zero value, excepted the fender forces and the tension of the side-by-side lines, which are measured with respect to the absolute zero.

6. Due to small movement of the LNGC, the loads between the lines and fenders is redistributed. A measurement is performed to check the equilibrium position of the LNGC with respect to the FLNG (the FLNG is still fixed).

7. The FLNG is released from the stiff rods and the side-by-side tests can be performed.

APPENDIX P9

Experimental procedure for model tests in irregular waves

Revision	Date	Description of revision	Author
0	September 19, 2014	First version of the appendix	FJ

Experimental procedure for model tests in irregular waves

The model tests in irregular waves are performed according to the procedure described below.

7. The model is completely at rest in its zero position in calm water. The model is at the correct draft and correct trim with a zero heel angle.

8. The signals of all quantities are set to zero. This means that all quantities are measured relative to their values in the equilibrium position.

9. The wave generators are started, together with the measurement system. The first 30 minutes (1,800 s) of irregular seas are generated to let possible transient phenomena vanish ("start-up time"). Subsequently, irregular seas are generated for the actual duration of the model test.

10. The model motions, line tensions, accelerations and all other signals are measured and recorded.

APPENDIX P10

Experimental Procedure for Transducer Calibration

Revision	Date	Description of revision	Author
0	October 09, 2009	First version of the appendix	JJS
1	February 01, 2017	Second version of the appendix	JJS

Experimental procedure for transducer calibration

Calibrations of transducers are in general carried out in MARIN's calibration department. Some calibrations (wave probes, motion measurements) are carried out in the basin. The general calibration procedure is as follows:

1. Before use, all transducers are cleaned and checked visually.

2. From all transducers the relation between the measured quantity and the output voltage of the transducer is determined. The measurement quantity is applied in a number of steps within the measurement range of the transducer. The measurement quantities that are applied during the calibration are known quantities, for instance calibration weights (forces and moments).

3. Based on the relation between voltage and measured quantity a linearity check of the transducer is carried out. Normally there should be a linear relation between voltage and measurement quantity.

4. The linear multiplication factor between voltage and measurement quantity is determined and stored. This is the input for the relation between voltage and measurement quantity during the test.

The electronic equipment in the calibration department is identical to the equipment in the basin. The equipment in the basin is checked regularly by giving a certain input voltage and checking the output of the system.

M A R I N
P.O. Box 28

6700 AA Wageningen
The Netherlands

T +31 317 49 39 11
E info@marin.nl

I www.marin.nl